



University  
of Glasgow

Heathcote, Helen Rachel (2016) *The regulation of AMP-activated protein kinase by vascular endothelial growth factor*. PhD thesis.

<https://theses.gla.ac.uk/7375/>

Copyright and moral rights for this work are retained by the author

A copy can be downloaded for personal non-commercial research or study, without prior permission or charge

This work cannot be reproduced or quoted extensively from without first obtaining permission in writing from the author

The content must not be changed in any way or sold commercially in any format or medium without the formal permission of the author

When referring to this work, full bibliographic details including the author, title, awarding institution and date of the thesis must be given

Enlighten: Theses

<https://theses.gla.ac.uk/>  
[research-enlighten@glasgow.ac.uk](mailto:research-enlighten@glasgow.ac.uk)

**The regulation of  
AMP-activated protein kinase  
by vascular endothelial growth factor**

**Helen Rachel Heathcote MRes, BSc (Hons)**

Submitted in fulfilment of the requirements  
for the Degree of Doctor of Philosophy

February 2016

Institute of Cardiovascular and Medical Science,  
School of Medical Veterinary and Life Sciences,  
University of Glasgow

## Abstract

The function of the vascular endothelium is to maintain vascular homeostasis, by providing an anti-thrombotic, anti-inflammatory and vasodilatory interface between circulating blood and the vessel wall, meanwhile facilitating the selective passage of blood components such as signaling molecules and immune cells. Dysfunction of the vascular endothelium is implicated in a number of pathological states including atherosclerosis and hypertension, and is thought to precede atherogenesis by a number of years. Vascular endothelial growth factor A (VEGF) is a crucial mitogenic signaling molecule, not only essential for embryonic development, but also in the adult for regulating both physiological and pathological angiogenesis. Previous studies by our laboratory have demonstrated that VEGF-A activates AMP-activated protein kinase (AMPK), the downstream component of a signaling cascade important in the regulation of whole body and cellular energy status. Furthermore, studies in our laboratory have indicated that AMPK is essential for VEGF-A-stimulated vascular endothelial cell proliferation. AMPK activation typically stimulates anabolic processes and inhibits catabolic processes including cell proliferation, with the ultimate aim of redressing energy imbalance, and as such is an attractive therapeutic target for the treatment of obesity, metabolic syndromes, and type 2 diabetes. Metabolic diseases are associated with adverse cardiovascular outcomes and AMPK activation is reported to have beneficial effects on the vascular endothelium. The mechanism by which VEGF-A stimulates AMPK, and the functional consequences of VEGF-A-stimulated AMPK activation remain uncertain.

The present study therefore aimed to identify the specific mechanism(s) by which VEGF-A regulates the activity of AMPK in endothelial cells, and how this might differ from the activation of AMPK by other agents. Furthermore, the role of AMPK in the proliferative actions of VEGF-A was further examined. Human aortic and umbilical vein endothelial cells were therefore used as a model system to characterise the specific effect(s) of VEGF-A stimulation on AMPK activation.

The present study reports that AMPK  $\alpha 1$  containing AMPK complexes account for the vast majority of both basal and VEGF-A-stimulated AMPK activity. Furthermore, AMPK  $\alpha 1$  is localized to the endoplasmic reticulum when sub-confluent, but translocated to the Golgi apparatus when cells are cultured to confluence. AMPK  $\alpha 2$  appears to be associated with a structural cellular component, but neither  $\alpha 1$  nor  $\alpha 2$  complexes appear to translocate in response to VEGF-A stimulation. The present study confirms previous reports that when

measured using the MTS cell proliferation assay, AMPK is required for VEGF-A-stimulated endothelial cell proliferation. However, parallel experiments measuring cell proliferation using the Real-Time Cell Analyzer xCELLigence system, do not agree with these previous reports, suggesting that AMPK may in fact be required for an aspect of mitochondrial metabolism which is enhanced by VEGF-A. Studies into the mitochondrial activity of endothelial cells have proved inconclusive at this time, but further studies into this are warranted.

During previous studies in our laboratory, it was suggested that VEGF-A-stimulated AMPK activation may be mediated via the diacylglycerol (DAG)-sensitive transient receptor potential cation channel (TRPCs -3, -6 or -7) family of ion channels. The present study can neither confirm, nor exclude the expression of TRPCs in vascular endothelial cells, nor rule out their involvement in VEGF-A-stimulated AMPK activation; more specific investigative tools are required in order to characterise their involvement. Furthermore, nicotinic acid adenine dinucleotide phosphate (NAADP)-stimulated  $\text{Ca}^{2+}$  release from acidic intracellular organelles is not required for AMPK activation by VEGF-A.

Despite what is known about the mechanisms by which AMPK is activated, far less is known concerning the downregulation of AMPK activity, as observed in human and animal models of metabolic disease. Phosphorylation of AMPK  $\alpha 1$  Ser485 ( $\alpha 2$  Ser491) has recently been characterised as a mechanism by which the activity of AMPK is negatively regulated. We report here for the first time that VEGF-A stimulates AMPK  $\alpha 1$  Ser485 phosphorylation independently of the previously reported AMPK  $\alpha 1$  Ser485 kinases Akt (protein kinase B) and ERK1/2 (extracellular signal-regulated kinase 1/2). Furthermore, inhibition of protein kinase C (PKC), the activity of which is reported to be elevated in metabolic disease, attenuates VEGF-A- and phorbol 12-myristate 13-acetate (PMA)-stimulated AMPK  $\alpha 1$  Ser485 phosphorylation, and increases basal AMPK activity. In contrast to this, PKC activation reduces AMPK activity in human vascular endothelial cells. Attempts to identify the PKC isoform responsible for inhibiting AMPK activity suggest that it is one (or more) of the  $\text{Ca}^{2+}$ -regulated DAG-sensitive isoforms of PKC, however cross regulation of PKC isoform expression has limited the present study. Furthermore, AMPK  $\alpha 1$  Ser485 phosphorylation was inversely correlated with human muscle insulin sensitivity. As such, enhanced AMPK  $\alpha 1$  Ser485 phosphorylation, potentially mediated by increased PKC activation may help explain some of the reduced AMPK activity observed in metabolic disease.

# Contents

<b>Abstract</b> .....	<b>i</b>
<b>Contents</b> .....	<b>iii</b>
<b>List of Figures</b> .....	<b>vi</b>
<b>List of Tables</b> .....	<b>ix</b>
<b>Acknowledgements</b> .....	<b>x</b>
<b>Author's declaration</b> .....	<b>xi</b>
<b>Abbreviations</b> .....	<b>xii</b>
<b>Chapter 1 – Introduction</b> .....	<b>1</b>
1.1 Cell signalling .....	2
1.1.1 Phosphorylation & protein kinases .....	2
1.1.2 The discovery of AMPK .....	2
1.2 AMPK.....	3
1.2.1 Overview .....	3
1.2.2 AMPK subunit structure .....	4
1.2.3 Regulation of AMPK activity by AMP/ADP .....	6
1.2.4 Phosphorylation of AMPK at Thr172 .....	6
1.2.5 AMPK Thr172 kinases.....	7
1.2.6 Phosphorylation of AMPK at Ser485/491 .....	8
1.2.7 Effects of AMPK activation.....	9
1.2.8 Pharmacological activation of AMPK .....	13
1.2.9 The vascular endothelium .....	15
1.2.10 Endothelial dysfunction .....	16
1.2.11 AMPK activation in the vascular endothelium .....	17
1.3 Vascular Endothelial Growth Factor Signalling.....	20
1.3.1 VEGF .....	20
1.3.2 Regulation of VEGF production .....	22
1.3.3 VEGF receptors.....	24
1.3.4 VEGF activates AMPK.....	32
1.4 Project aims .....	33
<b>Chapter 2 – Materials and Methods</b> .....	<b>34</b>
2.1 Materials .....	35
2.1.1 General reagents.....	35
2.1.2 Kits .....	38
2.1.3 Specialist equipment .....	39
2.1.4 Cells and specialist media .....	40

2.1.5	Antisera .....	41
2.1.6	Plasmids .....	44
2.1.7	Reverse transcriptase PCR primers .....	45
2.1.8	Standard solutions .....	46
2.2	Methods .....	49
2.2.1	Cell culture .....	49
2.2.2	Propagation and purification of recombinant adenoviral vectors .....	51
2.2.3	siRNA transfection .....	54
2.2.4	Plasmid transfection of HeLa cells .....	54
2.2.5	Cell proliferation .....	54
2.2.6	Measurement of mitochondrial function using the Seahorse Bioscience XF24 Analyzer .....	56
2.2.7	Preparation of cell lysates .....	59
2.2.8	<i>In vitro</i> phosphorylation of AMPK .....	61
2.2.9	SDS polyacrylamide gel electrophoresis .....	61
2.2.10	Western blotting .....	62
2.2.11	AMPK activity assay .....	63
2.2.12	Immunofluorescence methods .....	64
2.3	Molecular biology protocols.....	66
2.3.1	Transformation of competent <i>E.coli</i> .....	66
2.3.2	Preparation of plasmid DNA.....	66
2.3.3	DNA sequencing .....	66
2.3.4	RNA extraction .....	67
2.3.5	First cDNA strand synthesis .....	67
2.3.6	Reverse transcriptase PCR .....	68
2.3.7	Agarose gel electrophoretic resolution, visualisation and imaging of PCR products .....	68
2.3.8	Quantitative (TaqMan®) Real time-PCR .....	68
2.4	Statistical analysis .....	69
<b>Chapter 3 – Investigating the effect of VEGF on AMPK.....</b>		<b>70</b>
3.1	Introduction .....	71
3.2	Results .....	72
3.3	Discussion.....	100
3.4	Conclusion.....	107
<b>Chapter 4 - Investigating the mechanism by which VEGF stimulates increased [Ca<sup>2+</sup>]<sub>i</sub> and AMPK activation .....</b>		<b>108</b>
4.1	Introduction .....	109
4.2	Results .....	113

4.3	Discussion.....	124
4.3.1	TRPC channels.....	124
4.3.2	NAADP-mediated Ca <sup>2+</sup> mobilisation from acidic organelles.....	131
4.4	Conclusion.....	135
<b>Chapter 5 - Regulation of AMPK activity by PKC.....</b>		<b>136</b>
5.1	Introduction .....	137
5.2	Results .....	138
5.3	Discussion.....	171
5.3.1	VEGF and AICAR stimulate both AMPK Thr172 and Ser485 phosphorylation by different mechanisms .....	171
5.3.2	Investigating the Akt and ERK1/2 dependence of AMPK $\alpha$ 1 Ser485 phosphorylation.....	172
5.3.3	Investigating the mechanism of VEGF-stimulated AMPK $\alpha$ 1 Ser485 phosphorylation.....	174
5.3.4	Characterising the PKC isoform(s) responsible for PKC-mediated AMPK $\alpha$ 1 Ser485 phosphorylation.....	176
5.3.5	PKC inhibition as a therapeutic approach for ameliorating reduced AMPK activity in metabolic disease.....	178
5.3.6	AMPK $\alpha$ 1 Ser485 phosphorylation in mouse and human models of metabolic disease .....	179
5.4	Conclusion.....	182
<b>Chapter 6 – Discussion .....</b>		<b>183</b>
6.1	Final discussion .....	184
6.2	Future work .....	186
<b>Summary.....</b>		<b>190</b>
<b>References .....</b>		<b>191</b>

## List of Figures

Figure 1-1: Summary of the mechanism of AMPK activation.....	3
Figure 1-2: AMPK subunit domain composition .....	4
Figure 1-3: Effects of AMPK activation .....	12
Figure 1-4: Pharmacological activation of AMPK.....	13
Figure 1-5: The multiple effects of AMPK activation on the vascular endothelium .....	17
Figure 1-6: Exon structure of VEGF-A mRNA splice variants in human. ....	21
Figure 1-7: Interactions between the VEGF family members and their receptors .....	25
Figure 1-8: VEGF-R2 signalling mediates cell proliferation, migration and survival via numerous signalling effectors .....	28
Figure 1-9: PKC domain structure.....	31
Figure 2-1: Immunostaining of HAEC with anti-CD31 antibody and haematoxylin .....	50
Figure 2-2: A schematic of a Seahorse XF Cell Mito Stress Test profile, showing the key parameters of cellular respiration .....	56
Figure 3-1: VEGF stimulates AMPK activity .....	73
Figure 3-2: $\alpha 1$ containing complexes account for the vast majority of basal and VEGF- or AICAR- simulated AMPK activity in HAEC.....	74
Figure 3-3: AMPK $\alpha$ isoform specific subcellular distribution in HAEC.....	76
Figure 3-4: Characterisation of structural and subcellular organelles in HAEC.....	77
Figure 3-5: AMPK $\alpha 1$ co-localises with both PDI and Hsp47 .....	78
Figure 3-6: AMPK $\alpha 2$ in HAEC.....	79
Figure 3-7: AMPK $\alpha 1$ subcellular distribution in VEGF treated HAEC .....	81
Figure 3-8: AMPK $\alpha 2$ subcellular distribution in VEGF treated HAEC .....	82
Figure 3-9: AMPK $\alpha 1$ is concentrated in the Golgi of confluent HAEC .....	84
Figure 3-10: AMPK $\alpha 1$ subcellular localisation is dependent on confluency .....	85
Figure 3-11: Assessment of virus transduction efficiency .....	88
Figure 3-12: Infection with Ad.AMPK-DN prevents VEGF-stimulated HUVEC proliferation as measured by MTS assay .....	89
Figure 3-13: Infection with Ad.AMPK-DN has no effect on VEGF-stimulated HUVEC proliferation as measured using the xCELLigence system.....	90
Figure 3-14: Assessment of mitochondria morphology in HUVEC .....	92
Figure 3-15: Complex I-V expression in HUVEC .....	93
Figure 3-16: Optimisation of oligomycin and FCCP concentrations for oxygen consumption rate (OCR) experiments .....	95
Figure 3-17: Oxygen consumption rate profiles for HUVEC .....	97
Figure 3-18: Key parameters of metabolism in HUVEC .....	99
Figure 4-1: Proposed mechanism of AMPK activation by VEGF .....	110
Figure 4-2: Immunoblotting assessment of TRPC expression in HAEC .....	114
Figure 4-3: Reverse transcriptase PCR assessment of TRPC expression in HAEC.....	115
Figure 4-4: Hyperforin stimulates AMPK Thr172 phosphorylation .....	117

Figure 4-5: Hyperforin-stimulated AMPK Thr172 phosphorylation is not sensitive to STO-609 .....	118
Figure 4-6: Hyperforin-stimulated AMPK Thr172 phosphorylation is not sensitive to the removal of extracellular calcium .....	119
Figure 4-7: The TRPC inhibitor Pry3 stimulates AMPK Thr172 phosphorylation .....	120
Figure 4-8: The NAADP antagonist Ned 19 has no effect on VEGF-stimulated MARCKS or AMPK Thr172 phosphorylation .....	123
Figure 4-9: Phylogenetic relationship of the TRPC protein family .....	124
Figure 5-1: VEGF stimulates both AMPK $\alpha$ Thr172 and Ser485/491 phosphorylation in HAECs and HUVECs .....	140
Figure 5-2: VEGF stimulates both ERK1/2 Thr202/Tyr204 and Akt Ser473 phosphorylation in HAECs .....	141
Figure 5-3: VEGF-stimulated AMPK $\alpha$ Thr172 and Ser485/491 phosphorylation is independent of Akt and ERK1/2 .....	142
Figure 5-4: Wortmannin has no effect on VEGF-stimulated AMPK $\alpha$ 1 Ser485 phosphorylation .....	143
Figure 5-5: Insulin-mediated Akt activation has no effect on AMPK $\alpha$ 1 Ser485 phosphorylation .....	144
Figure 5-6: VEGF-stimulated AMPK $\alpha$ 1 Ser485 phosphorylation is insensitive to STO-609 .....	146
Figure 5-7: VEGF-stimulated AMPK $\alpha$ 1 Ser485 phosphorylation is sensitive to $Ca^{2+}$ removal .....	147
Figure 5-8: Effect of $Ca^{2+}$ chelation on VEGF-stimulated AMPK phosphorylation .....	148
Figure 5-9: PKC inhibitors ablate VEGF-stimulated AMPK $\alpha$ 1 Ser485 phosphorylation and stimulate AMPK activity .....	152
Figure 5-10: PKC activators preferentially stimulate AMPK $\alpha$ 1 Ser485 phosphorylation .....	153
Figure 5-11: PKC activators stimulate AMPK $\alpha$ 1 Ser485 phosphorylation .....	154
Figure 5-12: The sensitivity of VEGF- and PMA-stimulated AMPK $\alpha$ 1 Ser485 and MARCKS phosphorylation to PKC inhibition by LY333531 .....	155
Figure 5-13: PMA does not stimulate Akt phosphorylation at either Thr308 or Ser473 ..	156
Figure 5-14: <i>In vitro</i> phosphorylation of AMPK by PKC and Akt .....	158
Figure 5-15: Chronic down regulation of PKC prevents VEGF-stimulated $\alpha$ 1 Ser485 phosphorylation .....	160
Figure 5-16: siRNA-mediated downregulation of PKC $\alpha$ has no effect on VEGF-stimulated AMPK $\alpha$ 1 Ser485 phosphorylation .....	161
Figure 5-17: Overexpression of PKC is sufficient to increase basal AMPK $\alpha$ 1 Ser485 phosphorylation .....	162
Figure 5-18: PMA stimulates AMPK $\alpha$ 1 Ser485 phosphorylation in HeLa independently of CaMKK .....	164
Figure 5-19: PMA stimulates AMPK $\alpha$ 1 Ser485 phosphorylation and inhibits AICAR-stimulated ACC Ser79 phosphorylation in HeLa cells expressing LKB1 .....	165
Figure 5-20: PMA stimulates AMPK $\alpha$ 1 Ser485 phosphorylation in MEFs .....	166

Figure 5-21: Assessment of Akt and AMPK Ser485/491 phosphorylation in murine tissue .....	168
Figure 5-22: AMPK $\alpha$ 1 Ser485 phosphorylation is inversely related to insulin sensitivity in human muscle.....	169
Figure 5-23: The effect of CRT0066101 on VEGF-stimulated AMPK phosphorylation .....	170
Figure 6-1: Mechanism of VEGF-stimulated phosphorylation of AMPK at Thr172 and Ser485 .....	190

## List of Tables

Table 2-1:	Cells used and their conditions of culture.....	40
Table 2-2:	Primary antibodies used for immunoblotting .....	41
Table 2-3:	Secondary detection agents used for immunoblotting .....	43
Table 2-4:	Primary antibodies used for immunofluorescence.....	43
Table 2-5:	Secondary detection agents for immunofluorescence .....	44
Table 2-6:	Plasmid DNA.....	44
Table 2-7:	Custom primers designed for reverse transcriptase-PCR .....	45
Table 2-8:	XF Cell Mito Stress Test kit reagents and injection protocol.....	58
Table 2-9:	XF Cell Mito Stress Test Kit OCR measurement protocol .....	58
Table 3-1:	Numerical summary of data presented in Figure 3-17 – Effect of VEGF .....	98
Table 3-2:	Numerical summary of data presented in Figure 3-17 – Effect of recombinant adenoviral transduction.....	98
Table 5-1:	Protein kinase C subfamily categorisation and co-factor requirements .....	175

## Acknowledgements

I would like to take this opportunity to extend my thanks to the British Heart Foundation for sponsoring this project and also to the many people who so generously contributed to the work presented in this thesis.

My most sincere thanks go to my supervisor Ian, not only for his academic support but for his endless encouragement and patience with me. My thanks must also go to Gwyn for being my second supervisor and his support, in matters both academic and personal.

I could not have made it through the last three years if it were not for the people I have had the pleasure of working with, thank you for making it a mostly enjoyable experience – there are too many people to mention but extra special thanks to Sarah, Silvia, Mairi, Anna and Jess.

I would also like to thank Craig, the most patient caring man I have ever met, without whose support this would not have been possible. And finally, to my mum and my family, for their unwavering belief in my abilities and for supporting me through the darkest time of my life, I only wish my Dad were here to see me reach this milestone.

I dedicate this thesis to him.

## **Author's declaration**

I declare that the work presented in this thesis has been carried out by me unless otherwise stated. It is of my own composition and has not in whole or in part been submitted for any other degree.

Helen R. Heathcote

February 2016

## Abbreviations

3T3-L1	fibroblast cell line isolated from 3T3 mouse embryo
A769662	6,7-Dihydro-4-hydroxy-3-(2'-hydroxy[1,1'-biphenyl]-4-yl)-6-oxo-thieno[2,3-b]pyridine-5-carbonitrile
aa.	amino acid
ABCG1	ATP-binding cassette sub-family G member 1
ACC	acetyl-CoA carboxylase
Ad.AMPK-CA	constitutively active AMPK recombinant adenoviral vector
Ad.AMPK-DN	dominant negative AMPK recombinant adenoviral vector
Ad.GFP	GFP recombinant adenoviral vector
ADAMTS3	ADAM metalloproteinase with thrombospondin type 1 motif 3
AIS	auto-inhibitory sequence
Akt	protein kinase B
Akti	3-[1-[4-(7-Phenyl-3H-imidazo[4,5-g]quinoxalin-6-yl)phenyl]methyl]piperidin-4-yl]-1H-benzimidazol-2-one
AMP	adenosine monophosphate
AMPK	AMP-activated protein kinase
ANOVA	analysis of variance
APS	ammonium peroxodisulphate
Bad	Bcl-2-associated death promoter
BAPTA-AM	1,2-Bis(2-aminophenoxy)ethane-N,N,N',N'-tetraacetic acid tetrakis (acetoxymethyl ester)
Bcl2	B-cell lymphoma 2
C2C12	murine derived myoblast cell line
cADPR	cyclic ADP-ribose
CaM	calmodulin
CaMK	CaM kinase
CaMKK	CaMK-kinase
CBS	cystathionine beta synthase
CCL2	chemokine (C-C motif) ligand 2 also known as monocyte chemoattractant protein 1
Cdc42	cell division control protein 42
cDNA	complementary DNA
CHO	chinese hamster ovary
CIAP	calf intestinal alkaline phosphatase
cPMA	chronic PMA
CTD	C-terminal domain
Ctl	control
CVD	cardiovascular disease

DAB	diaminobenzidine
DAG	diacylglycerol
DMEM	Dulbecco's modified Eagles media
DMSO	dimethylsulphoxide
DNA	deoxyribonucleic acid
dNTP	deoxynucleoside triphosphates
DTT	dithiothreitol
EC	endothelial cell
EDTA	ethylenediamine tetra-acetic acid
eEF2	eukaryotic elongation factor-2;
EGF	epidermal growth factor
EGTA	ethylene glycol-bis(2-aminoethylether)- <i>N,N,N',N'</i> -tetraacetic acid
eNOS	endothelial NO synthase
ER	endoplasmic reticulum
ERK1/2	extracellular signal related kinases 1 and 2
ERR $\alpha$	estrogen-related receptor $\alpha$
FA	fatty acid
FABPpm	fatty acid binding protein
FAT/CD36	fatty acid transporter
FCCP	carbonyl cyanide-4-phenylhydrazone
FFA	free fatty acid
FGF	Fibroblast growth factor
Flk1	Fetal Liver Kinase 1, also known as VEGF-receptor 2
Flt1	Fms-Related Tyrosine Kinase 1, also known as VEGF-receptor 1
Flt4	Fms-Related Tyrosine Kinase 4, also known as VEGF-receptor 3
FWD	forward (primer)
Fyn	a proto-oncogene tyrosine-protein kinase
GAPDH	glyceraldehyde-3-phosphate dehydrogenase
GBD	glycogen binding domain
GF109203X	2-[1-(3-Dimethylaminopropyl)indol-3-yl]-3-(indol-3-yl) maleimide
GFP	green fluorescent protein
GLUT4	glucose transporter 4
GM130	Golgi marker 130
GPN	glycyl-1-phenylalanine- $\beta$ -naphthylamide
HAEC	human aortic endothelial cells
HBD	HEPES-Brij-DTT buffer
HEK-293	human embryonic kidney 293 cells
HeLa	cervical carcinoma cells

HEPES	2-[4-(2-hydroxyethyl)piperazin-1-yl]ethanesulphonic acid
HepG2	hepatic carcinoma cells
HFD	high fat diet
HIF	hypoxia inducible factor
HMG-CoA	3-hydroxy-3-methylglutaryl-coenzyme A
HMGCR	HMG-CoA reductase
HRE	hypoxia response element
HRMEC	human retinal microvascular endothelial cells
Hsp	heat shock protein
HuR	Hu antigen R
HUVEC	human umbilical vein endothelial cells
HYP	hyperforin
ICAM1	intercellular adhesion molecule 1
IFB	immunofluorescence buffer
IGF-1	insulin-like growth factor 1
IgG	immunoglobulin G
IKK	I $\kappa$ B kinase
IL	interleukin
IP	immunoprecipitation
IP <sub>3</sub>	inositol trisphosphate
ISI	insulin sensitivity index
JNK	c-Jun N-terminal kinases
KO	knockout
KRH	Krebs-Ringer bicarbonate buffer
LDL	low density lipoprotein
LKB1	liver kinase B 1
LPS	lipopolysaccharide
LY333531	ruboxistaurin; (9S)-9-[(dimethylamino)methyl]-6,7,10,11-tetrahydro-9H,18H-5,21:12,17-di(metheno)dibenzo[e,k]pyrrolo[3,4h][1,4,13]oxadiazacyclohexadecine-18,20-dione hydrochloride
Mac-1	macrophage-1 antigen
MAPKAPK2	mitogen-activated protein kinase-activated protein kinase 2
MARCKS	myristoylated alanine-rich C-kinase substrate
MCP-1	monocyte chemoattractant 1
MEF	mouse embryonic fibroblast
MEK1/2	mitogen activated protein kinase
MEM	Minimum Essential Media
ML-9	1-(5-Chloronaphthalene-1-sulfonyl)-1H-hexahydro-1,4-diazepine hydrochloride
M-MLV	Moloney Murine Leukemia Virus

MO25	mouse protein-25
mRNA	messenger RNA
mTOR	mammalian target of rapamycin
mTORC2	mTOR complex 2
MTS	[3-(4,5-dimethylthiazol-2-yl)-5-(3-carboxymethoxyphenyl)-2-(4-sulfophenyl)-2H-tetrazolium, inner salt
MTT	3-(4, 5-dimethylthiazolyl-2)-2, 5-diphenyltetrazolium bromide
MV2	endothelial cell culture media
NAAD <sup>+</sup>	nicotinic acid adenine-dinucleotide
NAADP	nicotinic acid adenine-dinucleotide phosphate
NADH	reduced nicotinamide adenine dinucleotide
NADP <sup>+</sup>	nicotinamide adenine dinucleotide phosphate
NADPH	reduced NADP <sup>+</sup>
Nck	non-catalytic region of tyrosine kinase adaptor protein 1
Ned 19	<i>trans</i> -Ned 19; ((1R,3S)-1-[3-[[4-(2-Fluorophenyl)piperazin-1-yl]methyl]-4-methoxyphenyl]-2,3,4,9-tetrahydro-1H-pyrido[3,4-b]indole-3-carboxylic acid)
NF-κB	nuclear factor κB
NTD	N-terminal domain
OAG	1-oleoyl 2-acetyl- <i>sn</i> glycerol
<i>ob/ob</i>	leptin deficient mouse strain
OCR	oxygen consumption rate, typically expressed as pmol/min
OGTT	oral glucose tolerance test
p38 MAPK	p38 mitogen-activated protein kinases
PAK2	P21 protein (Cdc42/Rac)-activated kinase 2
P-ase	phosphatase
PBS	phosphate buffered saline
PBS-T	PBS with Tween-20
PCG-1α	peroxisome proliferator-activated receptor-γ coactivator 1α
PCR	polymerase chain reaction
PD184352	cyclopropylmethoxy-3,4-difluorobenzamide
PDGF	placental derived growth factor
PDI	protein disulphide isomerase
PDK1	3-phosphoinositide-dependent protein kinase-1
PFK2	phosphofructokinase-2
pfu	plaque forming units
PHLPP1/2	PH domain leucine-rich repeat-containing protein phosphatase 1
PI3K	phosphoinositide 3-kinase
PIP <sub>2</sub>	phosphatidylinositol 4,5-bisphosphate
PIP <sub>3</sub>	phosphatidylinositol (3,4,5)-trisphosphate

PKA	protein kinase A
PKC	protein kinase C
PLC $\gamma$	phospholipase C- $\gamma$
PIGF	placental growth factor
PMA	phorbol-12-myristate-13-acetate
PMSF	phenylmethylsulphonyl fluoride
PP2A	protein phosphatase 2A
PP2C	protein phosphatase 2C
PPAR $\gamma$	peroxisome proliferator-activated receptor gamma
PtdSer	phosphatidylserine
PTEN	phosphatase and tensin homolog
Pyr3	1-[4-[(2,3,3-Trichloro-1-oxo-2-propen-1-yl)amino]phenyl]-5-(trifluoromethyl)-1 <i>H</i> -pyrazole-4-carboxylic acid
qRT-PCR	quantitative real-time PCR
Rac	Rho family of GTPases
Raf	rapidly accelerated fibrosarcoma
RAW264.7	murine derived macrophage cell line
REV	reverse (primer)
RNA	ribonucleic acid
ROS	reactive oxygen species
RTCA	Real Time Cell Analyser
RT-PCR	reverse transcriptase PCR
RyR	ryanodine receptor
S.O.C. medium	super optimal broth
SAMS peptide	specific peptide substrate of AMPK (HMRSAMSGHLVKRR)
SBTI	soya bean trypsin inhibitor
SDS-PAGE	sodium dodecyl sulphate-polyacrylamide gel electrophoresis
SEM	standard error of the mean
Shb	Src homology 2 domain containing adaptor protein B
siRNA	small interfering RNA
SKF96365	1-[2-(4-Methoxyphenyl)-2-[3-(4-methoxyphenyl)propoxy]ethyl]-1 <i>H</i> -imidazole hydrochloride
SOC	store-operated channels
Ssp1	sporulation-specific gene 1, the yeast homologue of CaMKK
Ssp2	sporulation-specific gene 2
STO-609	7-Oxo-7 <i>H</i> -benzimidazo[2,1- <i>a</i> ]benz[de]isoquinoline-3-carboxylic acid acetate
STRAD	STE20-related kinase adapter protein alpha
TE	Tris-EDTA
TEMED	<i>N,N,N',N'</i> -tetramethylethylenediamine

TGF- $\beta$	transforming growth factor $\beta$
TNF $\alpha$	tumor necrosis factor $\alpha$
TPC	two-pore channel
Tris base	tris-(hydroxymethyl)-amonoethane
TRPC	transient receptor potential cation channel
TRPP	transient receptor potential channel (polycystin)
TRPV	transient receptor potential channel (vanilloid)
TSad	T cell-specific adapter
TZD	thiazolidinediones
U-73122	1-[6-[[[(17 $\beta$ )-3-Methoxyestra-1,3,5(10)-trien-17-yl]amino]hexyl]-1 <i>H</i> -pyrrole-2,5-dione
ULK-1	Unc-51-like kinase
VCAM1	vascular cell adhesion molecule 1
VEGF	vascular endothelial growth factor
VEGF-R	VEGF receptor
Veh	vehicle
vHL	Von Hippel-Lindau tumour suppressor
VSMC	vascular smooth muscle cell
WT	wild type
ZMP	AICAR; 5-aminoimidazole-4-carboxamide-1- $\beta$ -D-furanosyl 5' monophosphate

# Chapter 1 – Introduction

## **1.1 Cell signalling**

### **1.1.1 Phosphorylation & protein kinases**

The ability of cells to perceive and respond appropriately to external stimuli is central to survival; cell signalling is the communication mechanism by which cells perceive and respond to their environment. Signalling molecules such as peptides, hormones, steroids, lipids and dissolved gases act in autocrine, paracrine and endocrine manners facilitating the coordinated behaviour of individual cells, larger organs and whole organisms. In the simplest linear form, cells detect an external stimulus, transmit the signal internally and then effect the appropriate biological response. Cell signalling pathways are however not linear, but rather form complex signalling networks which process, encode, integrate and amplify signals, such that a single stimuli has the capacity to affect a diverse range of responses. Protein kinases and phosphatases, which catalyse the protein phosphorylation and de-phosphorylation respectively, of serine, threonine and tyrosine residues within their substrates, are a major component of signalling cascades. The modification of proteins by phosphorylation has the capacity to induce reversible conformational change, alters subcellular localisation, half-life and interaction with other proteins, with the effect of regulating the biological activity of the protein and its substrates.

### **1.1.2 The discovery of AMPK**

In 1973, two groups independently observed the inhibition of HMG-CoA reductase (HMGCR) and acetyl-CoA carboxylase (ACC) by an, as yet uncharacterised soluble protein kinase, effects which were found to be stimulated by AMP and inhibited by ATP (Beg et al. 1973, Carlson and Kim 1973). It wasn't until 1987 that these effects were reported to be the function of the same enzyme (Carling et al. 1987). In line with the precedent set by the cyclic-AMP dependent protein kinase (PKA), the new kinase was later named AMP-activated protein kinase or AMPK, after its allosteric activator (Munday et al. 1988). AMPK has since been characterised as the downstream component of a protein kinase signalling cascade, which plays a central role in the regulation of whole-body and cellular energy status serving to redress energy imbalance under times of metabolic stress.

## 1.2 AMPK

### 1.2.1 Overview

AMPK is activated by an increase in the ratio of AMP (or ADP) to ATP caused by metabolic stress due to either increased ATP consumption *e.g.* exercise in muscle, or the inhibition of ATP production *e.g.* nutrient or oxygen deprivation. AMPK is a heterotrimeric complex, consisting of a catalytic ( $\alpha$ ) and regulatory ( $\beta$  and  $\gamma$ ) subunits. The  $\gamma$  subunit contains domains responsible for sensing cellular adenine nucleotide levels, whereas amongst other functions the  $\beta$  subunit acts as a scaffold stabilising the interaction between the  $\alpha$  and  $\gamma$  subunits. AMPK can be allosterically activated by the binding of AMP to the  $\gamma$  subunit, however maximal activation of AMPK is achieved by phosphorylation of Thr172 on the  $\alpha$  subunit by the upstream AMPK-kinases liver kinase B1 (LKB1) in complex with STE20-related adaptor (STRAD) and the adaptor protein MO25, or  $\text{Ca}^{2+}$ /calmodulin-dependent protein kinase kinase- $\beta$  (CaMKK $\beta$ ) (Figure 1-1). Activated AMPK acts to redress energy imbalance in the short-term by inhibiting ATP consuming processes and stimulating ATP production, but also has long-term effects on gene and protein expression. AMPK is highly conserved, such that orthologues have been identified in almost every eukaryote for which a genome sequence has been completed (Hardie 2011), highlighting the importance of this regulatory mechanism in different species.

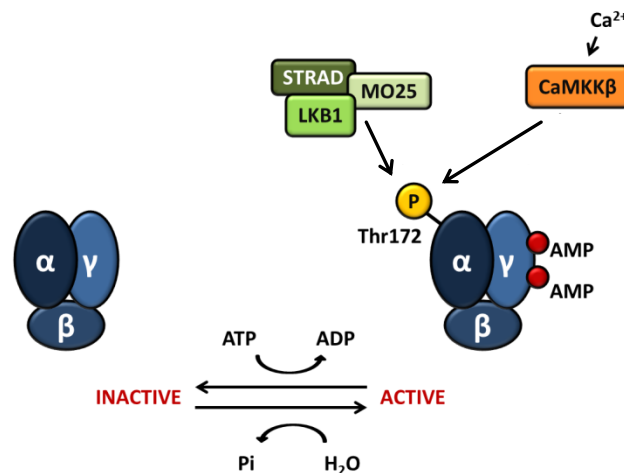


**Figure 1-1: Summary of the mechanism of AMPK activation**

AMPK is a heterotrimeric complex consisting of a catalytic ( $\alpha$ ) and regulatory ( $\beta$  and  $\gamma$ ) subunits. AMPK is activated allosterically by the binding of AMP to the  $\gamma$  subunit, or by phosphorylation of Thr172 within the activation loop of the  $\alpha$  subunit, catalysed by LKB1 complexed with STRAD and MO25, or in response to elevated intracellular  $\text{Ca}^{2+}$  by CaMKK $\beta$ . AMPK is dephosphorylated by phosphatases reverting AMPK to the inactive form. (Redrawn from Viollet et al. 2009).

## 1.2.2 AMPK subunit structure

AMPK is a heterotrimeric complex, consisting of a catalytic ( $\alpha$ ) and non-catalytic, regulatory ( $\beta$  and  $\gamma$ ) subunits (Figure 1-2). Each subunit has a distinct role in the activity or stability of the AMPK complex, and are coded for by seven distinct genes ( $\alpha 1$ -*PRKAA1*,  $\alpha 2$ -*PRKAA2*,  $\beta 1$ -*PRKAB1*,  $\beta 2$ -*PRKAB2*,  $\gamma 1$ -*PRKAG1*,  $\gamma 2$ -*PRKAG2* and  $\gamma 3$ -*PRKAG3*). Twelve different heterotrimeric complex combinations are therefore theoretically possible however alternative splicing of the different genes further increases this variation (Kahn et al. 2005).

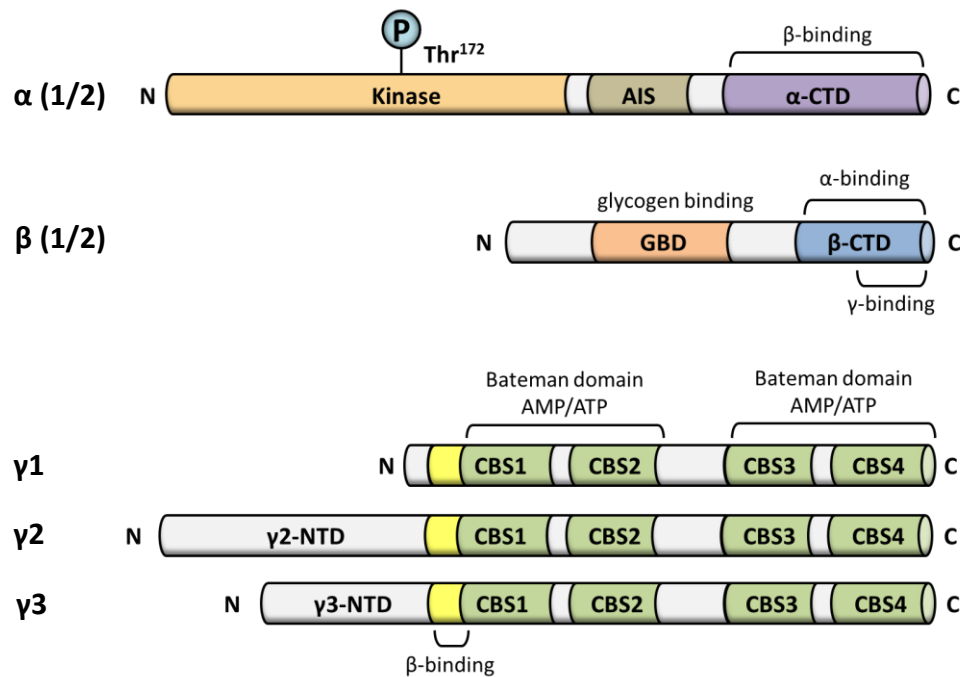


**Figure 1-2: AMPK protein domain structure**

The mammalian AMPK  $\alpha$ ,  $\beta$  and  $\gamma 1$ ,  $\gamma 2$ ,  $\gamma 3$  proteins are shown. The  $\alpha$  subunit contains a conserved phosphorylation (P) site at Thr172 within the kinase domain and a central auto-inhibitory sequence (AIS). The  $\beta$  subunit contains a glycogen binding domain (GBD) and C-terminal domain (CTD) necessary for complex formation with  $\alpha$  and  $\gamma$ . The  $\gamma$  subunits have variable N-terminal domains (NTD) and four conserved cystathione- $\beta$ -synthase (CBS) motifs. These act in pairs to form Bateman domains, which act as adenine nucleotide binding sites. (Redrawn from Hardie, 2007).

### 1.2.2.1 Alpha ( $\alpha$ ) subunit

The catalytic  $\alpha$  subunits ( $\alpha 1$  and  $\alpha 2$ ) are highly conserved within their catalytic core (~90 % identical) but diverge substantially outwith this conserved region (61 % shared identity) (Stapleton et al. 1996). The N-terminal catalytic serine/threonine kinase domain contains a conserved threonine at position 172; phosphorylation of which is essential for full activation of AMPK (Woods et al. 1994). The remainder of AMPK  $\alpha$  consists of an auto-inhibitory sequence (AIS) which negatively regulates AMPK activity via interaction with

the catalytic  $\alpha$  kinase domain (L. Chen et al. 2009), and C-terminal domain which is required for AMPK complex assembly (Crute et al. 1998). Although Thr172 is the major activating phosphorylation site on AMPK  $\alpha$ , other phosphorylated residues have been identified including  $\alpha 1$  Ser485 ( $\alpha 2$  Ser491) and Thr258, although these are not involved in the *activation* of AMPK (Woods et al. 2003b).

AMPK  $\alpha 1$  is widely expressed, however  $\alpha 2$  is reported to be the predominant isoform expressed in cardiac and striated muscle, specific expression patterns are however likely to vary markedly between species. Northern blot analysis by Stapleton and co-workers determined the presence of AMPK  $\alpha 2$  mRNA in rat skeletal muscle, with lesser amounts found in liver, heart and kidney, whereas low levels of AMPK  $\alpha 1$  mRNA was found in all the tissues examined in this particular study (heart, brain, spleen, lungs, liver, kidney and testis) (Stapleton et al. 1996). These findings were supported by immunoblot analysis, again demonstrating abundant AMPK  $\alpha 2$  expression in heart, liver and skeletal muscle whereas AMPK  $\alpha 1$  protein was again found to be widely expressed (Stapleton et al. 1996). Later studies using immunohistochemical methods measured the expression of AMPK  $\alpha 1$  and  $\alpha 2$  in human tissue biopsies from various tissues (heart, striated muscle, stomach, pancreas, kidney, liver, gut, breast, lung) (Quentin et al. 2011). This study however had the advantage of being able to determine AMPK expression patterns within the discreet cell populations that make up most organs *e.g.* identify differential  $\alpha$  isoform expression patterns in the islets of Langerhans and pancreatic acini cells.

#### **1.2.2.2 Beta ( $\beta$ ) subunit**

The  $\beta$  subunit facilitates the assembly of the AMPK complex, by stabilising the interaction between the  $\alpha$  and  $\gamma$  subunits. The  $\beta$  subunit contains a glycogen-binding domain (GBD). Binding of the oligosaccharide component of glycogen to AMPK acts to inhibit its activity (McBride et al. 2009). Therefore glycogen binding to the  $\beta$  subunit provides another mechanism by which AMPK can sense and regulate energy homeostasis. The C-terminal domain of AMPK  $\beta$  is necessary for AMPK  $\alpha/\beta/\gamma$  complex formation (Hudson et al. 2003). AMPK  $\beta$  is also reported to contain N-terminal myristoylation sites which may regulate the subcellular distribution of the AMPK complex (Mitchelhill et al. 1997).

#### **1.2.2.3 Gamma ( $\gamma$ ) subunit**

The  $\gamma$  subunits are characterised by the presence of four cystathione- $\beta$ -synthase (CBS) motifs. These occur in tandem pairs forming structures called Bateman domains, the site of

nucleotide binding thereby controlling the allosteric activity of the AMPK complex (Bateman 1997). Crystallisation studies revealed that three of the four mammalian CBS motifs facilitate nucleotide binding; two sites readily exchange AMP, ADP or ATP, whereas the third site is occupied by a non-exchangeable molecule of AMP (Xiao et al. 2007). The importance of the  $\gamma$  subunit is highlighted by the observation that the sensitivity of an AMPK complex to regulation by AMP is dependent upon the  $\gamma$  isoform present (Cheung et al. 2000).

### 1.2.3 Regulation of AMPK activity by AMP/ADP

When the reaction catalysed by adenylate kinase ( $2 \text{ ADP} \leftrightarrow \text{ATP} + \text{AMP}$ ) is assumed to be maintained at or near equilibrium, the AMP:ATP ratio will vary by the approximate square of the ADP:ATP ratio (*e.g.*  $[\text{AMP}]/[\text{ATP}] \approx ([\text{ADP}]/[\text{ATP}])^2$ ) making the former a more sensitive indicator of cellular energy status (Hardie et al. 1998). Binding of AMP or ADP to the  $\gamma$  subunit allosterically activates AMPK, and promotes the phosphorylation of Thr172 by upstream kinases. Furthermore, allosteric activation renders AMPK a poorer substrate for protein phosphatases (*e.g.* PP2C) effectively inhibiting Thr172 de-phosphorylation (Sanders et al. 2007b). In contrast, ATP binding to the  $\gamma$  subunit competitively antagonises AMP/ADP-mediated allosteric activation of AMPK and further Thr172 phosphorylation. It has been suggested that ADP rather than AMP is the principal nucleotide regulating the activation of AMPK (Xiao et al. 2011). The cellular ADP and ATP concentrations are far greater than AMP such that ADP:ATP may be a more physiologically relevant stimulus for AMPK activation. Contrary to this, AMP was later reported to be a more potent inhibitor of Thr172 de-phosphorylation than ADP (Gowans et al. 2013). Furthermore, allosteric activation of AMPK by AMP was sufficient to stimulate ACC phosphorylation in the absence of Thr172 phosphorylation suggesting that the allosteric activation of AMPK by AMP also contributes significantly to overall AMPK activity (Gowans et al. 2013).

### 1.2.4 Phosphorylation of AMPK at Thr172

Despite being named because of its allosteric activation by AMP, the effect of AMP on AMPK activity is relatively modest (<5-fold increase) (Carling et al. 1987) compared to the effect of Thr172 phosphorylation (>100-fold increase) (Suter et al. 2006). Thr172 phosphorylation is essential for the full activation of AMPK, as mutation of Thr172 to alanine abolishes AMPK activity (Crute et al. 1998). AMPK can be rapidly dephosphorylated upon cessation of the activating stimulus, however the identity of the

protein phosphatases that dephosphorylate Thr172 in different tissues *in vivo* remains elusive.

### 1.2.5 AMPK Thr172 kinases

The identity of the kinase(s) mediating Thr172 phosphorylation remained elusive for many years and it was studies in yeast that ultimately led to their identification. Two groups independently reported that Tos3 and Sak1, along with a further closely related kinase Elm1 phosphorylated and activated Snf1, the yeast homologue of AMPK (Hong et al. 2003, Sutherland et al. 2003). The closest related mammalian kinases to these yeast Snf1-kinases are the Ca<sup>2+</sup>/calmodulin-dependent kinase-kinase (CaMKK) family and the tumour suppressor liver kinase B1 (LKB1).

#### 1.2.5.1 LKB1

LKB1 much like AMPK, exists as a heterotrimeric complex, formed with MO25 and STRAD. It was debated for some time as to whether or not AMP directly stimulated LKB1 activity, however two independent groups published reports arguing against direct AMP-stimulated LKB1 activation (Hawley et al. 2003, Woods et al. 2003a). Currently, LKB1 is largely thought to be constitutively active and elevated levels of AMP allosterically increase AMPK activity while inhibiting the de-phosphorylation of Thr172 by protein phosphatases such as PP2C (Suter et al. 2006, Sanders et al. 2007b).

#### 1.2.5.2 CaMKK $\beta$

Despite LKB1 being identified as the major AMPK-kinase, several lines of evidence reported that AMPK could be activated in cells lacking LKB1 expression. In HeLa cells, which naturally lack LKB1 expression, AMPK activity was retained, and furthermore Thr172 phosphorylation was observed (Hawley et al. 2005), suggesting the presence of an AMPK-kinase other than LKB1. Three independent studies subsequently reported that CaMKK $\beta$  is an AMPK-kinase (Hawley et al. 2005, Hurley et al. 2005, Woods et al. 2005).

CaMKK $\beta$  consists of unique N- and C-terminal domains separated by a Ser/Thr kinase domain and a regulatory domain, composed of overlapping auto-inhibitory and CaM-binding regions. CaMKK $\beta$  has autonomous activity for Ca<sup>2+</sup>/calmodulin-dependent-kinase I (CaMKI) and Ca<sup>2+</sup>/calmodulin-dependent-kinase IV (CaMKIV), with phosphorylation of Ser129, -133 and 137 within an N-terminal region reported to be important regulator of

CaMKK $\beta$ 's autonomous activity (Tokumitsu et al. 2001). Furthermore, relieving auto-inhibition is reported to promote the auto-phosphorylation of Thr482, further contributing to the regulation of CaMKK $\beta$ 's autonomous activity (Tokumitsu et al. 2011). Other substrates including AMPK however, require Ca<sup>2+</sup>/CaM-mediated activation of CaMKK $\beta$  for kinase activity (Hurley et al. 2005) and CaMKK $\beta$ -AMPK interactions are reported to occur between the kinase domains of both proteins (Green et al. 2011). CaMKK $\beta$  is expressed in numerous tissue culture models including murine pre-adipocytes, embryonic fibroblasts and isolated hepatocytes, as well as human umbilical vein endothelial cells (Anderson et al. 2012, Lin et al. 2011, Stahmann et al. 2006). CaMKK $\beta$  is also present in many areas of the brain and nervous system, and to a lesser extent in testis, spleen and lung (Anderson et al. 1998, Ohmstede et al. 1989). When Ca<sup>2+</sup> levels fall, Thr172 is rapidly dephosphorylated by protein phosphatases, such as PP2C, accounting for the transient nature of AMPK activity after CaMKK $\beta$ -mediated activation (Carling et al. 2008).

### **1.2.6 Phosphorylation of AMPK at Ser485/491**

Despite the well-characterised mechanisms of activating-Thr172 phosphorylation, far less is known concerning the phosphorylation of AMPK at other residues, including  $\alpha$ 1 Ser485 (Ser485 is the murine designation and equivalent to human  $\alpha$ 1 Ser487) and  $\alpha$ 2 491. AMPK Ser485/491 phosphorylation is reported to be associated with reduced AMPK activity (Horman et al. 2006, Soltys et al. 2006, Berggreen et al. 2009, Ning et al. 2011) and can therefore be thought of as an inhibitory event. Initial studies reported that insulin or IGF-1-stimulated Akt (protein kinase B) activation reduced AMPK activity due to Akt-mediated Ser485 phosphorylation, in heart (Horman et al. 2006), cardiac myocytes (Soltys et al. 2006), adipocytes (Berggreen et al. 2009) and vascular smooth muscle (Ning et al. 2011). During the current study AMPK  $\alpha$ 2 Ser491 was reported to be a poor Akt substrate and is rather more likely to be modified by auto-phosphorylation (Hawley et al. 2014). More recently however, insulin/IGF-1 and Akt-independent mechanisms of Ser485 phosphorylation have been reported. LPS stimulated AMPK  $\alpha$ 1 Ser485 phosphorylation in RAW264.7 cells, in a manner sensitive to IKK but not Akt inhibition (Park et al. 2014). Furthermore, inhibitors of the mitogen/extracellular signal-regulated kinase (MEK1/2)-extracellular-signal-regulated kinases (ERK1/2) pathway are reported to inhibit cytokine (CCL21)-stimulated AMPK  $\alpha$ 1 Ser485 phosphorylation in human dendritic cells, independently of Akt (Lopez-Cotarelo et al. 2015).

### **1.2.7 Effects of AMPK activation**

Activation of AMPK exerts short-term effects via the rapid phosphorylation of specific substrates, and long-term effects via gene and protein expression. The pleiotropic effects of AMPK activation aim to redress energy imbalance by stimulating catabolic processes to generate ATP (*e.g.* fatty acid uptake and oxidation, glucose uptake and glycolysis, and mitochondrial biogenesis) and inhibiting anabolic/ATP consuming processes (*e.g.* the synthesis of fatty acids, triglycerides, cholesterol and glycogen, gluconeogenesis and protein synthesis), effects which can be observed in a diverse range of tissues, including liver, skeletal muscle, adipose, heart, brain and the vasculature (Figure 1-3).

#### **1.2.7.1 Lipid metabolism**

Under times of metabolic stress, AMPK activation seeks to stimulate energy availability by stimulating fatty acid oxidation. AMPK phosphorylates and inhibits ACC, the key regulated enzyme catalysing the conversion of acetyl-CoA to malonyl-CoA. Decreased malonyl-CoA synthesis relieves the inhibitory effect of malonyl-CoA on carnitine palmitoyl transferase stimulating fatty acid (FA) transport into mitochondria where they are subsequently oxidised to yield ATP (McGarry 1995). Furthermore, AMPK activation is reported to stimulate the expression of the fatty acid transporters FAT/CD36 and FABPpm in cardiomyocytes and Langendorff perfused hearts (Chabowski et al. 2006), in addition to previous reports that AMPK increased their trafficking to the plasma membrane (Chabowski et al. 2005). These effects have the combined effect of increasing fatty acid transport and subsequent oxidation.

HMGCR is a key enzyme regulating the synthesis of cholesterol. AMPK was first identified as the enzyme that phosphorylated HMGCR (Beg et al. 1973, Carling et al. 1987), resulting in its inhibition. AMPK-mediated inhibition of HMGCR decreases mevalonate synthesis, and the synthesis of its downstream products, including cholesterol. More recently statins (HMGCR inhibitors) have also been shown to activate AMPK (Sun et al. 2006), and it has been suggested that the vaso- and cardio-protective effects of statins may act at least in part via AMPK.

#### **1.2.7.2 Glucose metabolism**

AMPK is an important regulator of glucose metabolism, influencing glucose transport, glycolysis, gluconeogenesis and glycogen synthesis. Glucose uptake into muscle and

adipose is facilitated by the recruitment of glucose transporters such as GLUT4 from intracellular vesicles to the plasma membrane. AMPK is reported to increase GLUT4 expression, and regulate insulin-stimulated trafficking of GLUT4 to the plasma membrane (Holmes et al. 1999, Buhl et al. 2001). AMPK is also reported to phosphorylate phosphofructokinase-2 (PFK-2) in ischemic cardiac muscle (Marsin et al. 2001). PFK-2 is a key enzyme catalysing the conversion of fructose-6-phosphate to fructose-2,6-bisphosphate, which itself stimulates PFK-1, further accelerating glycolysis. AMPK activation is further reported to suppress hepatic gluconeogenesis in an AMPK-dependent manner by downregulating PEPCK and G6Pase (Foretz et al. 2005), key gluconeogenic enzymes. Furthermore, AMPK is reported to phosphorylate and inhibit glycogen synthase at Ser7, and stimulate glycogen phosphorylase (Inoue and Yamauchi 2006) thereby promoting the breakdown of glycogen and suppressing its synthesis.

### **1.2.7.3 Protein synthesis and cell growth**

The mammalian target of rapamycin (mTOR) is a key regulator of organismal growth and homeostasis. mTOR combines with different proteins to form two complexes (mTORC1 and mTORC2) which have distinct mechanisms of regulation and downstream signalling. AMPK regulates the activity of mTORC1 by directly phosphorylating Raptor, stimulating its binding to 14-3-3, thereby preventing the association of Raptor with mTOR. Furthermore, AMPK phosphorylates the negative regulator of mTORC1, TSC2 (Inoki et al. 2006), which stimulates the conversion of Rheb to its inactive (GDP-bound) state. Inactive Rheb is therefore no longer able to stimulate the kinase activity of mTORC1. Inhibition of mTORC1 reduces the phosphorylation a number of downstream translation initiators thereby inhibiting protein synthesis.

### **1.2.7.4 Mitochondrial biogenesis**

Mitochondrial biogenesis is stimulated in response to a numerous signals during times of metabolic stress, or in response to environmental stimuli. The transcription factor peroxisome proliferator-activated receptor  $\gamma$  co-activator 1 $\alpha$  (PGC-1 $\alpha$ ) is activated by AMPK, which stimulates the transcription of a number of mitochondrial genes (Lin et al. 2005). PGC-1 $\alpha$  is reported to be downregulated in *PRKAA2*<sup>-/-</sup> mice (Um et al. 2010), whereas AMPK activation using AICAR is reported to upregulate the mRNA expression of NFR-1 and mtTFA stimulating mitochondrial biogenesis in HUVEC (Kukidome et al. 2006).

### 1.2.7.5 Vascular homeostasis (NO synthesis)

eNOS plays a critical role in maintaining vascular homeostasis via the synthesis of NO. AMPK (Thr172) and eNOS (Ser633) phosphorylation are reported to be stimulated by shear stress, atorvastatin and adiponectin, and eNOS phosphorylation was prevented by prior inhibition or genetic ablation of AMPK (Z. Chen et al. 2009). Furthermore, the aorta of *PRKAA2*<sup>-/-</sup> mice showed attenuated atorvastatin-induced eNOS phosphorylation (Z. Chen et al. 2009).

### 1.2.7.6 Ischemic preconditioning

Sukhodub and colleagues report that AMPK activation is crucial for ischemic preconditioning, as the cardio-protective effect of preconditioning is lost in dominant-negative *PRKAA2* transgenic mice (Sukhodub et al. 2007). AMPK  $\alpha 2$  appears to be essential for preconditioning-stimulated recruitment of the  $K_{ATP}$  channel to the sarcolemmal membrane, decreasing the sarcolemmal action potential, and preventing  $Ca^{2+}$  overload and cell death (Sukhodub et al. 2007).

### 1.2.7.7 Autophagy

Under conditions of glucose deprivation, AMPK promotes autophagy to ensure cell viability, and is reported to achieve this by stimulating the activity of the mammalian autophagy initiating kinase 1 (Ulk1) (Kim et al. 2011). When glucose is abundant, mTORC1 is reported to phosphorylate Ulk1 on Ser757 preventing its association with AMPK. However, when glucose supplies are diminished, AMPK is activated which inhibits mTORC1 activity via the phosphorylation of TSC2 and Raptor. Ulk1 Ser757 phosphorylation is no longer sustained, and the de-phosphorylation of Ser757 permits the interaction of AMPK with Ulk1. AMPK subsequently phosphorylates Ulk1 at Ser317 and Ser777, thus initiating autophagy (Kim et al. 2011).

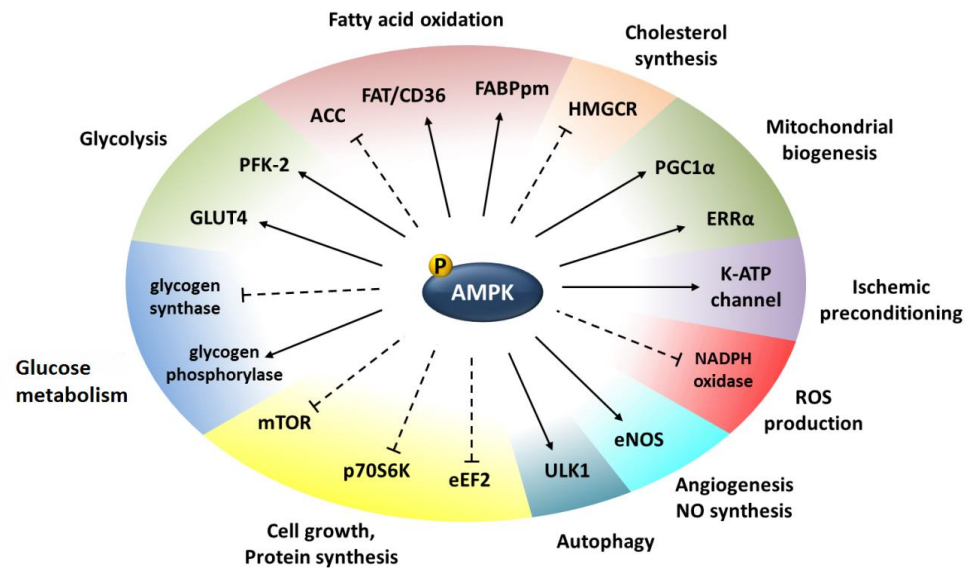


**Figure 1-3: Effects of AMPK activation**

AMPK targets and regulates a diverse range of proteins and processes, including fatty acid and glucose metabolism, cholesterol biosynthesis, the generation of ROS and vasoactive mediators, and regulating cell growth and protein synthesis. Targets which are positively regulated by AMPK are indicated by arrows, and those negatively regulated are indicated by a dashed/blunt ended line and the processes which they regulate are indicated around the periphery. ACC - acetyl-CoA carboxylase; eEF2 - eukaryotic elongation factor-2; eNOS - endothelial NO synthase; ERR $\alpha$  - oestrogen-related receptor  $\alpha$ ; FABPpm - fatty acid binding protein; FAT/CD36 - fatty acid transporter; GLUT4 - glucose transporter 4; HMGCR - 3-hydroxy 3-methylglutaryl CoA reductase; mTOR - mammalian target of rapamycin; PGC-1 $\alpha$  -transcriptional coactivator peroxisome proliferator-activated receptor- $\gamma$  coactivator 1 $\alpha$ ; PFK2 - phosphofructokinase-2; ULK-1 - Unc-51-like kinase; ROS - reactive oxygen species; NADPH - nicotinamide adenine dinucleotide phosphate. (Redrawn with modifications from Harada et al. 2012).

## 1.2.8 Pharmacological activation of AMPK

A number of compounds are used experimentally to activate AMPK including plant derived compounds and drugs currently used in the treatment of type 2 diabetes (Figure 1-4).

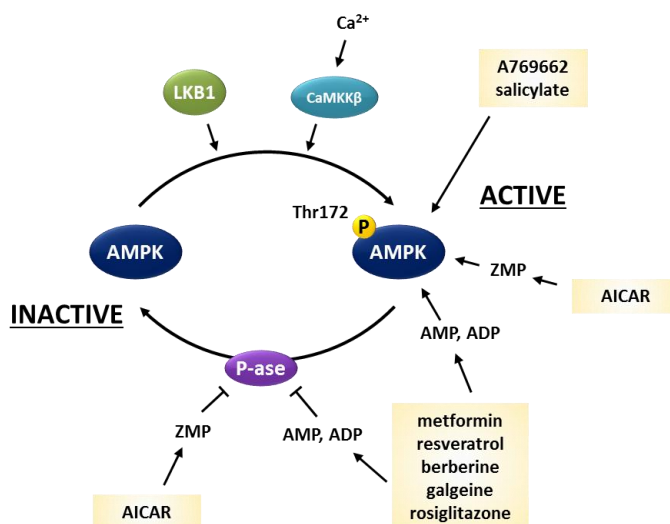


**Figure 1-4: Pharmacological activation of AMPK**

AMPK is activated by phosphorylation of Thr172 within the catalytic  $\alpha$  subunit catalysed by LKB1 or CaMKK $\beta$ , or allosterically by sensing changes in cellular energy. Elevated levels of AMP or ADP (relative to ATP) bind to the  $\gamma$  subunit inhibiting the activity of AMPK phosphatases (P-ase). The antidiabetic drugs metformin and rosiglitazone, and the plant derived compounds resveratrol, berberine and galgeine activate AMPK by increasing the ratio of AMP or ADP to ATP. The adenosine analogue AICAR is phosphorylated to ZMP mimicking the effect of AMP without altering adenine nucleotide ratios. Furthermore, A769662 and salicylate activate AMPK via binding directly to the  $\beta$ 1 subunit. Increases in intracellular calcium stimulate CaMKK $\beta$ -mediated AMPK activation, independently of adenine nucleotide levels. (Redrawn from Bijland et al. 2013).

### 1.2.8.1 Metformin

The biguanide drug metformin is now the first-line agent for the treatment of type 2 diabetes and was first reported to activate AMPK in hepatocytes (Zhou et al. 2001), although the extent to which AMPK activation contributes to its clinical effect remains disputed. The major action of metformin is the suppression of hepatic gluconeogenesis, however it is thought to activate AMPK via inhibition of NADH dehydrogenase (mitochondrial complex I) (El-Mir et al. 2000, Owen et al. 2000) thereby altering cellular nucleotide levels, although nucleotide-independent mechanisms have also been suggested (Hawley et al. 2002).

### 1.2.8.2 AICAR

AICAR is an adenosine analogue which is transported into cells via adenosine transporters and subsequently phosphorylated to the AMP mimetic ZMP (5-aminoimidazole-4-carboxamide-1- $\beta$ -D-furanosyl 5' monophosphate). In the laboratory setting, AICAR is widely used in studies of glucose and lipid metabolism, and insulin signalling. AICAR has been shown to stimulate adiponectin secretion and inhibit pro-inflammatory signalling (Lihn et al. 2004). AICAR is also reported to reverse various aspects of dysfunctional metabolism in animal models, but unfortunately has a short half-life, requires intravenous infusion and caused bradycardia and hypoglycaemia (Wong et al. 2009), making it a less than ideal therapeutic compound.

### 1.2.8.3 A769662 and salicylate

A769662 is a member of the thienopyridine family and directly activates AMPK (Sanders et al. 2007a). A769662 stimulates the allosteric activation of AMPK and inhibits its dephosphorylation, mimicking the effect of, but independent of AMP binding (Goransson et al. 2007). A769662-stimulated activation of AMPK is dependent upon interaction with the glycogen binding domain of the  $\beta$ 1 subunit, and residues in the  $\gamma$  subunit which are not involved in AMP binding. For reasons yet to be fully understood, A769662 activates only complexes containing the  $\beta$ 1 subunit and not  $\beta$ 2 (Scott et al. 2008). Treating *ob/ob* mice with A769662 is reported to reduce plasma glucose and weight gain, and significantly decrease plasma and liver triacylglycerol levels (Cool et al. 2006), indicating that targeting AMPK using small molecules is a feasible therapeutic strategy for metabolic disease.

Salicylate is a derivative of aspirin and salicylate administered orally, which at concentrations used therapeutically stimulates ACC phosphorylation and suppresses *de novo* lipogenesis, effects that were further enhanced by dual therapy with metformin (O'Brien et al. 2015). Salicylate directly activates AMPK by binding at the same site as A769662 on the  $\beta$ 1 subunit. Furthermore, salicylate stimulates hepatic ACC phosphorylation and fatty acid oxidation in *PRKAB1*<sup>WT</sup> mice, an effect that is lost in *PRKAB1*<sup>-/-</sup> mice, indicating that salicylate has AMPK-dependent effects *in vivo* (Hawley et al. 2012).

#### 1.2.8.4 Thiazolidinediones (troglitazone, rosiglitazone, pioglitazone)

Thiazolidinediones (TZDs) are insulin-sensitising agents and their mechanism of action is thought to be mainly mediated via peroxisome proliferator-activated receptor  $\gamma$  (PPAR $\gamma$ )-mediated gene transcription in adipocytes (Lehmann et al. 1995). TZDs stimulate adipogenesis, reduce plasma free fatty acids and mediate the release of adiponectin and other adipokines (Kubota et al. 2006). PPAR $\gamma$  and adipocyte-independent actions of TZDs have also been reported, including the rapid activation of AMPK by troglitazone in both isolated skeletal muscle and mammalian tissues *in vivo* (gastrocnemius and soleus muscles, liver, and epididymal fat) (LeBrasseur et al. 2006). In this particular study AMPK activation was found to correlate with changes in adenine nucleotide levels (increased AMP:ATP), glucose uptake and fatty acid oxidation in skeletal muscle (LeBrasseur et al. 2006).

#### 1.2.9 The vascular endothelium

The vascular endothelium acts as the interface between circulating blood and the underlying vessel wall. The endothelium comprises a single layer of flattened endothelial cells which line the entire vascular network, from largest arteries to the smallest capillaries. The vascular endothelium was previously thought of as a layer of inert cells, facilitating the selective passage of water and electrolytes. More recently however the distinct and unique functions of the vascular endothelium have become apparent. The vascular endothelium is now understood to act in both sensory and effector capacities, inhibiting thrombosis, facilitating the interaction of platelets and immune cells with the endothelium, regulating vascular tone and initiating angiogenesis.

Where the integrity of the endothelium is compromised, thrombin promotes fibrin formation and platelet aggregation. In the intact endothelium, thrombin interacts with thrombomodulin, subsequently activating protein C, which inhibits coagulation by stimulating the degradation of key clotting enzymes and neutralising fibrinolytic inhibitors (Popovic et al. 2011). A healthy vascular endothelium has the ability to balance pro-thrombotic and anti-thrombotic actions in accordance with local conditions for example, when haemostasis is required to restore vascular integrity after injury.

Vascular endothelial cells express a number of adhesion molecules, including integrins and adhesion molecules such as ICAM-1 and VCAM-1, which along with circulating soluble factors (cytokines) and components of the extracellular matrix, facilitate endothelial-

leukocyte interactions (Davies et al. 1993), *e.g.* fibrinogen mediates the interaction between endothelial ICAM-1 and Mac-1 which is expressed on the cell surface of leukocytes (Altieri et al. 1995).

Endothelial cells also produce a number of vasoactive factors: endothelium derived nitric oxide and prostacyclins induce vascular relaxation and inhibit platelet activation. Furthermore endothelial cells can produce vasoconstrictive factors *e.g.* endothelin, thromboxane A<sub>2</sub>, Angiotensin II and superoxide to regulate appropriate vascular tone (Cohen 1995).

Angiogenesis, the formation of new blood vessels from a pre-existing vascular network, requires the coordinated proliferation and migration of a number of cell types including endothelial cells, smooth muscle cells and pericytes. This process is exquisitely dependent upon signals being exchanged between these cells. Vascular endothelial growth factor (VEGF) provided the first example of a mitogen specific for the vascular endothelium (Leung et al. 1989). VEGF-A initiates angiogenesis whereas other endothelial factors for example angiopoietin and ephrin are required for subsequent remodelling and the maturation of the newly formed vessels. The vascular endothelium is therefore highly dynamic, acting as an anti-thrombotic surface facilitating the free passage of plasma and blood constituents, regulating the adhesion of inflammatory cells, regulating vascular tone and initiating angiogenesis, with the net effect of maintaining vascular homeostasis.

### **1.2.10 Endothelial dysfunction**

Endothelial dysfunction is an imbalance in the function of the vascular endothelium characterised by a shift towards enhanced vessel constriction, cell proliferation, thrombosis and chronic inflammation (Endemann and Schiffrin 2004). Vascular dysfunction is associated with numerous pathological states including metabolic syndrome, diabetes, heart failure, chronic kidney disease and hypertension. Endothelial dysfunction impairs the ability of the endothelium to regulate thrombosis, immune responses, fluid balance and vascular tone.

### 1.2.11 AMPK activation in the vascular endothelium

The diverse effects of AMPK activation in the vasculature (Figure 1-5), make it an attractive therapeutic target in the treatment of vascular disease, especially those related to dysfunctional metabolism (Motoshima et al. 2006, Kodiha and Stochaj 2011, García-Prieto et al. 2015).

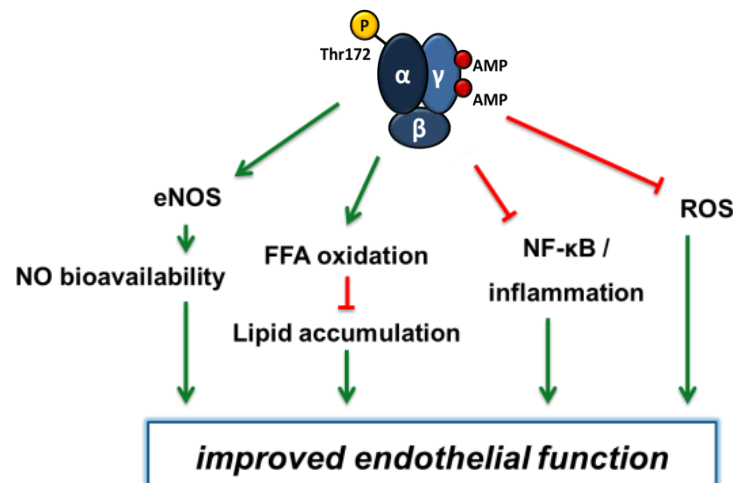


**Figure 1-5: The multiple effects of AMPK activation on the vascular endothelium**

AMPK activation acts via multiple mechanisms to improve endothelial function, stimulating eNOS activity and NO bioavailability, ameliorating lipotoxicity by inhibiting lipid accumulation and suppressing pro-inflammatory signalling and the generation of reactive oxygen species (ROS). (Adapted from Shirwany and Zou, 2010).

Highlighting the importance of LKB1 in the vasculature is a study reporting that endothelial specific knockout of LKB1 in mice (*STK11<sup>endo-/-</sup>*) results in significantly decreased eNOS activity, impaired endothelial function and acetylcholine-induced vessel relaxation (Zhang et al. 2014). Furthermore, the *STK11<sup>endo-/-</sup>* mice develop hypertension and ventricular hypertrophy. Administration of a constitutively active AMPK recombinant adenoviral vector however, alleviated endothelial dysfunction and lowered blood pressure in these animals (Zhang et al. 2014). In human endothelial cells, thrombin is reported to activate AMPK via increased intracellular  $\text{Ca}^{2+}$  and CaMKK $\beta$  activation, in the absence of detectable changes of AMP and crucially, independently of LKB1 inhibition (Stahmann et al. 2006).

Vascular endothelial cells express both isoforms of the AMPK  $\alpha$  subunit, but it is thought that  $\alpha 1$  expression is higher than  $\alpha 2$  (Schulz et al. 2005, Goirand et al. 2007, Zou et al. 2004). Less is known about vascular smooth muscle, however reports indicate that AMPK

$\alpha 1$  is the predominant catalytic isoform, with very little AMPK  $\alpha 2$  activity detected in smooth muscle of porcine carotid arteries (Rubin et al. 2005).

AMPK activators used clinically have been shown to ameliorate endothelial dysfunction. Metformin is reported to have cardio-protective effects independent of its anti-hyperglycaemic actions, including activating eNOS increasing NO bioactivity, and stimulating fatty acid oxidation (Calvert et al. 2008, Saeedi et al. 2008). Furthermore, rosiglitazone and pioglitazone are reported to have additional anti-atherosclerotic, anti-inflammatory and other beneficial effects on endothelial function (Wong et al. 2009).

#### **1.2.11.1 eNOS and NO bioavailability**

The endothelium regulates vascular tone via the synthesis and secretion of vasoactive substances with nitric oxide (NO), synthesised from L-arginine by endothelial NO synthase (eNOS) being one of the most important. eNOS expression is reduced via TNF $\alpha$ -stimulated inhibition of the eNOS promoter and by destabilising eNOS mRNA (Neumann et al. 2004, Kleinbongard et al. 2010). Furthermore, superoxide rapidly reacts with NO to produce peroxynitrite, and ROS contribute to eNOS uncoupling leading to increased superoxide generation and decreased NO production. AMPK activates eNOS by phosphorylating Ser1177 (Morrow et al. 2003) and Ser633 (Z. Chen et al. 2009), and by promoting its association with Hsp90 (Davis et al. 2006, Wang et al. 2009). A number of factors have been reported to stimulate eNOS activity in an AMPK-dependent manner including VEGF-A (Reihill et al. 2011), PPAR $\gamma$  agonists (Boyle et al. 2008), leptin (Procopio et al. 2009), adiponectin (Chen et al. 2003), and AICAR and metformin (Davis et al. 2006). Evidence has also emerged reporting that NO activates AMPK, via a CaMKK-dependent mechanism providing evidence for a positive feedback loop (Zhang et al. 2008).

#### **1.2.11.2 Lipid metabolism**

The statin class of HMGCR inhibitors exhibit cardio-protective effects beyond cholesterol reduction (Nissen et al. 2006), and furthermore are reported to activate AMPK (Sun et al. 2006). Excess fatty acids promote the *de novo* synthesis of diacylglycerol (DAG) which activates certain isoforms of protein kinase C (PKC). PKC activation stimulates NAPDH-oxidase, and pro-inflammatory intermediates, and reduces eNOS activity and insulin sensitivity, exacerbating endothelial dysfunction (Geraldès and King 2010). Another consequence of AMPK activation is reported to be increased endothelial cholesterol efflux via upregulated expression of the cholesterol efflux pump ATP-binding cassette G1

(ABCG1). AICAR treatment in hypercholesterolaemic mice inhibited atherosclerotic lesion progression which was associated with elevated ABCG1 expression (Li et al. 2010). AMPK activation is therefore able to regulate the energy demands of endothelial cells while protecting against endothelial lipotoxicity due to elevated levels of FAs.

### **1.2.11.3 Anti-inflammatory effects**

Chronic inflammation and the recruitment and infiltration of immune cells are early steps in the development of CVD. Cytokines such as TNF $\alpha$  and IL-1 $\beta$  increase nuclear-factor  $\kappa$ B (NF- $\kappa$ B)-mediated transcription of pro-inflammatory intermediates such as monocyte chemoattractant protein 1 (MCP-1) and interleukin 6 (IL-6) as well as adhesion molecules such as ICAM-1 and VCAM-1, thereby facilitating the recruitment and migration of inflammatory cells. In HUVECs, AMPK activation is reported to reduce inflammatory cell adhesion and migration (Ewart et al. 2008). Furthermore, berberine treatment inhibited the expression of the adhesion molecules ICAM-1 and VCAM-1 in HUVEC, suppressing monocyte (THP1) adhesion (Wang et al. 2009).

### **1.2.11.4 Inhibition of reactive oxygen species**

Redox balance is perturbed by increased oxidative stress and/or a reduction in anti-oxidant capacity; a major source of ROS in the vasculature is the NADPH oxidase system. Superoxide synthesised by NADPH oxidase is a major contributing factor to atherogenesis, removing bioavailable NO and by forming damaging species such as peroxynitrite. AMPK activation by rosiglitazone has been reported to reduce the generation of ROS stimulated by hyperglycaemia (Ceolotto et al. 2007). Mitochondrial-derived ROS however, generated in response to hypoxia, are reported to activate AMPK (Emerling et al. 2009), and stimulate the transcription of genes involved in antioxidant defences *e.g.* catalase, thioredoxin and manganese superoxide dismutase suggesting a positive role for sub-pathological levels of ROS in an ‘early warning system’. Furthermore, maintaining redox balance has knock on effects on NO availability and reduced adhesion molecule expression, ameliorating vascular inflammation.

## 1.3 Vascular Endothelial Growth Factor Signalling

Vascular endothelial growth factors are secreted mitogens which are highly specific for the vascular endothelium (Leung et al. 1989). The different VEGF isoforms signal to cells by selectively binding to three receptor tyrosine kinases (VEGF-Rs). VEGF-A is required for physiological angiogenesis being essential for normal development, while also having been implicated in a wide range of pathological states including atherogenesis, diabetic vasculopathies, neoangiogenesis and tumour metastasis, in addition to inflammatory diseases such as rheumatoid arthritis. Manipulation of VEGF signalling is therefore an attractive therapeutic strategy for pathologies involving aberrant angiogenesis.

### 1.3.1 VEGF

There are five isoforms of VEGF coded for by distinct genes in humans: VEGF-A, -B, -C, -D and placenta growth factor (PlGF), with splice variants and post-translational modifications adding further variation. Further VEGF-related proteins were later identified, encoded by viruses (VEGF-E) (Ogawa et al. 1998) or found in the venom of some snakes (VEGF-F) (Yamazaki et al. 2003).

#### 1.3.1.1 VEGF-A

The human gene for VEGF-A (hereafter referred to as VEGF) is organised into eight exons separated by seven introns, and is localised to chromosome *6p21.3* (Vincenti et al. 1996). Alternative splicing of the pre-mRNA transcript results in several distinct variants (Figure 1-6). VEGF<sub>165</sub> lacks the residues coded for by exon 6, but is the most biologically potent and abundant of the variants found in humans (Houck et al. 1991). VEGF-A<sub>165</sub> is also the isoform and variant used in the present study unless otherwise stated. The other VEGF splice variants are characterised by the presence or absence of exons 6 and 7, and the affinity and subsequent activity of specific VEGF splice variants is somewhat dependent upon the ability to bind to VEGF-receptor cofactors such as neuropilin and heparin sulphate proteoglycans (Cébe Suarez et al. 2006). VEGF is essential for vasculogenesis in the developing embryo, as demonstrated by the observation that the loss of a single allele in *VEGF-A*<sup>+/-</sup> mice is embryonically lethal at day E11-12 due to defective vascular development (Carmeliet et al. 1996, Ferrara et al. 1996).

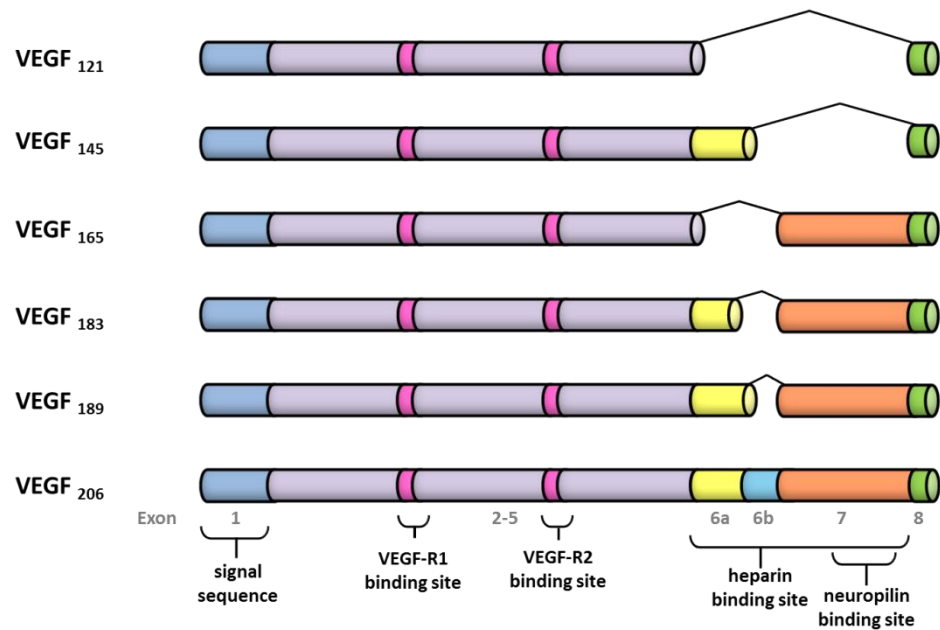


**Figure 1-6: Exon structure of VEGF-A mRNA splice variants in human.**

The VEGF-A gene comprises eight exons (1-8) and alternative mRNA splicing leads to the formation of multiple VEGF isoforms which vary in their amino acid number. VEGF<sub>165</sub> is the predominant variant found in humans. (Redrawn with modifications from Cross et al. 2003).

### 1.3.1.2 VEGF-B

VEGF-B is widely expressed but is particularly abundant in the heart, skeletal muscle and pancreas (Olofsson et al. 1996a). Human VEGF-B is found in two variants, VEGF-B<sub>167</sub> and VEGF-B<sub>186</sub>, which bind and activate VEGF-R1 (Olofsson et al. 1996b). Unlike *VEGF-A*<sup>+/-</sup> or <sup>-/-</sup> knock out mice, *VEGF-B*<sup>-/-</sup> mice are viable and fertile, and are reported to display only subtle cardiac phenotypes. *VEGF-B*<sup>-/-</sup> mice are reported to have smaller hearts, dysfunctional coronary vasculature and demonstrate impaired recovery after ischemic insult (Bellomo et al. 2000), suggesting a role for VEGF-B in vascular maintenance and the response to stress, rather than in development.

### 1.3.1.3 VEGF-C, -D and PlGF

VEGF-C primarily binds to and activates VEGF receptor 3 but can also activate VEGF-receptor 2 as a secondary target (Leppänen et al. 2010). While the primary function of VEGF-C is promoting the survival, growth and migration of lymphatic endothelial cells during development and lymphangiogenesis, VEGF-C is also a mitogenic stimulus for cultured vascular endothelial cells (Tammela et al. 2008). VEGF-C is synthesised in a ‘pro-protein’ form and is required to undergo sequential proteolytic processing at the C- and N-termini, catalysed by pro-protein convertases and ADAMTS3/plasmin respectively

to generate the mature, active form of VEGF-C (Siegfried et al. 2003, McColl et al. 2003, Jeltsch et al. 2014). The affinity of VEGF-C for VEGF receptor 3 increases with sequential cleavage, but only the fully cleaved/mature protein demonstrates significant affinity for its secondary receptor VEGF receptor 2 (Joukov et al. 1997). VEGF-D is structurally and functionally very similar to VEGF-C, and likewise requires complex proteolytic maturation, however far less is known about the function of VEGF-D. VEGF-D deficiency (*VEGF-D<sup>null</sup>* mice) does not affect embryonic or post-natal lymphangiogenesis, but VEGF-D contributes to peritumoral lymphangiogenesis and lymph node metastasis, suggesting that VEGF-D may contribute to lymphatic metastasis but is dispensable for normal lymphatic development (Baldwin et al. 2005, Koch et al. 2009).

PlGF is expressed in the early embryonic trophoblast and placenta during all stages of gestation (Clark et al. 1998) and has vasodilatory effects in human and rat resistance arteries (Osol et al. 2008). Alternative mRNA splicing generates multiple variants: PlGF<sub>131</sub>, -152, -204 and -224, and both serum and placental levels of PlGF are reported to be reduced in early and late-onset preeclampsia while levels of the soluble form of VEGF receptor 1 (sVEGF-R1) are reported to be elevated (Maynard et al. 2003). PlGF levels are therefore considered a useful biomarker for identifying patients at high risk of developing placental dysfunction and pre-eclampsia (Chappell et al. 2013).

### **1.3.2 Regulation of VEGF production**

Hypoxia and a number of cytokines and growth factors stimulate VEGF expression. Hypoxia-induced VEGF expression is mediated largely via a hypoxia response element (HRE) acting as a transcription enhancer upstream of the VEGF gene (Levy et al. 1995, Liu et al. 1995). The HRE contains a binding motif for the hypoxia inducible factor (HIF-1) which under normoxic conditions is highly O<sub>2</sub>-labile, therefore only under hypoxic conditions does HIF-1 accumulate sufficiently to influence gene transcription. The product of the von Hippel-Lindau (vHL) tumour suppressor gene is reported to negatively regulate HIF-1 activity as part of a ubiquitin-ligase complex which targets HIF-1 for degradation by the proteasome; oxygen promotes the hydroxylation of HIF-1, a requirement for association with vHL (Maxwell et al. 1999). Hypoxia also enhances the DNA binding ability of HIF-1, and increases the half-life of VEGF mRNA via association with the RNA binding protein HuR. Together these have the combined effect of stabilising HIF-1 and increasing transcription of the VEGF gene. Furthermore adenosine released by hypoxic

cells upregulates VEGF expression via binding to the adenosine A<sub>2</sub> receptor and activating the PKA pathway (Takagi et al. 1996).

Many cytokines and growth factors upregulate VEGF mRNA expression or induce its release including the epidermal (EGF) (Goldman et al. 1993), transforming (TGF- $\beta$ ) (Brogi et al. 1994, Pertovaara et al. 1994), fibroblast (FGF) (Seghezzi et al. 1998), insulin-like-1 (IGF-1) (Goad et al. 1996) and platelet-derived (PDGF) (Brogi et al. 1994) growth factors. Inflammatory cytokines such as TGF- $\beta$  and IL-1 upregulate VEGF expression in a number of cell types, including synovial fibroblasts (Berse et al. 1999), consistent with the hypothesis that VEGF is a mediator of inflammatory disorders, whereas the anti-inflammatory cytokine IL-10, and IL-13 are reported to inhibit VEGF release (Matsumoto et al. 1997).

### **1.3.2.1 Regulation of VEGF production by AMPK**

Whilst we and others have reported that VEGF activates AMPK (Reihill et al. 2007, Stahmann et al. 2010), there are now numerous reports suggesting that AMPK positively regulates VEGF synthesis. Lee and co-workers report that in a range of human cancer cell lines (DU145 prostate cancer, HeLa cervical carcinoma, HepG2 hepatocellular carcinoma and MCF7 breast adenocarcinoma), AMPK activity is required for hypoxia induced HIF-1 transcriptional activity and therefore expression of hypoxia responsive genes, including VEGF (Lee et al. 2003). The same group later reported that glucose deprivation increases VEGF mRNA stability via AMPK in DU145 cells (Yun et al. 2005), and furthermore that the carcinogenic metals cobalt, vanadate and arsenite activate AMPK, stimulating VEGF expression, but via HIF-1 dependent and independent mechanisms depending upon the carcinogenic metal the DU145 cells were exposed to (Lee et al. 2006). Mizrachy-Schwartz also report that in primary keratinocytes transformed with the human papillomavirus (HPV), AMPK inhibition reduced the levels of c-Myc, HIF-1 $\alpha$ , and VEGF in transformed cells cultured to 'late-passages' and in cells exposed to benzo[a]pyrene (a carcinogen that is present in cigarette smoke) (Mizrachy-Schwartz et al. 2007).

This effect is however not limited to cell models of cancer; Ouchi and colleagues demonstrated that in both cultured C2C12 myotubes and a mouse model of hind-limb ischemia AICAR stimulates increased VEGF expression via AMPK and p38 MAPK, by increasing the stability of VEGF mRNA (Ouchi et al. 2005). Furthermore, in osteoblast-like MC3T3-E1 cells, Kato and colleagues report that AMPK positively regulates FGF-2-

stimulated VEGF secretion via ERK1/2 and/or SAPK/JNK (Kato et al. 2010). Mizutani and co-workers further report that AMPK positively regulates TGF- $\beta$ -stimulated VEGF synthesis via MEK1/2 and ERK1/2 in the same osteoblast-like MC3T3-E1 cell line, as well as normal human osteoblasts (NHOst) (Mizutani et al. 2012). Finally, Ahluwalia and co-workers report that in myocardial microvascular endothelial cells, AICAR stimulates VEGF production and angiogenesis via AMPK, and identified MAPK/ERK1/2 as a likely mechanism for mediating this (Ahluwalia and Tarnawski 2011). Together, these studies suggest that AMPK also regulates VEGF expression levels, suggesting that a positive feedback mechanism could theoretically exist, whereby AMPK stimulates VEGF production and VEGF activates AMPK.

### **1.3.3 VEGF receptors**

The different isoforms of VEGF transmit signals into cells via selectively binding to one of three receptors (VEGF-Rs) (Figure 1-7). The VEGF-Rs consist of an extracellular ligand binding domain organised into seven immunoglobulin-like loops, a single trans-membrane domain, a tyrosine kinase domain interrupted by a 70 amino-acid insert, and a C-terminal tail. Binding of VEGF to its receptor induces receptor dimerization, accompanied by activation of receptor kinase activity leading to receptor auto-phosphorylation. Receptor phosphorylation recruits interacting proteins which activate a variety of signalling pathways regulating cell proliferation, migration and survival (Stuttfield and Ballmer-Hofer 2009).

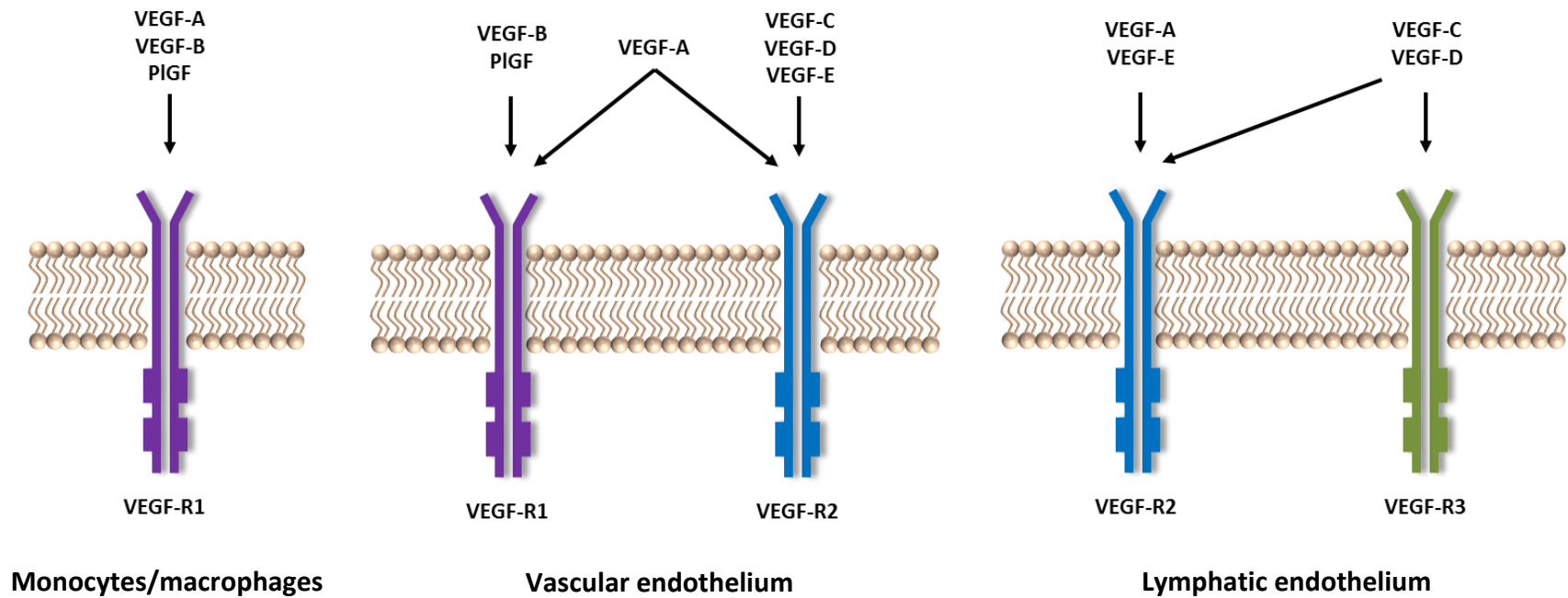


**Figure 1-7: Interactions between the VEGF family members and their receptors**

The VEGF ligand family includes VEGF -A, -B, -C, -D, -E and placenta growth factor (PlGF), which bind in a specific manner to the three VEGF receptors VEGF-R1, -2 and -3. VEGF-A and -B, in addition to PlGF bind to VEGF-R1, whereas VEGF-A, -C, -D and -E are ligands for VEGF-R2. VEGF-R3, whose expression is limited to the lymphatic system, is a receptor for VEGFs -C and -D (Matsumoto and Mugishima 2006).

### 1.3.3.1 VEGF-R1

VEGF-R1 (Flt1) is activated in response to VEGF-A, VEGF-B and PlGF binding. VEGF-R1 is widely expressed in endothelial cells in both the embryo during development and postnatally. Furthermore, VEGF-R1 expression is found in a range of non-endothelial cells including monocytes and macrophages, vascular smooth muscle cells and tumour cells (Barleon et al. 1996, Ishida et al. 2001, Fan et al. 2005). VEGF-R1 expression is regulated by hypoxia via a hypoxia-inducible enhancer element within the *FLT1* promoter. Alternative splicing of *FLT1* results in a soluble version of the receptor (sVEGF-R1) consisting of the six N-terminal extracellular Ig-like loops.

VEGF-R1 binds VEGF-A with a higher affinity than VEGF-R2 ( $K_d = 16$  pM vs 760 pM) however VEGF-R1 tyrosine-kinase activity is only weakly stimulated by ligand binding (Waltenberger et al. 1994). It has been argued that VEGF-R1 negatively regulates VEGF signalling via VEGF-R2: VEGF-R1 (or indeed sVEGF-R1) is proposed to sequester VEGF preventing its interaction with VEGF-R2, or form VEGF-R1/R2 heterodimers resulting in assembly of less active signalling complexes (Cudmore et al. 2012). Supporting this role in negative regulation was the finding that *FLT1*<sup>-/-</sup> mice die between E8.5 and E9 due to endothelial cell overgrowth and disorganisation of the vascular network (Fong et al. 1995) whereas mice expressing tyrosine kinase activity-deficient VEGF-R1 are viable (Hiratsuka et al. 1998), although display impaired immune responses. The presence of the receptor and not its activity is therefore essential for normal development.

### 1.3.3.2 VEGF-R3

VEGF-R3 (Flt4) is synthesised as a precursor protein prior to maturation by proteolytic cleavage. VEGF-R3 exists as two alternative splice variants in humans, long and short variants (Pajusola et al. 1993), with the long variant the predominant isoform. VEGF-R3 expression in mice is initiated at day E8.5 and is a critical regulator of both the developing vasculature and lymphatic system. *FLT4* knockout in mice is lethal at day E10.5, due to cardiovascular failure and impaired organisation of the vasculature preceding the development of the lymphatic system (Dumont et al. 1998). A naturally-occurring A to G substitution mutation, corresponding to a histidine to arginine (H1035R) substitution in the catalytic loop of VEGF-R3 results in a loss of VEGF-R3 auto-phosphorylation and tyrosine kinase activity (Irrthum et al. 2000). The resulting reduction in VEGF-R3 activity is associated with congenital lymphoedema, highlighting the importance of VEGF-R3 in maintaining lymphendothelial function in adults.

### 1.3.3.3 VEGF-R2

VEGF-R2 (KDR) expression is predominant in vascular endothelial cells and their embryonic precursors, with the highest levels of expression observed during vasculogenesis and angiogenesis (Matsumoto and Claesson-Welsh 2001). The receptor was also found to be expressed in a range of non-endothelial cells, including pancreatic duct cells, retinal progenitor cells, megakaryocytes and haemopoietic stem cells (Kato et al. 1995). VEGF-R2 expression is upregulated during physiological processes such as the female reproductive cycle, and pathological processes including tumour neovascularisation (McMahon 2000). *KDR*<sup>-/-</sup> mice die at E8.5 from impaired vascular development, a phenotype similar to that of *VEGF-A*<sup>-/-</sup> mice. Furthermore, mice with a *KDR*<sup>Y1173F</sup> knock-in mutation die between E8.5 and E8.9 (Shalaby et al. 1995, Sakurai et al. 2005) highlighting the importance of VEGF-R2 tyrosine kinase activity in embryogenesis.

Although both VEGF-R1 and -R2 are expressed in the vascular endothelium, the angiogenic effects of VEGF are thought to be mainly mediated via VEGF-R2 (Matsumoto and Mugishima 2006). Several tyrosine residues on VEGF-R2 have been identified as being key in mediating VEGFs angiogenic effects, specifically Tyr951 in the insert domain, Tyr1054 and Tyr1059 in the kinase domain and Tyr1175 and Tyr1214 in the C-terminal domain (Cross et al. 2003). A summary of the signalling cascades downstream of VEGF-R2 is presented in Figure 1-8.

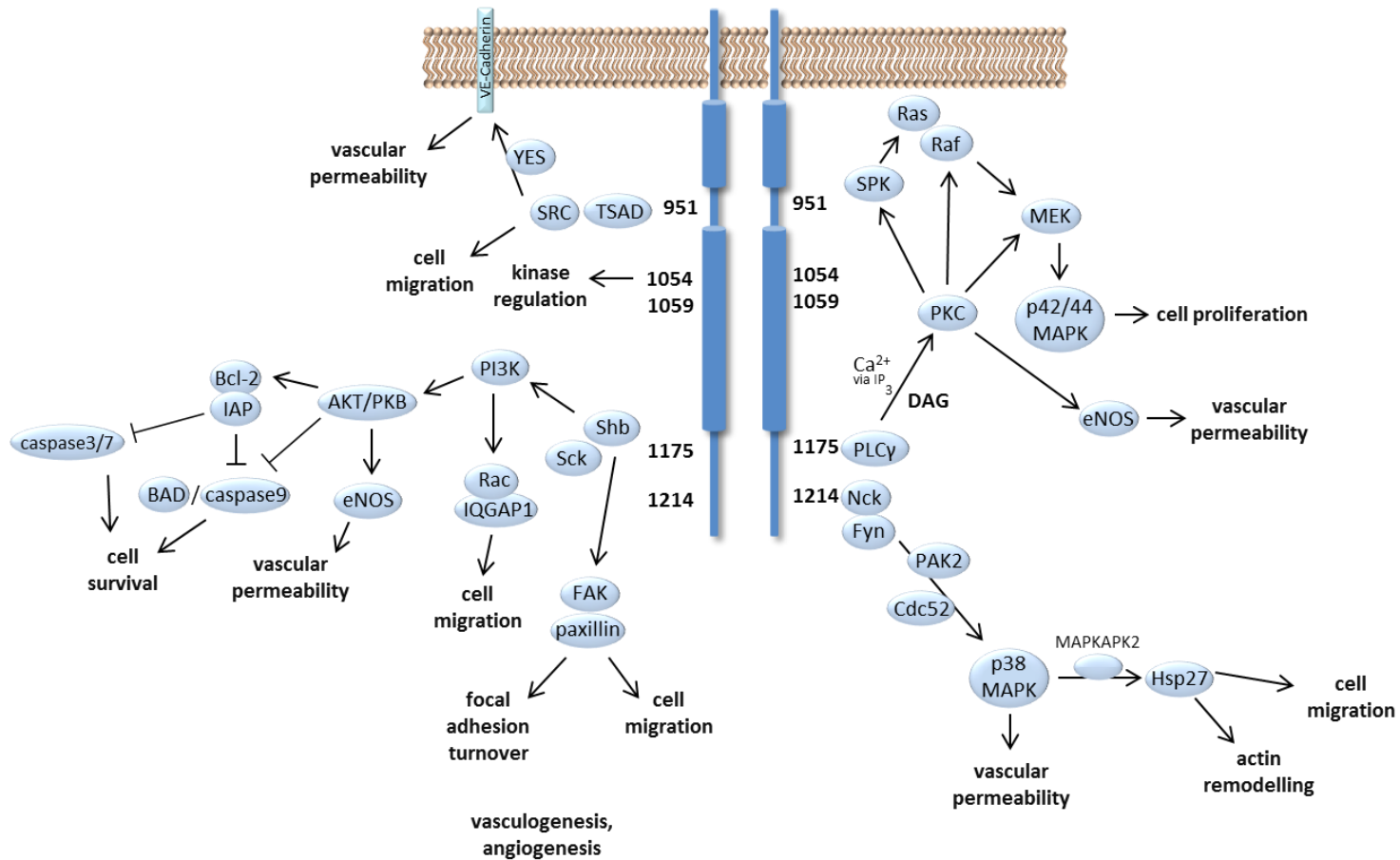


**Figure 1-8: VEGF-R2 signalling mediates cell proliferation, migration and survival via numerous signalling effectors**

Binding of VEGF to its receptor stimulates the receptor tyrosine kinase activity stimulating multiple signalling pathways. (Adapted from Olsson et al. 2006, and Koch et al. 2011).

Phosphorylated Tyr951 acts as a binding site for the adaptor protein TSAD (T-cell specific adaptor molecule) and activation of the tyrosine kinase Src mediating vascular permeability via further interaction with VE-cadherin (Matsumoto et al. 2005). Tyr1054 and Tyr1059 are critical for the receptor's kinase activity, acting as positive regulators by promoting the auto-phosphorylation of other Tyr residues including Tyr1175 (Dougher and Terman 1999). Phosphorylation of Tyr1175 provides a binding site for PLC $\gamma$ , inducing Ca<sup>2+</sup> release from intracellular stores (via IP<sub>3</sub> production) and diacylglycerol (DAG) synthesis. These in turn can activate PKC, which further induces activation of the Raf-MEK-ERK pathway promoting cell proliferation (Takahashi et al. 2001). DAG may also act on non-selective cation channels in the plasma membrane such as the transient receptor potential (TRP) family C (specifically TRPCs 3, 6 and 7), and it has previously been reported that functional TRPC6 is required for VEGF-stimulated angiogenesis (Hamdollah Zadeh et al. 2008). Tyr1175 also acts as a binding site for the adaptor protein Shb which further mediates PI3K (phosphoinositide 3-kinase) signalling. PI3K activates Akt/PKB which phosphorylates and therefore inhibits the pro-apoptotic proteins BAD and caspase 9, promoting cell survival (Gerber et al. 1998). Akt/PKB also activates eNOS, stimulating NO production (Fulton et al. 1999). Further to this, PI3K-mediated activation of Rac has also been implicated in vascular permeability and cell motility. Following the recruitment of Nck and Fyn to phospho-Tyr1214, p21-activated protein kinase-2 (PAK2) is activated and subsequently Cdc42 and p38 MAPK, mediating vascular permeability (Lamallice et al. 2004). Further downstream of phospho-Tyr1214, Hsp27 has been implicated in actin remodelling and cell migration in a MAPKAPK2 (mitogen-activated protein kinase-activated protein kinase 2)-dependent manner (Olsson et al. 2006, Koch et al. 2011).

#### **1.3.3.3.1 *Akt***

Akt is a serine/threonine kinase with a key role in multiple cellular processes including cell survival, proliferation and glucose metabolism. The two isoforms of Akt, Akt 1 and 2 are implicated in inhibiting apoptosis and stimulating cell proliferation with the net effect of enhancing cell survival, and in the insulin receptor-signalling pathway respectively. The role of Akt3 is however less clear (Martini et al. 2014). Akt is activated by PI3K-mediated PIP<sub>2</sub> phosphorylation (to generate PIP<sub>3</sub>), in response to receptor (G-protein or RTK) activation. Akt can then be activated via phosphorylation by PDK1 (phosphoinositide-dependent kinase-1) at Thr308, and mTORC2 (mTOR complex 2) at Ser473, however PI3K-independent mechanisms have also been reported (Martini et al. 2014). The de-phosphorylation of Akt Thr308 by PP2A and Ser473 by PHLPP1/2 antagonise Akt

activation, as does the activity of PTEN (phosphatase and tensin homolog) which catalyses the de-phosphorylation of PIP<sub>3</sub>, essentially the reverse reaction catalysed by PI3K (Song et al. 2012). Akt inhibits pro-apoptotic caspase and BAD proteins, and stimulates the transcription of pro-survival genes via NF-κB (Manning and Cantley 2007). Furthermore, Akt activation is reported to overcome cell cycle arrest, such that changes in Akt activity are one of the most frequently reported alterations in human cancer (Martini et al. 2014).

#### **1.3.3.3.2 *ERK1/2***

ERK1 and ERK2 are highly homologous protein kinases (83 % amino acid identity) sharing many if not all functions, and are widely expressed in most mammalian tissues. ERK1/2 is activated in response to growth factors *e.g.* VEGF and PDGF, insulin, and also by ligands for GPCRs (Raman et al. 2007). Furthermore, ERK1/2 can be activated by shear stress, osmotic stress and disorganisation of the microtubule network (Chen et al. 2001). As with other mitogen activated protein kinase (MAPK) cascades, the ERK1/2 signalling cascade consists of three tiers, the MAPK-kinase kinases A-Raf, B-Raf and Raf-1, the MAPK kinases MEK1 and MEK2, and the MAPKs ERK1 and ERK2. ERK1/2 is activated by dual threonine-tyrosine phosphorylation (Thr202/Tyr204 and Thr185/Tyr187 of ERK1 and 2 respectively) and their activity can be negatively regulated further by dual-specificity phosphatases *e.g.* MPK3 and 4, and PAC1 (phosphatase of activated cells 1) (Ward et al. 1994, Dickinson and Keyse 2006). Activated ERK1/2 regulates growth factor responsive targets in the cytosol, such as the mitogen- and stress-activated protein kinases (MSKs) which phosphorylate and activate AP-1 (activator protein 1). ERK1/2 can also be translocated to the nucleus where it phosphorylates a number of transcription factors and accessory proteins *e.g.* Elk1, Sap1/2 and c-Myc (Mebratu and Tesfaigzi 2009). ERK1/2 therefore participates in a large variety of processes including cell adhesion, cell cycle progression, cell migration, cell survival, differentiation, metabolism, proliferation and transcription. Aberrant signalling of the Ras-Raf-MEK1/2-ERK1/2 cascade is observed in a high proportion of cancers, such that inhibitors of Raf and MEK1/2 have been investigated as potential therapeutic agents for human cancers (Friday and Adjei 2008).

#### **1.3.3.3.3 *Protein kinase C (PKC)***

The PKC family of protein kinases play important roles in several signal transduction cascades, including VEGF. Fifteen isozymes have been identified in humans, and they can be classified according to their domain structure and second messenger requirements (Figure 1-9) (Parker and Murray-Rust 2004). The classical or conventional PKCs ( $\alpha$ ,  $\beta$ 1/2

and  $\gamma$ ) require  $\text{Ca}^{2+}$ , DAG and phospholipid for activation, whereas the novel PKCs ( $\delta$ ,  $\epsilon$ ,  $\eta$  and  $\theta$ ) require DAG but not  $\text{Ca}^{2+}$ . As such both the classical and novel PKC isoforms can be activated by phospholipase-C signal transduction cascades. On the other hand, given the absence of  $\text{Ca}^{2+}$  and DAG/phorbol ester binding domains, atypical PKCs ( $\zeta$  and  $\iota/\lambda$ ) require neither  $\text{Ca}^{2+}$  nor DAG for activation (Soetikno et al. 2012). Elevated levels of DAG and PKC activity are reported in various vascular tissues in models of over-nutrition/diabetes including retina (Shiba et al. 1993), aorta and heart (Inoguchi et al. 1992), renal glomeruli (Craven and DeRubertis 1989), and liver and skeletal muscle (Itani et al. 2000). Furthermore, several studies have reported that PKC inhibition using the compound LY333531 is efficacious in treating abnormalities in the retinal and renal vasculature in both animal models of diabetes and human patients (Adis 2007) making PKC inhibition an attractive therapeutic strategy.

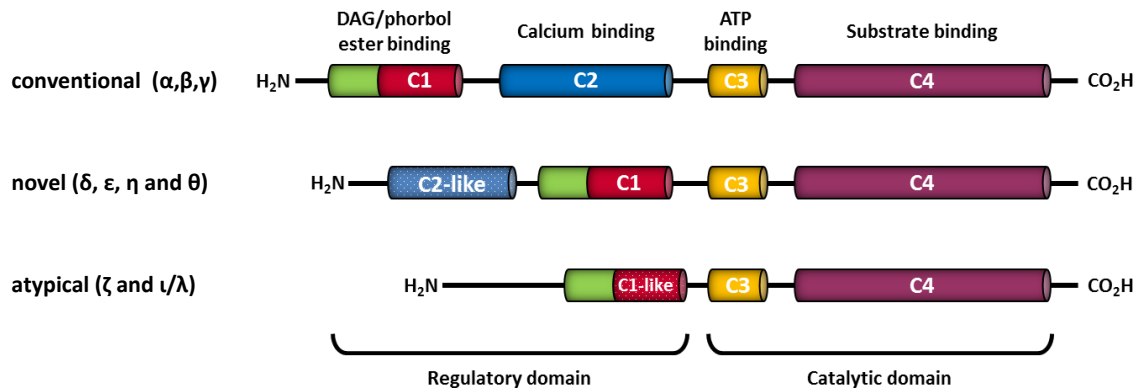


**Figure 1-9: PKC domain structure**

The domain structures of classical, novel, and atypical protein kinase Cs (PKC). All PKCs have a pseudo-substrate domain (green) in addition to which, the conventional and novel PKCs contain a C1 domain which facilitates binding to diacylglycerol (DAG) and phorbol 12-myristate 13-acetate (PMA). The C2 domain confers  $\text{Ca}^{2+}$  sensitivity to the conventional subfamily of PKCs but not to the novel. The atypical PKCs are not activated by  $\text{Ca}^{2+}$  or DAG, but their activation depends on phosphatidylserine and *cis*-unsaturated fatty acids. (Redrawn from Soetikno et al. 2012).

Protein kinase D-1 (PKD1 in mice, PKC  $\mu$  in humans), is related to the atypical family of PKC proteins (Valverde et al. 1994, Johannes et al. 1994) with two further proteins PKD2 and PKD3 subsequently identified as sharing significant homology with PKD1. PKD1 is activated by a diverse range of stimuli including hormones, chemokines, GPCR agonists, bioactive lipids and growth factors, and is reported to regulate a diverse range of biological responses including cell proliferation and differentiation, membrane trafficking, immune regulation, angiogenesis and cancer (Rozengurt 2011). PKD1 is reported to be activated in response to growth factors in a PKC-dependent manner, as PKC inhibition in 3T3 cells and MEFs prevented serum-induced PKD activation (Zugaza et al. 1996).

PKD1 activation is dependent upon PKC-dependent trans-phosphorylation of Ser744 and Ser748 in the kinase domain activation loop (Iglesias et al. 1998) and once activated, PKD1 subsequently undergo auto-phosphorylation at Ser916, within its C-terminal domain (Matthews et al. 1999), the measurement of which is used as a surrogate marker of PKD1 activity. PKD1 shares significant catalytic domain homology with myosin light chain kinase and the CAMKs, such that the three isoforms of PKD1 are classified as belonging to the CAMK family of protein kinases, and distinct from the 'AGC' kinases (PKA, PKG and PKC) (Hanks 2003).

### 1.3.4 VEGF activates AMPK

Previous reports from our laboratory indicated that physiologically relevant concentrations of VEGF (10 ng/mL) activated AMPK in HAEC (Reihill et al. 2007). AMPK was also shown to contribute to VEGF-stimulated eNOS Ser1177 phosphorylation and NO production via a PI3K/Akt-independent, PLC/CaMKK/AMPK-dependent signalling axis (Reihill et al. 2007). AMPK was later shown to be required for VEGF-stimulated HAEC proliferation and migration, whereas AMPK activation by other compounds (AICAR, A769662) or expression of constitutively active AMPK (Ad.AMPK-CA) in the absence of VEGF inhibited HAEC proliferation (Reihill et al. 2011). Furthermore, VEGF-stimulated HAEC chemokinesis was inhibited by CaMKK inhibition or infection with Ad.AMPK-DN whereas enhanced chemokinesis was mimicked by infection with Ad.AMPK-CA, even in the absence of VEGF (Reihill et al. 2011). It remains possible that this is a mechanism by which endothelial cells actively seek nutrients under conditions of nutrient deprivation/AMPK activation. Furthermore, expression of kinase-inactive AMPK in HUVEC under hypoxic conditions is reported to inhibit VEGF-stimulated migration and tube formation (Nagata et al. 2003). Stahmann and colleagues also report that AMPK contributes to angiogenesis *in vitro* and *in vivo* (Stahmann et al. 2010). VEGF-stimulated tube formation was inhibited in microvascular lung endothelial cells from *PRKAA1*<sup>-/-</sup> mice compared to wild type mice, and similarly VEGF-stimulated sprout formation was inhibited by down-regulation of AMPK expression in HUVEC by siRNA (Stahmann et al. 2010). Furthermore in *PRKAA1*<sup>WT</sup> mice, VEGF stimulated a 4-fold increase in the vascularisation of Matrigel plugs, an effect that was not present in *PRKAA1*<sup>-/-</sup> mice (Stahmann et al. 2010), highlighting the requirement of AMPK in VEGF-stimulated angiogenic processes *in vivo*.

## 1.4 Overall hypothesis and experimental aims

Despite previous reports, the mechanism by which VEGF stimulates AMPK activation has not been fully characterised, nor have the effects of VEGF on subsequent AMPK signalling been determined. This thesis sought to test the hypothesis that AMPK activation underlies the physiological consequences of VEGF in human endothelial cells. Specifically, the following experimental research questions were addressed:

- To what extent does VEGF influence the activity of a particular catalytic isoform containing AMPK complex, and does VEGF effect the subcellular localisation of AMPK in order to facilitate the functional proliferative actions of VEGF? This was examined in cultured human endothelial cells stimulated with exogenous recombinant VEGF by immunoprecipitation kinase assays with specific subunit isoform-specific antibodies, confocal immunofluorescence microscopy and analysis of endothelial cell proliferation.
- Do transient receptor potential cation channels (TRPCs) mediate the VEGF-stimulated extracellular  $\text{Ca}^{2+}$  influx, and CaMKK activation which has previously been reported to be required for VEGF-stimulated AMPK activation (Reihill et al. 2007)? This was examined using pharmacological agents to down- or upregulate TRPC activity in VEGF-stimulated cultured endothelial cells.
- Does VEGF influence inhibitory phosphorylation of AMPK  $\alpha 1/2$  Ser485/491? This was examined using specific antibodies to phosphorylated AMPK in cultured endothelial cells stimulated with VEGF, and the mechanisms by which VEGF influenced Ser485/491 phosphorylation were assessed using pharmacological and genetic strategies, to up- and down-regulate the activity of VEGF-stimulated signalling pathway proteins.

## **Chapter 2 – Materials and Methods**

## **2.1 Materials**

### **2.1.1 General reagents**

#### **Abcam, Cambridge, UK**

A769662, BAPTA-AM

#### **Acros Organics**

Brij-35

#### **BDH Laboratory Supplies, Poole, UK**

Coomassie brilliant blue G-250, tetra-sodium pyrophosphate ( $\text{Na}_4\text{P}_2\text{O}_7$ )

#### **Beckman Coulter, Pasadena, CA, USA**

Ultra-Clear™ ultracentrifuge tubes

#### **Biafin Gmb & Co, Kassel, Germany**

Akt (human recombinant)

#### **Biotium, Hayward, CA, USA**

RedDot™2

#### **Cambridge Bioscience, Cambridge, UK**

E-Plate 96

#### **EMD Chemicals Inc. (Calbiochem) San Diego, CA, USA**

LY333531, OAG, PD184352, PMA

#### **Fisher Scientific UK Ltd, Loughborough, Leicestershire, UK**

APS (ammonium persulphate), Corning™ tissue culture T75/T150 flasks and 12/6 well plates, DMSO (dimethylsulphoxide), ethidium bromide, Tris base (Tris-(hydroxymethyl)-amonoethane)

#### **Formedium, Hustanton, Norfolk, UK**

Bacterial agar, tryptone, yeast extract powder

#### **GE Healthcare, Little Chalford, Buckinghamshire, UK**

Protein G Sepharose 4 Fast Flow

**Thermo Fisher Scientific (including Life Technologies, Applied Bio Systems, GIBCO, and Invitrogen), Carlsbad, CA, USA**

Blasticidin, dNTPs (dATP, dCTP, dGTP, dTTP), Dulbecco's modified Eagles media (DMEM), Eagle's Minimum Essential Medium (EMEM), foetal calf serum (FCS; EU origin), L-glutamine, Lipofectamine® 2000 Reagent, Medium 199, Minimum Essential Medium (MEM), MitroTracker® Mitochondrion-Selective Probes, newborn calf serum (NCS), Non-Essential Amino Acids Solution (100X), One Shot chemically competent *E.coli*, Opti-MEM® reduced serum media, Penicillin-Streptomycin (10,000 U/mL), S.O.C. medium, *Taq* DNA Polymerase, TaqMan® Gene Expression Assay (FAM labelled probes), TaqMan® Universal Master Mix II no UNG, trypsin-EDTA, sodium pyruvate, zeocin

**LI-COR BioSciences, Lincoln, NE, USA**

LI-COR Odyssey Blocking Buffer

**Melford Laboratories Ltd, Chelworth, Ipswich, Suffolk, UK**

DTT (dithiothreitol)

**Merck Millipore Chemicals Ltd, Nottingham, UK**

Compound C, TRPC3 Channel Inhibitor Pyr3, ML-9 hydrochloride, Akt inhibitor VIII (isozyme-selective Akti1/2)

**National Diagnostics (UK) Ltd, Hessle, East Riding of Yorkshire, UK**

Ecoscint A

**New England Biolabs, Ipswich, MA, USA**

Gel loading dye (6 X), Low molecular weight DNA marker (100 bp), Pre-stained protein marker (broad range 6-175 kDa)

**Pall Life Sciences Pensacola, FL, USA**

Nitrocellulose transfer membrane (0.45 µm pore size)

**Perkin Elmer, Beaconsfield, Buckinghamshire, UK**

[ $\gamma$ -<sup>32</sup>P] ATP

**Pierce, Perbio Science UK Ltd, Tettenhall, Cheshire, UK**

10,000 MWCO Slide-A-Lyzer

**Premier International Foods, Cheshire, UK**

Dried skimmed milk

**Promega Corporation, Madison, WI, USA**

CIAP (calf intestinal alkaline phosphatase), M-MLV Reverse Transcriptase, Oligo(dT), PKC (Protein Kinase C) from rat brain

**Roche Diagnostics Ltd, Burgess Hill, UK**

Agarose MP

**Severn Biotech Ltd, Kidderminster, Hereford, UK**

Acrylamide:bisacrylamide (37.5:1; 30 % (w/v) acrylamide)

**Seahorse Bioscience, North Billierica, MA, USA**

XF24 Cell Culture Microplates, XF24 Flux Pak, XF Assay Medium, XF Calibrant Solution

**Sigma-Aldrich Ltd, Gillingham, Dorset, UK**

AMP (adenosine monophosphate), ATP (adenosine triphosphate), BSA (bovine serum albumin) benzamidine, D-mannitol, EDTA, EGTA, hyperforin (dicyclohexylammonium) salt, kanamycin, paraformaldehyde, PMSF (phenylmethylsulphonyl fluoride), Ponceau S, porcine insulin, SBTI (soyabean trypsin inhibitor), TEMED, Triton X-100, Tween-20, VEGF (Vascular Endothelial Growth Factor - recombinant human), reverse transcription PCR primers, wortmannin

**Thermo Scientific, Waltham, MA, USA**

ImmunoMount™

**R&D Systems, Inc. (Tocris Bioscience), Minneapolis, MN, USA**

STO-609 acetate, *trans*-Ned 19, GF109203X, CRT0066101

**Toronto Research Chemicals Inc, Ontario, Canada**

AICAR

**VWR International Ltd., Lutterworth, Leicestershire, UK**

Falcon branded cell culture plastics (96/24/12/6 well plates and 10 cm diameter dishes), HEPES

**Pepceuticals Ltd, Leicester, UK**

SAMS peptide

**Qiagen, Venlo, Netherlands**

HiPerFect® Transfection Reagent, siRNA

## **2.1.2 Kits**

### **Cell Biolabs, San Diego, CA, USA**

QuickTiter™ Adenovirus Titer Immunoassay Kit

### **Promega Corporation, Madison, WI, USA**

CellTiter 96® Aqueous One Solution Cell Proliferation Assay, Wizard® *Plus SV* Minipreps DNA Purification System

### **Qiagen, Venlo, Netherlands**

RNeasy Mini Kit

### **Seahorse Bioscience, North Billierica, MA, USA**

XF Cell Mito Stress Test Kit

### **2.1.3 Specialist equipment**

#### **ACEA Biosciences, San Diego, CA, USA**

RTCA SP Station, Analyzer and Control Unit (RTCA xCELLigence system)

#### **Beckman Coulter™, Pasadena, CA, USA**

Optima™ XL-80K ultracentrifuge, SW40 rotor, multipurpose scintillation counter LS 6500, Allegra® X-12 centrifuge

#### **Bio-Rad Laboratories, Hemel Hempstead, UK**

Protein gel casting and Western blotting equipment (Mini-Protean III), Gel Doc imaging system, Mini-Sub Cell GT Gel System

#### **BMG Labtech, Ortenberg, Germany**

FLUORstar OPTIMA Microplate Reader

#### **Carl Zeiss Ltd., Cambridge, UK**

LSM Exciter laser scanning microscope

#### **LI-COR BioSciences, Lincoln, NE, USA**

LI-COR Odyssey® Sa Infrared Imaging System

#### **Seahorse Bioscience, North Billierica, MA, USA**

XF24 Extracellular Flux Analyzer

#### **Techne, Bibby Scientific Ltd, Staffordshire, UK**

Progene FPR0G050 thermocycler

#### **Thermo Scientific, Waltham, MA, USA**

Nanodrop spectrophotometer

#### **WPA, Cambridge UK**

S2000 spectrophotometer

## 2.1.4 Cells and specialist media

### ATCC, Manassas, Virginia, USA

3T3-L1 fibroblasts , HEK-293 and HeLa

### Promocell, Heidelberg, Germany

Human aortic endothelial cells, human umbilical vein endothelial cells, MV2 endothelial cell growth media (with supplement)

HeLa cells stably expressing LKB1 were kindly provided by Prof. D. Alessi (University of Dundee, UK) and have been described previously (Sapkota et al. 2002).

**Table 2-1: Cell lines used and their conditions of culture**

Cell type	Culture media and supplements	Additional information
3T3-L1 MEFs (mouse embryonic fibroblasts)	DMEM with 10 % (v/v) newborn calf serum, 100 U/mL penicillin and 100 µg/mL streptomycin	Maintained between passage 2 and 12, Cultured at 37 °C, 10 % (v/v) CO <sub>2</sub>
HAEC (human aortic endothelial cells)	MV2 with MV2 supplement mix	Primary cells from single donors, Maintained until passage 6, Cultured at 37 °C, 5 % (v/v) CO <sub>2</sub>
HEK-293 (human embryonic kidney)	DMEM with 10 % (v/v) foetal calf serum and 2 mM glutamine	Cultured at 37 °C, 5 % (v/v) CO <sub>2</sub>
HeLa	DMEM with 10 % (v/v) foetal calf serum and 2 mM glutamine	Cultured at 37 °C, 5 % (v/v) CO <sub>2</sub>
HeLa <sup>LKB1-KD/WT</sup>	EMEM with 10 % (v/v) foetal calf serum, 2 mM glutamine, 100 U/mL penicillin, 100 µg/mL streptomycin, 2 mM non-essential amino acids, 5 µg/mL blasticidin and 100 µg/mL zeocin	Cultured at 37 °C, 5 % (v/v) CO <sub>2</sub>
HUVEC (human umbilical vein endothelial cells)	MV2, with supplement mix	Primary endothelial cells pooled from 6 donors, Maintained until passage 6, Cultured at 37 °C, 5 % (v/v) CO <sub>2</sub>

## 2.1.5 Antisera

### 2.1.5.1 Antibodies for immunoblotting

Unless otherwise stated, all antibodies for immunoblotting were prepared in 50 % (v/v) LI-COR Odyssey Blocking Buffer, 50 % (v/v) PBS-T

**Table 2-2: Primary antibodies used for immunoblotting**

Epitope (Clone)	Host Species	Dilution	Source (Cat #)
Akt (pan)	Mouse	1:2000	Cell Signalling Technology (#2920)
AMPK $\alpha$ 1	Sheep	1 $\mu$ g/mL	A kind gift from Prof. D.G. Hardie, The University of Dundee, UK (Woods et al. 1996)
AMPK $\alpha$ 1	Mouse	1:1000	Abcam (ab110036)
AMPK $\alpha$ 2	Sheep	1 $\mu$ g/mL	A kind gift from Prof. D.G. Hardie, The University of Dundee, UK (Woods et al. 1996)
AMPK $\alpha$ 2	Rabbit	1:1000	Cell Signalling Technology (#2537)
c-Myc (9E10)	Mouse	1:500	Santa Cruz Biotechnology (sc-40)
GAPDH	Mouse	1:80,000	Ambion, Cambridgeshire, UK (#4300)
GFP	Rabbit	1:3000	Abcam (ab290)
JNK	Rabbit	1:1000	Cell Signalling Technology (#9252)
OXPHOS Antibody Cocktail	Rodent	1:250	Abcam (ab110413)
p38 MAPK	Rabbit	1:1000	Cell Signalling Technology (#9212)
p44/42 MAPK (Erk1/2)	Rabbit	1:1000	Cell Signalling Technology (#9102)
Phospho-Acetyl-CoA Carboxylase (Ser79)	Rabbit	1:1000	Cell Signalling Technology (#3661)
Phospho-Akt (Ser473)(193H12)	Rabbit	1:1000	Cell Signalling Technology (#4058)
Phospho-Akt (Thr308)	Rabbit	1:1000	Cell Signalling Technology (#9275)
Phospho-AMPK $\alpha$ (Thr172)(40H9)	Rabbit	1:1000	Cell Signalling Technology (#2535)
Phospho-AMPK $\alpha$ 1 (Ser485)(45F5)	Rabbit	1:1000	Cell Signalling Technology (#2537)

Phospho-AMPK $\alpha$ 1(Ser485) /AMPK $\alpha$ 2(Ser491)	Rabbit	1:1000	Cell Signalling Technology (#4185)
Phospho-JNK (Thr183/Tyr185)	Mouse	1:1000	Cell Signalling Technology (#9255)
Phospho-MARCKS (Ser152/156)	Rabbit	1:1000	Cell Signalling Technology (#2741)
Phospho-p38 MAPK (Thr180/Tyr182) (28B10)	Mouse	1:1000	Cell Signalling Technology (#9216)
Phospho-p44/42 MAPK (Erk1/2) (Thr202/Tyr204) E10	Mouse	1:2000	Cell Signalling Technology (#9106)
Phospho-PKD/PKC $\mu$ (Ser916)	Rabbit	1:1000	Cell Signalling Technology (#2051)
PKC (A-9)	Mouse	1:500	Santa Cruz Biotechnology Inc. (sc-17804)
PKC (H-300)	Rabbit	1:500	Santa Cruz Biotechnology Inc. (sc-10800)
PKC $\alpha$ (alpha)	Rabbit	1:1000	Cell Signalling Technology (#2056)
PKC $\beta$ I (beta 1)	Rabbit	1:500	Santa Cruz Biotechnology Inc. (sc-209)
PKC $\beta$ II (F7) (beta 2)	Mouse	1:500	Santa Cruz Biotechnology Inc. (sc-13149)
PKC $\delta$ (delta)	Rabbit	1:1000	Cell Signalling Technology (#9616)
PKC $\epsilon$ (epsilon)	Mouse	1:1000	BD Transduction Laboratories (#610085)
PKC $\zeta$ (zeta)	Rabbit	1:1000	Cell Signalling Technology (#9368)
PKC $\eta$ (eta)	Rabbit	1:500	Santa Cruz Biotechnology Inc. (sc-215)
PKC $\theta$ (theta)	Mouse	1:500	BD Transduction Laboratories (#610089)
PKC $\lambda$ (lambda)	Mouse	1:500	BD Transduction Laboratories (#610207)
PKD1/PKC $\mu$ (mu)	Rabbit	1:1000	Cell Signalling Technology (#2052)
TRPC3	Rabbit	1:1000	Abnova (PAB13224)
TRPC6	Goat	1:5000	Abnova (PAB18696)
TRPC7 (extracellular)	Rabbit	1:200	Alamone Labs (ACC-066)

**Table 2-3: Secondary detection agents used for immunoblotting**

Conjugate	Epitope	Host species	Dilution	Source
IRDye® 800CW	Goat IgG	Donkey	1:5000	LI-COR Biosciences, Lincoln, NE, USA (#92632214)
IRDye® 800CW	Mouse IgG	Donkey	1:5000	LI-COR Biosciences, Lincoln, NE, USA (#926-32210)
IRDye® 800CW	Rabbit IgG	Donkey	1:5000	LI-COR Biosciences, Lincoln, NE, USA (#926-32213)
IRDye® 680LT	Rabbit IgG	Donkey	1:5000	LI-COR Biosciences, Lincoln, NE, USA (#926-68023)
Alexa Fluor® 680	Sheep IgG	Donkey	1:5000	Life Technologies Ltd, Paisley, UK (#A21102)

### 2.1.5.2 Antibodies for immunofluorescence

**Table 2-4: Primary antibodies used for immunofluorescence**

Epitope (Clone)	Host species	Dilution	Source (Cat #)
AMPK $\alpha$ 1 (aa. 344-358)	Sheep	1 $\mu$ g/mL	A kind gift from Prof. D.G. Hardie, The University of Dundee, UK (Woods et al. 1996)
AMPK $\alpha$ 1 (aa. 357-524)	Mouse	1:750	Abcam (ab110036)
AMPK $\alpha$ 2 (aa. 352-366)	Sheep	1 $\mu$ g/mL	A kind gift from Prof. D.G. Hardie, The University of Dundee, UK (Woods et al. 1996)
AMPK $\alpha$ 2	Sheep	1:100	A kind gift from Prof. D.G. Hardie, The University of Dundee, UK
c-Myc (9E10)	Mouse	1:300	Santa Cruz Biotechnology (sc-40)
GM130	Mouse	1:200	BD Transduction Laboratories (#610823)
Hsp47	Mouse	1:200	A kind gift from Dr Tom Van Agtmael, The University of Glasgow
PDI	Rabbit	1:200	A kind gift from Prof. Neil Bullied, The University of Glasgow
tubulin [YL1/2]	Rat	1:100	Abcam (ab6160)

**Table 2-5: Secondary detection agents for immunofluorescence**

<b>Epitope</b>	<b>Host Species</b>	<b>Conjugate</b>	<b>Dilution</b>	<b>Source (Cat#)</b>
Mouse IgG (H+L)	Donkey	Alexa Fluor® 488	1:100	Invitrogen (A-21202)
Rabbit IgG (H+L)	Goat	Alexa Fluor® 488	1:100	Invitrogen (A-11008)
Rabbit IgG (H+L)	Donkey	Alexa Fluor® 488	1:100	Invitrogen (A-21206)
Rat IgG (H+L)	Donkey	Alexa Fluor® 488	1:400	Invitrogen (A-21208)
Sheep IgG (H+L)	Donkey	Alexa Fluor® 488	1:100	Invitrogen (A-11015)
Sheep IgG (H+L)	Donkey	Alexa Fluor® 568	1:100	Invitrogen (A-21099)

## 2.1.6 Plasmids

**Table 2-6: Plasmid DNA**

<b>Insert (species)</b>	<b>Vector (antibiotic resistance)</b>	<b>Source</b>
PKC $\alpha$ (bovine)	pB $\Delta$ G (kanamycin)	A kind gift from Prof. T.M. Palmer, The University of Bradford, UK (Palmer and Stiles 1999)
PKC $\beta$ 1 (human)		
PKC $\beta$ 2 (human)		

## 2.1.7 Reverse transcriptase PCR primers

**Table 2-7: Custom primers designed for reverse transcriptase-PCR**

Target	Direction	Sequence 5' to 3'	Primer length (bp)	Product length (bp)
TRPC1	FWD	TTCTGTGGATTATTGGGATGA	21	505
TRPC1	REV	CAGAACAAAGCAAAGCAGGTG	21	
TRPC3	FWD	ATGCTGCTTTTACCACTGTAG	21	372
TRPC3	REV	TCCTTCTGCATTTGGGAAA	19	
TRPC4	FWD	GGCGGACTTCAGGACTACAT	20	499
TRPC4	REV	GCTGTGCTTTGACATTGGTC	20	
TRPC5	FWD	CTCTCAAGAAACTGGGTCTCCTATTC	26	325
TRPC5	REV	GTTTCAAATACATCCTCTGAGGAGTC	26	
TRPC6	FWD	GGCAAAACAAATGAAGCC	18	509
TRPC6	REV	CCCAACCTGTTTTTTGTCAA	20	
TRPC7	FWD	TCAACAACCTCAGCGA	15	187
TRPC7	REV	TTCGTGTCCTAGAGGAG	17	
18S	FWD	AAACGGCTACCACATCCAAG	20	250
18S	REV	CGCTCCCAAGATCCAACCTAC	20	

### **2.1.8 Standard solutions**

Unless otherwise stated, all solutions were made in distilled water (dH<sub>2</sub>O).

#### **2YT**

1.6 % (w/v) tryptone, 1 % (w/v) yeast extract, 0.5 % (w/v) NaCl

2YT was autoclaved before use.

#### **2YT-agar**

1.6 % (w/v) tryptone, 1 % (w/v) yeast extract, 0.5 % (w/v) NaCl, 1 % (w/v) agar

2YT-agar was autoclaved and allowed to cool before the appropriate antibiotic was added and poured into petri-dishes.

#### **Bradford's reagent**

35 mg/L Coomassie brilliant blue, 5 % (v/v) ethanol, 5.1 % (v/v) ortho-phosphoric acid

Bradford's reagent was filtered and stored in the dark

#### **Cell lysis buffer**

50 mM Tris-HCl (pH 7.4 at 4 °C), 50 mM NaF, 1 mM Na<sub>4</sub>P<sub>2</sub>O<sub>7</sub>, 1 mM EDTA, 1 mM EGTA, 1 % (v/v) Triton-X 100, 250 mM mannitol, 1 mM DTT, 1 mM Na<sub>3</sub>VO<sub>4</sub>, 0.1 mM benzamidine, 0.1 mM PMSF, 5 µg/mL SBTI.

Prior to use, cell lysis buffer was stored on ice.

#### **HEPES-Brij DTT (HBD) buffer**

50 mM HEPES-NaOH (pH 7.4 at 4 °C), 1 mM DTT, 0.02 % (v/v) Brij-35

#### **HEPES-Brij DTT (HBD) buffer (high salt)**

50 mM HEPES-NaOH, (pH 7.4 at 4 °C), 1 mM DTT, 0.02 % (v/v) Brij-35, 850 mM NaCl

#### **HEPES-EDTA-SUCROSE (HES)**

20 mM HEPES-NaOH (pH 7.4), 1 mM EDTA, 250 mM sucrose

**Immunoprecipitation (IP) buffer**

50 mM Tris-HCl (pH 7.4 at 4 °C), 150 mM NaCl, 50 mM NaF, 5 mM Na<sub>4</sub>P<sub>2</sub>O<sub>7</sub>, 1 mM EDTA, 1 mM EGTA, 1 % (v/v) Triton-X 100, 1 % (v/v) glycerol, 1 mM DTT, 1 mM Na<sub>3</sub>VO<sub>4</sub>, 0.1 mM benzamidine, 0.1 mM PMSF, 5 µg/mL SBTI.

Prior to use, IP buffer was stored on ice.

**Krebs-Ringer-HEPES (KRH) buffer**

20 mM HEPES-NaOH (pH 7.4), 119 mM NaCl, 5 mM NaHCO<sub>3</sub>, 5 mM glucose, 4.8 mM KCl, 2.5 mM CaCl<sub>2</sub>, 1.2 mM MgSO<sub>4</sub>, 1.2 mM NaH<sub>2</sub>PO<sub>4</sub>

**KRH (Ca<sup>2+</sup> free)**

20 mM HEPES-NaOH (pH 7.4), 119 mM NaCl, 5 mM NaHCO<sub>3</sub>, 5 mM glucose, 4.8 mM KCl, 1.2 mM MgSO<sub>4</sub>, 1.2 mM NaH<sub>2</sub>PO<sub>4</sub>, 1 mM EGTA

**KRH (high K<sup>+</sup>)**

20 mM HEPES-NaOH (pH 7.4), 59.5 mM NaCl, 5 mM NaHCO<sub>3</sub>, 5 mM glucose, 64.3 mM KCl, 2.5 mM CaCl<sub>2</sub>, 1.2 mM MgSO<sub>4</sub>, 1.2 mM NaH<sub>2</sub>PO<sub>4</sub>

**Phosphate-buffered saline (PBS)**

85 mM NaCl, 1.7 mM KCl, 5 mM Na<sub>2</sub>HPO<sub>4</sub>, 0.9 mM KH<sub>2</sub>PO<sub>4</sub>

**Phosphate-buffered saline-Tween 20 (PBS-T)**

85 mM NaCl, 1.7 mM KCl, 5 mM Na<sub>2</sub>HPO<sub>4</sub>, 0.9 mM KH<sub>2</sub>PO<sub>4</sub>, 0.1 % (v/v) Tween 20

**Ponceau S stain**

0.2 % (w/v) Ponceau S, 1 % (v/v) acetic acid

**SDS-PAGE resolving gel**

6-15 % (v/v) acrylamide/0.163-0.408 % (v/v) bisacrylamide in 125 mM Tris-HCl (pH 6.8), 0.1 % (w/v) SDS, 0.1 % (w/v) APS and 0.05 % (v/v) TEMED

**SDS-PAGE running buffer**

190 mM glycine, 62 mM Tris base, 0.1 % (w/v) SDS

**SDS-PAGE sample buffer (4X)**

200 mM Tris-HCl (pH 6.8), 8 % (w/v) SDS, 40 % (v/v) glycerol, 0.4 % (w/v) bromophenol blue. 200 mM DTT was added fresh on the day of use.

**SDS-PAGE stacking gel**

5 % (v/v) acrylamide/0.136 % (v/v) bisacrylamide in 125 mM Tris-HCl (pH 6.8), 0.1 % (w/v) SDS, 0.1 % (w/v) APS and 0.05 % (v/v) TEMED

**TAE buffer (50X)**

40 mM Tris-acetate (pH 8.2), 1 mM EDTA

**Tris-EDTA (TE buffer)**

10 mM Tris-HCl, (pH 8.0), 1 mM EDTA

**Transfer buffer**

25 mM Tris base, 192 mM glycine, 20 % (v/v) ethanol

## **2.2 Methods**

### **2.2.1 Cell culture**

#### **2.2.1.1 Plastic ware**

All cultured cells were maintained in Corning T25, T75 or T150 vented flasks. For experimental conditions, all endothelial cells (aortic endothelial cells and umbilical vein endothelial cells) were cultured in Falcon 6 and 12-well plates, or Falcon 10 cm diameter dishes. For experimental conditions, all other cell lines (HEK-293 cells, HeLa, 3T3-L1 fibroblasts, MEFs) were cultured in Corning 6, 12 and 24-well plates, or 10 cm diameter dishes.

#### **2.2.1.1 Recovery and culture of cryopreserved cells**

Cryopreserved cells were removed from liquid nitrogen and rapidly thawed, before being added to media pre-warmed and equilibrated to 37 °C and 5-10 % (v/v) CO<sub>2</sub>. Cells were incubated overnight, or until the cells had adhered before the media was replaced. Thereafter, cell culture media was replaced every 48 hours or until cells were passaged as described in 2.2.1.2.

#### **2.2.1.2 Passaging of cells**

All cells were routinely subdivided 1/5 – 1/10 when 80-90 % confluent. Cell culture media was aspirated and the cells were washed with pre-warmed sterile PBS. Cells were detached by the addition of trypsin-EDTA (0.05 % (v/v)) and incubated at 37 °C with 5-10 % (v/v) CO<sub>2</sub> until cells fully detached when agitated by sharp tapping of the flask. The trypsin was neutralised by the addition of at least an equal volume of complete cell culture media and the cell suspension was divided as required, or cells were pelleted by centrifugation at 150 x g for 5 min. The pelleted cells were then suspended and counted using a haemocytometer before further dilution and division as required.

#### **2.2.1.3 Determination of endothelial cell phenotype**

To determine whether cultured endothelial cells were maintaining their phenotype over sequential passages, HAEC from several batches and passages were assessed for the expression of endothelial cell marker CD31 (PECAM1), by immunostaining.

Cells were cultured on coverslips coated with type-I collagen, prior to fixing with ice cold methanol for 10 min. After washing, coverslips were attached to glass slides using petroleum jelly, and were circled using a Dako PAP pen to form a water tight seal. Coverslips were rinsed in PBS, and blocked with 3 % (v/v) goat serum in PBS. Coverslips were then incubated in anti-CD31 antibody, diluted 1:40 in PBS with 1 % (w/v) BSA, for 1 hour at room temperature on an orbital shaker. After further washes in PBS, coverslips were incubated for 30 min with biotinylated goat anti-mouse IgG diluted 1:20 in PBS with 1 % (w/v) BSA. After thorough washing in PBS, the coverslips were incubated for a further 30 min in ExtrAvidin Peroxidase diluted 1:20 in PBS with 1 % (w/v) BSA. Coverslips were further washed and incubated for 10 min in AEC substrate. After washing with distilled water, the coverslips were incubated in haematoxylin for 1 min, prior to a further rinse with distilled water. The coverslips were gently removed, and mounted on fresh slides using Aquamount and left to set overnight. Stained preparations were imaged using a Zeiss Axiophot microscope, and images captured using a JVC camera with AverCAP video card, in a Viglen computer.

Positive cells were identified by reddish-brown staining in the cytoplasm, whereas nuclei were observed as blueish-purple (Figure 2-1). Control cells were stained in the absence of primary antibody.

**Figure 2-1**

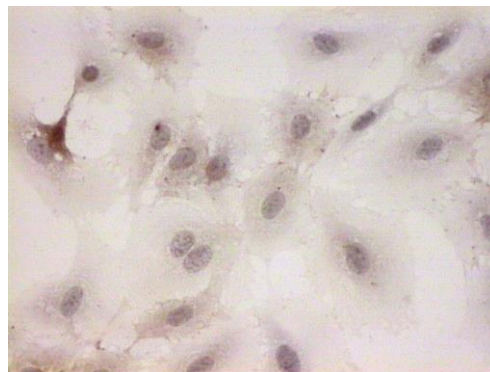


**Figure 2-1: Immunostaining of HAEC with anti-CD31 antibody and haematoxylin**

Immunostaining was carried out by Dr Ian Montgomery as described in 2.2.1.3. Cells positive for CD31 staining appear reddish-brown, whereas the nuclei appear blueish-purple.

#### **2.2.1.4 Cryopreservation of cells**

Confluent T75 flasks of cells were trypsinised as described in 2.2.1.2 and cells pelleted by centrifugation at 150 x g for 5 min. The cell pellet was suspended in 2 mLs of complete cell culture media with the addition of 10 % (v/v) DMSO. Cells were stored overnight at -80 °C, in a Mr. Frosty™ freezing container buffered with isopropyl alcohol, to achieve a freezing rate of -1 °C/min. Cells were transferred to a liquid nitrogen storage facility the next day.

### **2.2.2 Propagation and purification of recombinant adenoviral vectors**

#### **2.2.2.1 Recombinant AMPK adenoviral vector**

Recombinant adenoviral vector encoding Myc tagged dominant negative AMPK  $\alpha$ 1 (full length AMPK  $\alpha$ 1 containing a D157A mutation; Ad.AMPK-DN) and GFP (Ad.GFP) have been described previously (Woods et al. 2000), and were a generous gift from Dr F. Foufelle, Centre Biomédical des Cordeliers, Paris.

#### **2.2.2.2 HEK-293 cell culture and propagation of adenoviral vectors**

HEK-293 cells were cultured and passaged as described in 2.2, and were expanded with subsequent passages. For the propagation of recombinant adenoviral vectors, 25 x T150 flasks were seeded with HEK-293s and cultured until approximately 80 % confluent.

A pellet of cells infected with adenoviral vector was prepared by infecting five T75 flasks of HEK-293 cells with 2  $\mu$ L each of pure recombinant virus which were cultured until attachment failed. The cells were pelleted at 600 x g for 15 min and the supernatant aspirated. The cell pellets were re-suspended in a final volume of 10 mL PBS, and the cells were lysed by the addition of an equal volume of Arklone P (trichlorotrifluoroethane), and mixed thoroughly by inverting the tube for 10 seconds. The lysed cells were centrifuged for 15 min (600 x g) and the upper phase (containing the virus) was decanted into a fresh tube. A further 10 mL of PBS was added to the Arklone P, which was mixed and centrifuged as before - the upper phase was then added to that collected from the initial centrifugation, and the Arklone P layer discarded. The clarified virus was then diluted in sufficient serum free media to allow for the addition of ~10 mLs to each of 25 T150 flasks of HEK-293 cells. Three hours after the addition of the diluted virus, a further 14 mLs of complete media was added to each flask and cells were cultured at 37 °C (5 % (v/v) CO<sub>2</sub>). When attachment failed (typically 48 hours after infection), the cells were collected by

centrifugation at 600 x g for 15 min. The cell pellets were then pooled, and re-suspended in 10 mL sterile PBS before being stored at -80 °C.

### **2.2.2.3 Purification of recombinant adenoviral vector**

The re-suspended cell pellet prepared in 2.2.2.2 was thawed on ice, and the recombinant adenoviral vector extracted twice with Arklone P as described in 2.2.2.2. Sterile caesium chloride (CsCl) was prepared in Tris-EDTA buffer (5 mM Tris-HCl (pH 7.8), 1 mM EDTA) to a final density of 1.33 g/mL, and 2.5 mL added to a sterile centrifuge tube. This was under-laid with 1.5 mL CsCl at a density of 1.45 g/mL. The virus suspension was layered on top and centrifuged at 100,000 x g using an SW40 rotor in an Optima™ XL-80K ultracentrifuge, at 8 °C for 90 min. The centrifuge tube was punctured just below the opaque virus layer with a sterile 21G needle and the virus was aspirated into a 2.5 mL syringe. This was transferred to a 10 micron Slide-A-Lyzer cassette and dialysed against TE buffer at 4 °C, overnight. The next day, the virus was dialysed for a further 2 hours against fresh TE buffer, with the addition of 10 % (v/v) glycerol. The purified virus was then removed from the cassette, the titre assessed as described in 2.2.2.4, and the virus was stored at -80 °C.

### **2.2.2.4 Determination of recombinant adenovirus titre**

To determine the recombinant adenoviral vector titre, a QuickTitre™ Adenovirus Titre Immunoassay kit was used as per the manufacturer's instructions. Where solutions were supplied by the manufacturer with unspecified concentrations (*e.g.* 10 X), they were prepared and diluted to the working concentration (1 X) as instructed by the manufacturer.

Briefly, HEK-293 cells were seeded into a 24-well tissue culture plate ( $2.5 \times 10^5$  cells/well) and cultured for 1 hour at 37 °C, with 5 % (v/v) CO<sub>2</sub>. 10-fold serial dilutions of virus from 2.2.2.3 were prepared in complete MEM, and 100 µL of diluted virus was added to each well. This was performed in duplicate. Infected cells were cultured for 48 hours. Culture medium was carefully aspirated and the cells fixed by the addition of 0.5 mL/well of ice cold methanol, taking care not to dislodge adhered cells. The plate was incubated at -20 °C for 20 min. Cells were then washed three times with PBS, before the addition of 1 % (w/v) BSA in PBS for 1 hour at room temperature. Anti-Hexon antibody (diluted to 1 X concentration) was added and incubated for 1 hour at room temperature on an orbital shaker, before a further three washes with PBS. 1 X HRP-conjugated secondary antibody was added and incubated for a further hour at room temperature on an orbital shaker. Cells

were then washed five times with PBS before 1 X diaminobenzidine (DAB) was added to each well for 10 min at room temperature.

The DAB solution was aspirated and the cells washed twice with PBS. 1 mL of PBS was added to each well, and positive (brown) cells for five separate fields, per well, were counted using a light microscope fitted with a 10 X objective lens. Recombinant adenoviral vector titre was determined as plaque forming units/mL (pfu/mL).

#### **2.2.2.5 Transduction of cells with pure recombinant adenoviral vector for lysate preparation**

When approximately 50-70 % confluent, endothelial cells were washed twice with serum free Medium 199. Virus was diluted in serum free Medium 199 to the appropriate titre and 1 mL typically added to each well of a 6-well plate. After the addition of the virus, cells were cultured at 37 °C, 5 % (v/v) CO<sub>2</sub> for three hours, before the addition of a further 1 mL of complete MV2. Cells were then cultured for at least 20 hours before being treated as described in 2.2.7.1.

### **2.2.3 siRNA transfection**

Volumes given are per well for cells cultured in a 6-well plate.

HUVECs were cultured as described (2.2) until 80 % confluent. The appropriate amount of siRNA was diluted in 150  $\mu\text{L}$  OptiMEM™ media and mixed by pipetting up and down multiple times. 12  $\mu\text{L}$  of HiPerFect® Transfection Reagent was added and the tubes were vortexed briefly. siRNA-transfection reagent complexes were allowed to form by incubating for 15 min at room temperature. Cells were washed with 1 mL/well OptiMEM™ before 750  $\mu\text{L}$  of OptiMEM™ was added per well. siRNA complexes were added dropwise to the wells, and cells were cultured at 37 °C, 5 % (v/v) CO<sub>2</sub>. Three hours after the addition of siRNA, a further 1.5 mLs of complete MV2 was added, and cells were cultured for a further 48 hours at 37 °C in 5 % (v/v) CO<sub>2</sub>.

### **2.2.4 Plasmid transfection of HeLa cells**

HeLa cells were seeded into 6-well plates and cultured until approximately 80 % confluent. On the day of transfection, culture media was replaced with 700  $\mu\text{L}$ /well culture medium.

Lipofectamine® 2000 was diluted 1:30 in 150  $\mu\text{L}$  OptiMEM™, vortex-mixed, and incubated at room temperature for 5 min. Plasmid DNA (2.5  $\mu\text{g}$ ) was diluted in 150  $\mu\text{L}$  OptiMEM™ and mixed by vigorous pipetting. The diluted Lipofectamine® 2000 and diluted DNA were combined, and further mixed by pipetting up and down. Complexes were allowed to form for 20 min at room temperature before 300  $\mu\text{L}$  of complexes were added to each well of cells. Cells were cultured for 4 hours (37 °C, 5 % (v/v) CO<sub>2</sub>) before the complexes were removed and 2 mL of complete culture media was added. Cells were further cultured overnight before treatment and lysis as required. For control transfections, Lipofectamine® 2000 and/or DNA was replaced with an equal volume of OptiMEM™ media.

### **2.2.5 Cell proliferation**

#### **2.2.5.1 Real-time cell proliferation using the RTCA xCELLigence system**

Real time proliferation of HUVECs was measured using the RTCA xCELLigence system. This method utilises gold coated 96-well E-Plates into which cells are seeded. The instrument measures electrical impedance through this gold surface; changes in which are proportional to the area of the well occupied by cells.

In an E-Plate (96-well plate format), 100  $\mu\text{L}$  of MV2 was dispensed into each well and the plate inserted into the RTCA xCELLigence instrument. At 1 min intervals 3 ‘sweeps’ were measured to obtain a background value. HUVEC were seeded, 2,000 cells/well in 50  $\mu\text{L}$  MV2 and allowed to rest in the cell culture hood for 30 min. The plate was returned to the xCELLigence instrument and 30 measurements (sweeps) were recorded, performed at 5 min intervals. The plate was removed and 30 pfu/cell of recombinant adenoviral vector was added in 25  $\mu\text{L}$  MV2. The plate was returned to the xCELLigence and sweeps were performed at 15 min intervals for the remaining duration of the experiment. 6 hours after the addition of virus, the sweeping protocol was paused, and treatments were added to the wells, in a volume of 25  $\mu\text{L}$  to achieve a final VEGF concentration of 10 ng/mL. The E-Plate was returned to the xCELLigence, the sweeping protocol was resumed, and measurements recorded for a further 48 hours.

### **2.2.5.2 MTS assay**

HUVEC proliferation was also determined using the CellTitre 96® Aqueous One Solution. This colourimetric assay relies on the reduction of a tetrazolium compound (3-(4,5-dimethylthiazol-2-yl)-5-(3-carboxymethoxyphenyl)-2-(4-sulphophenyl)-2H-tetrazolium inner salt; MTS) by living cells to a coloured formazan product which is soluble in cell culture medium. The quantity of formazan compound produced is measured by the absorbance at 490 nm, and is reported to be directly proportional to the number of living cells.

Briefly, cells were treated in parallel to the xCELLigence method (2.2.5.1) in Falcon 96-well cell culture plates, except for the absence of the addition of the initial 100  $\mu\text{L}$  cell culture media. Two hours prior to completion of the xCELLigence protocol, 20  $\mu\text{L}$  of CellTitre 96® Aqueous One Solution was added to each well and the cells were incubated under normal cell culture conditions (37 °C in 5 % (v/v) CO<sub>2</sub>). Upon completion of the xCELLigence protocol, the absorbance at 490 nm was measured using a FLUORstar OPTIMA Microplate Reader. Wells into which no cells had been seeded were taken as background.

## 2.2.6 Measurement of mitochondrial function using the Seahorse Bioscience XF24 Analyzer

HUVEC mitochondrial function was assessed using the XF Cell Mito Stress Test Kit. The oxygen consumption rate (OCR) of cells is measured directly by the Seahorse XF24 Extracellular Flux Analyzer, and serial injections of oligomycin, carbonyl cyanide-4 (trifluoromethoxy) phenylhydrazone (FCCP) and a combination of rotenone and antimycin A allows for the measurement of cellular ATP production, maximal respiration and non-mitochondrial respiration respectively. From these parameters proton leak and spare respiratory capacity can be determined. A schematic of an OCR profile is presented (Figure 2-2).

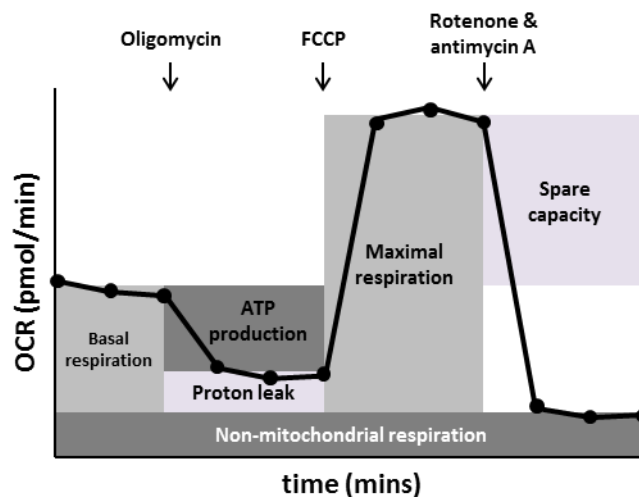


**Figure 2-2: A schematic of a Seahorse XF Cell Mito Stress Test profile, showing the key parameters of cellular respiration**

The sequential addition of oligomycin, FCCP and Rotenone/antimycin A allows cellular basal respiration, ATP production, proton leak, maximal respiration and spare capacity to be calculated, Redrawn from Seahorse XF Cell Mito Stress Test Kit User Guide (Seahorse Bioscience).

HUVEC (at passage 3) were plated into an XF24 Cell Culture Microplate at a density of 65,000 cells per well using a two-step seeding method to achieve an even monolayer of cells. Briefly, HUVEC were cultured, trypsinised and counted as described in 2.2. Cell density was adjusted to  $6.5 \times 10^5$  cells per mL in complete endothelial cell culture media (MV2) and 100  $\mu$ L added to each well. Cell culture media with no cells was added to the control wells A1, B4, C3 and D6. Cells were allowed to adhere for 1 hour at 37 °C, 5 % (v/v) CO<sub>2</sub> before a further 400  $\mu$ L un-supplemented MV2 was added to each well, with or without the addition of 30 pfu/cell virus (Ad.GFP or Ad.AMPK.DN). After a further three hours of incubation (37 °C, 5 % (v/v) CO<sub>2</sub>), VEGF was added in an additional 100  $\mu$ L of 1 % (v/v) supplemented MV2 to achieve a final in well concentration of 10 ng/mL and MV2

supplement concentration of 1 % (v/v). The next day, culture media was replaced with 500  $\mu$ L of 1 % (v/v) supplemented MV2 with the addition of 10 ng/mL VEGF in the appropriate wells. On the evening prior to the assay, an XF24 Flux Pak was hydrated in the Utility Plate provided, by the addition of 1 mL/well XF Calibrant Solution. This was incubated overnight at 37 °C in the absence of supplemental CO<sub>2</sub>. The XF24 Analyzer was turned on and XF24 Software loaded, to ensure the XF24 Analyzer was running at a temperature of 37 °C on the day of the assay.

XF Assay Media was prepared on the day of the assay by the addition of 5.5 mM glucose, 1 mM sodium pyruvate and 2 mM glutamine, to basal XF Assay Medium. The pH was adjusted with dilute NaOH to 7.4, at 37 °C. The XF Assay Media was then filter sterilised and kept at 37 °C until required. HUVEC cell morphology was observed to ensure cell health and that a confluent monolayer had been achieved, before the cells were washed with XF Assay Medium. Cells were washed by removing all but 50  $\mu$ L of the cell culture medium, taking care not to disturb the cell monolayer, and adding 1 mL/well of XF Assay Media. This was performed a further two times with a final addition of 500  $\mu$ L XF Assay Media. The cells were incubated at 37 °C without supplemental CO<sub>2</sub> for 1 hour to allow equilibration. The XF24 Flux Pak was loaded with compounds as per Table 2-8, with final in well concentrations ([in well]) having been determined previously using the protocol described by Seahorse Bioscience, available on their website at:

[www.seahorsebio.com/resources/documentation/basicprocedures/XFe24.php?xfe24](http://www.seahorsebio.com/resources/documentation/basicprocedures/XFe24.php?xfe24)

The OCR measurement protocol was designed and run as described in Table 2-9. Upon completion of the protocol, the XF Assay Media was removed and cells lysed by the direct addition of 15  $\mu$ L/well complete sample buffer. Cells were scraped and pooled according to experimental conditions and used for further analysis as described in 2.2.9 and 2.2.10.

**Table 2-8: XF Cell Mito Stress Test kit reagents and injection protocol**

Compound	Target	Port	[Port] ( $\mu\text{M}$ )	Port volume ( $\mu\text{L}$ )	[In-well] ( $\mu\text{M}$ )
Oligomycin	ATP synthase (complex V)	A	5	56	0.5
FCCP	inner mitochondrial membrane	B	1.25	62	0.125
Rotenone & antimycin A	complex I and III respectively	C	5	69	0.5

**Table 2-9: XF Cell Mito Stress Test Kit OCR measurement protocol**

Step	Cycles	
1.	1	Calibrate probes and insert cell plate
2.	1	Equilibrate cells
3.	x 3	mix - 3 min, wait - 2 min, measure - 3 min
4.	1	Inject port A
5.	x 3	mix - 3 min, wait - 2 min, measure - 3 min
6.	1	Inject port B
7.	x 3	mix - 3 min, wait - 2 min, measure - 3 min
8.	1	Inject port C
9.	x 3	mix - 3 min, wait - 2 min, measure - 3 min
End of protocol.		

## **2.2.7 Preparation of cell lysates**

### **2.2.7.1 Treatment of cells prior to lysis**

Cells, typically cultured in 6-well plates, were incubated in 1 mL/well Medium 199 or KRH after a brief wash with 1 mL/well Medium 199 or KRH (volumes were adjusted accordingly for other plastic ware). Test substances were added for various durations as described, and cells were maintained at 37 °C, 5 % (v/v) CO<sub>2</sub> for the duration of the experiments.

### **2.2.7.2 Preparation of lysates**

#### **2.2.7.2.1 *Preparation of lysates from cultured cells***

With the cells on ice, cold cell lysis buffer (50-500 µL depending on plasticware used) was added and cells vigorously scraped with a cell lifter. Lysates were transferred to a pre-chilled 1.5 mL microcentrifuge tubes, vortex-mixed then incubated on ice for 30 min. Lysates were centrifuged (20,000 x g, 5 min, 4 °C) before supernatant was transferred to fresh microcentrifuge tubes and used for protein quantification.

#### **2.2.7.2.2 *Preparation of lysates from murine tissue***

Female mice were housed under standard conditions, under the personal project license No. 60/4504, Mechanisms of Aging, following the “principles of laboratory animal care” (NIH Publication No. 86-23, revised 1985) and experiments were approved by the University of Glasgow ethical review board. Mice had free access to water and food (D12450B, Research Diets Inc., New Brunswick, NJ, USA; protein 20 kcal%, carbohydrate 70 kcal% and fat 10 kcal%), and were fasted overnight prior to culling via a Schedule 1 procedure between 16 and 20 weeks of age. Tissues were harvested and snap frozen in liquid N<sub>2</sub>. Tissue was homogenised by the addition of 4 volumes of lysis buffer and by 20 passes in a Dounce homogeniser at 4 °C. Cell debris was pelleted by centrifugation (20,000 x g, 10 min, 4 °C), the supernatant was removed and subjected to a further centrifugation (20,000 x g, 10 min, 4 °C). Cleared lysate was used for the determination of protein concentration.

#### **2.2.7.2.3 *Preparation of lysates from human muscle biopsies***

Particulate membrane fractions from human muscle (vastus lateralis) biopsy lysates were prepared in a previous study (Hall et al. 2010) from volunteers of European descent in which the insulin sensitivity index (ISI) derived by Matsuda and DeFonzo (Matsuda and

DeFronzo 1999) was also calculated from data obtained during oral glucose tolerance tests whereby:

$$\text{ISI} = 10,000/\sqrt{([\text{fasting glucose}][\text{fasting insulin}]) \times ([\bar{x} \text{ glucose}][\bar{x} \text{ insulin}] \text{ during OGTT})}$$

The study was approved by the North Glasgow NHS Trust Research Ethics Committee and was conducted according to the principles expressed in the Declaration of Helsinki. Additional analyses received ethical approval from the National Research Ethics Service (Proportionate Review Sub-committee of the NRES Committee West Midlands – Solihull, REC ref 15/WM/0186).

All participants were recruited via a study website and local advertising, and resided in Glasgow at the time of the original study (Hall et al. 2010). All participants reported low/moderate activity levels (physically inactive job and <2 hours of planned exercise per week), were non-smokers aged 18-40 years old with blood pressure <160/90 mmHg, and reported no previous history of diabetes or cardiovascular disease. All participants gave written informed consent. Volunteers attended the laboratory after 12-hour overnight fast with at least a 60-hour abstention from planned exercise. Fasting metabolic parameters and blood samples were taken followed by a muscle biopsy from the vastus lateralis of the right leg, 20 cm above the patella, under local anaesthesia using a ‘semi-open’ technique. Visible fat and connective tissue was removed with sterile forceps and samples were snap-frozen in liquid N<sub>2</sub>. Muscle biopsies were thawed, weighed and homogenised in 8 volumes of homogenisation buffer (50 mM Tris-HCl (pH 7.4 at 4 °C), 250 mM sucrose, 1 mM EDTA, 1 mM EGTA, 5 mM NaF, 5 mM Na<sub>4</sub>P<sub>2</sub>O<sub>7</sub>, 1 mM DTT, 1 mM Na<sub>3</sub>VO<sub>4</sub>, 0.1 mM benzamidine, 0.1 mM PMSF, 5 µg/mL SBTI) by 20 passes in a Dounce homogeniser at 4 °C. Homogenates were centrifuged at 350,000 x g (30 min, 4°C) to obtain cytosolic supernatant fractions. Pellets were then re-suspended in 150 µl homogenisation buffer supplemented with 1% (v/v) NP-40 and incubated on ice for 30 min prior to centrifugation (100,000 x g, 30 min, 4 °C) to obtain microsomal supernatant fractions which were stored at -80 °C. These were re-suspended in 80 µL HES buffer (20 mM HEPES (pH 7.4 at 4 °C), 250 mM sucrose, 1 mM EDTA) prior to determining the protein concentration, and combination with SDS-PAGE sample buffer as described in 2.2.7.3 and 2.2.9.

### **2.2.7.3 Determination of protein concentration**

To determine cell lysate protein concentration, spectrophotometric analysis was performed according to the method of Bradford (Bradford 1976).

Using disposable plastic cuvettes and in duplicate, 2, 4 and 6  $\mu\text{g}$  of bovine serum albumin was diluted in 100  $\mu\text{L}$   $\text{dH}_2\text{O}$ , to be used as reference standards. Cell lysates, again in duplicate, were diluted 1:19 in  $\text{dH}_2\text{O}$  to a final volume of 100  $\mu\text{L}$ . To all standards and samples, 1 mL Bradford's reagent was added, and spectrophotometric analysis performed using a WPA S2000 spectrophotometer. The mean absorbance (mean  $A_{595}$ ) of each duplicate sample was calculated and protein concentration determined by comparison to the reference standards prepared (mean  $A_{595}/\mu\text{g}$  BSA derived from the linear portion of the BSA standards curve).

### **2.2.8 *In vitro* phosphorylation of AMPK**

HEK-293 cells were infected with Ad.AMPK-DN prepared as described in 2.2.2 and cell lysates prepared (2.2.7.2 and 2.2.7.3). AMPK was immunoprecipitated from 500  $\mu\text{g}$  total protein (modified from 2.2.11.1) and incubated with 0.1 U/ $\mu\text{L}$  CIAP (calf intestinal alkaline phosphatase) for 30 min at 30 °C. The immunoprecipitated AMPK-bead complexes were washed once with high salt IP buffer, and a further two times with IP buffer prior to incubation in the presence or absence of 0.02 U or 0.1 U of PKC (active rat brain) or Akt (recombinant human), 1.7 mM  $\text{Ca}^{2+}$ , 0.6 mg/mL PtdSer (phosphatidyl serine), 0.2 mM ATP, and 6 mM  $\text{MgCl}_2$  for 30 min at 30 °C. AMPK-bead complexes were pelleted by centrifugation and washed with IP buffer and HEPES-DTT prior to the addition of complete 1 X sample buffer and heating to 95 °C, then SDS-PAGE and immunoblotting (2.2.9 and 2.2.10).

### **2.2.9 SDS polyacrylamide gel electrophoresis**

Protein samples were resolved by SDS-polyacrylamide gel electrophoresis (SDS-PAGE). SDS-gels used were typically 6-15 % (v/v) acrylamide, 1.5 mm thick, and were prepared as described previously (Sambrook 1989) using Bio-Rad mini-Protean III gel units. Cell lysates were combined with 4 X complete sample buffer in a ratio of 3:1 and heated to 95 °C for 5 min. Equal amounts of protein were loaded per well (typically 10-12  $\mu\text{g}$ ) with a broad range pre-stained molecular mass marker included in at least one well. Proteins were stacked by electrophoresis at 80 V then, when in the resolving gel, the voltage was increased to 120-150 V, until the dye front had migrated the length of the gel and good resolution of the molecular mass markers had been achieved.

## **2.2.10 Western blotting**

### **2.2.10.1 Electrophoretic transfer of protein**

Proteins were resolved by SDS-PAGE as described in 2.2.9, before being transferred onto nitrocellulose membrane (0.45 µm pore size). Gels were removed from their glass supports and placed on an equal sized sheet of nitrocellulose membrane pre-wetted with transfer buffer. These were placed between sheets of 3 mm filter paper and transfer sponges, all pre-wetted with transfer buffer. This was then placed in a Bio-Rad mini Protean transfer cassette and electrophoretic transfer performed in a Bio-Rad mini Protean III Transblot Cell filled with transfer buffer. Electrophoretic transfer was performed at 60 V for 135 min. After transfer, membranes were briefly stained with Ponceau S to visualise protein and ensure even loading, before being washed three times with PBS.

### **2.2.10.2 Blocking of membranes and primary antibody incubation**

Non-specific binding to the nitrocellulose membrane was blocked by incubating the membrane in 5 % (w/v) milk powder made up in PBS for 30 min at room temperature on a shaking platform. Unbound milk protein was then removed by washing the membrane three times in PBS-T (~5 min for each wash, with shaking). Primary antibody (Table 2-2) in 50 % (v/v) LI-COR Odyssey Blocking Buffer, 50 % (v/v) PBS-T was added and the membranes incubated overnight at 4 °C, with shaking.

### **2.2.10.3 Secondary antibody and immunodetection of proteins using the LI-COR Odyssey® imaging system**

Following an overnight incubation in primary antibody, membranes were washed three times in PBS-T, before secondary antibody with the appropriate fluorescent conjugate was added (Table 2-3), and incubated at room temperature for 1 hour, in the dark. After a final three washes with PBS-T, membranes were washed once with PBS before image acquisition was performed using the LI-COR Odyssey® Sa infrared imaging system.

### **2.2.10.4 Densitometric quantification of protein bands**

Images were exported from the LI-COR Odyssey® Sa imaging program as a grey scale .tif and edited (cropped/rotated) using photo editing software. Protein band intensity was measured using ImageJ and subtracted from a representative background value. Densitometric quantification of protein bands is typically expressed here as a ratio of

phospho-specific immunoreactivity:total immunoreactivity, or immunoreactivity compared to an independent loading control, as indicated.

### **2.2.11 AMPK activity assay**

Total catalytic AMPK was immunoprecipitated from cell lysates and AMPK activity was assessed by measuring the incorporation of [ $\gamma$ - $^{32}$ P] ATP into SAMS peptide, a synthetic AMPK substrate.

#### **2.2.11.1 Immunoprecipitation of AMPK**

Protein-G Sepharose beads (10  $\mu$ L of 50 % (v/v) slurry per immunoprecipitation) were washed by the addition of 1 mL immunoprecipitation (IP) buffer and centrifuged at 17,500 x g at 4 °C for 1 min, three times. The bead density was adjusted with IP buffer to 25 % (v/v) beads, and 1  $\mu$ g of (each) antibody per IP reaction was added to the beads. Antibody-bead complexes were allowed to form by incubating for 1 hour at 4 °C on a rotating platform. Beads were collected by centrifugation and again washed three times with 1 mL IP buffer. Antibody-bead complexes were distributed to give a final volume of 5  $\mu$ L packed beads per IP reaction. Cell lysate prepared as described in 2.2.7 (volume equal to 100  $\mu$ g protein) was added to the antibody-bead complexes and the volumes adjusted with IP buffer, so as to be equal across all the samples. Protein was allowed to bind to the antibody-bead complexes by incubation for 3 hours at 4 °C on a rotating platform. IP reactions were centrifuged and washed as follows: 2 x high salt IP buffer (IP buffer with a final concentration of 1 M NaCl), 2 x IP buffer and finally with HEPES-Brij-DTT (HBD) buffer (50 mM HEPES-NaOH pH 7.4 at 4 °C, 0.02 % (v/v) Brij-35, 1 mM DTT). The supernatant was completely aspirated and the pellets were stored at -20 °C.

#### **2.2.11.2 AMPK activity assay**

Immunoprecipitated AMPK-Sepharose bead pellets were re-suspended by the addition of 20  $\mu$ L HBD buffer. Kinase reactions were prepared in chilled microfuge tubes as follows: 5  $\mu$ L re-suspended immunoprecipitated AMPK-beads, 5  $\mu$ L HBD, 5  $\mu$ L 1 mM AMP and 5  $\mu$ L 1 mM SAMS peptide. Reactions were started by the addition of 5  $\mu$ L of 0.2  $\mu$ Ci/ $\mu$ L [ $\gamma$ - $^{32}$ P]-ATP, diluted in HBD containing 1 mM ATP and 25 mM MgCl<sub>2</sub>. All samples were incubated at 30 °C on a vibrating platform. 15  $\mu$ L was removed from each tube and spotted onto a square of P-81 Whatman phosphocellulose paper which was submerged in 500 mL of 0.1 % (v/v) H<sub>3</sub>PO<sub>4</sub> 10 min after the addition of the [ $\gamma$ - $^{32}$ P]-ATP to each reaction. The

paper squares were then washed as follows: two water rinses, a further 0.1 % (v/v) H<sub>3</sub>PO<sub>4</sub> wash for 5 min, finally two further water rinses. The paper squares were allowed to air dry before being added to 5 mL scintillation fluid. Counts were obtained for 1 min using a Beckman LS6500 scintillation counter. All samples were assayed in duplicate, with an additional reaction for each sample omitting the SAMS peptide (replaced by an equal volume of HBD). To measure total counts, 5 µL of the [ $\gamma$ -<sup>32</sup>P]-ATP preparation was spotted onto phosphocellulose paper and added immediately to scintillation fluid for counting.

## **2.2.12 Immunofluorescence methods**

For all incubations and washes, a volume of liquid sufficient to immerse the coverslips were used.

### **2.2.12.1 Preparing, and seeding cells onto, coverslips**

Glass coverslips were immersed in 100 % (v/v) ethanol, placed into cell culture plates and allowed to dry completely in a laminar flow hood. When the coverslips were dry, cell culture plates were exposed to UV light (~30 min) to ensure sterility. Cells were trypsinised, as described in 2.2, and seeded into the culture plates with coverslips. Cells were cultured under normal culture conditions (2.2) until cells had reached the required density.

### **2.2.12.2 Treatment and fixation of cells**

Cells were washed with, and then quiesced in Medium 199 for 2-3 hours prior to stimulation with compounds as previously described in 2.2.7.1. Cells were washed twice with PBS before the addition of 3 % (w/v) paraformaldehyde in PBS for 20 min at room temperature. After fixing, cells were washed again, three times with PBS before the coverslips were transferred to fresh cell culture plates containing PBS. Coverslips were either stained immediately or sealed with paraffin film and stored at 4 °C overnight.

### **2.2.12.3 Staining of cells and mounting coverslips**

Fixed cells on coverslips were allowed to warm to room temperature and unless otherwise indicated, all staining incubations and washes were performed at room temperature. Cells were permeabilised by the addition of 0.1 % (v/v) Triton X-100 in PBS for 10 min before coverslips were washed three times with immunofluorescence buffer (IFB; 0.1 % (v/v)

Triton X-100, 1 % (w/v) BSA, in PBS). Non-specific staining was reduced by ‘blocking’ the coverslips with 10 % (v/v) donkey serum in IFB for 20 min before a further three washes with IFB. Primary antibodies were diluted as indicated (Table 2-4) in IFB and applied to the coverslips for 2 hours, before a further three washes with IFB. Secondary antibody was diluted as indicated (Table 2-5), and applied to coverslips for 1 hour; this step and all subsequent incubations/washes were performed in the dark. Coverslips were washed a further three times before the addition of RedDot™2, diluted 1:200 in IFB; cells were incubated for 10 min. Coverslips were washed three times with IFB before a final wash with PBS. Excess PBS was blotted from the coverslip before they were mounted onto glass slides using ImmunoMount™ mounting media and allowed to set at room temperature overnight.

#### **2.2.12.4 Visualisation and image acquisition**

Images of immunolabelled cells were acquired using a Zeiss LSM Exciter laser scanning microscope utilising LSM imaging software. Images were obtained with a Plan-Apochromat 63X/1.4 NA oil DIC objective lens and relevant filters. Images were exported from the LSM software in .tif format.

## **2.3 Molecular biology protocols**

### **2.3.1 Transformation of competent *E.coli***

Chemically competent *E.coli* were thawed on ice and combined with 1  $\mu$ L plasmid DNA (Table 2-6). Cells and DNA were incubated on ice for 30 min before being subjected to heatshock at 42 °C for 45 seconds. Cells were rested on ice for 2 min before the addition of 300  $\mu$ L SOC media. Cells were allowed to recover for 1 hour at 37 °C, with shaking. 75-100  $\mu$ L of transformed *E.coli* was spread onto pre-warmed 2YT-agar plates with the appropriate antibiotic (50  $\mu$ g/mL kanamycin). Plates were allowed to dry briefly before being inverted and incubated at 37 °C overnight. Small-scale cultures were prepared by inoculating 5-10 mL 2YT (with appropriate antibiotic) with a single colony picked from a plate and incubating overnight with vigorous shaking. The next day, amplified plasmid DNA was prepared.

### **2.3.2 Preparation of plasmid DNA**

Small scale plasmid DNA preparations were made from *E.coli* using Promega's Wizard<sup>®</sup> Plus SV Miniprep DNA Purification System.

Briefly, overnight cultures (2.3.1) were pelleted by centrifugation 1500 x g for 5 min. The cell pellet was re-suspended with Cell Re-suspension Solution and mixed thoroughly. Cells were lysed by the addition of Cell Lysis Solution and Alkaline Protease Solution was added. After 5 min of incubation, Neutralization Solution was added and cell debris pelleted by centrifugation using a bench-top centrifuge at 20,000 x g. The cleared cell lysate containing the plasmid DNA was passed through the Spin Columns provided by centrifugation 1500 x g for 1 min. Columns were washed twice with Wash Solution before a further 2 min centrifugation to remove residual Wash Solution. Columns were transferred to sterile 1.5 mL microfuge tubes and nuclease free water applied directly to the membrane. DNA was eluted from the column by centrifuging the columns for 1 min 1500 x g. DNA concentration was determined at A<sub>260</sub> using a Nanodrop spectrophotometer and stored at -20 °C.

### **2.3.3 DNA sequencing**

All DNA sequencing was performed by DNA Sequencing & Services (MRCPPU, College of Life Sciences, University of Dundee, Scotland, [www.dnaseq.co.uk](http://www.dnaseq.co.uk)) using Applied

Biosystems Big-Dye Ver 3.1 chemistry on an Applied Biosystems model 3730 automated capillary DNA sequencer. For each sequence, 600 ng of plasmid DNA was provided in a volume of 30  $\mu$ L. Standard primers were provided by DNA Sequencing & Services. Custom sequencing primers were designed with the aid of primer-BLAST software, available at <http://www.ncbi.nlm.nih.gov/tools/primer-blast/>. Sequencing data was analysed using Chromas Lite version 2.2.1 and Serial Cloner version 1.3r11.

### **2.3.4 RNA extraction**

Cells were cultured to near 100 % confluence in 10 cm diameter culture dishes before total cellular RNA was isolated using a Qiagen RNeasy Mini Kit according to the manufacturer's instructions. All buffers were supplied by the manufacturer.

Briefly, cells were directly lysed by the addition of 350  $\mu$ L lysis buffer ('RLT') and collected with a cell scraper. Cell lysates were homogenised by passage through a sterile/RNase-free 21-gauge needle and syringe several times. An equal volume of 70 % (v/v) ethanol was added to the lysate, mixed by pipetting up and down, and then applied to an RNeasy Mini column in 700  $\mu$ L aliquots which were then centrifuged at full speed in a benchtop centrifuge for 1 min, until the whole volume had passed through the column. Columns were washed with 700  $\mu$ L of wash buffer ('RW1'). The columns were washed twice with 500  $\mu$ L of buffer 'RPE', with the second centrifugation performed for 2 min. The RNeasy columns were transferred to fresh collection tubes and centrifuged for a further min. The columns were transferred to fresh 1.5 mL collection tube and 30  $\mu$ L of RNase-free water applied directly to the membrane and columns were centrifuged for 1 min. Elute was reapplied to the membrane and centrifuged for a further min. Eluted RNA was quantified using a Nanodrop spectrophotometer before storage at -80 °C.

### **2.3.5 First cDNA strand synthesis**

To synthesise cDNA, total RNA extracted (as described in 2.3.4) was reverse transcribed using M-MLV Reverse Transcriptase. 2  $\mu$ g of RNA was combined with 1  $\mu$ g of Oligo(dT) and made up to a final volume  $\leq$  14  $\mu$ L in sterile water. Secondary mRNA structures were melted by heating the tubes to 70 °C for 5 min before tubes were chilled on ice and briefly centrifuged to collect all the solution. The following was added to each reaction: 5  $\mu$ L M-MLV 5X Reaction Buffer, 1.25  $\mu$ L of each dNTP (10 mM stock of dATP, dCTP, dGTP and dTTP), 200 units of M-MLV Reverse Transcriptase. Each reaction was made up to a

final volume of 25  $\mu\text{L}$  with nuclease free water and reactions were heated to 42  $^{\circ}\text{C}$  for 60 min, before storage at -20  $^{\circ}\text{C}$ .

### **2.3.6 Reverse transcriptase PCR**

PCR reactions were assembled on ice, in thin-walled PCR tubes as follows: 1 X *Taq* DNA polymerase buffer (20 mM Tris HCl pH 8.0, 50 mM KCl), 1.5 mM  $\text{MgCl}_2$ , 0.2 mM dNTPs, 0.5  $\mu\text{M}$  forward primer, 0.5  $\mu\text{M}$  reverse primer (Table 2-7), 1  $\mu\text{g}$  of template cDNA, 2.5 units of *Taq* DNA polymerase and sterile/RNase free  $\text{dH}_2\text{O}$  to a final volume of 50  $\mu\text{L}$ . Reactions were subjected to thermocycling in a Progene FPR0G050 thermocycler as follows: 94  $^{\circ}\text{C}$  for 2 min, followed by 25-50 cycles of 94  $^{\circ}\text{C}$  for 2 min, 58  $^{\circ}\text{C}$  for 1 min and 72  $^{\circ}\text{C}$  for 50 seconds. A final extension step was performed at 72  $^{\circ}\text{C}$  for 5 min before reactions were chilled to 4  $^{\circ}\text{C}$  for overnight storage.

### **2.3.7 Agarose gel electrophoretic resolution, visualisation and imaging of PCR products**

PCR products were separated on agarose gels (typically 1 % (w/v)) with 0.2  $\mu\text{g}/\text{mL}$  ethidium bromide using a Mini-Sub Cell GT gel system (Bio-Rad). PCR products were combined 5:1 with 6 X DNA loading buffer and equal volumes of PCR products loaded per well. An appropriate DNA ladder was included in at least one well. PCR products were resolved for 20-40 min at 100 V.

DNA was visualised on a UV trans-illuminator, before being photographed using a Gel Doc imaging system (BioRad).

### **2.3.8 Quantitative (TaqMan®) Real time-PCR**

RNA was extracted and cDNA synthesised as described previously (2.3.4 and 2.3.5). Quantitative RT-PCR was performed in a 384-well plate using ABI-PRISM 7900HT Sequence Detection System. For each reaction, 1.5  $\mu\text{L}$  cDNA, 0.5  $\mu\text{L}$  FAM-labelled TaqMan® probe, 5  $\mu\text{L}$  TaqMan® Universal Mastermix II (no UNG) and 3  $\mu\text{L}$  RNase/DNase free  $\text{H}_2\text{O}$  was combined and subjected to thermal cycling as follows: 2 min 50  $^{\circ}\text{C}$ , 10 min 95  $^{\circ}\text{C}$ , then 40 cycles of 15 seconds 95  $^{\circ}\text{C}$  and 1 min 60  $^{\circ}\text{C}$ . All RNA isolates/synthesized cDNA were assessed for GAPDH expression levels and all PCR reactions were carried out in duplicate.

## 2.4 Statistical analysis

Unless stated otherwise, results are expressed as the mean  $\pm$  SEM. Graphs were generated and statistically significant differences were determined using a two-tailed Student's *t*-test using GraphPad Prism® software, with  $p < 0.05$  deemed to be statistically significant.

## **Chapter 3 – Investigating the effect of VEGF on AMPK**

### **3.1 Introduction**

Previous work in our laboratory reported that AMPK is activated by VEGF in vascular endothelial cells in a CaMKK-dependent manner, and that AMPK is required for endothelial cell proliferation (Reihill et al. 2011); this is in contrast to the anti-proliferative actions of AMPK activation in other cell types. AMPK activation is reported to inhibit VSMC proliferation (Stone et al. 2013), suggesting that targeting VEGF-stimulated AMPK signalling in endothelial cells may be an attractive therapeutic strategy for promoting the re-endothelialisation of damaged vessels, thereby preventing the maladaptive remodelling that often follows vascular injury. This, in addition to the beneficial metabolic and anti-inflammatory effects of AMPK activation in the vasculature, makes AMPK an attractive therapeutic target for a number of vascular pathologies. The current study therefore aimed to characterise the specific effect(s) of VEGF on AMPK to clarify the mechanism by which VEGF-stimulated AMPK activity is required for the proliferation of endothelial cells.

## 3.2 Results

VEGF activates AMPK when measured by immunoblotting for activating AMPK Thr172 phosphorylation, phosphorylation of the AMPK substrate ACC, and assessment of kinase activity (Figure 3-1). VEGF treatment (10 ng/mL, 5 min) stimulated a significant increase in both AMPK Thr172 phosphorylation and phosphorylation ACC at Ser79 (Figure 3-1A). When measured by kinase assay (Figure 3-1B), VEGF significantly stimulated AMPK activity >2-fold, a level which is comparable to AMPK activation stimulated by AICAR.

To assess the relative contributions of the AMPK  $\alpha$ 1 and  $\alpha$ 2 catalytic subunits in both basal and VEGF/AICAR-stimulated AMPK activity, AMPK  $\alpha$ 1 and  $\alpha$ 2 containing complexes were separated by immunoprecipitation prior to the measurement of AMPK kinase activity (Figure 3-2). AMPK  $\alpha$ 1 activity accounts for the vast majority of both basal and VEGF-stimulated AMPK activity, with comparable levels of activity measured when AMPK was immunoprecipitated with antibodies against either AMPK  $\alpha$ 1 or a combination of antibodies recognising AMPK  $\alpha$ 1 and AMPK  $\alpha$ 2. AMPK  $\alpha$ 2 activity (both basal and VEGF-stimulated) was negligible in HAEC (Figure 3-2Ai). A similar pattern (AMPK  $\alpha$ 1 accounting for the majority of total AMPK activity) was measured for AMPK immunoprecipitated from HAEC treated with AICAR (Figure 3-2Aii). Successful separation of  $\alpha$  subunit containing complexes was determined by subsequent immunoblotting (Figure 3-2B), and the successful measurement of AMPK  $\alpha$ 2 activity was confirmed using AMPK immunoprecipitated from rat liver (Figure 3-2C) which gave a ratio of  $\alpha$ 1: $\alpha$ 2-mediated AMPK activity of 60:40.

Figure 3-1

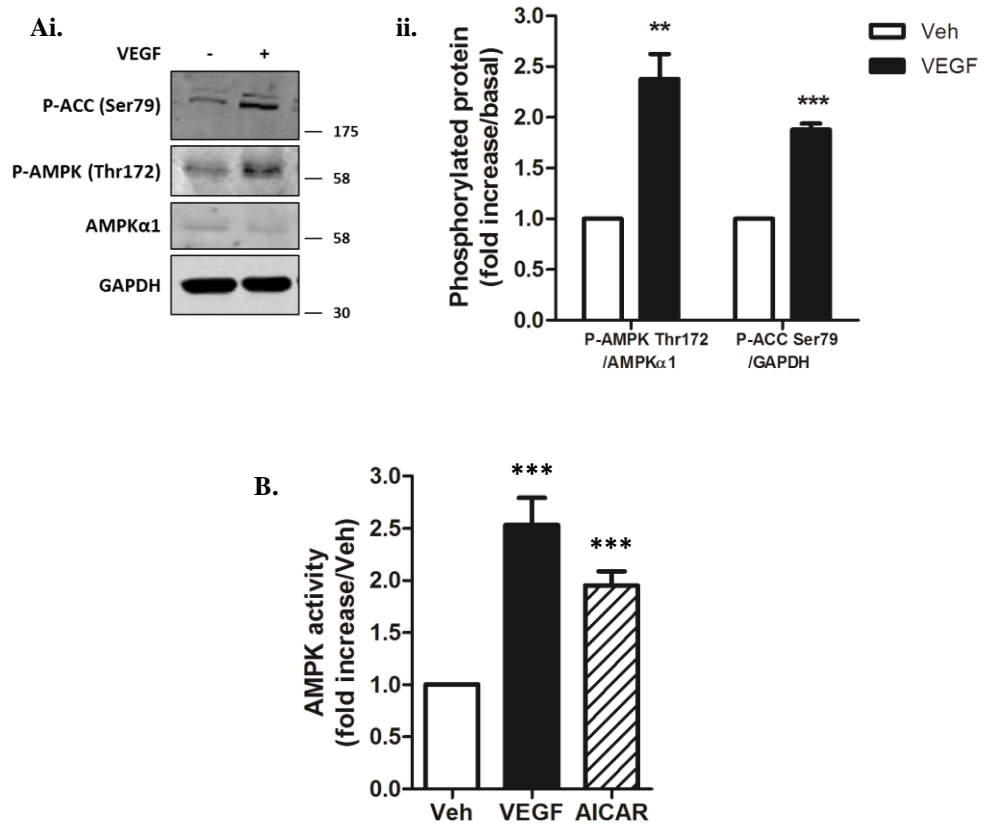
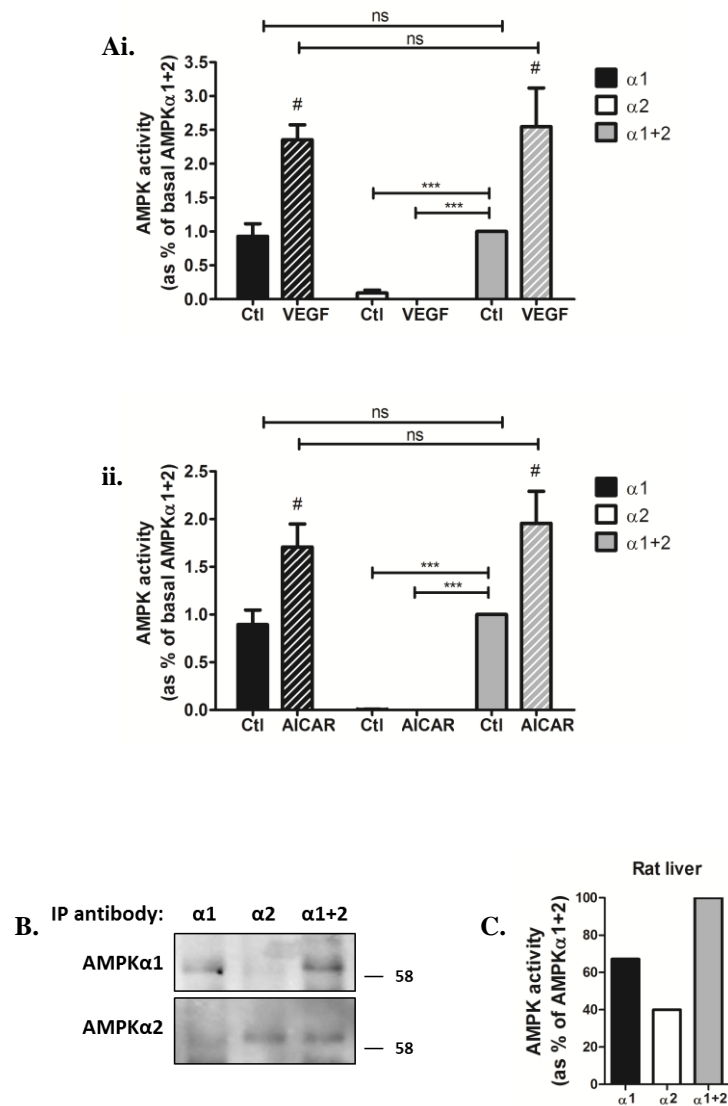


Figure 3-1: VEGF stimulates AMPK activity

HAEC were stimulated with 10 ng/mL VEGF (5 min) or 2 mM AICAR (45 min) prior to cell lysis and the preparation of cell lysates. **A.** Proteins were resolved by SDS-PAGE/gel electrophoresis and subjected to immunoblotting using the antibodies indicated. **i.** a representative immunoblot is shown with the migration of molecular mass markers indicated on the right and **ii.** quantification of immunoblots from three independent experiments  $\pm$  SEM. **B.** AMPK activity was also measured in HAEC lysate. Data in **B.** represents mean fold increase  $\pm$  SEM of AMPK activity for five independent experiments. \*\* $p < 0.01$  and \*\*\* $p < 0.001$  versus Veh.

Figure 3-2



**Figure 3-2:  $\alpha$ 1 containing complexes account for the vast majority of basal and VEGF- or AICAR-simulated AMPK activity in HAEC**

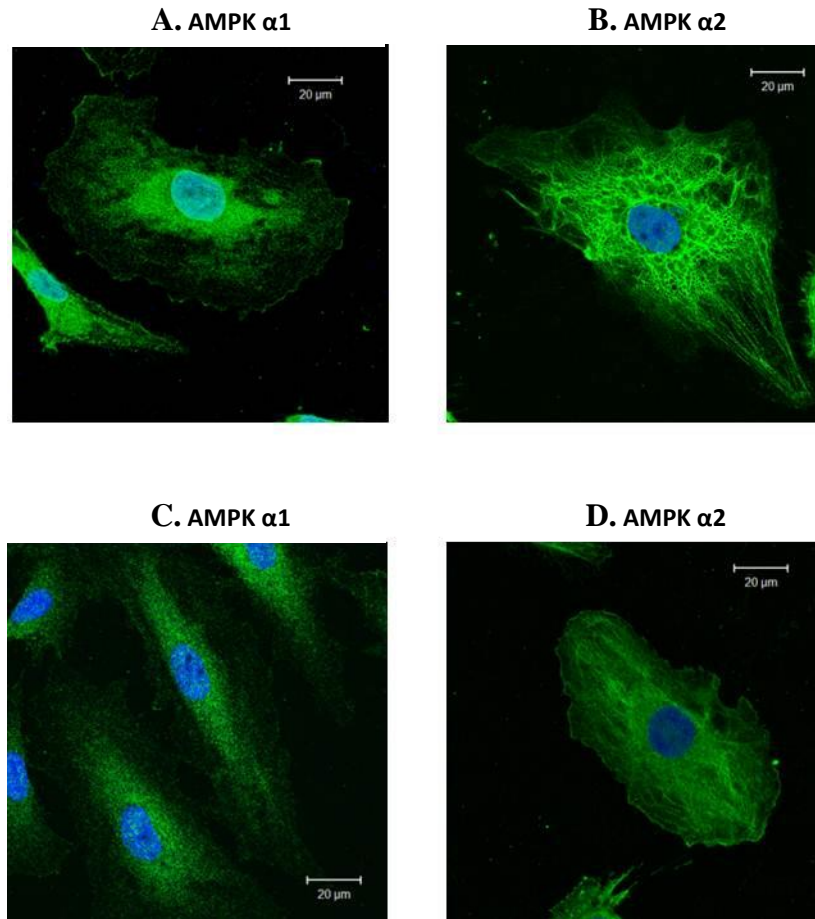
HAEC were treated with **A.** VEGF (10 ng/mL, 5 min) or **Aii.** AICAR (2 mM, 45 min) prior to cell lysis and the preparation of cell lysates. AMPK  $\alpha$ 1,  $\alpha$ 2 or both  $\alpha$ 1 and  $\alpha$ 2 were immunoprecipitated as described in 2.2.11, and AMPK activity measured. Data in **A.** represents AMPK activity from six independent experiments  $\pm$  SEM. The remaining AMPK was eluted from the Sepharose beads used in the immunoprecipitations and assessed by SDS-PAGE and immunoblotting with the antibodies indicated in **B.** The migration of molecular mass markers is indicated on the right. **C.** AMPK activity was also assessed in rat liver after separation of AMPK  $\alpha$ 1 and  $\alpha$ 2 containing complexes, n=1. ns=not significant. # $p < 0.05$  versus absence of VEGF/AICAR and \*\*\* $p < 0.001$  versus untreated total AMPK ( $\alpha$ 1+ $\alpha$ 2).

AMPK subcellular distribution was also determined in HAEC using indirect immunofluorescence and imaging by confocal microscopy. AMPK  $\alpha 1$  was observed to be localised to the cytoplasm of HAEC and highly concentrated in the perinuclear region (Figure 3-3A and C). Contrary to previous reports (Salt et al. 1998), AMPK  $\alpha 1$  staining was observed in the nucleus of these cells but was not present in the nucleolus. AMPK  $\alpha 2$  was found to have a fibrous staining pattern (Figure 3-3B and D). Furthermore AMPK  $\alpha 2$  was present in the nucleus but absent from the nucleolus. These findings were confirmed using antibodies recognising different epitopes of the AMPK  $\alpha 1$  and  $\alpha 2$  subunits respectively.

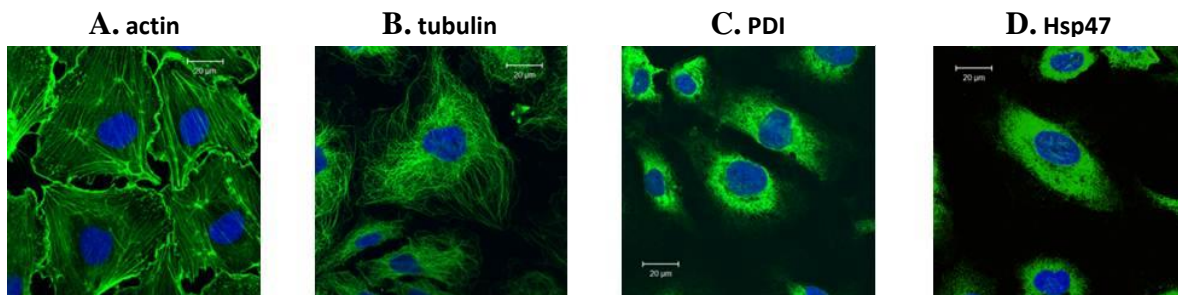
In order to characterise cell components with which AMPK might be interacting or localised to, HAEC were stained for the structural components actin and tubulin, and the endoplasmic reticulum resident proteins protein disulphide isomerase (PDI) or heat-shock protein 47 (Hsp47). Well defined actin fibres can be observed extending throughout the cells with distinct areas of actin deposition at the plasma membrane (Figure 3-4). Tubulin on the other hand, forms a fibrous network of filaments, concentrated around (but not inside) the nucleus and extending outwards towards the cell periphery (Figure 3-4B). Staining for both PDI and Hsp47 was concentrated in the perinuclear region and absent in the nucleus as might be expected for ER resident proteins (Figure 3-4C and D).

Co-staining patterns for AMPK  $\alpha 1$  and either PDI or Hsp47 showed a high level of overlap indicating that AMPK  $\alpha 1$ , may be concentrated in the ER of HAEC (Figure 3-5). AMPK  $\alpha 2$  and tubulin showed a similar pattern of immunostaining, however this was by no means a perfect match when overlaid (Figure 3-6). Areas where fibrous AMPK  $\alpha 2$  and tubulin staining ran in parallel were noted.

To assess whether VEGF altered the subcellular distribution of AMPK  $\alpha 1$  and  $\alpha 2$  containing complexes, HAEC were stimulated with VEGF (10 ng/mL) for 5-360 min ( $\alpha 1$ ) or up to 24 hours ( $\alpha 2$ ) prior to fixation and staining for AMPK  $\alpha 1$  and PDI (Figure 3-7), or AMPK  $\alpha 2$  and tubulin (Figure 3-8). No obvious redistribution of either AMPK  $\alpha 1$  or  $\alpha 2$  was observed within the cell population over the duration of these experiments.

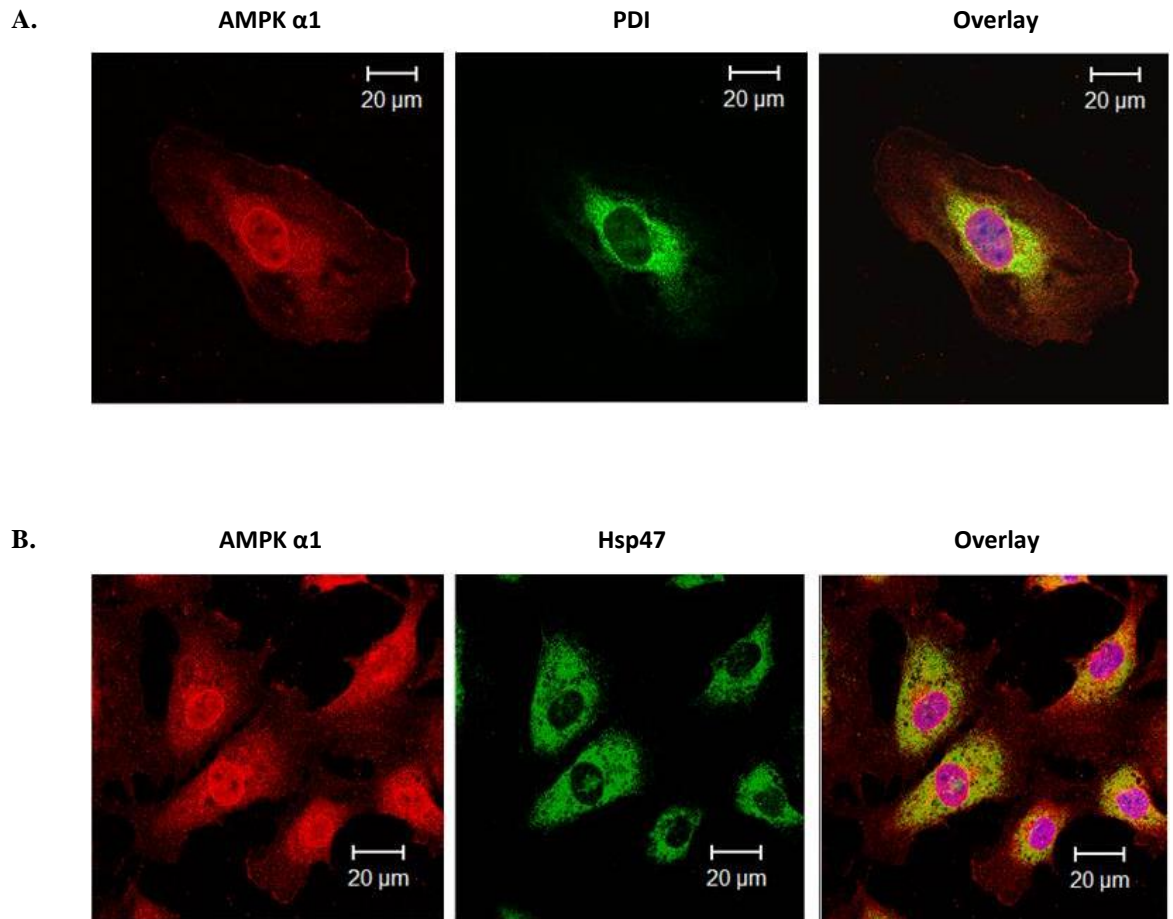
**Figure 3-3****Figure 3-3: AMPK  $\alpha$  isoform specific subcellular distribution in HAEC**

Unstimulated HAEC were fixed and incubated with antibodies against **A.** AMPK  $\alpha$ 1 (amino acids 344-358), **B.** AMPK  $\alpha$ 2, **C.** AMPK  $\alpha$ 1 (amino acids 357-524) and **D.** AMPK  $\alpha$ 2 (amino acids 352-366), (all in green). Cells were further stained with the far-red nuclear stain RedDot<sup>TM</sup>2 (blue) and localisation of antibodies assessed by immunofluorescence microscopy. Scale bar represents 20  $\mu$ m. Images shown are representative of six to ten fields of view from four independent experiments.

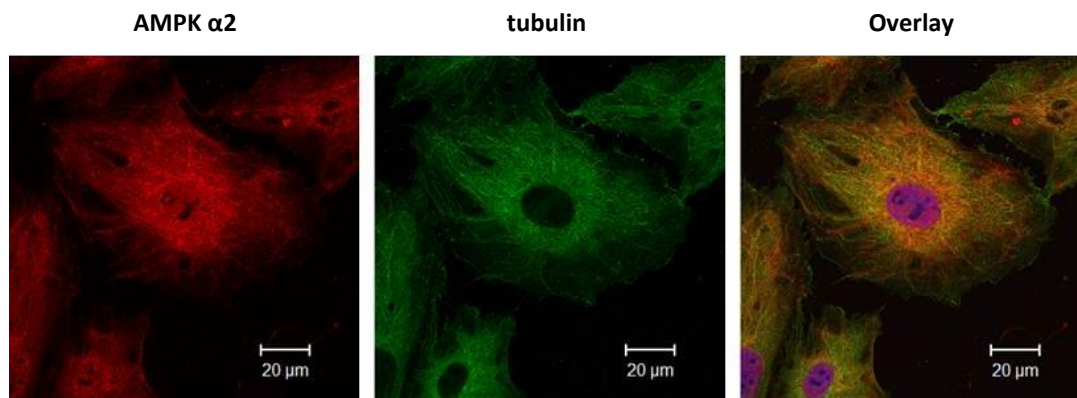
**Figure 3-4****Figure 3-4: Characterisation of structural and subcellular organelles in HAEC**

Unstimulated HAEC were fixed and incubated with antibodies against **A.** actin, **B.** tubulin, **C.** protein disulphide isomerase (PDI) or **D.** heat-shock protein 47 (Hsp47) (green). Cells were further stained with the far-red nuclear stain RedDot™2 (blue) and the localisation of antibodies was assessed by confocal microscopy. Scale bar represents 20 μm. Images shown are representative of five fields of view in a single experiment.

Figure 3-5

**Figure 3-5: AMPK  $\alpha$ 1 co-localises with both PDI and Hsp47**

Unstimulated HAEC were fixed and incubated with antibodies against **A.** AMPK  $\alpha$ 1 (red) and protein disulphide isomerase (PDI) (green) and **B.** AMPK  $\alpha$ 1 (red) and heat-shock protein 47 (Hsp47 - green). Cells were further stained with the far-red nuclear stain RedDot™2 (blue in overlay) and the localisation of antibodies assessed by immunofluorescence microscopy. Scale bar represents 20  $\mu$ m. Images shown are representative of 5 fields of view from two independent experiments.

**Figure 3-6****Figure 3-6: AMPK  $\alpha$ 2 in HAEC**

Unstimulated HAEC were fixed and incubated with antibodies against AMPK  $\alpha$ 2 (red) and tubulin (green). Cells were further stained with the far-red nuclear stain RedDot™2 (blue in overlay) and the localisation of antibodies assessed by immunofluorescence microscopy. Scale bar represents 20  $\mu$ m. Images shown are representative of six to nine fields of view from two independent experiments.

**Figure 3-7: AMPK  $\alpha$ 1 subcellular distribution in VEGF treated HAEC**

Figure on facing page. Quiesced HAEC were stimulated with VEGF (10 ng/mL) for the times indicated prior to being fixed and incubated with antibodies against AMPK  $\alpha$ 1 (red) and PDI (green). Cells were further stained with the far-red nuclear stain RedDot™2 (blue in overlay) and the localisation of antibodies assessed by immunofluorescence microscopy. Scale bar represents 20  $\mu$ m. Images shown are representative of six to nine fields of view from two independent experiments.

Figure 3-7

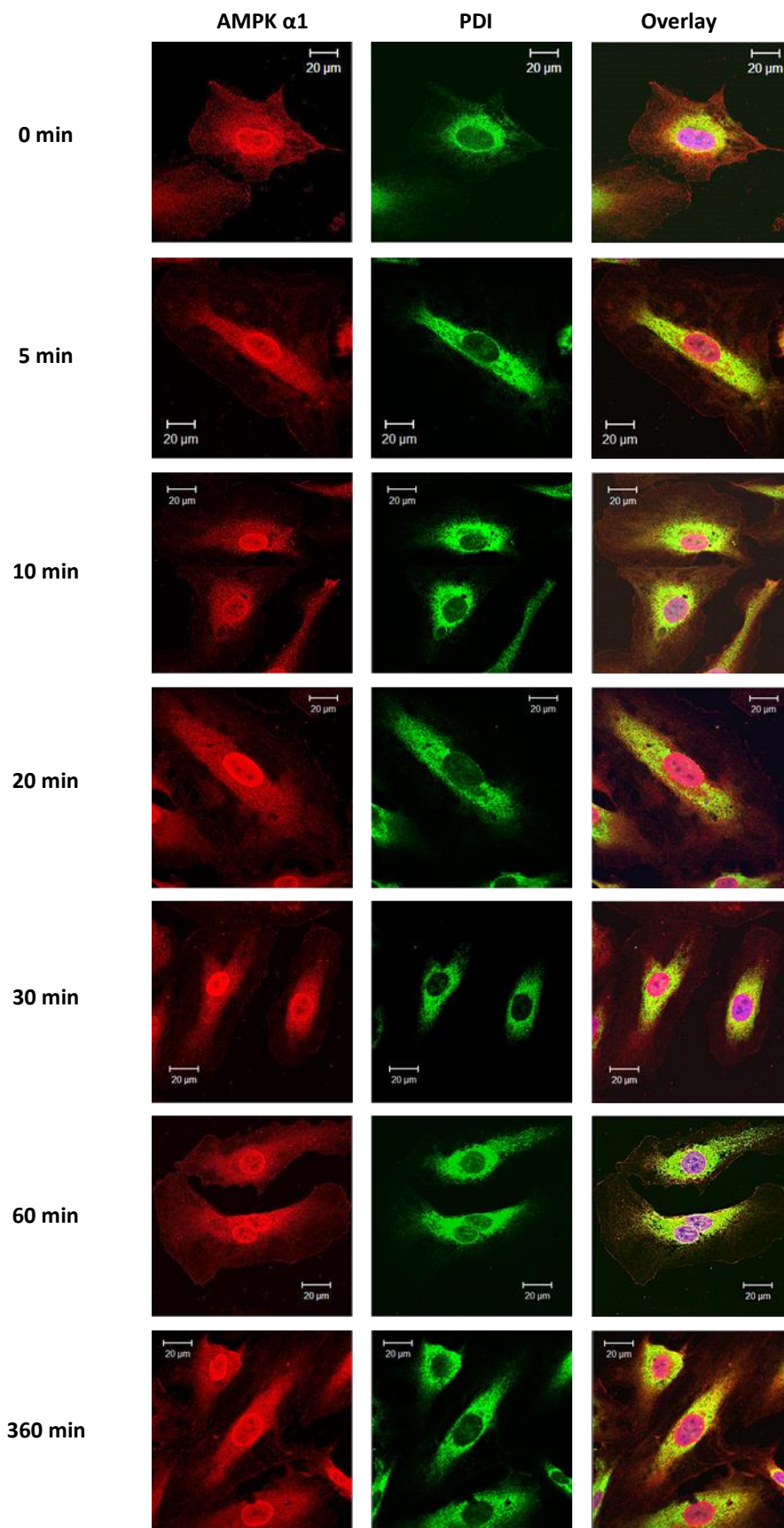
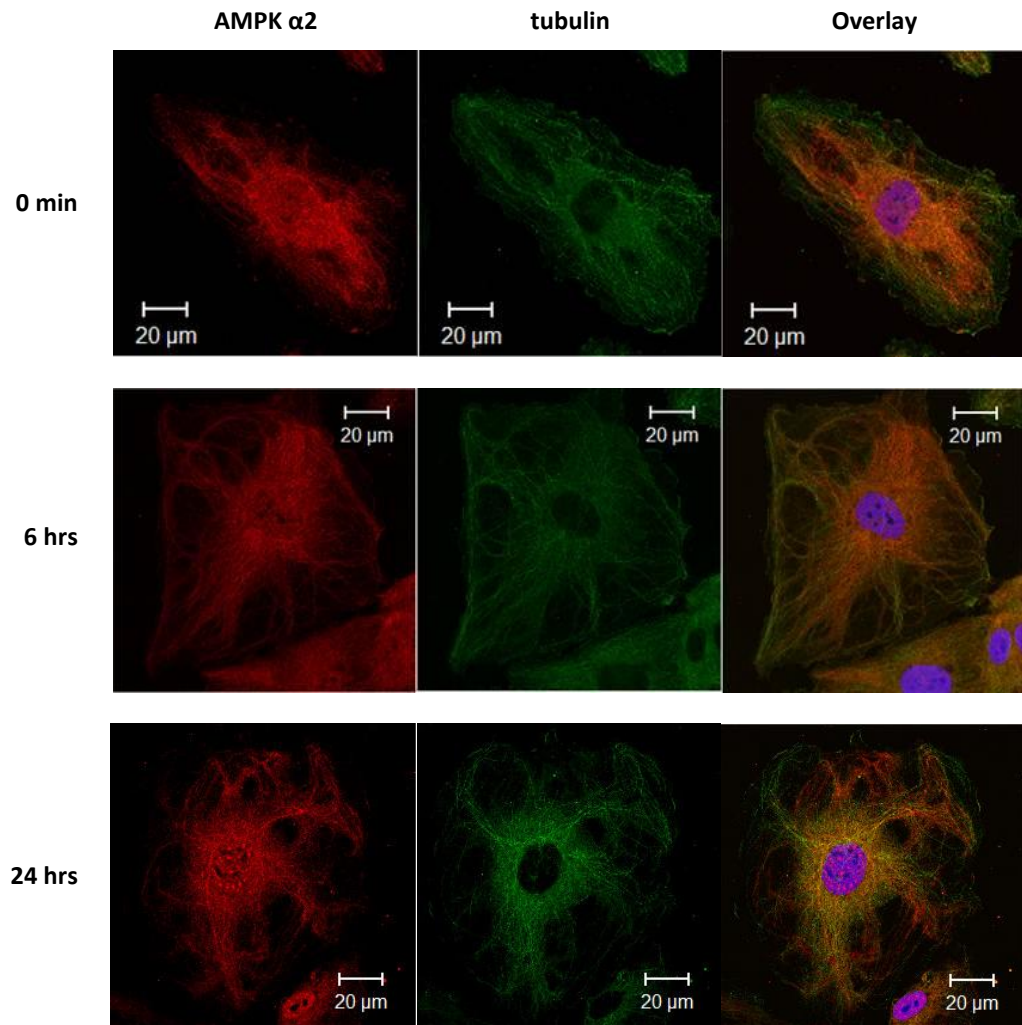


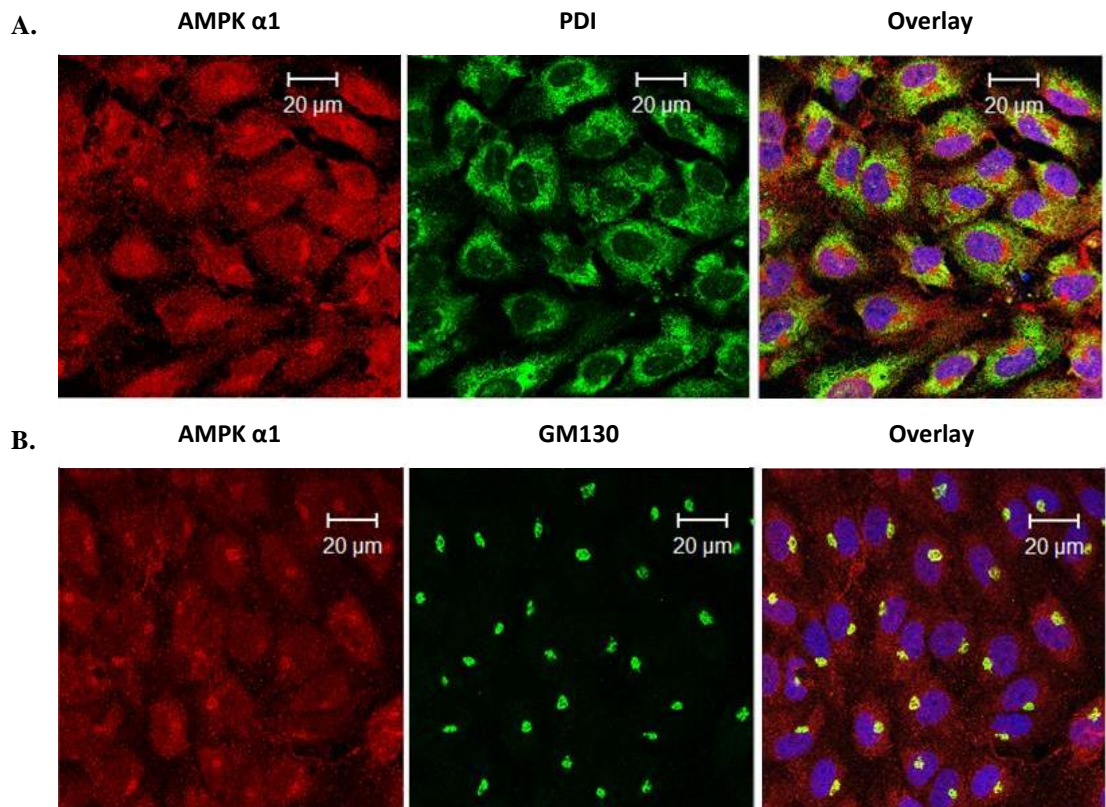
Figure 3-7: AMPK α1 subcellular distribution in VEGF treated HAEC

Legend on facing page

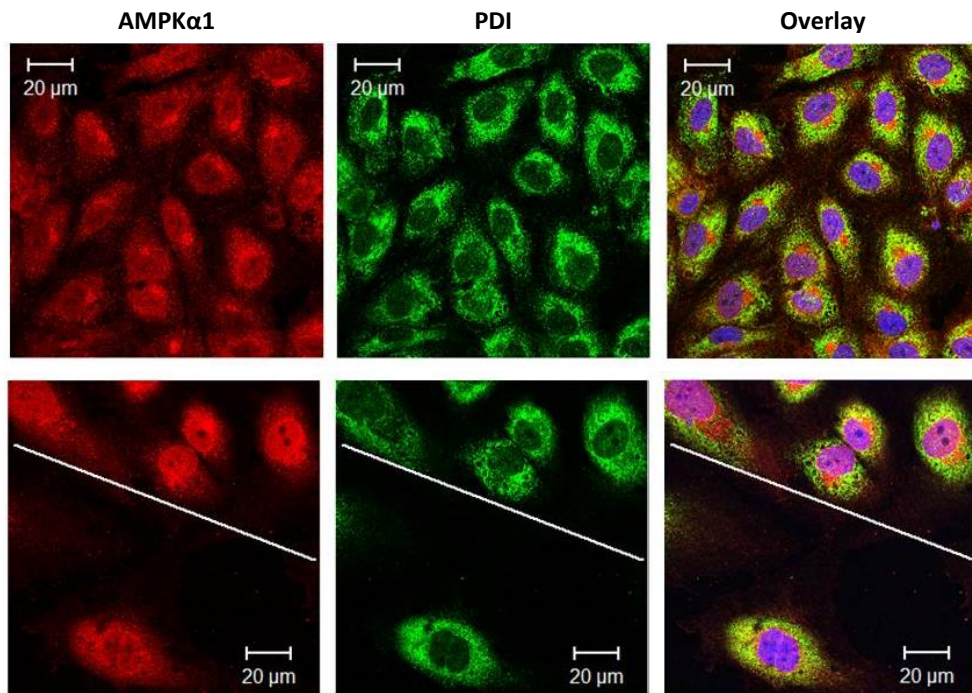
**Figure 3-8****Figure 3-8: AMPK  $\alpha$ 2 subcellular distribution in VEGF treated HAEC**

Quiesced HAEC were stimulated with VEGF (10 ng/mL) for the times indicated prior to being fixed and incubated with antibodies against AMPK  $\alpha$ 2 (red) and tubulin (green). Cells were further stained with the far-red nuclear stain RedDot™2 (blue in overlay) and the localisation of antibodies assessed by immunofluorescence microscopy. Scale bar represents 20  $\mu$ m. Images shown are representative of six to nine fields of view from two independent experiments.

The assessment of AMPK sub-cellular localisation reported here were performed in sub-confluent HAEC. Given the confluent nature of the vascular endothelium, we assessed the subcellular distribution of AMPK  $\alpha$ 1 containing complexes in confluent HAEC. Intriguingly, when cells were cultured to near 100 % confluence, AMPK  $\alpha$ 1 staining was characterised by a punctate distribution, with a single distinct area of AMPK  $\alpha$ 1 staining adjacent to the nucleus: diffuse staining was also observed throughout the cell. Further co-staining experiments identified the region in which AMPK  $\alpha$ 1 concentrates in confluent HAEC as being the Golgi body, assessed by co-staining with the Golgi matrix protein 130 (GM130) (Figure 3-9). Therefore to assess whether confluency determines the sub-cellular distribution of AMPK  $\alpha$ 1 containing complexes, a confluent monolayer of HAEC was wounded by scratching with a pipette tip, and allowed to recover overnight. AMPK  $\alpha$ 1 in cells remote to the wounded area was found to be concentrated in the Golgi body whereas cells which had migrated into the wounded area displayed a diffuse perinuclear staining pattern for AMPK  $\alpha$ 1, similar to that observed in previous experiments. Furthermore this was found to correlate with PDI staining. Cells at the wound periphery displayed a combination of AMPK  $\alpha$ 1 concentrated in either the Golgi body or ER (Figure 3-10).

**Figure 3-9****Figure 3-9: AMPK  $\alpha$ 1 is concentrated in the Golgi of confluent HAEC**

HAEC were cultured to confluence prior to fixing and incubating with antibodies against **A.** AMPK  $\alpha$ 1 (red) and PDI (green) or **B.** AMPK  $\alpha$ 1 and Golgi marker 130 (GM130; green). Cells were further stained with the far-red nuclear stain RedDot™2 (blue in overlay). The localisation of antibodies was assessed by immunofluorescence microscopy. Scale bar represents 20  $\mu$ m. Images shown are representative of six to nine fields of view from two independent experiments.

**Figure 3-10****Figure 3-10: AMPK  $\alpha$ 1 subcellular localisation is dependent on confluency**

HAEC were cultured to confluence before being 'wounded' by scratching with a pipette tip and then cultured overnight. Cells were fixed and incubated with antibodies against AMPK  $\alpha$ 1 (red) and PDI (green). Cells were further stained with the far-red nuclear stain RedDot™2 (blue in overlay). The localisation of antibodies was assessed by immunofluorescence microscopy. Scale bar represents 20  $\mu$ m. Images shown are representative of six to nine fields of view from two independent experiments. The upper panel shows an area of confluent cells not affected by wounding, and lower panel showing the periphery of the wound on the same coverslip (edge of wound indicated with white line).

We next re-examined the AMPK-dependence of VEGF-stimulated proliferation by infecting cells with a recombinant adenoviral vector expressing a dominant negative mutant AMPK (Ad.AMPK-DN). The resulting preparation of Ad.GFP and Ad.AMPK-DN was assessed for infection efficiency and the degree to which it inhibited AMPK activity (Figure 3-11). Treatment of HAEC with either 30 or 60 pfu/cell Ad.GFP resulted in >80 % GFP positive cells, whereas in cells transduced with Ad.AMPK-DN, 60 % of cells stained positive for Myc overexpression (Figure 3-11A and B). Increasing the amount of Ad.AMPK-DN virus to 60 pfu/cell caused a 10 % increase in the number of Myc-positive cells however at this titre, cells with atypical morphologies were observed (not shown). Subsequent experiments therefore used a titre of 30 pfu/cell Ad.GFP and Ad.AMPK-DN.

HAEC were transduced with 30 pfu/cell Ad.GFP or Ad.AMPK-DN prior to stimulation with the direct AMPK activator A769662. Substantial levels of GFP protein was measured in cell lysates prepared from cells transduced with Ad.GFP which was absent in cells not treated with virus, or Ad.AMPK-DN transduced cells. Conversely, high levels of Myc and AMPK  $\alpha$ 1 were measured in cells transduced with Ad.AMPK-DN compared to untransduced or GFP-transduced HAEC (Figure 3-11C). In the presence of A769662, ACC Ser79 phosphorylation is robustly stimulated in cells transduced with Ad.GFP whereas HAECs transduced with Ad.AMPK-DN, exhibited substantially reduced basal and A769662-stimulated ACC Ser79 phosphorylation compared to Ad.GFP-transduced cells (Figure 3-11Cii). Despite there being detectable levels of AMPK Thr172 phosphorylation after Ad.AMPK-DN infection, the ratio of Thr172 phosphorylated to total AMPK  $\alpha$ 1 indicates that although a proportion of AMPK is still phosphorylated after Ad.AMPK-DN treatment (Figure 3-11Ciii), by far the vast majority of AMPK present is exogenous adenoviral derived kinase-dead AMPK.

Previous studies in our laboratory reported that AMPK was required for VEGF-stimulated endothelial cell proliferation as assessed by MTS assay, as over expression of dominant-negative AMPK prevented VEGF-stimulated cell proliferation (Reihill et al. 2011). This assay determines the number of viable cells present using the reduction of a tetrazolium compound into a coloured formazan product which is soluble in tissue culture media. This reaction is presumed to be catalysed by NADPH or NADH, and produced by dehydrogenase enzymes in metabolically active cells (Berridge and Tan 1993). To confirm this previous report, cell proliferation was measured using the MTS assay as described previously (Reihill et al. 2011), in parallel with proliferation measured using the RTCA xCELLigence system. The xCELLigence system measures impedance of an electrical

current caused by cells actively growing on a gold substrate. Cell indices are generated, defined by:  $(R_n - R_b)/15$ , with  $R_n$  defined as the cell-electrode impedance and  $R_b$  the impedance of the well with cell culture media alone. As such, the xCELLigence system can be thought of as measuring the area of a well occupied by cells, in real time.

In agreement with previous studies (Reihill et al. 2011), infection of HUVEC with Ad.AMPK-DN prevents VEGF-stimulated cell proliferation when assessed using the MTS assay (Figure 3-12). Furthermore, AICAR inhibited HUVEC proliferation by approximately half in both un-transduced cells and cells transduced with either Ad.GFP or Ad.AMPK-DN. In contrast to this however, infection of HUVEC with Ad.AMPK-DN had no effect on VEGF-stimulated cell proliferation when measured using the RTCA xCELLigence system (Figure 3-13).

Figure 3-11

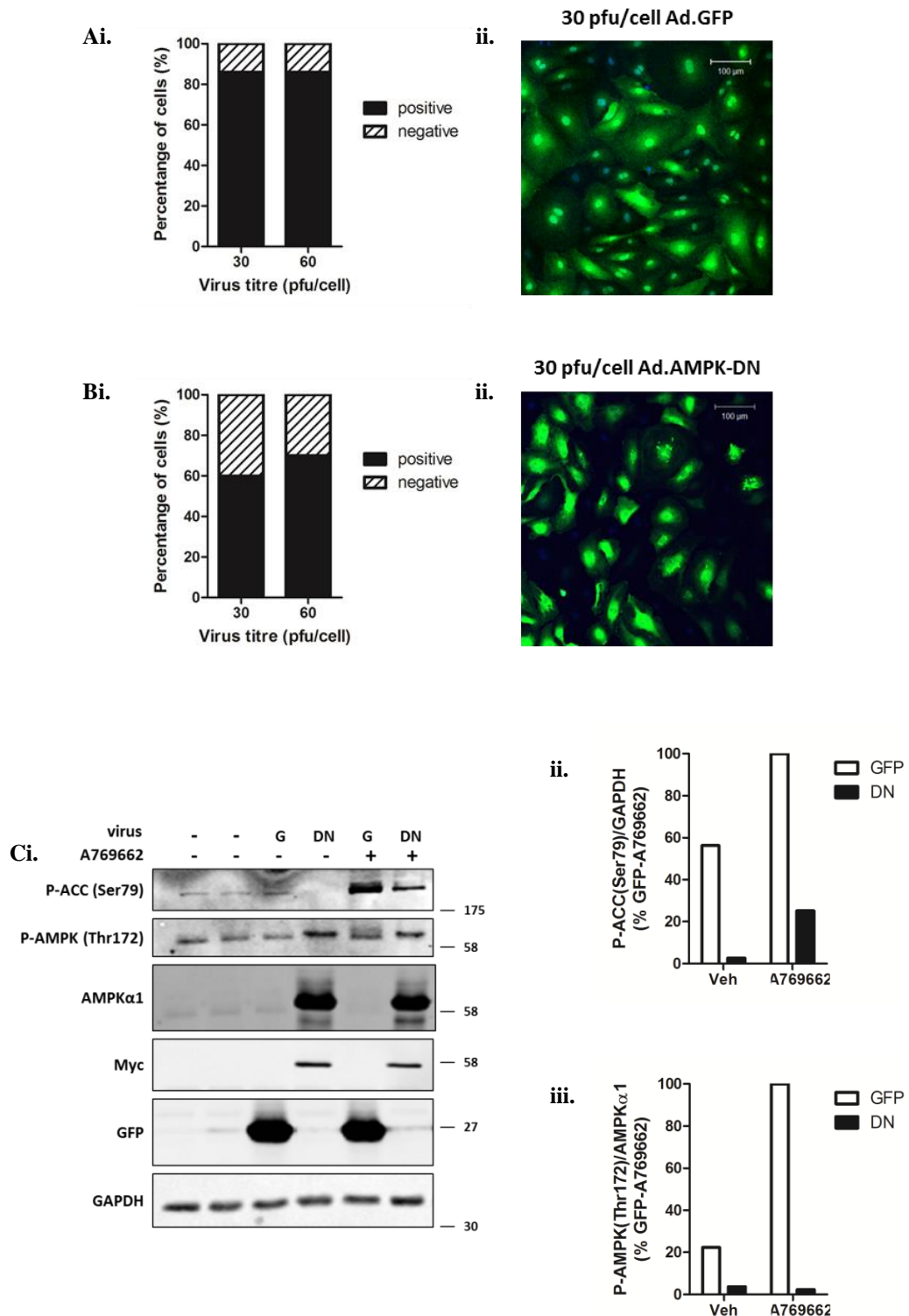
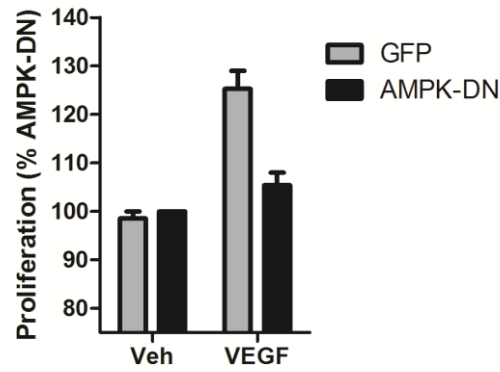


Figure 3-11: Assessment of virus transduction efficiency

HAEC were transduced with the indicated pfu/cell **A.** Ad.GFP or **B.** Ad.AMPK-DN. Ad.AMPK-DN-transduced cells were stained with anti-Myc (green) prior to imaging by confocal microscopy. Scale bar represents 20  $\mu\text{m}$ . Cells were further stained with the far-red nuclear stain RedDot™2 (blue) as shown in **Aii.** and **Bii.** Positive (green) cells were counted and expressed as a percentage of total cells, determined by the number of nuclei (blue) present. Representative fields of view are shown for HAEC transduced with 30 pfu/cell Ad.GFP and Ad.AMPK-DN in **Aii.** and **Bii.** respectively. **C.** HAEC were also transduced with 30 pfu/cell Ad.GFP or Ad.AMPK-DN prior to treatment with A769662 (100  $\mu\text{M}$ , 60 min) and the preparation of cell lysates. Proteins were resolved by SDS-PAGE/gel electrophoresis and immunoblotted with the antibodies indicated in **C.** Pixel densitometry analysis of immunoblots from **C** are shown in **ii.** and **iii.** Virus infection efficiency was assessed in a single experiment (data presented here,  $n=1$ ), and confirmed during subsequent experiments.

**Figure 3-12****Figure 3-12: Infection with Ad.AMPK-DN prevents VEGF-stimulated HUVEC proliferation as measured by MTS assay**

HUVEC were seeded, into 96-well plate (2000 cells/well) and once adhered transduced with 30 pfu/cell Ad.GFP or Ad.AMPK-DN for 6 hours. VEGF (10 ng/mL) was then added to the cells, which were cultured for a further 48 hours. Two hours prior to the end of the experiment, 25  $\mu$ L/well MTS reagent was added. Proliferation of cells was determined by measuring the absorbance at 490 nm. Background values (wells into which no cells had been seeded) were subtracted and results were normalised to vehicle (Veh)-treated cells. Data represents the mean of triplicate measurements, for two independent experiments.

Figure 3-13

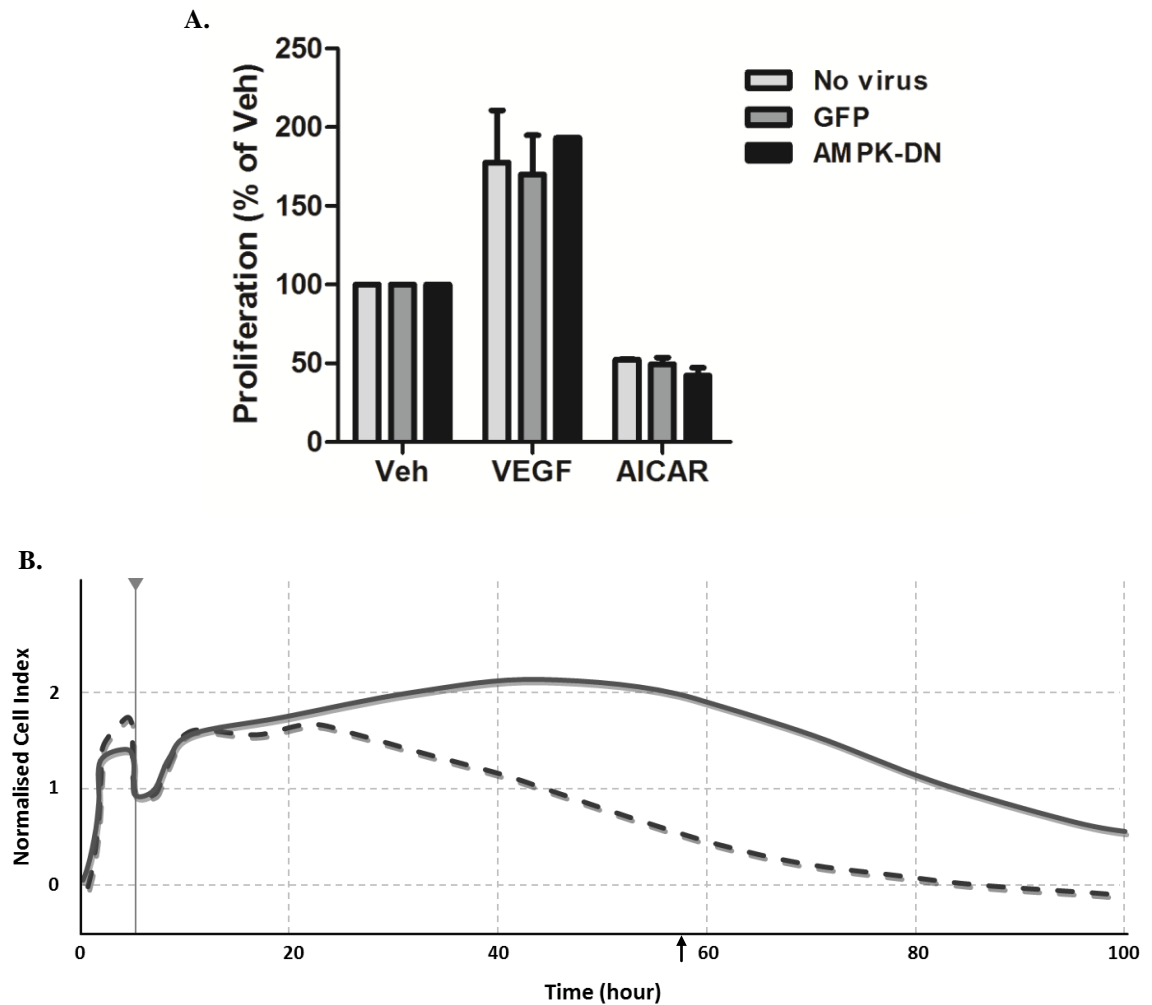


**Figure 3-13: Infection with Ad.AMPK-DN has no effect on VEGF-stimulated HUVEC proliferation as measured using the xCELLigence system**

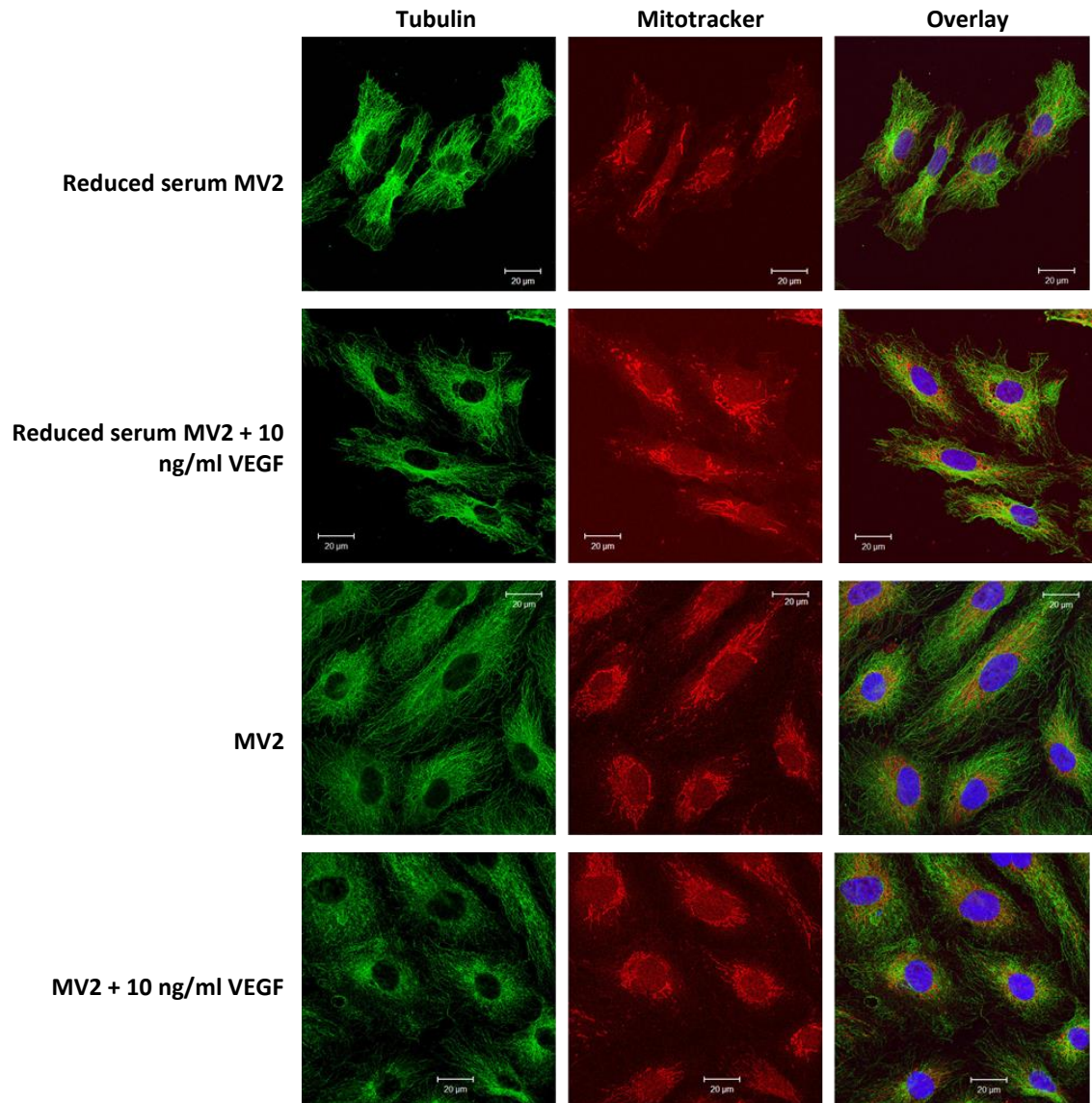
HUVEC were seeded, into 96-well E-plate (2000 cells/well) and once adhered transduced with 30 pfu/cell Ad.GFP or Ad.AMPK-DN for 6 hours. VEGF (10 ng/mL) was then added to the cells, which were cultured for a further four days in the xCELLigence instrument. **A.** Data represents the mean cell index of triplicate measurements for two independent experiments, normalised to vehicle (Veh)-treated cells. **B.** An example trace of the raw data from a single experiment is shown, lines represent the mean normalised cell index for triplicate measurements for vehicle (dashed line) and VEGF-stimulated cells (solid line) normalised to cell index measured at the addition of treatment, indicated by the vertical line and arrow (grey). For comparison with the end-point MTS assay Figure 3-12, the normalised cell index measured 48 hours after the addition of vehicle/VEGF was used (black arrow on x axis).

Given the discrepancy between the results in Figure 3-12 and Figure 3-13, we hypothesised that AMPK might be required for a VEGF-stimulated parameter of mitochondrial function, given that the MTS is not necessarily a direct measure of cell proliferation.

We therefore assessed whether VEGF alters mitochondrial morphology or complex composition. HUVEC were stained with MitoTracker Red and imaged by confocal microscopy (Figure 3-14). At the resolution we are currently able to achieve, it has not been possible to quantify mitochondrial mass, however mitochondria in HUVEC do appear to be concentrated within the perinuclear region.

To assess whether Ad.AMPK-DN or chronic VEGF treatment affected mitochondrial complex expression, mitochondrial complex protein levels were assessed by immunoblotting using an OXPHOS antibody cocktail (Figure 3-15). Robust complex I, IV and V expression was detected (Figure 3-15B, E and F respectively), with lesser amounts of complex II and III detected (Figure 3-15C and D). Neither Ad.AMPK-DN nor VEGF affected the expression of any of the complexes detected.

Figure 3-14

**Figure 3-14: Assessment of mitochondria morphology in HUVEC**

HUVEC were cultured in either reduced serum MV2 (0.5 % (v/v)) or 'complete' MV2 (5 % (v/v)), in the presence or absence of VEGF (10 ng/mL, 48 hours) prior to the addition of MitoTracker (red) to the cell culture medium for 30 min. After a brief washout period, cells were fixed and stained with anti-tubulin antibody (green) and the far-red nuclear stain RedDot™2 (blue) prior to imaging by confocal microscopy. Scale bar represents 20 µm. Representative images are shown from two independent experiments.

Figure 3-15

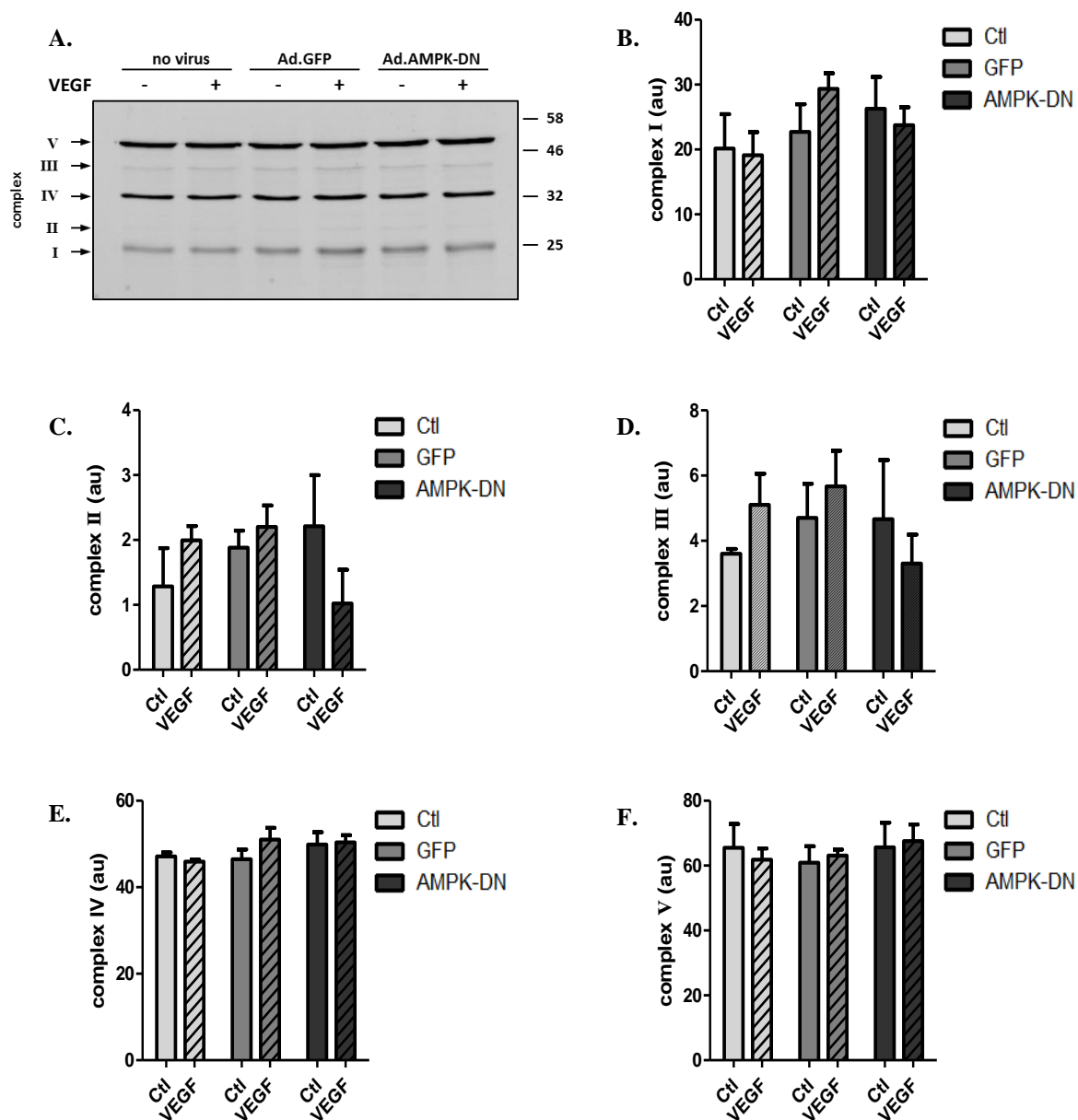


Figure 3-15: Complex I-V expression in HUVEC

Cells used for OCR measurements (Figure 3-17) were lysed by the direct addition of sample buffer and subjected to vigorous scraping and pooled according to virus and VEGF treatment regime. Equal volumes of protein were subjected to SDS-PAGE/gel electrophoresis and immunoblotted using an OXPHOS antibody cocktail (Table 2-2) **A.** A representative blot is shown with the complex identities indicated on the left and the migration of molecular mass standards on the right. **B-F.** Mean pixel density (au) of immunoblots for individual mitochondrial complexes are shown for two independent experiments.

Given that VEGF did not obviously alter mitochondrial morphology or complex composition, we characterised parameters of mitochondrial activity in HUVEC using the Seahorse Mito Stress Test kit. In the first instance 65,000 HUVEC/well were found to produce an oxygen consumption rate (OCR) of approximately 100 pmol/min, within the suggested optimal range (personal communication – Dr Amy Sinclair, University of Glasgow – not shown). Increasing concentrations of oligomycin or FCCP (final concentration of  $\leq 2$   $\mu\text{M}$ ) were injected and three OCR values were recorded (Figure 3-16). Oligomycin at all concentrations tested (0.5, 1 and 2  $\mu\text{M}$ ) significantly reduced the OCR of HUVEC by approximately half (Figure 3-16A). FCCP at the lowest concentration tested (0.125  $\mu\text{M}$ ) significantly increased the OCR to the greatest extent (~50% increase). At lower concentrations, FCCP (0.5  $\mu\text{M}$ ) stimulated a lesser but still significant increase in OCR, but at a concentration of 2  $\mu\text{M}$  OCR was not significantly increased above untreated HUVEC (Figure 3-16B).

OCRs were subsequently measured for cells transduced with either Ad.GFP or Ad.AMPK-DN (Figure 3-17B), in the presence and absence of VEGF (Figure 3-17C and D). For cells transduced with both Ad.GFP and Ad.AMPK-DN, VEGF caused a small vertical shift in the OCR profile, but this increase did not reach statistical significance. This increase however was found to be greater in cells transduced with Ad.GFP, when compared to cell transduced with Ad.AMPK-DN (Table 3-1).

Infection of HUVEC with Ad.AMPK-DN consistently decreased OCR in both the presence and absence of VEGF (Table 3-2), and this was more apparent in VEGF-stimulated cells, indicating that AMPK inhibition tends to attenuate the VEGF-induced increase in OCR.

Average OCRs was calculated for the three OCR measurements prior to the addition of compounds, and after the sequential addition of oligomycin, FCCP and a combination of rotenone and antimycin A. From these values, basal respiration (Figure 3-18A), ATP production (Figure 3-18B), proton leak (Figure 3-18C), maximal respiration (Figure 3-18D) and spare capacity (Figure 3-18E) were calculated for each treatment group. Neither VEGF nor infection of HUVEC with Ad.AMPK-DN significantly affected any parameters of metabolic activity calculated, although maximal respiration and spare capacity tended to be reduced by infection of HUVEC with Ad.AMPK-DN in both the presence and absence of VEGF (Figure 3-18D and E).

Figure 3-16

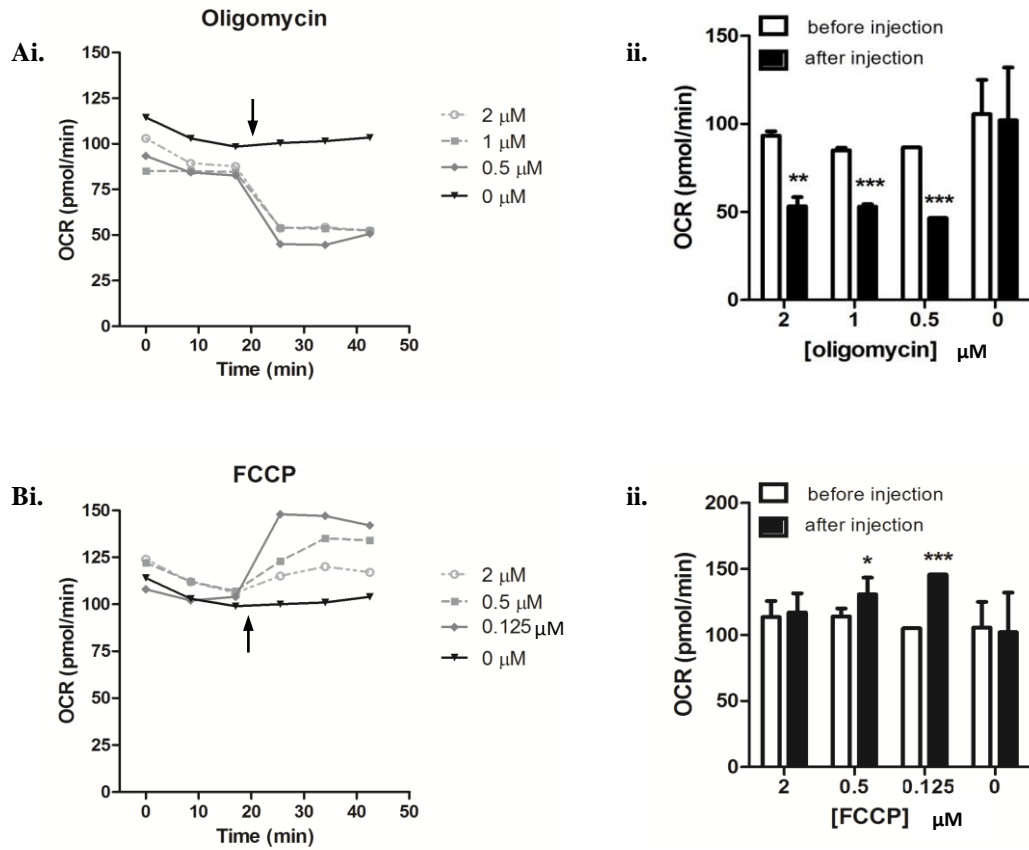


**Figure 3-16: Optimisation of oligomycin and FCCP concentrations for oxygen consumption rate (OCR) experiments**

HUVEC (65,000 cells/well) were seeded (as described in 2.2.6). Three OCR measurements were obtained prior to the addition of **A.** oligomycin (final concentration of 0 - 2  $\mu\text{M}$ ) and **B.** FCCP (final concentration of 0 - 2  $\mu\text{M}$ ) in a single reagent injection (arrow). A further three OCR measurements were then obtained. Values in **Ai.** and **Bi.** represent mean OCR (pmol/mL) for triplicate wells in a single experiment. **Aii.** and **Bii.** Mean OCR was determined for each well prior to and after the addition of oligomycin and FCCP. Bars represent the mean OCR  $\pm$  SEM for three wells before and after reagent addition, for a single experiment. \* $p < 0.05$  \*\* $p < 0.01$  and \*\*\* $p < 0.001$  compared to OCR before compound injection.

### Figure 3-17 Oxygen consumption rate profiles for HUVEC

Figure on facing page. HUVEC were seeded using the two-step method described in 2.2.6 and were transduced with **C.** Ad.GFP or **D.** Ad.AMPK-DN. Three hours after the addition of virus to the plate, cells were stimulated with VEGF (10 ng/mL) for a further 48 hours. OCR values were measured prior to reagent addition, and after the sequential addition of oligomycin (0.5  $\mu$ M), FCCP (0.125  $\mu$ M) and rotenone/antimycin A (0.5  $\mu$ M of both). **A.** An example OCR profile is shown and **B.** HUVEC used in **C.** and **D.** were lysed by the direct addition of SDS-PAGE sample buffer, vigorously scraped, and pooled according to the virus treatments received. Equal volumes of protein were resolved by SDS-PAGE/gel electrophoresis and immunoblotted using the antibodies indicated. The migration of molecular mass markers is indicated on the right. Data in **C.** and **D.** represents the mean OCR of triplicate measurements  $\pm$  SEM, for three independent experiments.

Figure 3-17

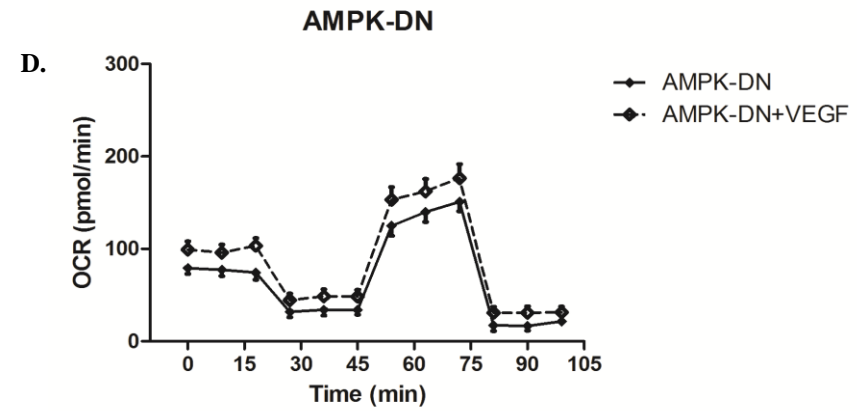
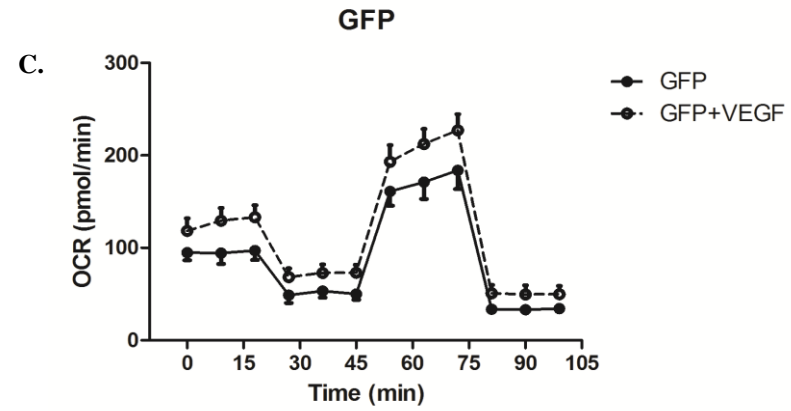
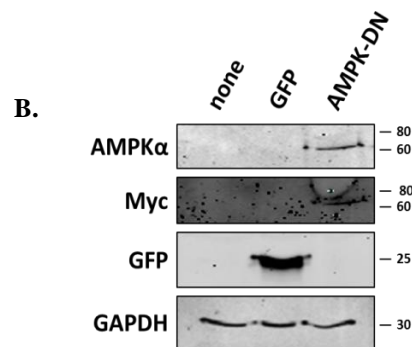
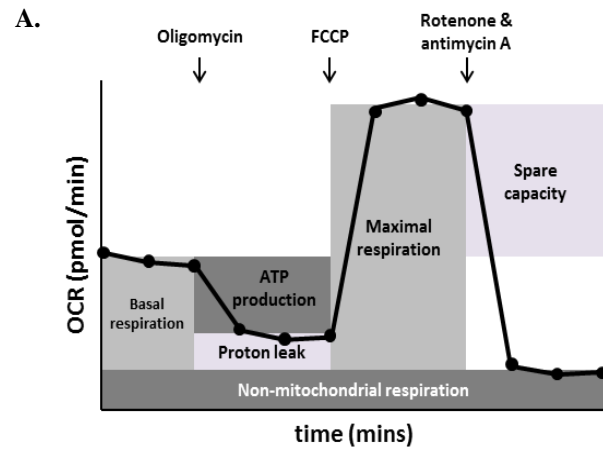


Figure 3-17: Oxygen consumption rate profiles for HUVEC

Legend on facing page

**Table 3-1: Numerical summary of data presented in Figure 3-17 – Effect of VEGF**

Numerical values demonstrating the effect of VEGF treatment ( $\Delta$ mean) on OCR (pmol/min) in GFP and AMPK-DN transduced HUVEC.  $\Delta(\Delta$ mean) indicates the difference in effect of VEGF for GFP vs AMPK-DN transduced HUVEC.

Time (min)	Mean OCR (pmol/min) $\pm$ SEM for 3 independent experiments						
	GFP	GFP +VEGF	$\Delta$ mean	AMPK-DN	AMPK-DN +VEGF	$\Delta$ mean	$\Delta(\Delta$ mean)
0	94.8 $\pm$ 1.6	118.4 $\pm$ 6.9	<b>+23.6</b>	79.1 $\pm$ 0.6	99.2 $\pm$ 3.0	<b>+20.1</b>	<b>-3.5</b>
9	94.3 $\pm$ 5.8	129.4 $\pm$ 6.5	<b>+35.1</b>	77.4 $\pm$ 1.6	95.9 $\pm$ 2.9	<b>+18.5</b>	<b>-16.6</b>
18	97.2 $\pm$ 4.9	133.0 $\pm$ 5.7	<b>+35.8</b>	74.4 $\pm$ 1.6	103.4 $\pm$ 1.8	<b>+29.0</b>	<b>-6.8</b>
27	49.6 $\pm$ 4.2	68.4 $\pm$ 4.3	<b>+18.8</b>	31.8 $\pm$ 0.5	44.4 $\pm$ 1.1	<b>+12.6</b>	<b>-6.2</b>
36	52.4 $\pm$ 3.0	73.0 $\pm$ 6.6	<b>+20.6</b>	34.0 $\pm$ 0.9	48.5 $\pm$ 1.8	<b>+14.5</b>	<b>-6.1</b>
45	49.5 $\pm$ 3.4	73.2 $\pm$ 5.3	<b>+23.8</b>	33.8 $\pm$ 1.1	48.4 $\pm$ 1.5	<b>+14.6</b>	<b>-9.2</b>
54	161.0 $\pm$ 2.0	193.2 $\pm$ 12.8	<b>+32.2</b>	125.0 $\pm$ 1.4	153.0 $\pm$ 7.2	<b>+28.0</b>	<b>-4.1</b>
63	171.2 $\pm$ 1.4	212.3 $\pm$ 10.4	<b>+41.1</b>	139.9 $\pm$ 0.9	162.0 $\pm$ 5.0	<b>+22.2</b>	<b>-18.9</b>
72	184.0 $\pm$ 0.7	227.2 $\pm$ 11.9	<b>+43.3</b>	151.0 $\pm$ 1.3	176.4 $\pm$ 5.0	<b>+25.4</b>	<b>-17.8</b>
81	34.2 $\pm$ 3.6	50.8 $\pm$ 4.7	<b>+16.5</b>	15.1 $\pm$ 2.7	30.8 $\pm$ 2.9	<b>+15.7</b>	<b>-0.9</b>
90	33.7 $\pm$ 3.4	49.7 $\pm$ 5.5	<b>+16.0</b>	15.7 $\pm$ 2.1	30.4 $\pm$ 3.9	<b>+14.7</b>	<b>-1.3</b>
99	34.6 $\pm$ 2.8	49.8 $\pm$ 4.9	<b>+15.2</b>	21.1 $\pm$ 1.8	31.2 $\pm$ 4.0	<b>+10.0</b>	<b>-5.2</b>

**Table 3-2: Numerical summary of data presented in Figure 3-17 – Effect of recombinant adenoviral transduction**

Effect ( $\Delta$ mean) of AMPK-DN vs GFP on OCR (pmol/min) in HUVEC, in the presence and absence of VEGF.

Time (min)	Mean OCR (pmol/min) $\pm$ SEM for 3 independent experiments					
	GFP	AMPK-DN	$\Delta$ mean	GFP +VEGF	AMPK-DN +VEGF	$\Delta$ mean
0	94.8 $\pm$ 1.6	79.1 $\pm$ 0.6	-15.8	118.4 $\pm$ 6.9	99.2 $\pm$ 3.0	-19.3
9	94.3 $\pm$ 5.8	77.4 $\pm$ 1.6	-16.9	129.4 $\pm$ 6.5	95.9 $\pm$ 2.9	-33.6
18	97.2 $\pm$ 4.9	74.4 $\pm$ 1.6	-22.8	133.0 $\pm$ 5.7	103.4 $\pm$ 1.8	-29.6
27	49.6 $\pm$ 4.2	31.8 $\pm$ 0.5	-17.8	68.4 $\pm$ 4.3	44.4 $\pm$ 1.1	-24.0
36	52.4 $\pm$ 3.0	34.0 $\pm$ 0.9	-18.3	73.0 $\pm$ 6.6	48.5 $\pm$ 1.8	-24.5
45	49.5 $\pm$ 3.4	33.8 $\pm$ 1.1	-15.7	73.2 $\pm$ 5.3	48.4 $\pm$ 1.5	-24.8
54	161.0 $\pm$ 2.0	125.0 $\pm$ 1.4	-36.1	193.2 $\pm$ 12.8	153.0 $\pm$ 7.2	-40.2
63	171.2 $\pm$ 1.4	139.9 $\pm$ 0.9	-31.4	212.3 $\pm$ 10.4	162.0 $\pm$ 5.0	-50.3
72	184.0 $\pm$ 0.7	151.0 $\pm$ 1.3	-33.0	227.2 $\pm$ 11.9	176.4 $\pm$ 5.0	-50.8
81	34.2 $\pm$ 3.6	15.1 $\pm$ 2.7	-19.1	50.8 $\pm$ 4.7	30.8 $\pm$ 2.9	-20.0
90	33.7 $\pm$ 3.4	15.7 $\pm$ 2.1	-18.0	49.7 $\pm$ 5.5	30.4 $\pm$ 3.9	-19.2
99	34.6 $\pm$ 2.8	21.1 $\pm$ 1.8	-13.5	49.8 $\pm$ 4.9	31.2 $\pm$ 4.0	-18.6

Figure 3-18

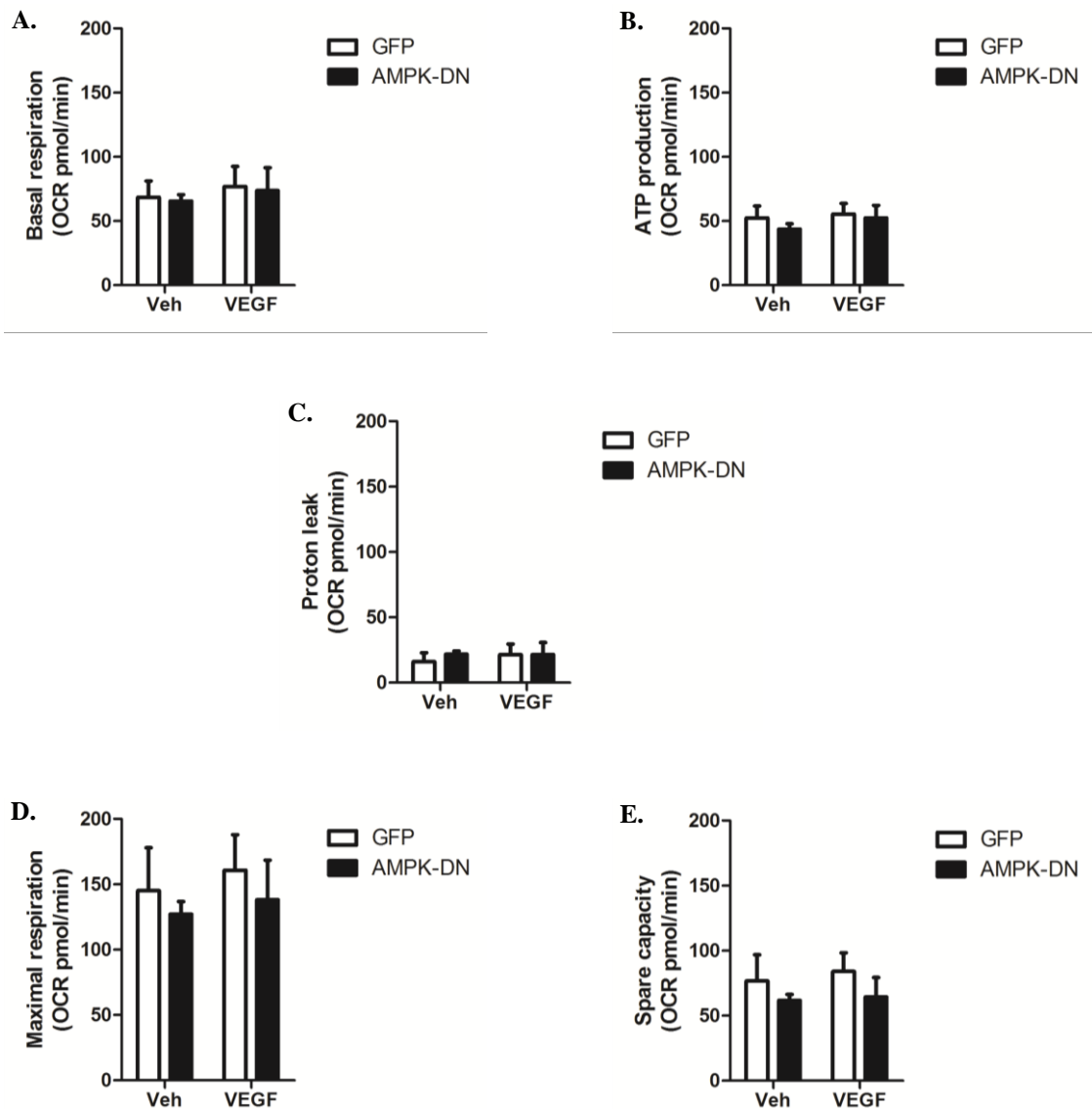


Figure 3-18: Key parameters of metabolism in HUVEC

Analysis of the data in Figure 3-17. C and D. calculating key parameters of mitochondrial metabolism. For each well, the mean OCR was calculated for each of the three measurements before any additions were made, and then after the sequential addition of oligomycin, FCCP, and a combination of rotenone and antimycin A. The mean of three wells were then used to calculate the key parameters of mitochondrial metabolism (as summarised in Figure 3-17A). **A.** basal respiration, **B.** ATP production, **C.** proton leak, **D.** maximal respiration and **E.** spare capacity for each of three independent experiments. Data represents the mean OCR for three independent experiments  $\pm$  SEM.

### 3.3 Discussion

Numerous reports suggest that AMPK is a viable therapeutic target for the treatment of cardiovascular disease however the activation of AMPK by VEGF, an essential growth factor is somewhat of a paradox. Previous studies report that AMPK activity is required for VEGF-stimulated endothelial cell proliferation, as measured by MTS assay, and migration (Reihill et al. 2011), effects in contrast to the anti-proliferative effects of AMPK activation by other agents *e.g.* AICAR, in the absence of growth factor stimulation (Igata et al. 2005). VEGF is also reported to promote local inflammation in VSMC (Koga et al. 2009), whereas AMPK activation by agents other than VEGF is reported to suppress inflammation and proliferation in VSMC (Ferri 2012). The specific activation of AMPK by VEGF may therefore facilitate, or permit endothelial cell proliferation and migration, while suppressing inflammation and proliferation in VSMC. This would be especially desirable in treating vascular pathologies such as restenosis, where the promotion of endothelial cell, but not VSMC proliferation is desired. We therefore sought to characterise the differential effects of AMPK activation by VEGF and AICAR, in order to determine the specific mechanisms by which AMPK is mediating VEGF-stimulated EC proliferation.

Two possible mechanisms explaining the opposing effects of VEGF and other AMPK activators such as AICAR, on cell proliferation are: 1. VEGF activates a different AMPK  $\alpha/\beta/\gamma$  isoform complex compared to other AMPK activators, or that 2. VEGF activates a discreet subcellular pool of AMPK and/or alters AMPK subcellular distribution to facilitate interaction with VEGF-specific signalling mediators. Targeting specific isoform containing complexes with pharmaceutical compounds is possible, as demonstrated by reports that A769662 activates only AMPK complexes containing the  $\beta 1$  subunit isoform (Scott et al. 2008). It is possible that VEGF specifically targets a specific isoform of the  $\alpha$ -catalytic subunit. AMPK  $\alpha 1$ -containing complexes contribute the vast majority of both basal and VEGF-stimulated AMPK activity in human vascular endothelial cells. This is consistent with previous reports that AMPK  $\alpha 1$  is the predominant isoform that is expressed and active in vascular cells (Schulz et al. 2005, Goirand et al. 2007, Zou et al. 2004). AICAR-stimulated AMPK activity is also mediated via  $\alpha 1$  containing complexes, making it unlikely that VEGF preferentially activates a particular  $\alpha$  isoform, different to that activated by other AMPK activators/mechanisms of activation.

Basal AMPK  $\alpha 1$  activity is reported to be a protective, redox-regulating element of vascular homeostasis. AICAR-induced activation of AMPK  $\alpha 1$ , but not  $\alpha 2$ , in VSMC

induces dose-dependent vasorelaxation in endothelium denuded aortic ring segments (Goirand et al. 2007). Furthermore in WT mice challenged with Ang II, AMPK activation protected the vasculature *in vivo* against superoxide production, inflammation and impaired endothelial function, a protective effect that was absent in *PRKAA1*<sup>-/-</sup> mice (Schuhmacher et al. 2011). A role for AMPK  $\alpha$ 2 in endothelial homeostasis cannot be excluded however. *PRKAA2*<sup>-/-</sup> mice are reported to demonstrate elevated expression of the subunits of NADPH-oxidase (p47<sup>phox</sup>, p67<sup>phox</sup>, gp91<sup>phox</sup> and Nox1 and -4), with an associated elevation in ROS levels (p22<sup>phox</sup> and p40<sup>phox</sup> levels were however not reported in this study) (Wang et al. 2010). AMPK  $\alpha$ 2 may therefore have a homeostatic role in suppressing vascular endothelial NADPH-oxidase expression and ROS generation.

Having determined that VEGF does not activate a different  $\alpha$  isoform-containing complex to that activated by AICAR, we assessed whether VEGF activated a specific subcellular pool of AMPK  $\alpha$ 1, and/or stimulated a change in the subcellular distribution of AMPK. Previous studies report that  $\alpha$ 2 containing complexes exhibit preferential nuclear localisation compared to  $\alpha$ 1 containing complexes, which are mostly cytosolic (Salt et al. 1998). The subcellular localisation of AMPK is reported to be sensitive to various stresses including heat shock, nutrient restriction and oxidants (Kodiha et al. 2007), and the cell cycle. It has been reported that AMPK complexes recruited to the cytokinetic apparatus of proliferating HUVEC exhibit distinct subunit isoform composition (Pinter et al. 2012). Furthermore, cellular fractionation identified enriched AMPK  $\alpha$ 1 in the cytoskeletal fraction whereas  $\alpha$ 2 was enriched in the cytosolic, cytoskeletal and membrane/particulate fractions, with lesser amounts found in the nucleus (Pinter et al. 2012). A number of reports now suggest that AMPK activation and function depend upon its subcellular localisation; studies in *Schizosaccharomyces pombe* report that the AMPK  $\alpha$  subunit homolog Ssp2 is phosphorylated at Thr189 (orthologous to Thr172) by the CaMKK homolog Ssp1, stimulating nuclear translocation and accumulation which is required for adaptation to nutritional stress (Valbuena and Moreno 2012). Aberrant AMPK  $\alpha$ 1 activation was also observed in the nuclei of striatal neurons of both mouse models and human patients with Huntington's disease, which was closely associated with mHtt-induced cell death (Ju et al. 2011). The authors of this study report that the activation and nuclear translocation of AMPK  $\alpha$ 1 suppresses Bcl2 expression promoting cell death, which was not observed in healthy control subjects (Ju et al. 2011).

Few reports agree on the subcellular distribution of AMPK in endothelial cells, we therefore assessed the basal and VEGF-stimulated subcellular distribution of AMPK  $\alpha$ 1

and  $\alpha 2$  containing complexes in human endothelial cells. Specific immunostaining and confocal imaging of  $\alpha 1$  and  $\alpha 2$  subunits suggests that  $\alpha 1$  containing complexes are localised to the perinuclear region of HAEC with lesser amounts diffusely distributed throughout the cytoplasm. Contrary to previous reports, AMPK  $\alpha 1$  was observed in the nucleus of HAEC, but exclusively absent in the nucleolus: this distribution pattern was confirmed using an independently sourced antibody recognising a different epitope of the  $\alpha 1$  subunit. Also in contrast to previous reports, substantial  $\alpha 2$  immunostaining was observed in the cytoplasm of HAEC, and appeared fibrous in nature: this was also confirmed using multiple anti-AMPK  $\alpha 2$  antibodies. Staining of actin with phalloidin revealed the characteristic filamentous staining pattern of actin fibres whereas tubulin exhibits a more delicate fibrous distribution, which is absent in the nucleus. The endoplasmic reticulum resident proteins protein disulphide isomerase (PDI) and heat shock protein 47 (Hsp47) were found to be concentrated in the perinuclear region and defined the subcellular extent of the ER; both PDI and Hsp47 were excluded from the nucleus as would be expected for ER resident proteins.

Co-staining of HAEC for  $\alpha 1$  and either PDI or Hsp47 indicates that AMPK  $\alpha 1$  is resident in the ER of sub confluent HAEC. Furthermore, acute and chronic VEGF treatment appears to have no obvious effect on AMPK distribution, with substantial amounts found in both the ER and nucleus (but not the nucleoli) in both the presence and absence of VEGF, however given the rapid nature of AMPK activation by VEGF we might have missed potential rapid, reversible changes in distribution of AMPK using this method.

By its very nature, the vascular endothelium is required to be a confluent monolayer of endothelial cells. Basal AMPK activity is reported to increase in keratinocytes as they approach confluence suggesting that AMPK is an endogenous inhibitor of proliferation (Saha et al. 2006). We have not assessed AMPK activity in cells at different densities during the current study, all experiments were performed when cells were >95 % confluent, however we did assess the distribution of AMPK  $\alpha 1$  in HAEC which had been cultured to confluence. Intriguingly, AMPK  $\alpha 1$  was found to be concentrated in the Golgi apparatus of confluent cells, as indicated by co-staining with the Golgi resident protein GM130. Furthermore, when confluent HAEC are subjected to ‘wounding’, two distinct populations with differential  $\alpha 1$  distributions were observed; ER resident  $\alpha 1$  in cells which had migrated into, or were adjacent to the wound, and Golgi resident AMPK  $\alpha 1$  in confluent cells remote from the wounded area.

The reversible redistribution of protein from the cytosol to Golgi apparatus has been reported previously. Herbert and colleagues reported that cytosolic phospholipase A<sub>2</sub>- $\alpha$  (cPLA<sub>2</sub> $\alpha$ ) is redistributed in HUVEC when cells are cultured to confluence and mature cell-cell contacts are established (Herbert et al. 2005). Furthermore, the activity of cPLA<sub>2</sub> $\alpha$  is reported to be inhibited by 87 % when associated with the Golgi apparatus, and this is a characteristic of contact-inhibition in endothelial cells, given that cPLA<sub>2</sub> $\alpha$  relocation and activation is required for the induction of Ki67 expression and entry into the cell cycle (Herbert et al. 2005). The reversible redistribution of cPLA<sub>2</sub> $\alpha$  has also been reported to be dependent upon the formation of VE-cadherin/ $\alpha$ -catenin/PAR3 complexes, facilitating the attachment of filamentous actin and subsequent direction to the Golgi apparatus (Odell et al. 2011). Additionally, a distinction was made between VEGF-A-stimulated signalling and cPLA<sub>2</sub> $\alpha$  localisation. VEGF-R2 activation and downstream signalling did not contribute to the relocation of cPLA<sub>2</sub> $\alpha$  to the Golgi, nor did depletion of cPLA<sub>2</sub> $\alpha$  affect short term VEGF-R2 signalling (>60 min) (Odell et al. 2011). At this time we can only speculate as to why AMPK  $\alpha$ 1 is localised in the ER when sub-confluent, and transported to the Golgi body upon reaching confluence but further studies into the significance of this are certainly warranted. There is evidence that AMPK is involved in regulating the cell cycle and sensing cell density, it therefore remains feasible that AMPK acts as a sensor to diminish cell proliferation when cells near confluence as has been previously suggested (Saha et al. 2006), and that this redistribution represents a mechanism for regulating AMPK activity/interactions when switching to this quiescence phenotype as has previously been reported for cPLA<sub>2</sub> $\alpha$  (Herbert et al. 2005, Odell et al. 2011).

So far we have shown that AMPK  $\alpha$ 1 accounts for the vast majority of VEGF-stimulated AMPK activity in vascular endothelial cells, and that this is also the case under basal and AICAR-stimulated conditions. Furthermore, we report that AMPK  $\alpha$ 1 appears to reside within the ER and nucleus whereas AMPK  $\alpha$ 2 appears to be associated with a structural cellular component. VEGF treatment doesn't stimulate a substantial redistribution of AMPK, however confluency does. Given these findings, we reassessed the previous reports that AMPK is required for VEGF-stimulated endothelial cell proliferation (Reihill et al. 2011). Consistent with this previous report, infection of HUVEC with Ad.AMPK-DN prevents VEGF-stimulated HUVEC proliferation when assessed by MTS assay. However, when assessed using the real-time RTCA xCELLigence system, expression of dominant negative AMPK had no effect on VEGF-stimulated HUVEC proliferation. Furthermore, assessment of the raw data generated during the xCELLigence experiments actually indicates that rather than stimulating cell proliferation by significantly increasing the cell

index, VEGF prevents cell death under nutrient deprived conditions, without significantly increasing the cell index.

This finding demonstrates that expressing end point assay data relative to the absence of VEGF does indeed suggest that VEGF stimulates cell proliferation despite there being no absolute increase in cell number. Unfortunately, due to factors beyond our control, data from a third replicate was not available for inclusion in the present analysis, and is something that is worth repeating and including at a later date. The current data however, suggests that the effect of Ad.AMPK-DN on cell proliferation depends on the technique used to measure proliferation and how data is interpreted. The MTS based assay relies on the conversion of a tetrazolium compound to form a coloured formazan compound that is soluble in tissue culture media, presumed to be accomplished by NADPH or NADH produced by dehydrogenase enzymes in metabolically active cells (Berridge and Tan 1993). The change in absorbance at 490 nm is reported to be directly proportional to the number of cells present, however this assay technically measures the metabolic capacity of the cells present in a well and as such would not necessarily distinguish between an increase in the metabolic capacity of a given number of cells, and an increase in the number of cells present but with no change in their metabolic activity. The RTCA xCELLigence system however measures the area of a well occupied by cells, although is again limited by a lack of distinction between cell proliferation and cell spreading. Together however, these data suggest that VEGF has an AMPK-dependent effect on HUVEC metabolism, without affecting the area occupied by cells (either changes in cell number or cell spreading). Endothelial cells from  $VEGF^{lox/lox}$  mice that were isolated and treated with Ad.Cre *in vitro*, demonstrated reduced basal glucose consumption, lactate production and triglyceride synthesis, in addition to reduced basal OCR and mitochondrial respiratory capacity in both the presence and absence of serum. Furthermore HUVEC subjected to siRNA-mediated VEGF knockdown exhibited fragmented mitochondria (indicated by Hsp60 staining) (Domigan et al. 2015), indicating that depletion of VEGF has detrimental effects on metabolism in the vasculature. Although anaerobic glycolysis appears sufficient to support the low metabolic demands of quiescent non-proliferating cells under aerobic conditions and where nutrients are in excess (Davidson and Duchon 2007), there are reports that anaerobic glycolysis can be supported or indeed replaced to some extent by the utilisation of fatty acids and glutamine as energy sources (Unterluggauer et al. 2008, Dagher et al. 2001), such that aberrant mitochondrial activity has the capacity to significantly affect HUVEC cell energetics.

We therefore hypothesised that AMPK is required for an element(s) of VEGF-stimulated mitochondrial function, which at this time is poorly characterised in human vascular endothelial cells. We went on to assess the AMPK dependence of a number of mitochondrial metabolic parameters using the XF Seahorse platform and Mito Stress Test kit. Optimisation experiments indicated that 65,000 cells per well are required to achieve oxygen consumption rates (OCR) within the range required to perform the XF Cell Mito Stress Test consistent with previous reports (Domigan et al. 2015), however it must be noted that this is a much higher cell density than that used in the previous proliferation experiments. It was also determined that 0.5  $\mu\text{M}$  of oligomycin and 0.125  $\mu\text{M}$  FCCP were the optimal concentrations for inhibiting complex V and uncoupling oxygen consumption from ATP production respectively, the lowest concentrations tested. Given that the experimental OCR values continued to rise after the addition of FCCP however suggests a delay for the full effect of FCCP to be achieved, which was not evident during the initial optimisation experiments, but could represent a window of recovery from the effects of the oligomycin. In two of the three Mito Stress Test experimental replicates, chronic VEGF treatment increased OCR at all the time points assessed in cells transduced with Ad.GFP. At the same time VEGF no longer increased OCR in cells transduced with Ad.AMPK-DN. When put together these data suggest that VEGF tends to increase HUVEC OCR, and that this effect is suppressed by prior infection with Ad.AMPK-DN. However, neither the VEGF-stimulated increase in OCR, nor its suppression by infection with Ad.AMPK-DN reached statistical significance. Increasing the number of experimental replicates may clarify whether this is in fact the case or not. Furthermore, VEGF did not significantly alter any of the metabolic parameters calculated (basal respiration, ATP production, proton leak, maximal respiration or spare capacity) but this is not unexpected given the vertical shift in all points of the OCR profile in response to VEGF. This suggests that VEGF increases overall mitochondrial activity, rather than a specific mitochondrial complex. To assess the relative expression of the mitochondrial complexes between treatments, lysates prepared from cells used in the Mito Stress Test were lysed and assessed by immunoblotting. We readily detected complex I, VI and V, however observed far lower immunoreactivity for complexes II and III. Together these data suggest that inhibiting AMPK activation by VEGF, using Ad.AMPK-DN, does not affect the expression of a single mitochondrial complex, but may still affect overall mitochondrial activity, potentially by influencing mitochondrial mass. We therefore also assessed whether mitochondrial mass and/or morphology might be altered in response to VEGF by fluorescence imaging. Using this method however it was not apparent whether VEGF treatment, or the presence or absence of serum in the culture media affected mitochondrial mass. The major limitation of using

this method is that assessing fluorescence and the fraction of the cell occupied by fluorescence is subjective. Furthermore, dyes previously used in the assessment of mitochondrial mass and thought to be membrane potential independent may in fact depend upon mitochondrial membrane potential (Gohil et al. 2005). Obtaining Z-stacks and assembling high resolution 3D models of mitochondria within individual cells or using transmission electron microscopy may provide more accurate ways of assessing mitochondrial volume (Medeiros 2008), and is something that should be considered optimising in the future.

Long term (6 hr) VEGF exposure caused the induction of several nuclear encoded mitochondrial genes in HUVEC, including COX8, TIM23 and TOM70 (Wright et al. 2008). Furthermore, VEGF has been linked to PGC-1 $\alpha$  activity *via* Akt3-dependent nuclear trafficking. Interestingly, VEGF is however reported to have no effect on PGC-1 $\alpha$  expression, and furthermore Wright and co-workers were not able to detect a direct interaction between Akt3 and PGC-1 $\alpha$  (Wright et al. 2008). AMPK activation is also reported to promote mitochondrial biogenesis and respiration in muscle, *via* PGC-1 $\alpha$  induced gene transcription (Jäger et al. 2007). The AMPK activators metformin and AICAR are reported to significantly inhibit mtROS production by stimulating increased MnSOD expression. Furthermore, metformin and AICAR induced the expression of NRF-1 and mtTFA mRNA, increased mitochondrial DNA content, and the absolute mitochondrial number; all these effects are reported to be inhibited by overexpression of dominant-negative AMPK (Kukidome et al. 2006), such that it would be interesting to assess whether VEGF has similar effects. Given the link between AMPK and mitochondrial biogenesis, it seems reasonable to speculate that as VEGF stimulates cell proliferation, the metabolic demands of endothelial cells increases, which can be compensated for to some degree by AMPK-regulated mitochondrial biogenesis. In the absence of functional AMPK, cells may no longer be able to compensate for the increased metabolic demand in response to VEGF. The methods we have employed here are not able to resolve mitochondrial morphology sufficiently to assess mitochondrial mass, but this might be assessed in the future using transmission electron microscopy. Furthermore, assessing the expression of genes such as PGC-1 $\alpha$ , NRF-1 and mtTFA in addition to mtDNA content should also be considered.

### 3.4 Conclusion

These data indicate that AMPK  $\alpha 1$  accounts for the vast majority of both basal and VEGF/AICAR-stimulated AMPK activity in human vascular endothelial cells. Furthermore, VEGF does not appear to alter the subcellular localisation of AMPK, suggesting that VEGF does not redistribute AMPK in order to facilitate binding with unique substrates. Data presented here also suggests that AMPK  $\alpha 1$  is concentrated in the Golgi apparatus of cells when they are cultured to near 100 % confluence, which may represent a mechanism of regulating AMPK activity.

Previous studies using the MTS assay may have generated misleading results, as the assay is essentially a measure of the cells metabolic activity, not absolute cell number. Conflicting data obtained using the RTCA xCELLigence system suggests that a direct measure of cell proliferation such as [<sup>3</sup>H]-thymidine or BrdU incorporation should be performed. At this time, the available data suggests that VEGF is actually promoting cell survival rather than proliferation in serum deprived endothelial cells.

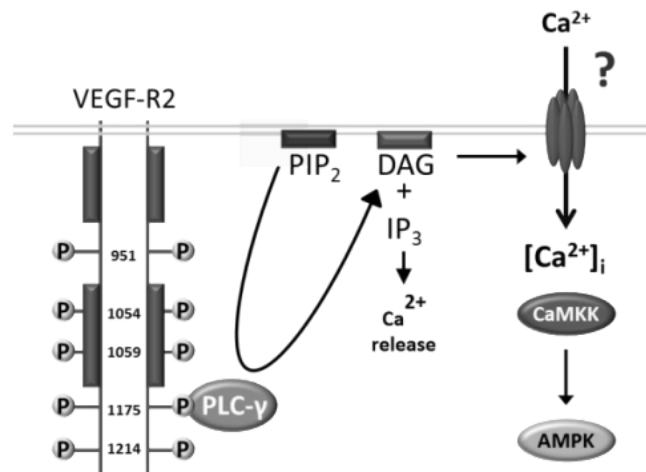
We also assessed cellular oxygen consumption using the Seahorse Mito Stress Test. Initial experiments suggest that VEGF increases all aspects of mitochondrial activity, as seen by a vertical shift in the OCR profile. There is a suggestion that whatever this effect of VEGF on OCR is, it may be dependent on AMPK, although further experiments are required to elucidate this.

## **Chapter 4 - Investigating the mechanism by which VEGF stimulates increased $[Ca^{2+}]_i$ and AMPK activation**

## 4.1 Introduction

Increasing the concentration of intracellular calcium ( $[Ca^{2+}]_i$ ) represents a fundamental mechanism by which VEGF stimulates endothelial cell proliferation and vascular permeability (Bates et al. 2001, Becker et al. 2001, Cullen et al. 2000). Binding of VEGF to its receptor stimulates PLC $\gamma$ -induced PIP<sub>2</sub> hydrolysis resulting in the generation of IP<sub>3</sub> and diacylglycerol (DAG). IP<sub>3</sub> stimulates Ca<sup>2+</sup> release via the IP<sub>3</sub> receptor (IP<sub>3</sub>R) on the endoplasmic reticulum, whereas DAG resulting from PIP<sub>2</sub> hydrolysis remains associated with the plasma membrane, signalling via downstream signalling cascades such as PKC, and stimulating the influx of extracellular Ca<sup>2+</sup> via DAG-sensitive Ca<sup>2+</sup> channels (Bates and Harper 2002). Increases in VEGF-stimulated endothelial permeability have previously been shown to be inhibited by prior treatment with anti-VEGF-R2 antibodies, the PLC inhibitor U-73122 (Wu et al. 1999), and calcium chelation by BAPTA-AM (Jho et al. 2005), indicating that endothelial cell permeability is regulated via a VEGF-R2, PLC $\gamma$  and Ca<sup>2+</sup>-dependent mechanism.

VEGF has previously been shown to activate AMPK in human vascular endothelial cells (Reihill et al. 2007). VEGF-stimulated AMPK activation was later shown to be dependent on CaMKK activation (Reihill et al. 2007), the influx of extracellular Ca<sup>2+</sup>, and not affected by LKB1 or IP<sub>3</sub>R antagonism (Reihill 2009). In addition to this, the phospholipase C inhibitor U-73122 inhibited VEGF-stimulated AMPK activation (Reihill et al. 2007), as did hyperpolarisation of the cells by replacing 60 mM of extracellular Na<sup>+</sup> with K<sup>+</sup> (Reihill 2009). The DAG mimetic OAG was also shown to activate AMPK in a manner that is similarly sensitive to CaMKK inhibition and cell hyperpolarisation (Reihill 2009). Together these findings suggest that VEGF, via PLC $\gamma$ , stimulates the production of DAG which then causes the influx of extracellular Ca<sup>2+</sup> via DAG-regulated cation channels (which can be inhibited by cell hyperpolarisation), subsequently activating CaMKK and AMPK (Figure 4-1).

**Figure 4-1****Figure 4-1: Proposed mechanism of AMPK activation by VEGF**

VEGF has previously been shown to activate AMPK in a PLC $\gamma$ , extracellular Ca<sup>2+</sup> and CaMKK $\gamma$ -dependent manner which is independent of both IP<sub>3</sub>-stimulated Ca<sup>2+</sup> release and LKB1 activation.

The identity of the calcium channel mediating VEGF-stimulated Ca<sup>2+</sup> influx and activation of AMPK however remains unclear. In non-excitable cells such as endothelial cells, Ca<sup>2+</sup> influx typically occurs via voltage-independent calcium channels; endothelial cells express several different types of voltage-independent non-selective cation channels including members of the cyclic gated nucleotide-gated channels, P2X purinoceptor subfamilies and transient receptor potential (TRP) cation channels, a subset of which (TRPCs 3,6 and 7) are directly regulated by DAG (Hofmann et al. 1999).

There is an ever-expanding body of evidence proposing a role for TRPCs in mediating VEGF/VEGF-R2-mediated Ca<sup>2+</sup> influx. Overexpression of TRPC6 was sufficient to enhance HUVEC proliferation in the absence of VEGF, whereas TRPC6 inhibition with SKF96365 prevented VEGF-stimulated HUVEC proliferation and caused cell cycle arrest at G<sub>2</sub>/M (Ge et al. 2009). Furthermore, SKF96365 caused inhibition of VEGF-induced angiogenesis *in vitro* (assessed by tube length and number of branch points) (Ge et al. 2009). This is in agreement with a previous report that expression of dominant negative TRPC6 in human microvascular endothelial cells (HMVEC) inhibits VEGF-stimulated HMVEC migration, sprout formation and reduces the percentage of cells in S-phase when treated with VEGF (Hamdollah Zadeh et al. 2008). Expression of dominant-negative TRPC6 also inhibited OAG-stimulated Ca<sup>2+</sup> entry (Hamdollah Zadeh et al. 2008). Frog mesenteric vessels which demonstrated increased permeability in response to VEGF treatment responded in a similar manner when stimulated with OAG, and this was not

dependent on PKC (Pocock et al. 2004) suggesting that VEGF and OAG might share a common mechanism to stimulate  $\text{Ca}^{2+}$  influx.

In HEK-293 cells co-transfected with VEGF-R2 and TRPC6, VEGF stimulation resulted in a robust  $\text{Ca}^{2+}$  transient similar to that measured *in vivo*, which was not present in cells transfected with either VEGF-R2 or TRPC6 alone suggesting a link between VEGF-R2 and TRPC-mediated  $\text{Ca}^{2+}$  influx (Pocock et al. 2004). This is in agreement with other studies reporting that co-transfection of CHO cells with VEGF-R2 and either TRPC6 or TRPC3 made these cells sensitive to VEGF stimulation (Cheng et al. 2006). In co-transfected cells VEGF-induced  $\text{Ca}^{2+}$  influx which was not observed when VEGF-R2 or the TRPC channels were expressed alone (Cheng et al. 2006).

Evidence suggesting a mechanism linking VEGF-R2 activation and TRPC  $\text{Ca}^{2+}$  influx is however not limited to TRPC6 and 3. TRPC4 expression was demonstrated to be elevated during hypoxia in human retinal microvascular endothelial cells (HRMEC), and siRNA-mediated suppression of TRPC4 expression prevented VEGF-induced retinal neovascularisation in a mouse model of oxygen-induced retinopathy and VEGF-stimulated angiogenesis in HRMEC *in vitro* (Song et al. 2015). It has also been suggested that TRPC-mediated VEGF-induced  $\text{Ca}^{2+}$  influx is not limited to mature vascular endothelial cells. A population of  $\text{CD133}^+$  adipose-resident immature endothelial progenitor stem cells were shown to express both VEGF-R2 and TRPC3. VEGF-stimulated  $\text{Ca}^{2+}$  transients in these cells were shown to be inhibited by  $\text{Gd}^{3+}$  or expression of a dominant negative TRPC3 fragment (Poteser et al. 2008).

In addition to the evidence supporting a role for TRPCs in VEGF-induced  $\text{Ca}^{2+}$  influx, TRPCs have also been shown to regulate AMPK activity. TRPC channels have been proposed to be a necessary component of thrombin-stimulated AMPK activation via  $\text{CaMKK}\beta$  activation (Bair et al. 2009) and more recently, in the presence of serum, *trans*-3,4,5-trimethoxy-stilbene, a methylated derivative of resveratrol, has been shown to induce autophagy via TRPC4-mediated  $\text{Ca}^{2+}$  influx in vascular endothelial cells. This  $\text{Ca}^{2+}$  influx was shown to stimulate the activation of  $\text{CaMKK}$  and AMPK, subsequently suppressing mTOR resulting in autophagy initiation (Zhang et al. 2015).

Other  $\text{Ca}^{2+}$  channels have been implicated in VEGF-stimulated endothelial cell  $\text{Ca}^{2+}$  influx. VEGF-R2 activation has been proposed to stimulate the synthesis of the incompletely characterised second messenger NAADP, which stimulates two-pore channel (TPC)-

dependent  $\text{Ca}^{2+}$  release from acidic intracellular  $\text{Ca}^{2+}$  stores (Favia et al. 2014). The authors further suggest that NAADP-dependent increases in  $[\text{Ca}^{2+}]_i$  and resulting downstream signalling contribute towards the angiogenic effects of VEGF.

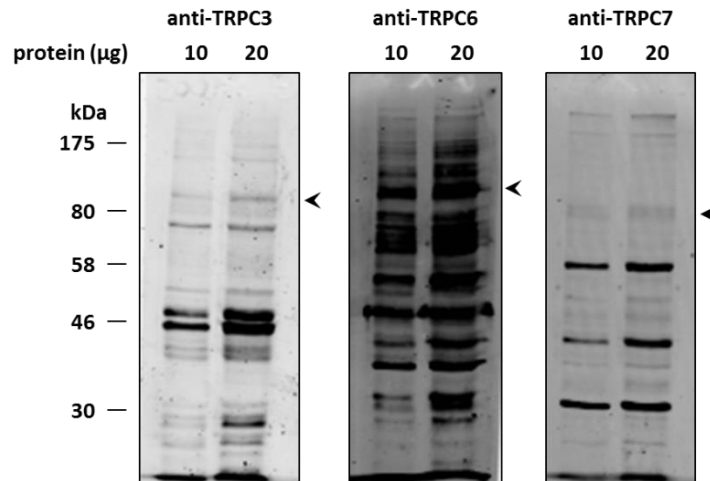
Given the dependence of VEGF-stimulated AMPK activation on extracellular  $\text{Ca}^{2+}$  influx, and that OAG mimics the effects of VEGF stimulation on AMPK, we sought to determine whether the DAG-sensitive TRPC channels (TRPCs 3, 6 and 7) mediate AMPK activation by VEGF. Data presented in this chapter therefore aims to clarify the isoform-specific expression of TRPC channels in cultured human vascular endothelial cells and to determine the specificity of pharmacological agents reported to be selective modulators of TRPC channel activity, with the aim of measuring the effect of inhibiting the activity of these channels on VEGF-stimulated AMPK activation. We also sought to determine the role of NAADP dependent  $\text{Ca}^{2+}$  release from acidic intracellular stores in the mechanism of AMPK activation by VEGF.

## 4.2 Results

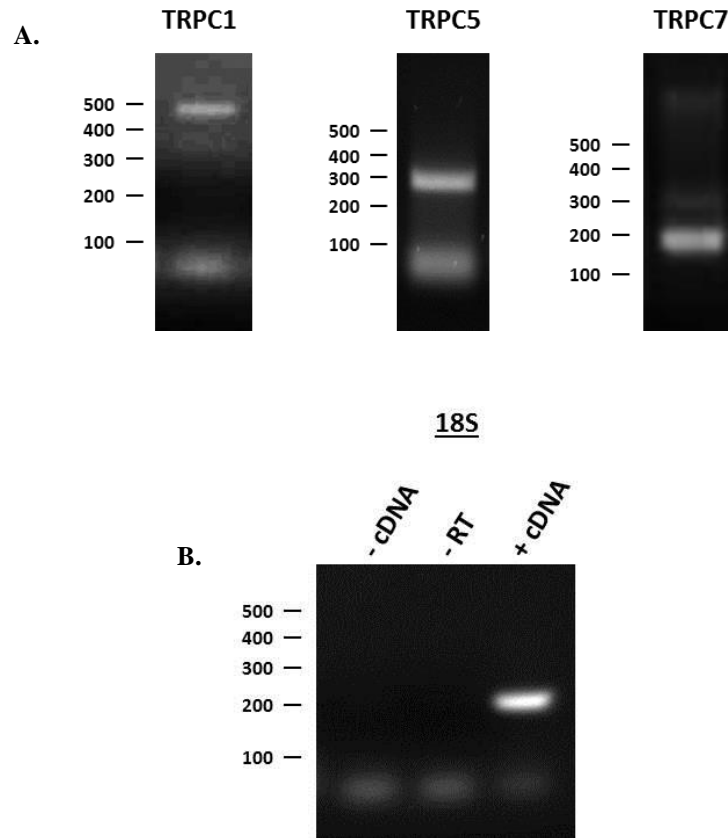
To assess the expression of TRPC channels in human vascular endothelial cells, immunoblot analysis was performed using commercially available antibodies recognising specific TRPC channel isoforms. Immunoblot analysis of HAEC lysates identified bands of the predicted molecular mass for the TRPC channels 3, 6 and 7 indicated by arrow heads in Figure 4-2 (97, 110 and 100 kDa respectively). However, antibodies commercially available at the time of this study also showed unacceptably high levels of non-specific immunoreactivity when used for immunoblotting (Figure 4-2).

To assess the expression of TRPC channels at the level of mRNA, RNA was also isolated from early passage HAECs and reverse transcription performed to synthesise cDNA. Reverse transcriptase PCR (RT-PCR) and quantitative real-time PCR (qRT-PCR) was then performed using the HAEC cDNA as the template. RT-PCR generated PCR products of the predicted size when primers designed to detect TRPCs 1, 5 and 7 were used (505, 325 and 187 base pairs respectively) (Figure 4-3). No PCR products were amplified when primers designed to detect TRPCs 3, 4 or 6 were used, despite a PCR product for the 18S ribosomal subunit being amplified from the same cDNA templates.

qRT-PCR also failed to detect expression of the DAG-sensitive TRPC channels 3, 6 and 7 however GAPDH expression was detected in all reactions, with Ct values of between 15 and 20 cycles. Additionally TRPC channel 3, -6 and -7 mRNA was detected, with the same TaqMan® probes, when using template cDNA synthesised from RNA isolated from human testes, with Ct values of between 37 and 38 (data not shown).

**Figure 4-2****Figure 4-2: Immunoblotting assessment of TRPC expression in HAEC**

HAEC were cultured and when confluent, the cells were washed briefly and lysates prepared. 10 or 20 µg of total cellular protein was subjected to SDS-PAGE and immunoblotting with the antibodies indicated. The predicted molecular mass of TRPCs 3, 6 and 7 are 97, 110 and 99 kDa respectively; arrowheads indicate corresponding bands. The migration of molecular mass markers is indicated on the left. Image shown is representative of immunoblots from three HAEC donors.

**Figure 4-3****Figure 4-3: Reverse transcriptase PCR assessment of TRPC expression in HAEC**

RNA was isolated from HAEC and used as a template to synthesise cDNA. RT-PCR was performed using the resultant cDNA as the template. **A.** Primers designed to amplify TRPCs 1 to 7 (with the exception of TRPC2) were tested. **B.** All experiments included positive control (detection of 18S RNA), and negative controls (no cDNA added to PCR reaction) and a genomic DNA control (no reverse transcriptase added to reverse transcription reaction) for all targets assessed (*e.g.* lower panel). Image shown is representative of TRPC1, 5 and 7 expression measured in four, three and a single experiment respectively. The migration of molecular mass markers is indicated on the left of each image.

Having experienced difficulties in measuring TRPC protein and mRNA expression, pharmacological agents reported to selectively modulate the activity of TRPC channels were therefore investigated. Hyperforin, a bicyclic polyprenylated acylphloroglucinol derivative, is reported to selectively activate TRPC6 (Leuner et al. 2007). Hyperforin (1  $\mu\text{M}$ , 5 min) stimulated a 2.3-fold increase in AMPK Thr172 phosphorylation, with comparable potency at 2.5  $\mu\text{M}$  (5 min) and 5  $\mu\text{M}$  when added for 5, 10 or 15 min (Figure 4-4). All subsequent experiments therefore used hyperforin at a concentration of 1  $\mu\text{M}$  for 5 min.

The sensitivity of hyperforin-stimulated AMPK phosphorylation to the CaMKK inhibitor STO-609 and to the removal of extracellular calcium was subsequently assessed. Hyperforin-stimulated AMPK Thr172 phosphorylation was not affected by either prior treatment with STO-609 (Figure 4-5) or the removal of extracellular  $\text{Ca}^{2+}$  (Figure 4-6). VEGF-stimulated AMPK Thr172 phosphorylation was inhibited by STO-609 treatment at a concentration that had no effect on AICAR-stimulated AMPK Thr172 phosphorylation (Figure 4-5). VEGF-stimulated AMPK Thr172 phosphorylation was inhibited, whereas AICAR-stimulated AMPK Thr172 phosphorylation was not affected, by the removal of extracellular  $\text{Ca}^{2+}$  (Figure 4-6).

Pyr3 and ML-9, the reported inhibitors of TRPC channels 3 and 6 respectively (Shi et al. 2007, Kiyonaka et al. 2009) had no effect on VEGF- or AICAR-stimulated AMPK Thr172 phosphorylation (Figure 4-7), however due to the calcium and CaMKK independent effects of hyperforin, a specific positive control for these inhibitors has been difficult to identify.

Figure 4-4

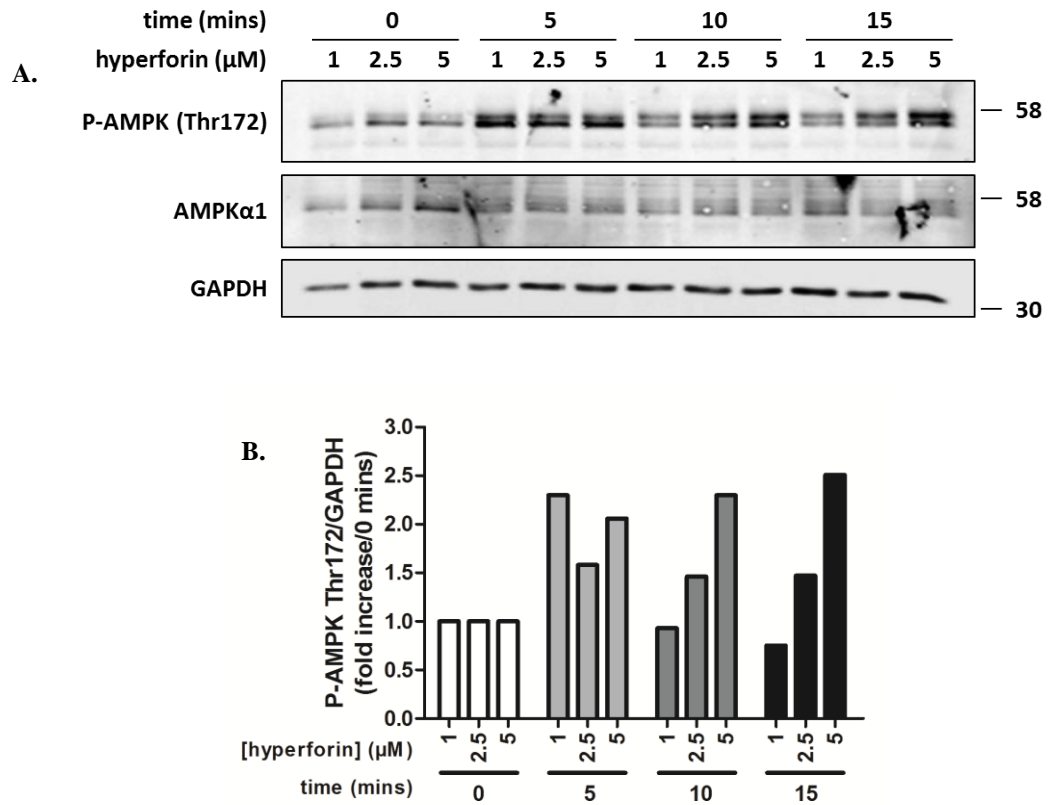
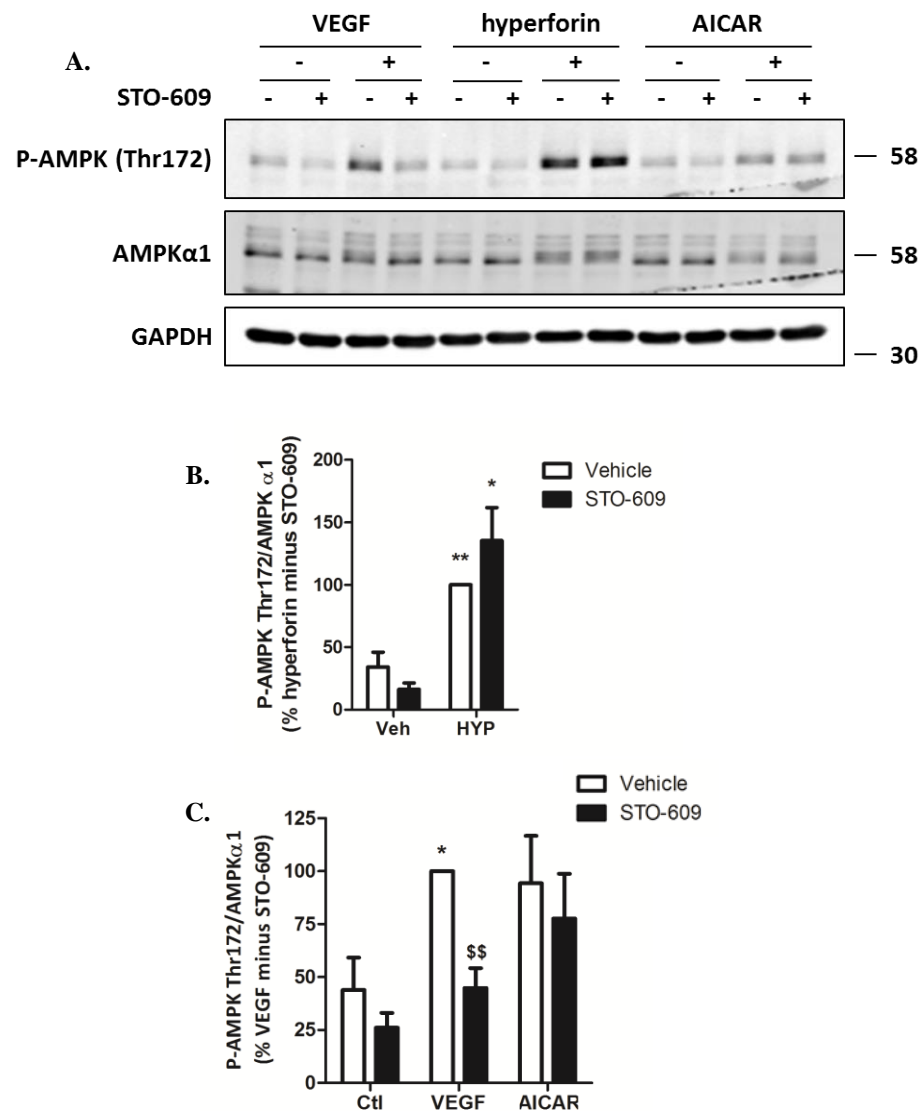


Figure 4-4: Hyperforin stimulates AMPK Thr172 phosphorylation

HAEC were stimulated with increasing concentrations of hyperforin (1, 2.5 or 5  $\mu\text{M}$ ) for the durations indicated before cell lysates were prepared. Cell lysates were then subjected to SDS-PAGE and immunoblotting using the primary antibodies as indicated in **A**. The migration of molecular mass standards are indicated on the right. **A**, the immunoblot and **B**, quantification of pixel density is shown for a single experiment.

Figure 4-5



**Figure 4-5: Hyperforin-stimulated AMPK Thr172 phosphorylation is not sensitive to STO-609**

HAEC were pre-treated with STO-609 (1  $\mu$ M) for 60 min. Cells were then stimulated with VEGF (10 ng/mL, 5 min), hyperforin (1  $\mu$ M, 5 min) or AICAR (2 mM, 45 min) and cell lysates prepared. Lysates were subjected to SDS-PAGE and immunoblotting using the primary antibodies as indicated. **A.** Image shown is representative of three independent experiments. The migration of molecular mass standards are indicated on the right. **B.** and **C.** Data are presented as mean pixel density  $\pm$  SEM, for three independent experiments in each case. \*\* $p$ <0.01 and \* $p$ <0.05 vs absence of hyperforin or VEGF, \$\$ $p$ <0.01 vs absence of STO-609.

Figure 4-6

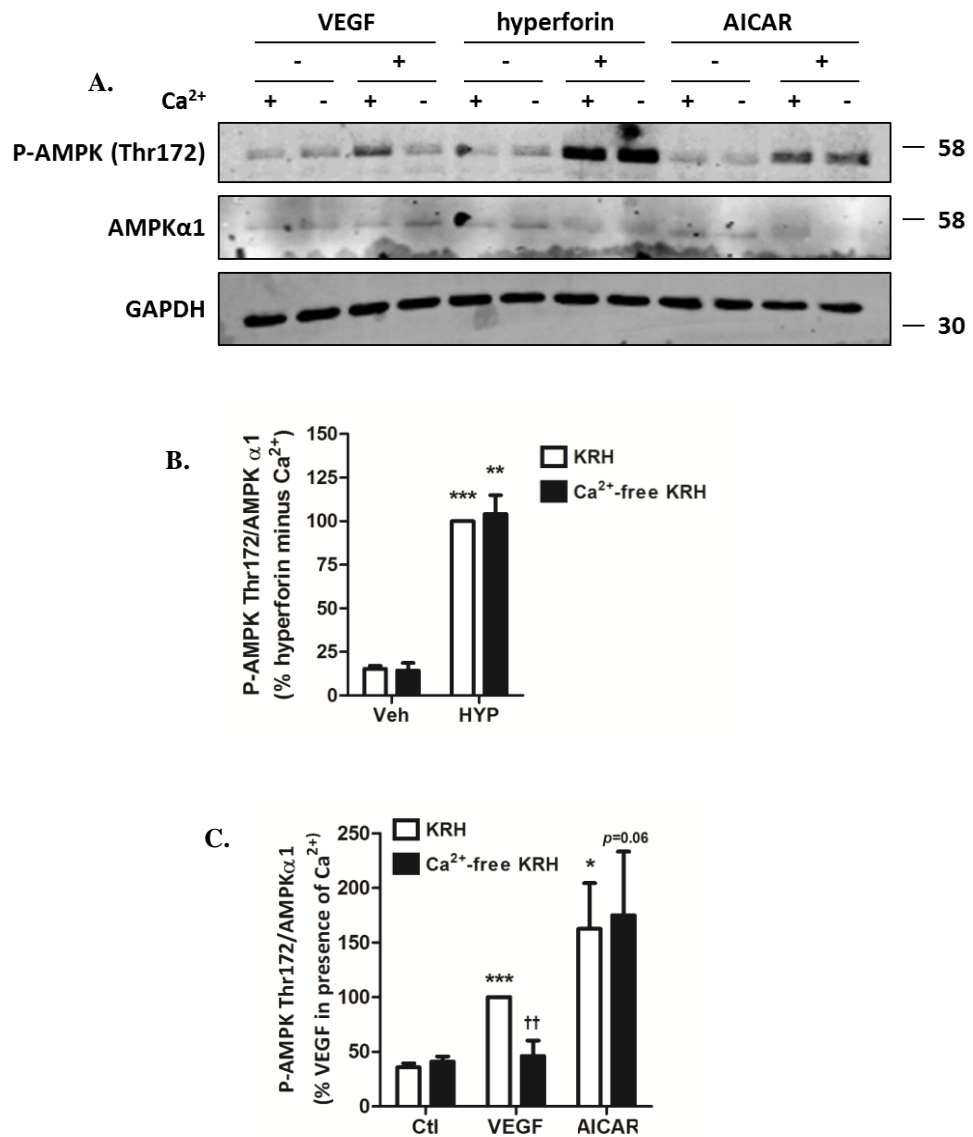


**Figure 4-6: Hyperforin-stimulated AMPK Thr172 phosphorylation is not sensitive to the removal of extracellular calcium**

HAEC were quiesced in KRH with the addition of 2.5 mM CaCl<sub>2</sub> or KRH with no Ca<sup>2+</sup> with the addition of 1 mM EGTA prior to stimulation with VEGF (10 ng/mL, 5 min), hyperforin (1 μM, 5 min) or AICAR (2 mM, 45 min). Cell lysates were prepared and subjected to SDS-PAGE and immunoblotting with the antibodies indicated. **A.** Blot shown is representative of three independent experiments and the migration of molecular mass standards are indicated on the right. **B.** and **C.** Data are presented as mean pixel density ± SEM, for three independent experiments in each case. \*\*\**p*<0.001, \*\**p*<0.01 and \**p*<0.05 vs absence of hyperforin, VEGF or AICAR. ††*p*<0.01 vs presence of Ca<sup>2+</sup>.

Figure 4-7

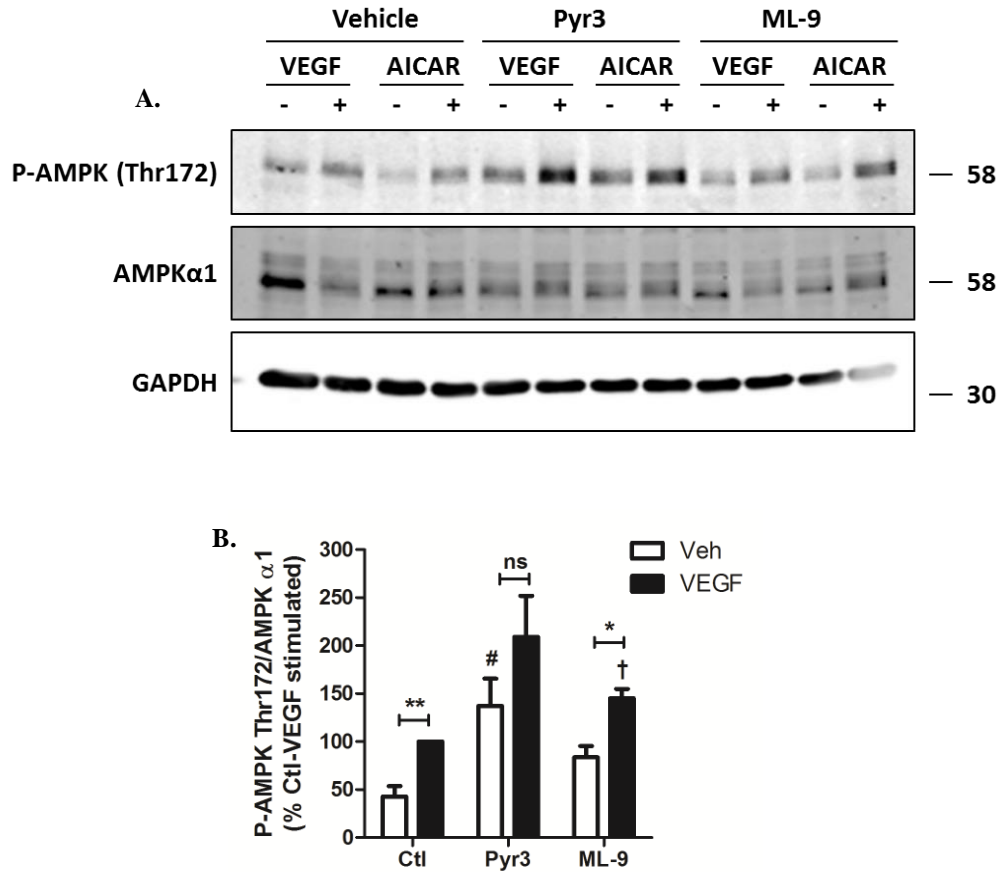
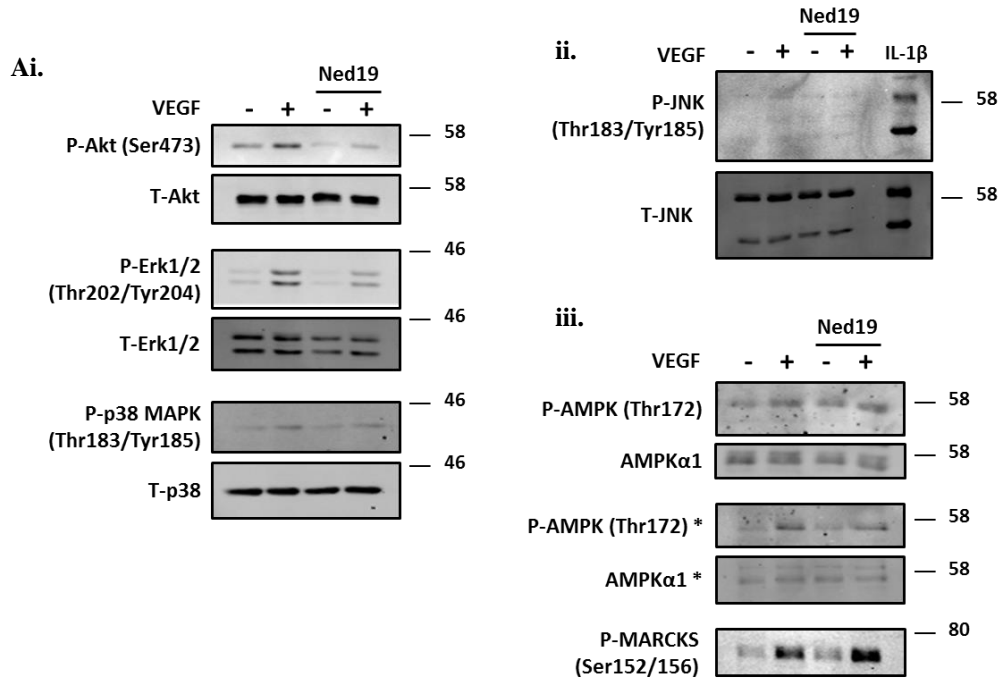


**Figure 4-7: The TRPC inhibitor Pry3 stimulates AMPK Thr172 phosphorylation**

HAEC were pre-treated with 20  $\mu$ M Pyr3, ML-9 or an equal volume of DMSO. Cells were stimulated with VEGF (10 ng/mL, 5 min) or AICAR (2 mM, 45 min) or an equal volume of vehicle before cell lysates were prepared. Cell lysates were subjected to SDS-PAGE and immunoblotting using antibodies as indicated. **A.** A representative immunoblot is shown with the migration of molecular mass standards indicated on the right and **B.** quantification of immunoblots from three independent experiments. \*\* $p < 0.01$  and \* $p < 0.05$  vs absence of VEGF, and # $p < 0.05$  and † $p < 0.05$  for Veh and VEGF-stimulation respectively vs the absence of inhibitor.

It has previously been reported that VEGF induced neoangiogenesis is mediated by the second messenger NAADP, and two-pore channel-2 (TPC-2)-dependent  $\text{Ca}^{2+}$  mobilisation from acidic intracellular stores (Favia et al. 2014). In agreement with this, the NAADP antagonist Ned 19 inhibited VEGF-stimulated phosphorylation of Akt and Erk1/2 (Figure 4-8A) whereas VEGF-stimulated p38 MAPK phosphorylation was not significantly altered. In contrast, VEGF-induced JNK phosphorylation was not observed (Figure 4-8Aii). In addition to the previous report of Ned 19 action in endothelial cells, neither VEGF-stimulated phosphorylation of the PKC substrate MARCKS (Ser152/156) nor AMPK Thr172 phosphorylation was inhibited by pre-treatment with Ned 19 (Figure 4-8Biv and v).

**Figure 4-8**



*Continued on facing page*

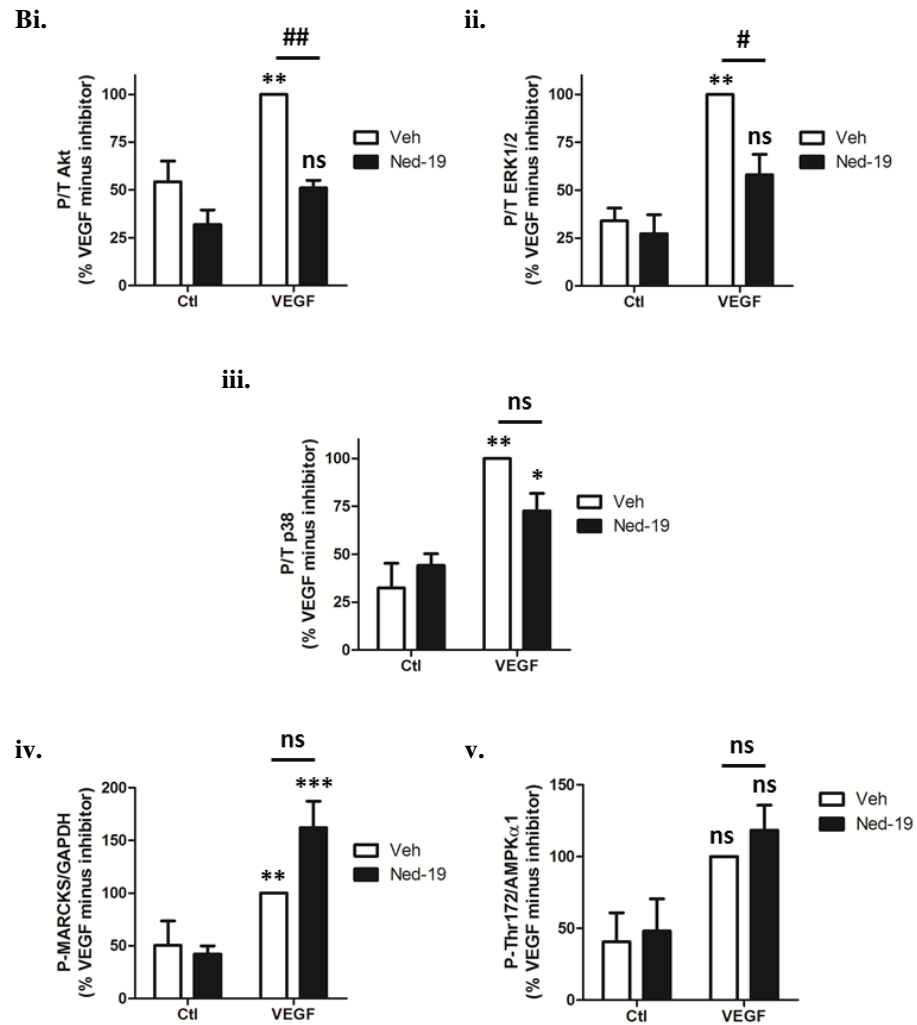


**Figure 4-8: The NAADP antagonist Ned 19 has no effect on VEGF-stimulated MARCKS or AMPK Thr172 phosphorylation**

HUVEC were pre-treated for 30 min in the presence or absence of 100  $\mu$ M Ned 19 prior to stimulation with 10 ng/mL VEGF for a further 15 min as previously described (Favia et al. 2014), or 5 min as indicated by \* in **Aiii**. Cell lysates were prepared and subjected to SDS-PAGE and immunoblotting with the antibodies indicated. **A**. Representative immunoblots are shown. **ii**. Cell lysate (40  $\mu$ g protein) from IL-1 $\beta$ -stimulated MEFs (10 ng/mL, 15 min – kind gift from Dr. Sarah Mancini) was included as a positive control for JNK phosphorylation, and the migration of molecular mass standards are indicated on the right. **B**. Data shown represent mean band intensity  $\pm$  SEM, relative to VEGF-stimulation in the absence of Ned 19, for three independent experiments in each case. # $p$ <0.05, and ## $p$ <0.01 vs absence of Ned 19, and \* $p$ <0.05, \*\* $p$ <0.01, \*\*\* $p$ <0.05 vs absence of VEGF.

## 4.3 Discussion

### 4.3.1 TRPC channels

VEGF signals via its cognate receptor, VEGF-R2, stimulating PLC $\gamma$ -mediated PIP $_2$  hydrolysis resulting in IP $_3$  and DAG synthesis. IP $_3$  diffuses freely into the cytoplasm where it activates IP $_3$  receptors (IP $_3$ R) on the membrane of the smooth endoplasmic reticulum stimulating calcium mobilization from intracellular stores. This initial rapid Ca $^{2+}$  release can induce further Ca $^{2+}$  influx via store-operated calcium (SOC) channels in the plasma membrane, resulting in sustained Ca $^{2+}$  influx. When it was initially characterised, VEGF was thought to increase vascular permeability via IP $_3$  induced Ca $^{2+}$  release from intracellular stores. It was however later shown by Pocock and colleagues that VEGF increases vascular permeability independently of thapsigargin-induced Ca $^{2+}$  store depletion, providing evidence that VEGF is acting via Ca $^{2+}$  store/IP $_3$  independent mechanism(s) to increase [Ca $^{2+}$ ] $_i$  (Pocock et al., 2000). DAG resulting from PIP $_2$  hydrolysis remains associated with the plasma membrane stimulating signalling cascades such as PKC and ERK1/2. DAG has also been shown to directly stimulate extracellular Ca $^{2+}$  influx via a number of the family of non-selective cation channels called transient receptor potential (TRP) channels (Hofmann et al. 1999).

Seven mammalian TRPC channel isoforms have been identified (TRPCs 1-7) which can be further sub-categorised into four groups based on their sequence homology and functional similarities; TRPCs 2, 1, 4/5, and 3/6/7. TRPC2 is a pseudogene in humans, old world monkeys and apes, but forms functional cation channels in other mammalian species, including rodents (Vannier et al. 1999). Consequently, most studies utilising human derived cell lines, including the present one, do not investigate the role of TRPC2.

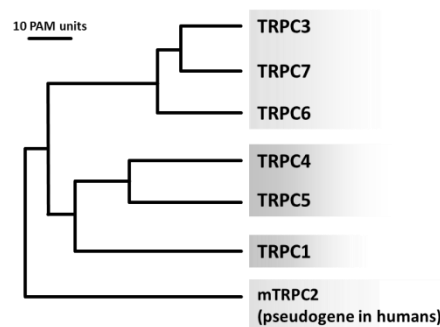


**Figure 4-9: Phylogenetic relationship of the TRPC protein family**

Evolutionary distance is shown by the total branch lengths in point accepted mutations (PAM) units, which is the mean number of substitutions per 100 residues, (Clapham et al. 2001).

Functional TRPC channels are tetrameric complexes with assembly typically occurring between the phylogenetically related TRPCs 1/4/5 and 3/6/7, although complexes containing other combinations have been reported (Zagranichnaya et al. 2005, Poteser et al. 2006, Antoniotti et al. 2006). Generally TRPCs 1, 4 and 5 are reported to form  $\text{Ca}^{2+}$  store-regulated channels while TRPCs 3, 6 and 7 are thought to be  $\text{Ca}^{2+}$  store independent, receptor (including DAG) activated calcium channels.

Many studies investigating the role of TRPC channels initially investigate the expression pattern of the different TRPC channel isoforms in the model system under investigation, an approach we have utilised here at both the level of protein and mRNA. Commercially available antibodies and qRT-PCR have recently become available for detecting TRPC channel expression. Immunoblot analysis of HAEC cell lysates generated immune-reactive bands corresponding to the predicted molecular mass of TRPC 3, 6 and 7 (97, 110 and 99 kDa respectively). The antibodies however show unacceptably high levels of non-specific immunoreactivity. Membrane containing fractions were isolated from HAEC and high ionic strength washes were used during the immunoblotting process in an attempt to reduce non-specific immunoreactivity, however unacceptably high levels of immunoreactivity were again observed (data not shown) consistent with previous reports critiquing the specificity of commercial antibodies for TRPCs (Flockerzi et al. 2005, Ong et al. 2002).

Ong and co-workers successfully employed a combined immunoprecipitation and immunoblotting protocol using two antibodies recognising different epitopes of endogenous TRPC1 (a polyclonal antibody recognising the C-terminal 18 amino acids of human TRPC1 for immunoprecipitation and then immunoblotting with a mouse monoclonal antibody representing the N-terminus of human TRPC1 - immunogen sequence not specified). Either antibody alone was not sufficient to detect endogenous levels of TRPC1 (Ong et al. 2002). Using this approach, proteins with a low copy number may be concentrated sufficiently by immunoprecipitation to detect by immunoblotting. In addition, partial purification by immunoprecipitation or isolation of membranes may remove proteins that would otherwise cross react with the antibody resulting in TRPC detection that is more specific. The failure of either antibody alone to detect endogenous TRPC expression might represent a low specificity or affinity of the antibody for the denatured protein. Given the degree of homology between TRPCs 3, 6 and 7 improvements to the specificity of TRPC antibodies is limited, we therefore also assessed TRPC mRNA levels in HAEC.

To measure TRPC expression at the level of mRNA, the methods employed by Yip and co-workers were utilised (Yip et al. 2004). In their study, the authors demonstrate the expression of TRPCs 1, 3, 4, 5, 6, and 7 in human coronary artery endothelial cells by RT-PCR (TRPC2 is a pseudogene in humans and was therefore not included in this study as mentioned previously). Using the methods described by the authors of this particular study, we detected PCR products of the predicted size for TRPCs 1, 5, and 7, but failed to detect TRPCs 3, 4 or 6. TRPC6 expression has previously been demonstrated in HAECs by our lab (Reihill 2009), however it was not detected during this present study. HAECs are derived from individual donors; HAEC cells from six individual donors, and over sequential passages, were therefore included in this study with inconsistent results. cDNA synthesised from RNA isolated from HUVEC (pooled from 6 individual isolations), HEK-293, HeLa cells and human brain was also assessed for TRPC mRNA expression, again with varying and inconsistent results (data not shown). On a technical note, it must be made apparent that 50 cycles of PCR were required to amplify the PCR products shown in Figure 4-3. Although consistent with the methods employed by Yip and co-workers, requiring this number of cycles to detect mRNA expression by RT-PCR suggests that the mRNA for these channels is present in negligible amounts, is highly susceptible to degradation or generates very stable protein, and is therefore expressed only under certain conditions yet to be determined. In addition to reverse transcriptase PCR, we have also used the more sensitive and quantitative approach of real-time PCR on HAEC derived cDNA using commercially available TaqMan® RT-PCR probes. Using this approach we again failed to detect the expression of TRPCs 3, 6 or 7 (data not shown) in any of the individual HAEC lines used. Expression of these TRPC channels was measured in cDNA derived from human testicular RNA using this method indicating that the probes are able to amplify the PCR product, and GAPDH expression levels measured in tandem indicated that good quality RNA isolation and efficient cDNA synthesis had been performed.

What is clear from the literature is that no consensus has been reached regarding the expression of TRPCs in commonly used vascular endothelial cells, and studies report different TRPC expression in cells isolated from different vascular beds of the same organism. In fact different expression patterns have even been reported in the same vascular endothelial cell type. The expression of TRPC channels 1, -3, -4, -6 and -7 have previously been reported in HUVEC (Paria et al. 2003) whereas other studies failed to detect TRPC4 or -6 in HUVEC (Kohler et al. 2001). We have presently used the same experimental conditions reported in detail by Yip and colleagues yet this failed to show the expression of TRPCs 3, 4 and 6 despite our lab having reported TRPC6 expression in

HAEC previously (Reihill 2009). Methods have been developed to allow the assessment of mRNA expression in single cells (Jones 2011, Kohler et al. 2001), however this is probably not representative of the organismal cell population as a whole and so is probably of little use. Although we demonstrate TRPC1, 5 and 7 expression at the level of mRNA, mRNA levels do not always reflect relative protein abundance therefore the significance of studies analysing mRNA levels is difficult to assess without also assessing protein levels, ideally by immunoblot or immunofluorescence.

TRPCs are not essential for the development of a mature vasculature, as mice deficient in each of the mammalian TRPCs have been generated (Freichel et al. 2005). The use of knockout models however might not be the solution to our technical issues, as TRPC3 expression has been shown to be elevated in ~2-3 fold in vascular smooth muscle of *TRPC6*<sup>-/-</sup> mice, and demonstrated enhanced responsiveness to agonists, suggesting that functional redundancy or compensatory mechanisms exists between the TRPC isoforms (Dietrich et al. 2005). Furthermore, deletion of either TRPC3 or TRPC6 is not protective against pressure overload induced cardiac hypertrophy *in vivo* whereas combined TRPC3 and -6 deletion is (Seo et al. 2014) suggesting TRPC isoforms may act in concert.

Much of the data describing the activities of TRPC channels has been obtained in experiments using heterologously expressed TRPC proteins in cell lines optimised for the expression of the protein being investigated, no cells with a truly TRPC null background have been described to our knowledge. Ectopic expression may result in TRPC channels being localised to intracellular compartments or form complexes with other TRP isoforms, not necessarily occurring *in vivo*. Ectopic TRPC expression may also result in the expression of TRPC channels at levels far greater than those observed *in vivo*. Although helpful, this may not be a useful strategy when extrapolating findings to native tissues/systems.

TRPC expression within a cell population may also be temporally and spatially regulated. TRPC4 has been shown to be absent in the plasma membrane of sub-confluent human microvascular endothelial cells (Graziani et al. 2010). Epidermal growth factor initiated the recruitment of TRPC4 to the plasma membrane which was retained there until the cells had formed mature cell-cell contacts. Upon growth factor stimulation of quiescent, barrier forming cells, TRPC4 was internalised, suggesting the subcellular distribution of TRPCs is cell cycle dependent (Koenig et al. 2013). The fate of the internalised TRPC4 was not reported in this study (*e.g.* whether it was retained in storage vesicles or degraded) but it is

interesting to speculate as to whether the same is true for other TRPC isoforms, adding further complication when attempting to determine their expression pattern.

It has previously been proposed that caution is required when interpreting data regarding the expression of TRP channels in cultured cells (Yao and Garland 2005). Culture under different conditions and the serial passaging of cells is believed to alter TRP channel expression. Therefore data obtained from cultured cell lines may not accurately represent native tissue expression (Yao and Garland 2005). Studies have measured TRPC expression in intact vessels (Yip et al. 2004), however studies using *in situ* hybridisation or immunohistochemistry are made technically difficult due to low specificity and cross reactivity of commercially available detection reagents, as is apparent in Figure 4-2.

A large number of the studies investigating the role of TRPCs use heterologous expression system culture models however given the variation in expression; it is not difficult to foresee how introducing heterologous TRPC proteins might further complicate the interpretation of TRPC channel activity. No consensus regarding the expression of TRPCs within a given cell model can be agreed upon. In fact, it has been suggested the TRP-channel expression is highly sensitive and dependent upon how tissue has been isolated, cultured and the method used to assess expression (Yao and Garland 2005). The cells we have used here therefore either express TRPC mRNA at a level too low to detect or the TRPC mRNA is rapidly turned over and the window of protein expression was missed, or the culture methodology was not conducive to TRPC expression. If this is the case and they are present either in low numbers or not at all, their functional relevance in VEGF signalling must be questioned, given the consistent response of vascular endothelial cells to VEGF. Numerous studies have demonstrated TRPC channel expression in vascular endothelial cells (Yip et al. 2004, Antoniotti et al. 2006, Pocock et al. 2004, Tirupathi et al. 2002, Riccio et al. 2002, Antoniotti et al. 2002, Hamdollah Zadeh et al. 2008, Ge et al. 2009, Graziani et al. 2010, Song et al. 2015), yet this study was unable to confirm their expression.

To add further complexity, TRPC channels exist as multimeric complexes in the plasma membrane. TRPCs form homo- or heteromeric complexes, typically within their related families *e.g.* TRPC1 will form complexes with TRPC4 or TRPC5 and complexes will form within the TRPC 3/6/7 family, although other complex combinations have been reported (J. Chen et al. 2009). The composition of native TRPC heteromeric complexes *in vivo* is however poorly understood. While TRPC1 is regarded to be a SOC channel, TRPCs 3 and

6 are regarded to be independent of calcium stores. If TRPC1 does complex with TRPCs 3 or 6 as suggested by Chen and co-workers, TRPC1 may confer SOC sensitivity to otherwise SOC insensitive complexes (J. Chen et al. 2009). TRPC1 also forms complexes with the other TRP superfamily members TRPP2 and TRPV6 (Kobori et al. 2009, Schindl et al. 2012). TRPC1 activity is also interesting given that it is not currently known whether TRPC1 forms homomeric channels, or acts to regulate the activity of the other TRP channels. With such diverse combinations of TRPC complexes possible, it is therefore not surprising that TRPC channels with a variety of biophysical and biological properties exist, which are entirely dependent upon the homo/heterogeneity of the complex (Kiselyov et al. 2005).

Given the difficulties in measuring the expression of TRPCs in vascular endothelial cells, the feasibility of pharmacologically modulating the activity of TRPCs was assessed. A number of compounds have been reported to selectively modulate the activity of TRPC channels, which we have utilised to assess the effect of VEGF-stimulation on AMPK Thr172 phosphorylation.

Hyperforin, the main anti-anxiolytic and anti-depressive compound found in St. John's wort has been proposed to specifically activate TRPC6 channels (Harteneck and Gollasch 2011). HAEC were therefore stimulated with hyperforin which, rapidly stimulates the phosphorylation of AMPK Thr172 in a concentration dependent manner up to 5  $\mu\text{M}$ . Activation of AMPK by hyperforin supports our hypothesis that TRPC-mediated  $\text{Ca}^{2+}$  influx is able to stimulate AMPK activation via CaMKK. Unfortunately, hyperforin-stimulated AMPK Thr172 phosphorylation was not affected by either the inhibition of CaMKK using STO-609 nor the removal of extracellular calcium. This data indicates that hyperforin is activating AMPK in a  $\text{Ca}^{2+}$  and CaMKK independent manner and not via TRPC6 induced  $\text{Ca}^{2+}$  influx. A mechanism describing hyperforin-stimulated AMPK activation has been described recently in HL-60 cells (a human promyelocytic leukemia cell line) (Wiechmann et al. 2015). Hyperforin stimulation of HL-60 cells reduced cell viability by approximately 90% at concentrations above 5  $\mu\text{M}$ , and caused a significant decrease in MTT reduction capacity by isolated mitochondria at concentrations as low as 0.01  $\mu\text{M}$ . This was demonstrated to be associated with disruption of  $\Delta\Psi\text{m}$  and suppression of ATP synthesis, thought to be the stimulus for AMPK activation, but whether AMPK activation contributes to, or facilitates hyperforin-stimulated apoptosis in this system remains to be determined (Wiechmann et al. 2015). Wiechmann and colleagues demonstrate a 6.5-fold increase in AMPK Thr172 phosphorylation, exclusively at a

hyperforin concentration of 3  $\mu\text{M}$  (10 min). In the present study, we demonstrate a lower, 2.3-fold increase, which may represent a difference in hyperforin sensitivity due to the cell lines used (*e.g.* immortalised vs primary, suspension vs adherent).

Hyperforin is therefore a poor tool for helping us determine whether VEGF-stimulated AMPK activation is via TRPC6-mediated  $\text{Ca}^{2+}$  influx. There are however an increasing number of studies utilising the compounds Pyr3 and ML-9, reported to be selective inhibitors of the TRPCs 3 and 6 respectively. Pyr3 is based on the structure of BTP2, an inhibitor of store operated calcium induced calcium release and has been reported to directly interact with and inhibit TRPC3 (Kiyonaka et al. 2009). Pyr3 is reported to significantly reduce carbamylcholine-induced  $\Delta[\text{Ca}^{2+}]_i$  in endothelial cells derived from WT and *TRPC1*<sup>-/-</sup> but not *TRPC3*<sup>-/-</sup> mice (Kochukov et al. 2012). Despite being reported to be a selective inhibitor of TRPC3, it was later shown that Pyr3 also inhibits store operated calcium entry in Jurkat cells with a similar potency to TRPC3 (Seo et al. 2014).

ML-9 inhibits both OAG and carbachol induced TRPC6-mediated  $\text{Ca}^{2+}$  influx with similar efficacy in HEK-293 cells heterologously expressing TRPC6 (Shi et al. 2007). Treatment of cells with 100  $\mu\text{M}$  ML-9 inhibits TRPC6-mediated relative current by ~90%, however at 100  $\mu\text{M}$ , the concentration required to achieve almost complete inhibition of TRPC6 channel conductance, ML-9 potentiates basal TRPC7 channel activity 2-3 fold (Shi et al. 2007). In addition to this, ML-9 may have other non-specific effects as it has also been reported to inhibit calmodulin activity in cell free assays (Harteneck and Gollasch 2011). In intact cells however, due to its structure, ML-9 is unlikely to cross the plasma membrane and so would likely act only via effectors present on the extracellular surface of the plasma membrane.

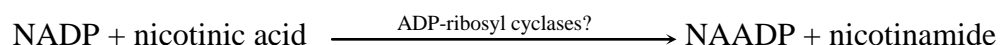
Despite the limitations of using these compounds, modulation of TRPC activity using Pyr3 is reported to have direct effects on vascular function, cell proliferation resulting in vessel remodelling, and cardiac hypertrophy. Pyr3 inhibited bradykinin-stimulated nitric oxide production and vasodilation in primary porcine coronary arteries. In addition, exposure of porcine coronary artery endothelial cells to hypoxia/re-oxygenation inhibited TRPC translocation to the plasma membrane and  $\text{Ca}^{2+}$  influx, proposed to underlie impaired NO production and vasodilation after ischemia-reperfusion (Yang et al. 2011). Pyr3 also demonstrated a concentration-dependent anti-proliferative effect on human coronary arterial smooth muscle (HCASM) cells (0.1-10  $\mu\text{M}$ ), an effect that was not observed in HMVEC across the same concentration range (Koenig et al. 2013). Significantly higher

TRPC3 expression was detected in human coronary artery smooth muscle cells compared to MVEC such that it has been suggested that TRPC3 may be a therapeutic target for preventing the development of neointimal hyperplasia after percutaneous coronary intervention (Koenig et al. 2013). Furthermore, Pyr3 suppressed pathological cardiac hypertrophy in response to pressure-overload *in vivo* (Seo et al. 2014). The use of ML-9 as a therapeutic agent is not possible due to systemic complications and non-specific effects on other kinases in whole organisms (Shen et al. 2010), however TRPC6 selective modulators are being developed that would allow greater insight into the function of TRPC6 channel activity (Urban et al. 2012).

Using a similar approach to Harteneck and colleagues, we had intended to use hyperforin as a positive control for measuring the degree of ML-9-mediated TRPC6 inhibition, however due to the non-TRPC6 effects of hyperforin that we and others have reported, this was not possible. Endothelial cells treated with Pyr3 and ML-9 at concentrations previously reported to inhibit TRPC3 and 6, had no inhibitory effect on VEGF- or AICAR-stimulated AMPK Thr172 phosphorylation. Pyr3 may in fact potentiate basal and VEGF-stimulated AMPK activation. At this time given the tools available, we are not able to conclude definitively whether TRPCs 3 and 6 are required, but neither can we rule out a role for them in the mechanism of VEGF-stimulated AMPK activation.

### 4.3.2 NAADP -mediated Ca<sup>2+</sup> mobilisation from acidic organelles

Extracellular stimuli stimulate the synthesis of the well characterised Ca<sup>2+</sup> mobilising second messengers IP<sub>3</sub> and cyclic ADP-ribose (cADPR) in addition to the less well characterised nicotinic acid adenine dinucleotide (NAADP) (Galione et al. 2010). NAADP differs from the co-factor NADP only by the substitution of the nicotinamide group for nicotinic acid, this substitution however confers potent Ca<sup>2+</sup> mobilising qualities not possessed by NADP. The mechanism and regulation of NAADP synthesis *in vitro* has not been determined empirically, but the best hypothesis suggests an ADP-ribosyl cyclase (specifically CD38)-mediated ‘*base-exchange*’ mechanism (Aarhus et al. 1995), whereby:



CD38 has been reported to catalyse the synthesis of NAADP *in vitro* via the base-exchange mechanism, but whether CD38 and base-exchange contribute to the *in vivo* synthesis of NAADP however is still to be determined. *In vivo*, the de-amination of NADP<sup>+</sup> or

phosphorylation of NAAD<sup>+</sup> represent mechanisms of NAADP synthesis that have not yet been excluded (Soares et al. 2007).

NAADP, much like IP<sub>3</sub> and cADPR, triggers Ca<sup>2+</sup> release by binding to and opening Ca<sup>2+</sup> channels on intracellular organelles. Unlike IP<sub>3</sub> and cADPR, which stimulate Ca<sup>2+</sup> release from the endoplasmic reticulum (via IP<sub>3</sub>R and the ryanodine receptor (RyR) respectively), NAADP specifically mobilises Ca<sup>2+</sup> from acidic stores such as endosomes and lysosomes, via two-pore channel (TPC) activation (Pitt et al. 2010). Three isoforms of TPCs exist (TPCs 1-3) however these isoforms exhibit differential organelle distribution; TPC1 is widely distributed throughout the endo-lysosomal system whereas while TPC2 expression is restricted to the late endo/lysosome (Calcraft et al. 2009). Ca<sup>2+</sup> uptake into acidic organelles is best characterised in yeast and plants and occurs via a thapsigargin insensitive high affinity Ca<sup>2+</sup>-ATPase, and a low affinity Ca<sup>2+</sup>/H<sup>+</sup> antiporter. In higher organisms however the mechanism is less clear but is usually thapsigargin independent, and dependent on H<sup>+</sup> gradient.

NAADP/TPC-mediated Ca<sup>2+</sup> release may further contribute to global Ca<sup>2+</sup> signalling via localised cross-talk with other Ca<sup>2+</sup> mobilisation mechanisms when in close proximity. Ca<sup>2+</sup> release from acidic organelles can act as a trigger for calcium induced calcium release from the sarco/endoplasmic reticulum, potentially dependent on IP<sub>3</sub>/cADPR. Additionally the release of Ca<sup>2+</sup> from acidic organelles in close proximity to the plasma membrane could stimulate extracellular Ca<sup>2+</sup> influx via Ca<sup>2+</sup>-activated plasma membrane channels.

Recent published data demonstrates that the cell-permeant, selective NAADP antagonist Ned 19 inhibits VEGF-induced neoangiogenic processes in HUVEC (Favia et al. 2014). The authors reported that VEGF-R activation leads to NAADP synthesis, and two pore channel (TPC)-mediated (specifically TPC2) Ca<sup>2+</sup> release from acidic Ca<sup>2+</sup> stores. Furthermore, VEGF-stimulated phosphorylation of ERK1/2, JNK, Akt and eNOS in HUVEC was prevented by prior-treatment with 100 μM Ned 19 (Favia et al. 2014). The authors proposed that NAADP-dependent Ca<sup>2+</sup> mobilisation is mediating the angiogenic effects of VEGF in HUVEC via these signalling mediators.

Given the dependence of Ca<sup>2+</sup> in AMPK activation by VEGF (Reihill 2009), we assessed the effect of NAADP antagonism with Ned 19 on VEGF-stimulated AMPK Thr172 phosphorylation in HUVEC. Using the reported concentration and duration of Ned 19 pre-treatment (100 μM, 30 min) and duration of VEGF treatment (15 min), Ned 19 pre-

treatment caused a significant decrease in VEGF-stimulated Akt (Ser473) and ERK1/2 (Thr183/Tyr185) phosphorylation, whereas pre-treatment of HUVEC with Ned 19 had no effect on VEGF-stimulated phospho-p38 MAPK; these results are in agreement with previous reports (Favia et al. 2014). In contrast to previous findings however, VEGF did not stimulate the phosphorylation of JNK (Thr183/Tyr185). The role of JNK in regulating the effects of VEGF is debated. It has been suggested that growth factor stimulated angiogenesis requires ERK1/2 activation and subsequent ERK1/2-stimulated JNK activation, and that JNK acts as the final effector of VEGF-stimulated angiogenesis (Pedram et al. 1998). On the other hand studies have also demonstrated the inhibition of stress (serum withdrawal or ceramide) induced JNK phosphorylation by VEGF (Gupta et al. 1999).

Ned 19 pre-treatment had no effect on VEGF-stimulated phosphorylation of the PKC substrate MARCKS (Ser152/156), nor AMPK Thr172 phosphorylation. This data showing that phosphorylation of the PKC substrate MARCKS is not affected by NAADP antagonism is interesting given that classical PKC isoforms are stimulated by VEGF and are  $\text{Ca}^{2+}$  regulated. It must be noted however that MARCKS is also a substrate for  $\text{Ca}^{2+}$ -independent PKC isoforms, therefore identifying unique substrates of the  $\text{Ca}^{2+}$ -dependent PKCs may be of benefit in elucidating any VEGF/NAADP/ $\text{Ca}^{2+}$ /classical PKC signalling axis. As reported previously (Reihill 2009) and replicated later (Figure 5-1), VEGF-stimulated AMPK Thr172 phosphorylation is rapid and transient, with phospho-Thr172 levels returning to basal levels 10-15 min after the addition of VEGF. It is therefore not surprising that VEGF-stimulated AMPK Thr172 phosphorylation was increased, but not significantly so above basal levels after 15 min of VEGF treatment. To address this, cells were pre-treated with Ned 19 as before, however VEGF was added for only 5 min prior to the preparation of cell lysates. VEGF retains the ability to stimulate the phosphorylation of AMPK Thr172 in the presence of Ned 19 after a relevant duration of VEGF treatment. This suggests that VEGF-stimulated AMPK activation is not dependent on  $\text{Ca}^{2+}$  mobilisation from acidic organelles stimulated by NAADP.

A major limitation of NAADP biology is that the mechanism coupling cell-surface receptor activation and stimulation of NAADP synthesis has not yet been determined. To our knowledge, no mechanistic link between VEGF-R2 activation and NAADP synthesis has been described. To determine the role of acidic  $\text{Ca}^{2+}$  mobilisation in VEGF-stimulated AMPK activation, the lysolytic agent GPN (glycyl-L-phenylalanine- $\beta$ -naphthylamide) could be utilised to assess VEGF-stimulated AMPK activation under conditions where the

endo/lysosomal acidic stores have been disrupted. It may also be prudent to test the effect of Ned 19 at lower concentrations although low nanomolar concentrations of Ned 19 (1-100 nM) have been shown to activate TPCs in cardiomyocytes in a dose dependent manner (Pitt et al. 2010). Treatment of cardiomyocytes with 1  $\mu$ M Ned 19 completely shuts TPCs, a concentration one hundred times lower than that used presently. At a concentration of 100  $\mu$ M, Ned 19 has been shown to significantly reduce the  $\text{Ca}^{2+}$  content of the sarcoplasmic reticulum of cardiomyocytes to a similar extent as treatment with 10  $\mu$ M ryanodine, or pre-empting the SR of  $\text{Ca}^{2+}$  with both caffeine and thapsigargin (10 mM and 100 nM respectively) (Pitt et al. 2010, Davidson et al. 2015). Ned 19 at higher concentrations may therefore have off-target effects on  $\text{Ca}^{2+}$  handling, which may explain some of the findings by (Favia et al. 2014) given that EKR1/2, Akt, eNOS and JNK can be regulated via  $\text{Ca}^{2+}$  dependent mechanisms.

## 4.4 Conclusion

TRPC channels represent a large family of proteins which exhibit differential expression among a variety of different cell types, even within a single cell type when cultured under different conditions. TRPCs are not essential for the development of a mature functional vasculature given the development of viable KO mouse strains, but may be involved in responding to chemical or physical insult such as growth factor stimulation. However, attributing an effect to a specific TRPC isoform is made problematic by the difficulties in assessing both native and homologous TRPC expression, and the degree to which TRPC channels form hetero/homomeric complexes: TRPC channels forming heteromeric complexes have been shown to differ in their electrophysical properties based upon the subunit composition of the complex. TRPC channels are regulated via multiple, complex and overlapping mechanisms:  $G_{\alpha q}$ ,  $PIP_2$ ,  $IP_3$ , DAG,  $IP_3Rs$ , fatty acids and their metabolites and intracellular  $Ca^{2+}$ -store depletion. Due to the interwoven nature of these signalling mechanisms, it may not be possible to resolve them sufficiently to characterise the mechanism resulting in AMPK activation by VEGF.

VEGF-stimulated AMPK activation has previously been shown to be dependent on  $Ca^{2+}$  influx, and independent of  $IP_3R$  antagonism and thapsigargin-mediated depletion of  $Ca^{2+}$  stores (Reihill et al. 2011), however NAADP-mediated  $Ca^{2+}$  release was not considered in these previous experiments. The present study has assessed the effect of NAADP antagonism on VEGF-stimulated AMPK activation and concludes that NAADP-mediated  $Ca^{2+}$  mobilisation is not mediating VEGF-stimulated AMPK activation.

## **Chapter 5 - Regulation of AMPK activity by PKC**

## 5.1 Introduction

VEGF has previously been demonstrated to activate AMPK in a CaMKK-dependent manner (Reihill et al. 2007). In addition to phosphorylation at the activating Thr172, recent studies have shown that AMPK can also be phosphorylated at  $\alpha 1$  Ser485/ $\alpha 2$  Ser491 (Woods et al. 2003b). Phosphorylation of AMPK  $\alpha$  at Ser485/491 is reported to be associated with reduced Thr172 phosphorylation and AMPK activity, so can be thought of as an inhibitory regulation mechanism (Horman et al. 2006, Hawley et al. 2014). Several studies have reported that Akt activation by insulin or IGF-1 stimulates AMPK Ser485 phosphorylation, and Akt has since been validated as a *bona fide* AMPK  $\alpha 1$  Ser485 kinase (Horman et al. 2006, Soltys et al. 2006, Berggreen et al. 2009, Ning et al. 2011). AMPK  $\alpha 2$  Ser491 has more recently been shown to be a poor Akt substrate *in vitro* and phosphorylation of this residue is therefore more likely to result from AMPK auto-phosphorylation (Hawley et al. 2014).

Further studies have also reported that inhibition of PKA, IKK and MEK-ERK1/2 attenuate AMPK Ser485 phosphorylation (Hurley et al. 2006, Park et al. 2014, Lopez-Cotarelo et al. 2015). The angiogenic effects of VEGF are effected via multiple signalling cascades including Akt and ERK1/2. Together these findings suggest that VEGF may be an endogenous AMPK activator which stimulates both activating Thr172 and inhibitory Ser485 phosphorylation, via CaMKK and Akt or ERK1/2 respectively. The current study therefore aimed to characterise the effect of VEGF on AMPK regulation by phosphorylation at both the activating Thr172 and inhibitory Ser485/491 residues.

## 5.2 Results

The effect of VEGF on the phosphorylation of AMPK  $\alpha$  Thr172 and Ser485/491 over 30 min was assessed in the human vascular endothelial cells HAEC and HUVEC. In HAEC, VEGF stimulation caused a rapid but transient increase in both Thr172 and Ser485/491 phosphorylation over the 30 min duration of the experiment (Figure 5-1A). AMPK  $\alpha$  Thr172 phosphorylation was significantly increased 2, 5 and 10 min after the addition of VEGF, with maximal (5-fold) increase in Thr172 phosphorylation measured after 5 min of VEGF treatment. By 15 min, Thr172 phosphorylation was no longer significantly elevated and at 20 min had returned to basal levels (Figure 5-1Aii). AMPK  $\alpha$ 1/2 Ser485/491 phosphorylation in response to VEGF-treatment mimicked the time course of Thr172 phosphorylation and maximal  $\alpha$  Ser485/491 phosphorylation was observed between 5 and 10 min of VEGF treatment (4-fold increase). Elevated AMPK  $\alpha$  Ser485/491 phosphorylation was maintained for 20 min, before returning to basal levels 30 min after the addition of VEGF. AMPK  $\alpha$ 1 specific Ser485 phosphorylation was found to have similar kinetics to that of AMPK  $\alpha$ 1/2 Ser485/491 in response to VEGF (Figure 5-1Ai). The effect of VEGF treatment over time on AMPK phosphorylation in HUVEC was also assessed (Figure 5-1B). A rapid and transient increase in AMPK  $\alpha$  phosphorylation was observed for both Thr172 and Ser485 in HUVEC which mimicked that observed in HAEC (Figure 5-1A).

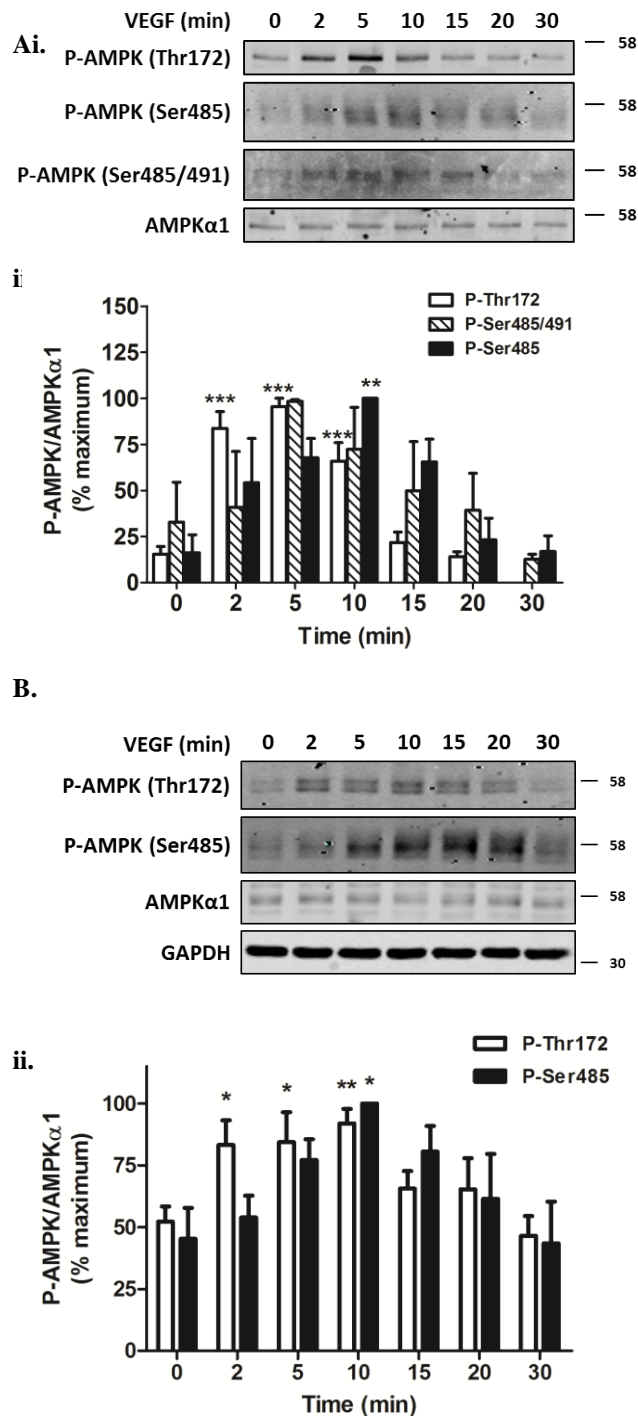
VEGF mediates some of its angiogenic effects via ERK1/2 and Akt. Therefore the effect of VEGF on ERK1/2 Tyr204/Thr202 and Akt Ser473 phosphorylation over time in HAEC was assessed. ERK1/2 phosphorylation was increased 3-fold ( $p < 0.05$ ) after 5 min of VEGF treatment with maximal phosphorylation observed between 5 and 10 min (Figure 5-2ii). ERK1/2 phosphorylation was submaximal 15 min after the addition of VEGF, but did not return to basal levels within the time course of this experiment. Akt phosphorylation was significantly increased after 10 min of VEGF treatment, and increased further 15 min after the addition of VEGF (Figure 5-2iii). The time taken to reach maximal Akt phosphorylation and return to basal levels was not determined over the course of this particular experiment.

Data presented in Chapter 4 of this study and elsewhere (Reihill et al. 2007, Reihill 2009), describes evidence for a PLC $\gamma$ , extracellular Ca<sup>2+</sup> and CaMKK-mediated mechanism of AMPK activation by VEGF, yet the mechanism of VEGF-stimulated AMPK

phosphorylation at Ser485/491 remains uncharacterised. Akt and ERK1/2 have previously been identified as AMPK Ser485 kinases (Hawley et al. 2014, Lopez-Cotarelo et al. 2015).

VEGF stimulates both ERK1/2 and Akt (Figure 5-2), therefore the effect of Akt and ERK1/2 inhibition on AMPK  $\alpha$  Ser485/491 phosphorylation in HAEC was assessed. Inhibition of Akt and ERK1/2, as indicated by the complete ablation of Akt Ser473 and ERK1/2 Thr202/Tyr204 phosphorylation with Akti-1/2 and PD184352 respectively had no effect on the phosphorylation of AMPK  $\alpha$ 1/2 at Ser485/491 or Thr172 in response to VEGF (Figure 5-3). To assess further the effect of Akt inhibition on VEGF-stimulated AMPK Ser485 phosphorylation, the PI3K inhibitor wortmannin was utilised. Pre-treatment of HUVEC with wortmannin significantly reduced Akt Ser473 phosphorylation in both the presence and absence of VEGF (Figure 5-4i) however inhibition of PI3K activity had no effect on basal or VEGF-stimulated AMPK  $\alpha$ 1 Ser485 phosphorylation (Figure 5-4ii) indicating that Akt is not *necessary* for AMPK  $\alpha$ 1 Ser485 phosphorylation. VEGF treatment (10 ng/mL, 5 min) however robustly stimulated AMPK  $\alpha$ 1 Ser485 phosphorylation in these cells. To determine whether activation of Akt is *sufficient* to stimulate the phosphorylation of AMPK  $\alpha$ 1 Ser485 in EC, HAEC were treated with insulin, a known activator of Akt which has previously been reported to stimulate AMPK Ser485 phosphorylation in other tissues (Horman et al. 2006, Berggreen et al. 2009). Insulin (1  $\mu$ M) robustly stimulated the phosphorylation of Akt Ser473 at all the time points assessed (5-30 min) (Figure 5-5), without also stimulating AMPK  $\alpha$ 1 Ser485 phosphorylation.

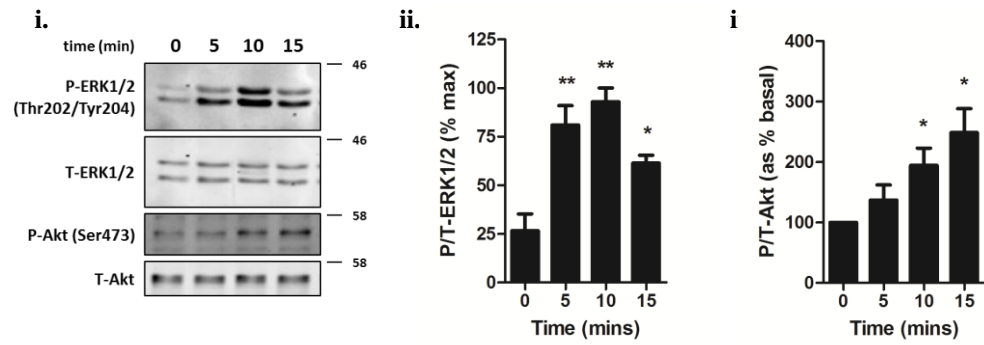
Figure 5-1



**Figure 5-1: VEGF stimulates both AMPK  $\alpha$  Thr172 and Ser485/491 phosphorylation in HAECs and HUVECs**

**A.** HAEC were stimulated with 10 ng/mL VEGF for the times indicated before cell lysates were prepared. Proteins were resolved by SDS-PAGE and immunoblotting using the antibodies indicated. **Ai.** A representative blot is shown and **ii.** densitometric quantification of immunoblots from three independent experiments. **B.** HUVECs were stimulated with 10 ng/mL VEGF for the times indicated before cell lysates were prepared. Proteins were resolved by SDS-PAGE and immunoblotting using the antibodies indicated. A representative immunoblot is shown with similar results observed on two further occasions. The migration of molecular mass markers is indicated on the right. \* $p < 0.05$ , \*\* $p < 0.01$  and \*\*\* $p < 0.001$  relative to time 0.

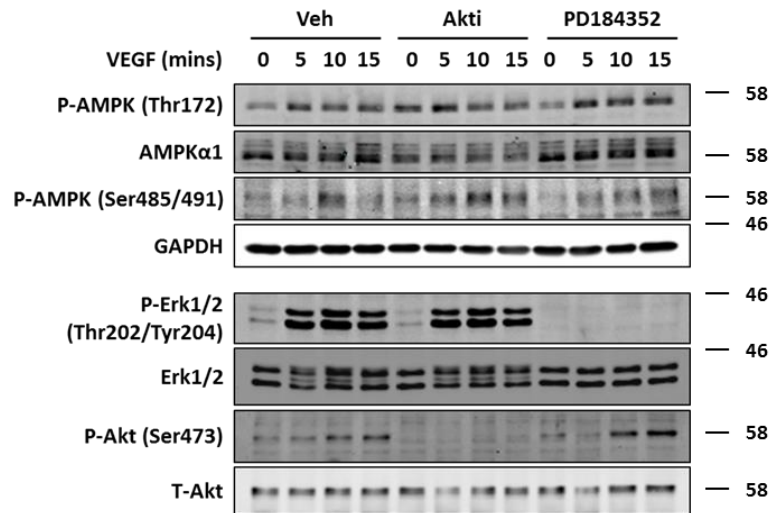
Figure 5-2



**Figure 5-2: VEGF stimulates both ERK1/2 Thr202/Tyr204 and Akt Ser473 phosphorylation in HAECs**

HAEC were stimulated with 10 ng/mL VEGF for the times indicated prior to the preparation of cell lysates. Proteins were resolved by SDS-PAGE and immunoblotted with the antibodies indicated. **i.** A representative blot is shown with the migration of molecular mass markers indicated on the right. **ii. and iii.** Densitometric quantification of immunoblots from three independent experiments \* $p < 0.05$  and \*\* $p < 0.01$  relative to time 0.

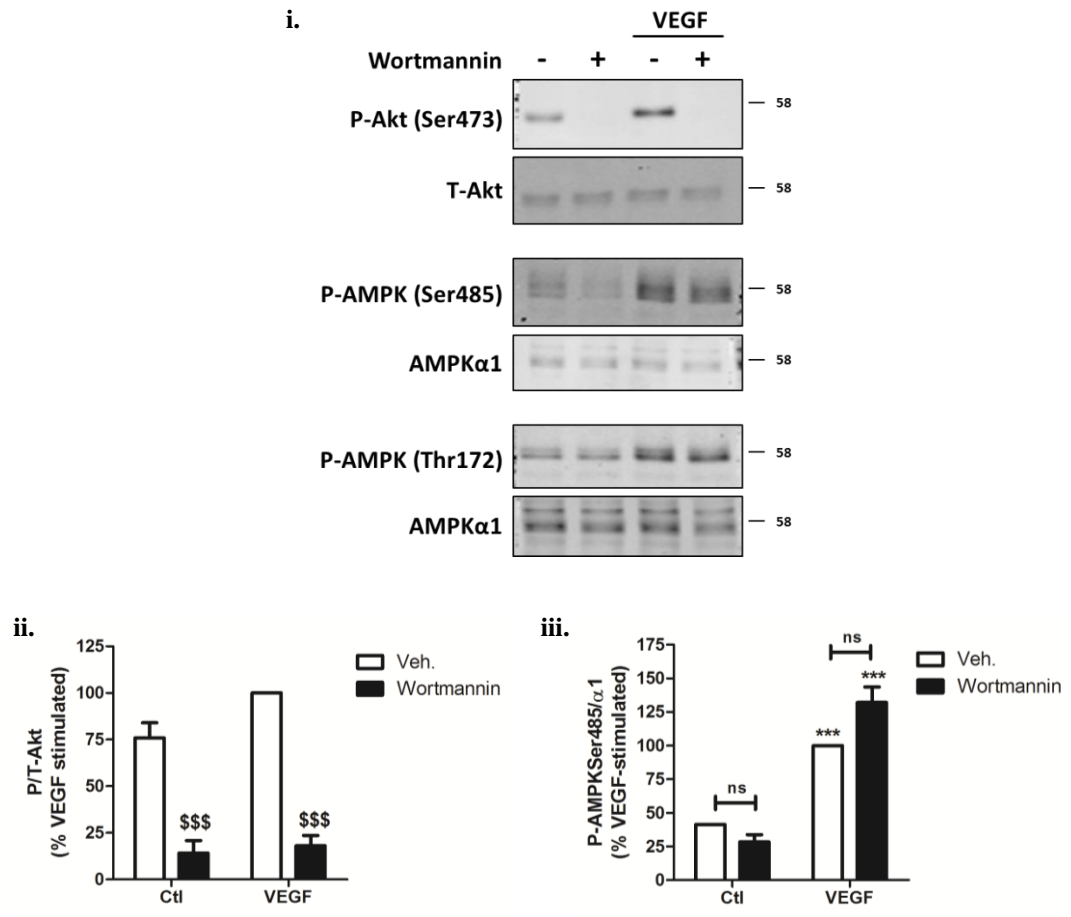
Figure 5-3



**Figure 5-3: VEGF-stimulated AMPK  $\alpha$  Thr172 and Ser485/491 phosphorylation is independent of Akt and ERK1/2**

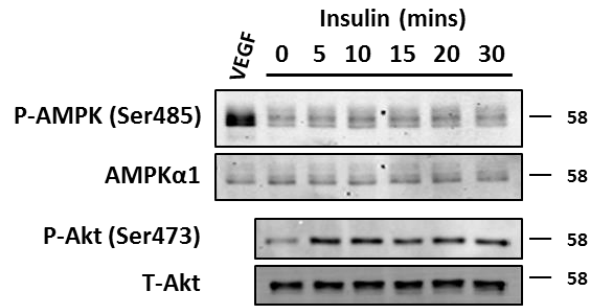
HAECs were pre-incubated in the presence or absence of 1  $\mu$ M Akti-1/2 (Akt inhibitor) or PD184352 (MEK inhibitor) for 60 min prior to VEGF stimulation (10 ng/mL, for the times indicated). Cell lysates were prepared, proteins resolved by SDS-PAGE and immunoblotted with the antibodies indicated. A representative immunoblot is shown with the migration of molecular mass markers indicated on the right. Immunoblot shown is representative of three independent experiments, with similar results.

Figure 5-4



**Figure 5-4: Wortmannin has no effect on VEGF-stimulated AMPK  $\alpha$ 1 Ser485 phosphorylation**

HUVEC were pre-incubated with 100 nM wortmannin for 45 min prior to stimulation with 10 ng/mL VEGF (5 min). Cell lysates were prepared and subjected to SDS-PAGE/immunoblotting with the antibodies indicated. **i.** A representative blot is shown with the migration of molecular mass markers indicated on the right, and **ii-iii.** Densitometric analysis of immunoblots from three independent experiments. Data represents mean band intensity relative to VEGF-stimulated in the absence of inhibitor. \*\*\* $p < 0.001$  relative to absence of VEGF, \$\$\$ $p < 0.001$  relative to absence of wortmannin.

**Figure 5-5****Figure 5-5: Insulin-mediated Akt activation has no effect on AMPK  $\alpha$ 1 Ser485 phosphorylation**

HAECs were stimulated with 1  $\mu$ M insulin for the times indicated, or 10 ng/mL VEGF for 5 min. Cell lysates were prepared and proteins resolved by SDS-PAGE/immunoblotting with the antibodies indicated. Representative immunoblots are shown, repeated on two further occasions with similar results.

As VEGF has previously been demonstrated to activate AMPK in a CaMKK-dependent manner (Reihill et al. 2007) and AMPK  $\alpha 2$  has previously been reported to auto-phosphorylate at Ser491 (Hawley et al. 2014), HUVEC were pre-treated with the CaMKK inhibitor STO-609 prior to stimulation with VEGF or AICAR. As has been shown previously (Reihill et al. 2007), STO-609 pre-treatment inhibited VEGF-stimulated AMPK Thr172 phosphorylation, and furthermore had no effect on AICAR-stimulated Thr172 phosphorylation (Figure 5-6ii). AICAR tended to increase Ser485 phosphorylation in both the presence and absence of STO-609, however this did not reach statistical significance. As previous studies indicated that removal of extracellular  $\text{Ca}^{2+}$  ablated VEGF-stimulated AMPK activation (Figure 4-6), the dependence of VEGF-stimulated Ser485 phosphorylation on  $\text{Ca}^{2+}$  influx was determined. HAEC were depleted of extracellular  $\text{Ca}^{2+}$  by incubation in KRH, or KRH without  $\text{Ca}^{2+}$  and the addition of 1 mM EGTA, prior to VEGF or AICAR stimulation. VEGF- but not AICAR-stimulated AMPK Thr172 phosphorylation was prevented by the depletion of extracellular  $\text{Ca}^{2+}$  (Figure 5-7ii) in agreement with previous reports (Reihill 2009) and Figure 4-6. VEGF-stimulated Ser485 phosphorylation was similarly prevented by prior depletion of extracellular calcium whereas AICAR-stimulated Ser485 phosphorylation was not affected by the removal of extracellular calcium (Figure 5-7iii).

In order to characterise the role of intracellular calcium in AMPK Ser485 phosphorylation, HUVEC were pre-treated with the membrane permeant  $\text{Ca}^{2+}$  chelator BAPTA-AM, prior to stimulation with VEGF. In the presence of BAPTA-AM, basal AMPK Thr172 phosphorylation was significantly increased; this was not further enhanced by VEGF treatment (Figure 5-8ii). The addition of BAPTA-AM tended to increase VEGF-stimulated AMPK Ser485 phosphorylation but this did not reach statistical significance (Figure 5-8iii).

Figure 5-6

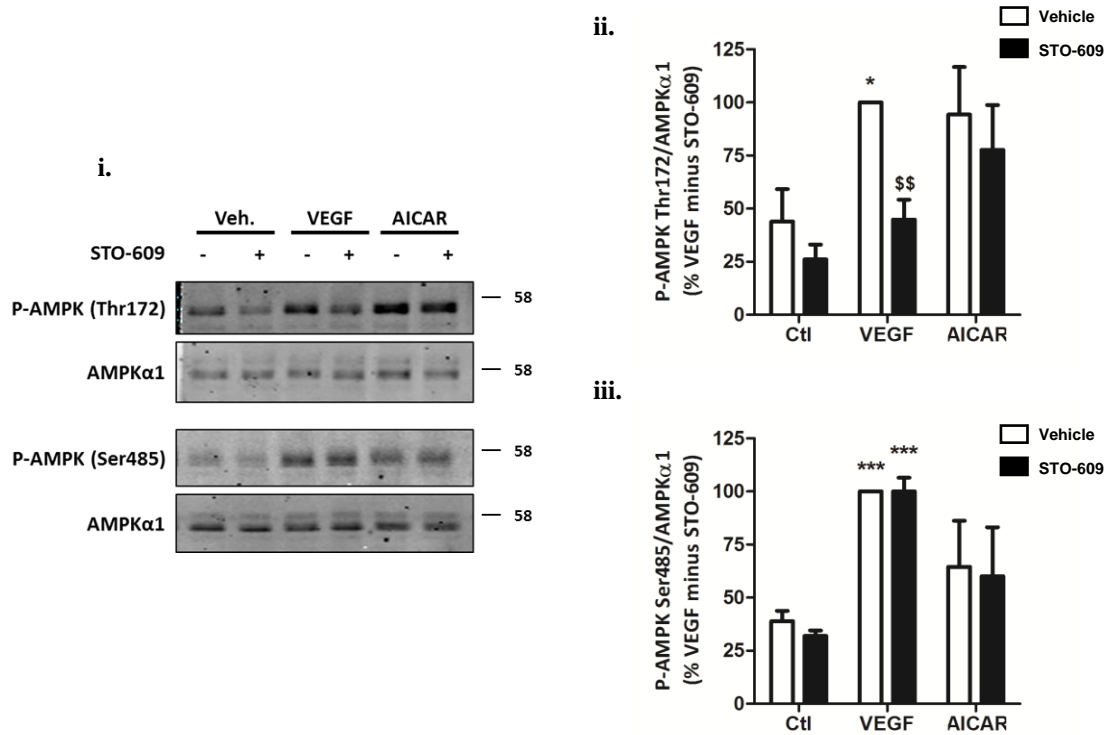


**Figure 5-6: VEGF-stimulated AMPK  $\alpha$ 1 Ser485 phosphorylation is insensitive to STO-609**

HAEC were incubated in the presence or absence of 10  $\mu$ M STO-609 for 60 min prior to stimulation with VEGF (10 ng/mL, 5 min) or AICAR (2 mM, 45 min). HAEC lysates were prepared, proteins resolved by SDS-PAGE and immunoblotted with the antibodies indicated. **i.** A representative immunoblot is shown. The migration of molecular mass markers is indicated on the right, and this was repeated with similar results on two further occasions. **ii and iii.** Densitometric quantification of immunoblots from three independent experiments displaying mean  $\pm$  SEM. \*  $p < 0.05$  and \*\*\*  $p < 0.001$  compared to absence of VEGF, \$\$  $p < 0.01$  compared to absence of STO-609.

Figure 5-7

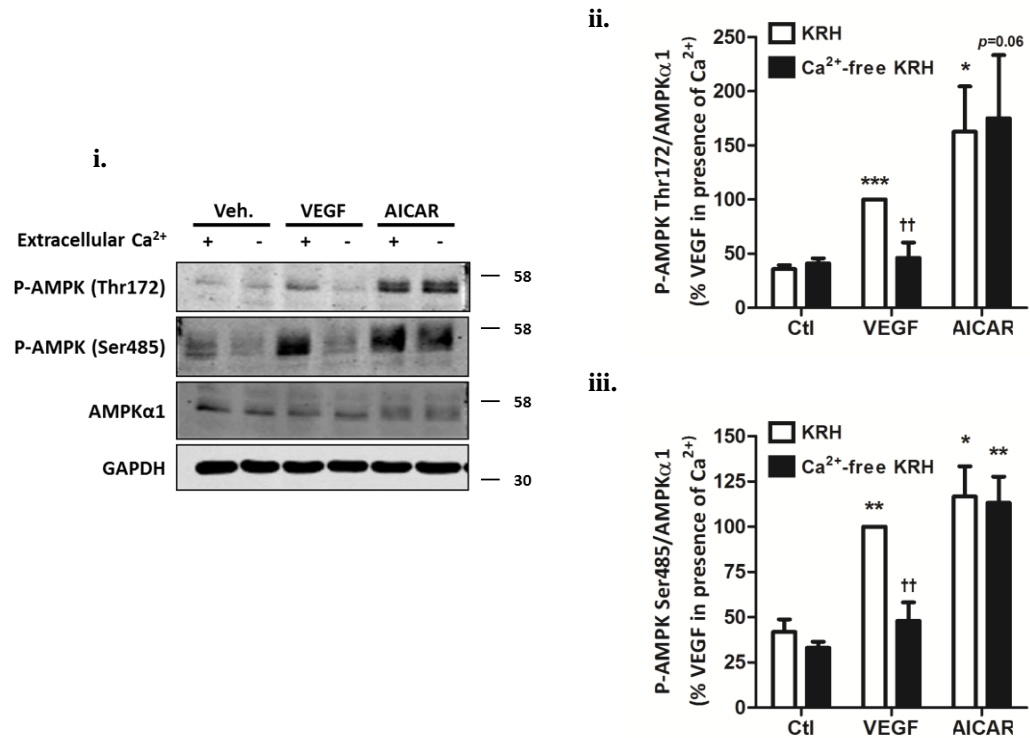


**Figure 5-7: VEGF-stimulated AMPK  $\alpha$ 1 Ser485 phosphorylation is sensitive to Ca<sup>2+</sup> removal**

HAEC were incubated in the presence or absence of extracellular Ca<sup>2+</sup> for 60 min, prior to stimulation with VEGF (10 ng/mL, 5 min) or AICAR (2 mM, 45 min). HAEC lysates were prepared, proteins resolved by SDS-PAGE and immunoblotted with the antibodies indicated. **i.** A representative immunoblot is shown. The migration of molecular mass markers is indicated on the right, and this was repeated with similar results on two further occasions. **ii and iii.** Densitometric quantification of immunoblots from three independent experiments displaying mean  $\pm$  SEM. \* $p$ <0.05, \*\* $p$ <0.01 and \*\*\* $p$ <0.001 compared to absence of VEGF/AICAR, †† $p$ <0.01 compared to KRH.

Figure 5-8

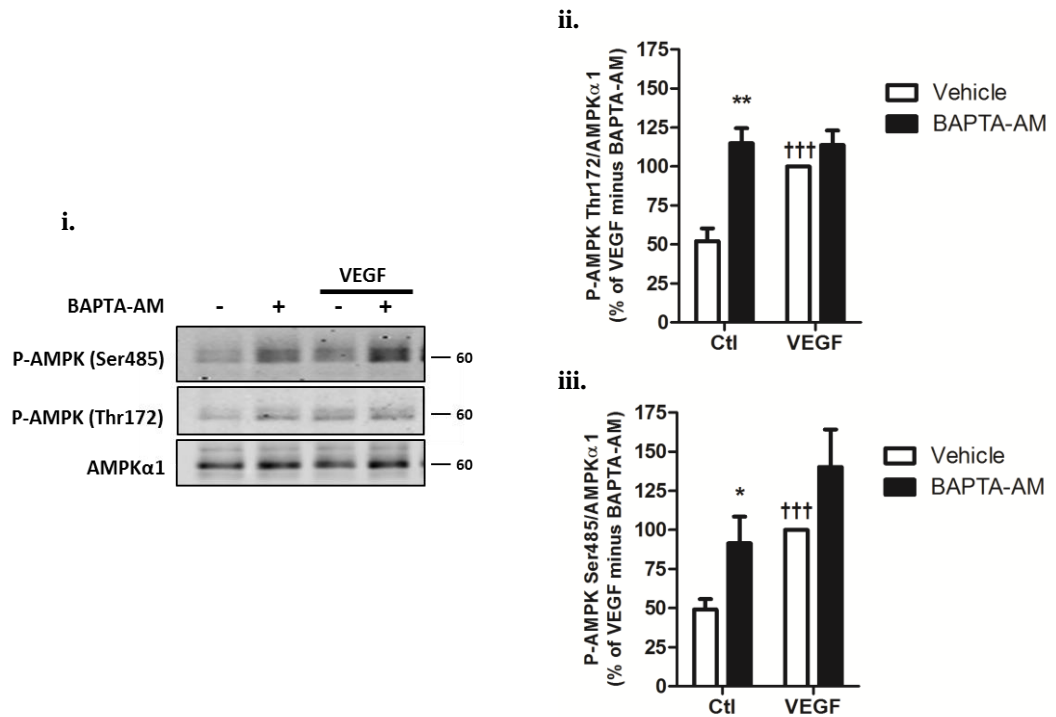


**Figure 5-8: Effect of Ca<sup>2+</sup> chelation on VEGF-stimulated AMPK phosphorylation**

HUVEC were incubated in the presence or absence of 25  $\mu$ M BAPTA-AM for 25 min, prior to stimulation with VEGF (10 ng/mL, 5 min). Cell lysates were prepared, proteins resolved by SDS-PAGE and immunoblotted with the antibodies indicated. **i.** A representative immunoblot is shown. The migration of molecular mass markers is indicated on the right, and this was repeated with similar results on two further occasions. **ii.** and **iii.** Densitometric quantification of immunoblots from three independent experiments displaying mean  $\pm$  SEM. \* $p$ <0.05, \*\* $p$ <0.01 compared to absence of BAPTA-AM, ††† $p$ <0.01 compared to absence of VEGF.

Previous data (Chapter 4) suggested a role for DAG-stimulated  $\text{Ca}^{2+}$  influx in AMPK activation induced by VEGF. VEGF stimulates members of the PKC family of protein kinases, and the conventional PKCs ( $\alpha$ ,  $\beta$ 1/2 and  $\gamma$ ) are regulated by DAG and  $\text{Ca}^{2+}$ . To assess the effect of PKC inhibition on VEGF-stimulated AMPK  $\alpha$  Thr172 and Ser485 phosphorylation, selective PKC inhibitors were utilised. Prior incubation of HUVEC with the classical PKC inhibitor GF109203X, or the PKC $\beta$  selective inhibitor LY333531 had no effect on Thr172 phosphorylation stimulated by VEGF (Figure 5-9Aii) however both GF109203X and LY333531 significantly inhibited VEGF-stimulated Ser485 phosphorylation (Figure 5-9Aiii). GF109203X treatment of HAEC resulted in a 40% increase in basal AMPK activity ( $p < 0.05$ ), and tended to increase AMPK activity after VEGF-stimulation (44% increase in mean activity) although this was not quite significant ( $\$p = 0.06$ ; Figure 5-9B). To determine whether the PKC inhibitor LY333531 directly influences AMPK activity, immunoprecipitated AMPK was incubated in the presence or absence of 0.2 mmol/L AMP, and LY333531 (0.1 or 1  $\mu\text{M}$ ). In the presence of AMP, purified AMPK activity was increased approximately 2-fold (Figure 5-9C) and this was not further increased by the inclusion of either 0.1 or 1  $\mu\text{M}$  LY333531.

Due to the inhibitory effect of GF109203X and LY333531 on VEGF-stimulated AMPK Ser485 phosphorylation, the effect of PKC activation on AMPK Ser485 phosphorylation was subsequently assessed, using the synthetic PKC activator phorbol 12-myristate 13-acetate (PMA) and the DAG mimetic OAG. AMPK  $\alpha$ 1 or  $\alpha$ 2 was immunoprecipitated from HUVEC previously stimulated with PMA or the DAG mimetic OAG, and phosphorylation of AMPK  $\alpha$ 1 Ser485 or  $\alpha$ 1/2 Ser485/491 was assessed (Figure 5-10). Both PMA and OAG stimulate  $\alpha$ 1 Ser485 phosphorylation and no immune reactive bands were observed in AMPK  $\alpha$ 1 immuno-depleted lysates when an antibody recognising both AMPK  $\alpha$ 1/2 Ser485/491 phosphorylation was used. Further to this, no  $\alpha$ 1/2 Ser485/491 immune reactive bands were observed in AMPK  $\alpha$ 2 immuno-precipitates but were present in AMPK  $\alpha$ 2 immuno-depleted cell lysates. This data indicates that PKC activation preferentially stimulates the Ser485 phosphorylation in AMPK  $\alpha$ 1 containing complexes.

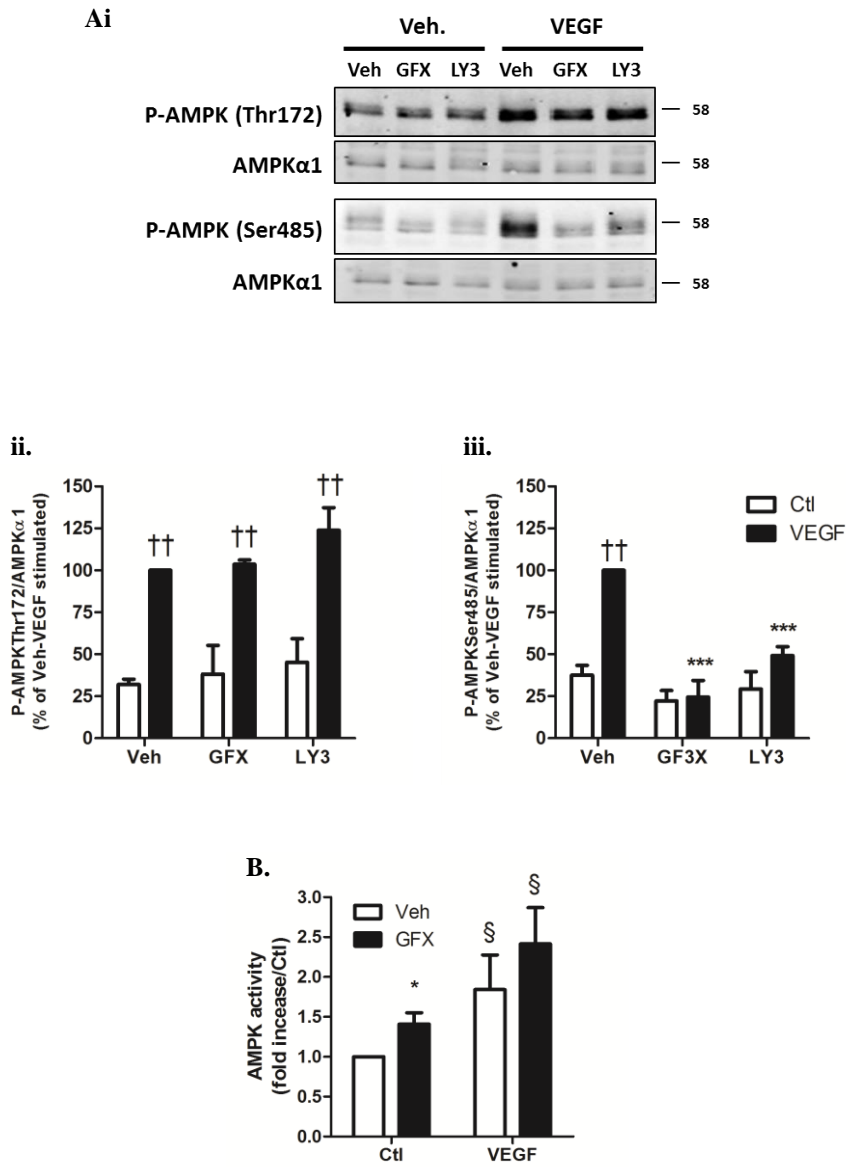
The phosphorylation of AMPK  $\alpha$ 1 Ser485 and the PKC substrate MARCKS (Ser152/156) was assessed after PMA treatment for various durations. In response to 1  $\mu\text{M}$  PMA, phosphorylation of the PKC substrate MARCKS at Ser152/156 was stimulated 8.8-fold ( $p < 0.001$ ) reaching maximal phosphorylation within 2 min (Figure 5-11). This maximal level of phosphorylation was maintained for the 20 min duration of this experiment (Figure 5-11). PMA-stimulated AMPK  $\alpha$ 1 Ser485 phosphorylation was also rapidly stimulated but

reached maximal phosphorylation only after 10 min of PMA treatment. The time taken to reach 50% max PMA-stimulated phosphorylation for MARCKS and AMPK  $\alpha$ 1 Ser485 were 1.0 and 2.6 min respectively.

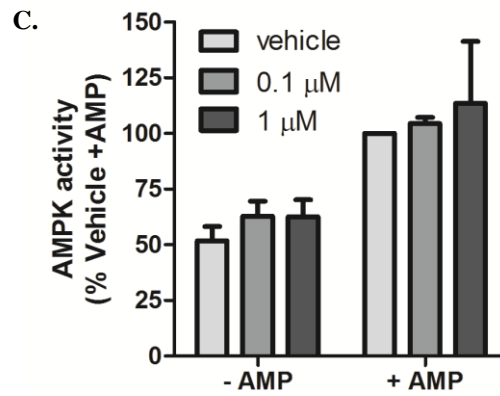
To assess the sensitivity of both VEGF- and PMA-stimulated AMPK Ser485 phosphorylation to PKC inhibition, HUVEC were pre-treated with increasing concentrations of LY333531 for 60 min prior to stimulation with VEGF or PMA. Phosphorylation of AMPK  $\alpha$ 1 Ser485 and MARCKS Ser152/156 was then assessed. PMA (1  $\mu$ M) stimulated the phosphorylation of both AMPK  $\alpha$ 1 Ser485 and MARCKS Ser152/156 to a greater extent than 10 ng/mL VEGF (Figure 5-12i). LY333531 concentration-dependent inhibition of VEGF-stimulated AMPK  $\alpha$ 1 Ser485 and MARCKS Ser152/156 phosphorylation was remarkably similar with an  $IC_{50}$  value of  $\sim$ 0.1-0.15  $\mu$ M (Figure 5-12ii). Significant inhibition of VEGF-stimulated AMPK Ser485 and MARCKS Ser152/156 phosphorylation was measured at all concentrations of LY333531 tested (0.1-1  $\mu$ M; Figure 5-12ii). In contrast, PMA-stimulated AMPK  $\alpha$ 1 Ser485 and MARCKS phosphorylation had  $IC_{50}$  values of  $\sim$ 0.1 and  $\sim$ 0.4  $\mu$ M respectively (Figure 5-12iii). Inhibition of PMA-stimulated AMPK  $\alpha$ 1 Ser485 phosphorylation was inhibited by all concentrations tested ( $p < 0.001$ ) whereas significant inhibition of PMA-stimulated MARCKS was only measured at LY333531 concentrations  $\geq$ 0.5  $\mu$ M (Figure 5-12iii).

Previous reports have suggested that, in certain cell lines (typically immune cells), PMA indirectly stimulates Akt activation (usually as assessed by increased Akt Ser473 or Thr308 phosphorylation) (Kawakami et al. 2004, Barragan et al. 2006, Douda et al. 2014). To assess whether PMA effects Akt phosphorylation, HUVEC were pre-treated with Akti or wortmannin, prior to stimulation with PMA or insulin. Insulin stimulated a robust increase in both Akt Thr308 and Ser473 phosphorylation (Figure 5-13A) which was ablated by prior treatment with either Akti or wortmannin. Similarly to VEGF (Figure 5-3 and Figure 5-4), PMA stimulation robustly increased AMPK Ser485 phosphorylation and this was not affected by either Akti or wortmannin treatment. PMA treatment in the absence of Akti or wortmannin actually reduced the intensity of phospho-Akt Thr308 and Ser473 immuno-reactive bands (Figure 5-13A). Furthermore, increasing the duration (Figure 5-13B) or concentration (Figure 5-13C) of PMA treatment results in the concurrent increase in AMPK Ser485 and reduced Akt Ser473 phosphorylation.

Figure 5-9



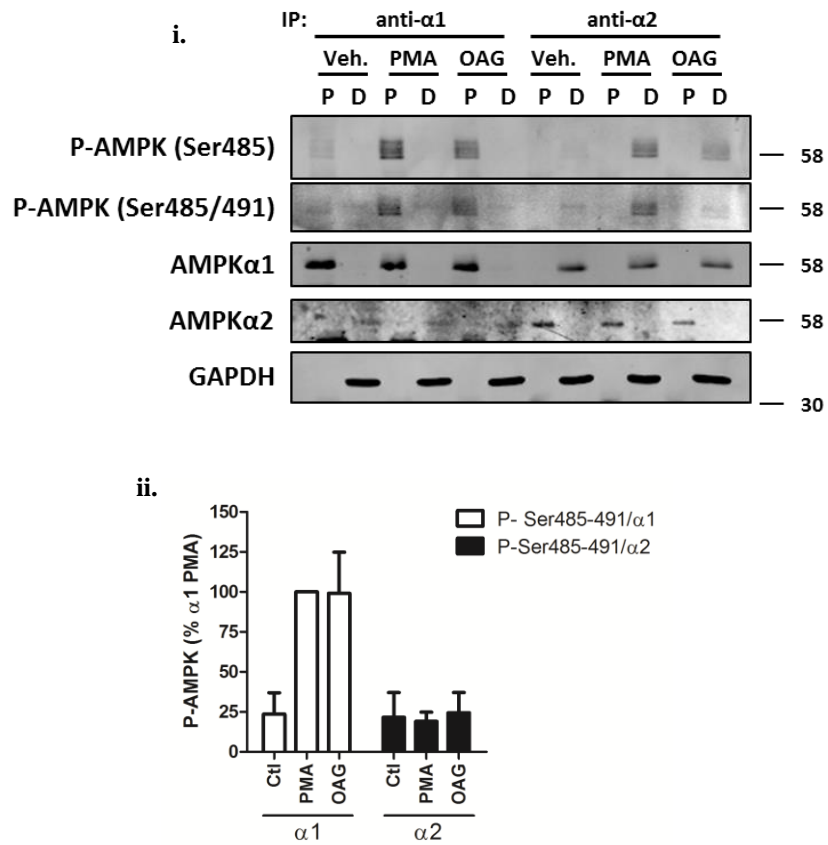
Continued on facing page...



**Figure 5-9: PKC inhibitors ablate VEGF-stimulated AMPK  $\alpha$ 1 Ser485 phosphorylation and stimulate AMPK activity**

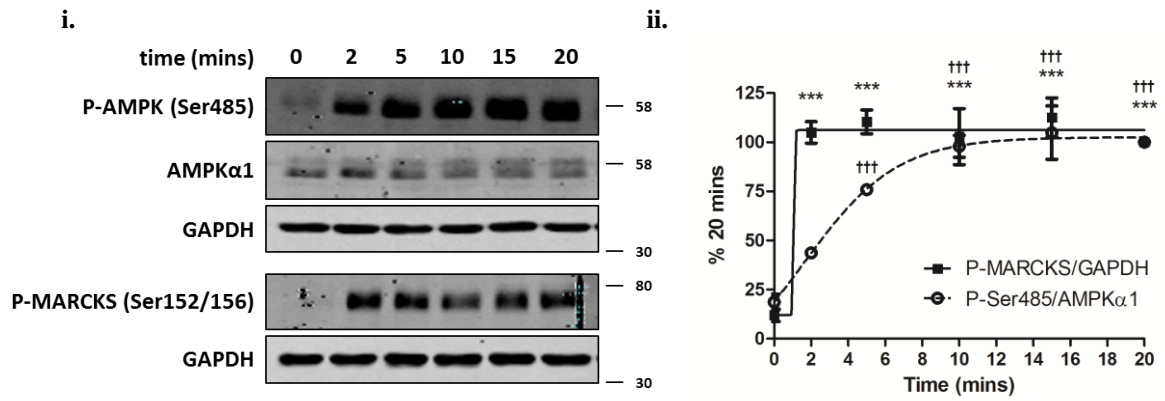
**A.** HUVEC or **B.** HAEC were pre-incubated in the presence or absence of either 1  $\mu$ M GF109203X (GFX) or LY333531 (LY3) for 1 hr prior to stimulation with VEGF (10 ng/mL, **A.** 5 min or **B.** 10 min). Cell lysates were prepared and **A.** subjected to SDS-PAGE and immunoblotting with the antibodies indicated, or **B.** AMPK immunoprecipitated and assayed for AMPK activity. **Ai.** Representative immunoblots are shown with the migration of molecular mass markers indicated on the right. **ii.** and **iii.** Densitometric quantification of immunoblots from three independent experiments. Data are expressed relative to VEGF-treated HUVECs in the absence of inhibitor.  $\dagger\dagger p < 0.01$  phospho-Thr172 relative to absence of VEGF,  $\# p < 0.05$  phospho-Ser485 relative to absence of VEGF and  $*** p < 0.001$  relative to absence of PKC inhibitor. **B.** AMPK activity from five independent experiments.  $* p < 0.05$  relative to absence of PKC inhibitor,  $\S p = 0.06$  relative to absence of VEGF. **C.** AMPK  $\alpha$ 1 was immunoprecipitated and activity was assayed in the presence or absence of AMP and LY333531 at the concentrations indicated. Data represents results from three independent experiments.

Figure 5-10

**Figure 5-10: PKC activators preferentially stimulate AMPK  $\alpha$ 1 Ser485 phosphorylation**

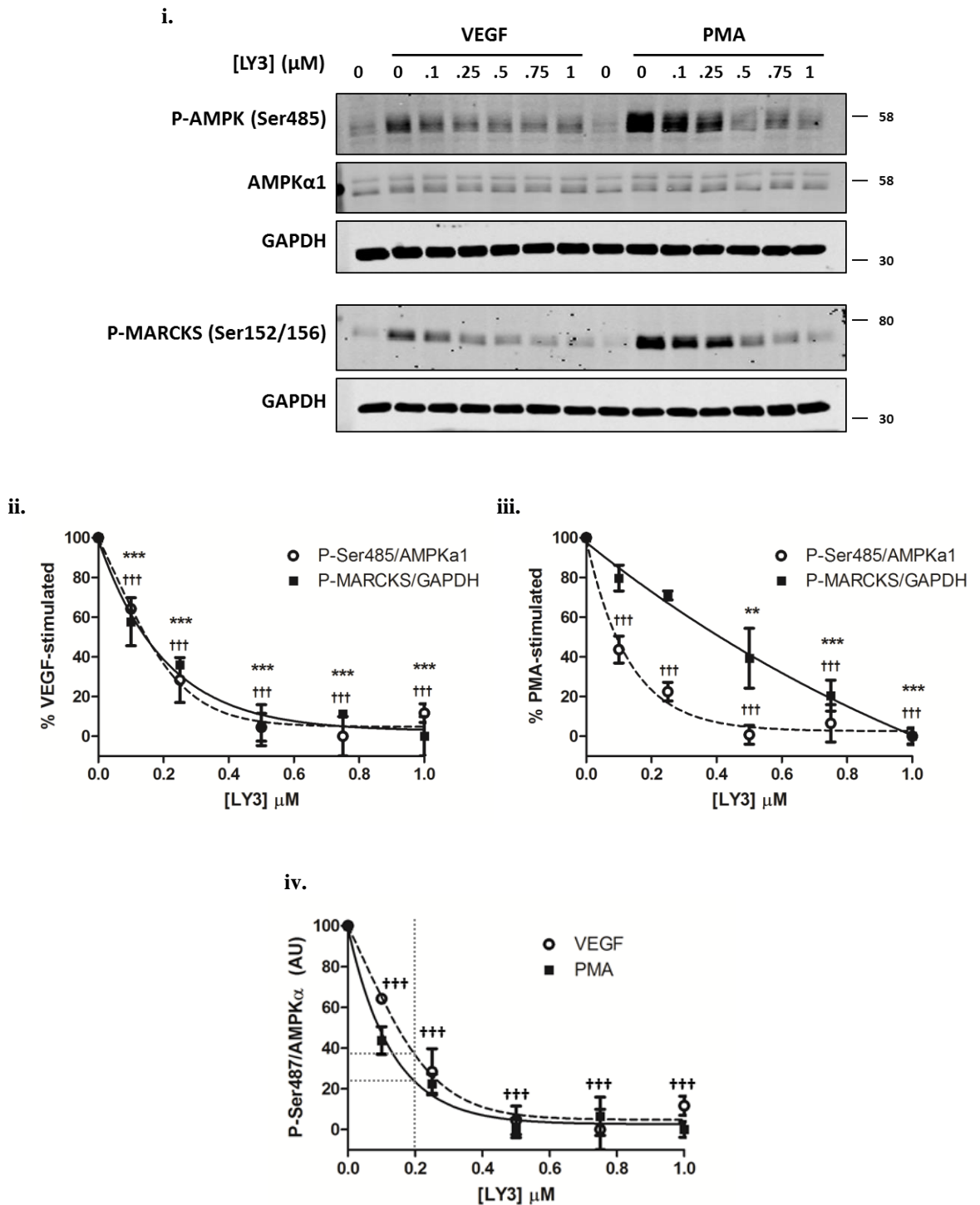
HUVEC were stimulated with 1  $\mu$ M PMA or 100  $\mu$ M OAG for 20 min prior to cell lysis. AMPK was immunoprecipitated (IP) using anti-AMPK  $\alpha$ 1 or anti-AMPK  $\alpha$ 2 antibodies. **i.** The AMPK immunoprecipitate (P) and immune-depleted lysate (D) samples were subjected to SDS-PAGE and immunoblotting with the antibodies indicated. **ii.** Densitometric quantification of immunoprecipitate (P) immunoblots from two independent experiments.

Figure 5-11

**Figure 5-11: PKC activators stimulate AMPK  $\alpha$ 1 Ser485 phosphorylation**

HUVEC were stimulated with PMA (1  $\mu$ M) for the indicated durations and lysates prepared. Proteins were resolved by SDS-PAGE and immunoblotted using the antibodies indicated. **i.** representative blots are shown with the migration of molecular mass markers indicated on the right, and **ii.** Densitometric quantification of immunoblots. Data represents mean  $\pm$  SEM relative to 20 min of treatment, for three independent experiments in each case. \*\*\* $p$ <0.001 for phospho-MARCKS and ††† $p$ <0.001 for phospho-Ser485 relative to absence of PMA stimulation.

Figure 5-12



**Figure 5-12: The sensitivity of VEGF- and PMA-stimulated AMPK  $\alpha$ 1 Ser485 and MARCKS phosphorylation to PKC inhibition by LY333531**

HUVEC were pre-treated with the indicated concentrations of LY333531 for 1 hour prior to stimulation with VEGF (10 ng/mL, 5 min) or PMA (1  $\mu\text{M}$ , 20 min). Lysates were resolved by SDS-PAGE and immunoblotted using the antibodies indicated. **i.** representative blots are shown with the migration of molecular mass markers indicated on the right. **ii-iv.** Densitometric quantification of immunoblots. **iv.** Dashed line indicates the plasma concentrations achieved in previous studies and indicate AMPK  $\alpha$ 1 Ser485 phosphorylation at this level. Data represents mean  $\pm$  SEM relative to % max phosphorylation for three independent experiments. \*\* $p < 0.01$  and \*\*\* $p < 0.001$  for phospho-MARCKS, ††† $p < 0.001$  for phospho-Ser485 relative to absence of LY333531.

Figure 5-13

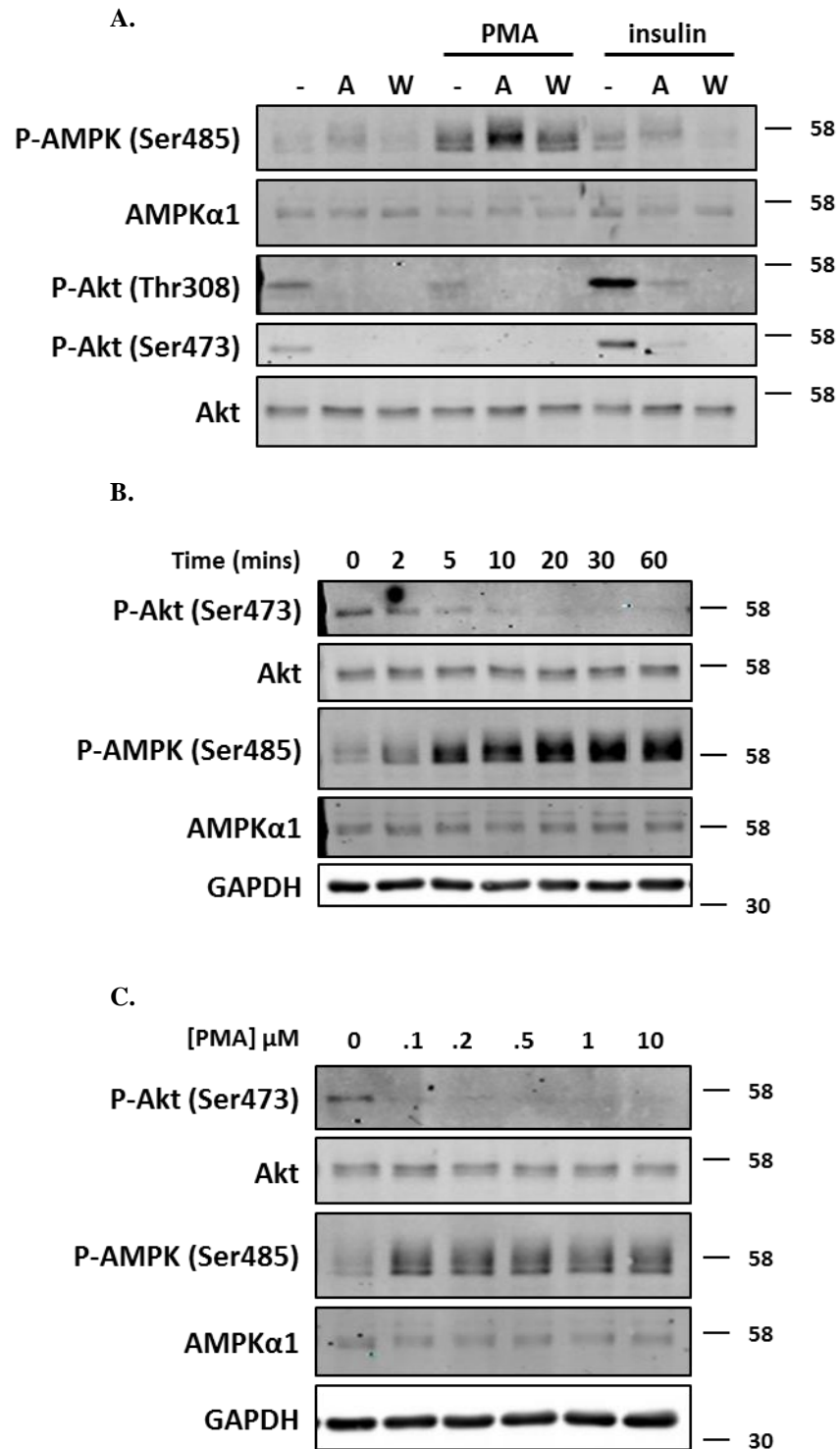


**Figure 5-13: PMA does not stimulate Akt phosphorylation at either Thr308 or Ser473**

**A.** HUVEC were pre-incubated with 1  $\mu$ M Akti-1/2 (A) or 100 nM wortmannin (W) prior to stimulation with 1  $\mu$ M PMA, or 1  $\mu$ M insulin for a further 15 min. **B.** HUVEC were stimulated with 1  $\mu$ M PMA for the times indicated or **C.** with the indicated concentration of PMA for 20 min. Cell lysates were prepared and proteins resolved by SDS-PAGE/immunoblotting using the antibodies indicated. Immunoblots shown are representative of **A.** two, **B** and **C.** single experiments respectively. The migration of molecular mass markers is indicated on the right.

Data to this point indicates that PKC activation stimulates AMPK  $\alpha$ 1 Ser485 phosphorylation independently of Akt. To assess the ability of PKC to phosphorylate AMPK *in vitro*, commercially purified PKC (reported by the manufacturers to be primarily  $\alpha$ ,  $\beta$  and  $\gamma$ , with lesser amounts of  $\delta$  and  $\zeta$ ) was incubated with immunoprecipitated kinase-inactive AMPK  $\alpha$ 1 in the presence of phosphatidylserine (PtdSer) and  $\text{Ca}^{2+}$ . PKC phosphorylates AMPK  $\alpha$ 1 Ser485 *in vitro* with similar efficiency to a comparable number of units of active recombinant human Akt (Figure 5-14).

The PKC family of protein kinases in humans consists of at least 15 members. To identify the PKC isoform(s) involved in the regulation of AMPK activity, HAEC and HUVEC were cultured overnight in the presence of 200 nM PMA prior to the preparation of cell lysates and immunoblotting with PKC isoform specific antibodies. Chronic PMA treatment downregulated the expression of PKC  $\alpha$ ,  $\beta$ 1,  $\gamma$ ,  $\eta$ ,  $\theta$  and  $\mu$ , whereas PKC  $\delta$  expression was unaffected (Figure 5-15A and B). PKC  $\beta$ 2,  $\epsilon$ ,  $\zeta$  and  $\lambda$  were not detected in endothelial cell lysates (data not shown). Upon determining the PKC isoforms downregulated by chronic PMA, HUVEC were then exposed to chronic PMA overnight, prior to stimulation with VEGF, AICAR, A769662 or OAG (Figure 5-15B). After PMA treatment PKC  $\beta$ 1 and pan immune-reactive bands were significantly reduced in endothelial cell lysates, to a level that was approximately 2 % of basal expression ( $p < 0.001$ ; Bii and iii). Down regulation of active PKC was indicated by significantly reduced VEGF-stimulated MARCKS phosphorylation after chronic PMA treatment (Figure 5-16Biv). Chronic PMA treatment also caused a significant reduction in both VEGF- and OAG-stimulated AMPK  $\alpha$ 1 Ser485 phosphorylation (Figure 5-16Bv). AICAR treatment stimulated an increase in AMPK  $\alpha$ 1 Ser485 phosphorylation which was not effected by PKC depletion, and AICAR did not affect phospho-MARCKS. A769662 did not alter the phosphorylation of AMPK at  $\alpha$ 1 Ser485, nor MARCKS Ser152/156.

siRNA-mediated downregulation of PKC  $\alpha$  by 90 % was measured, (Figure 5-16i and ii), however significant knockdown of PKC  $\alpha$  did not affect VEGF-stimulated AMPK  $\alpha$ 1 Ser485 phosphorylation (Figure 5-16iv). Intriguingly, downregulation of PKC  $\alpha$  also caused a significant reduction in PKC  $\beta$ 1 expression (Figure 5-16iii). Conversely, overexpression of PKC  $\alpha$  or  $\beta$ 1 (2.6-fold and 3.9-fold respectively,  $p < 0.001$ ; Figure 5-17i and ii) in HeLa was sufficient to significantly increase basal AMPK  $\alpha$ 1 Ser485 phosphorylation in the absence of a stimulus (Figure 5-17iii). Overexpression of PKC  $\beta$ 2 tended to increase AMPK Ser485 phosphorylation however increased PKC  $\beta$ 2 protein levels were not observed.

Figure 5-14

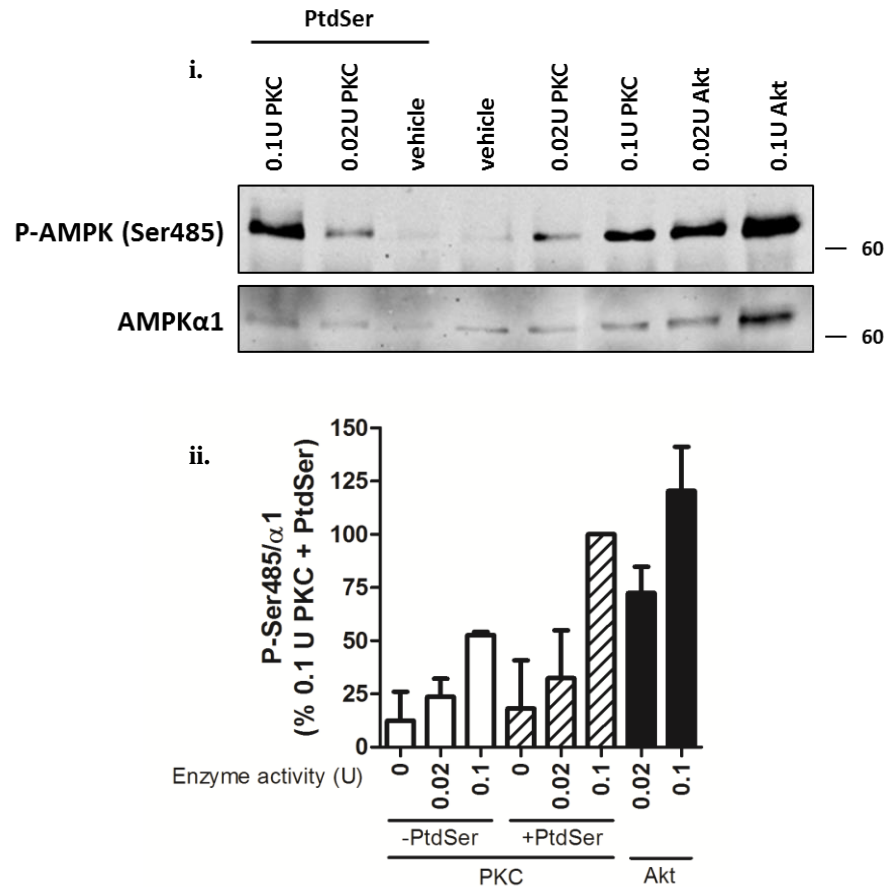


**Figure 5-14: *In vitro* phosphorylation of AMPK by PKC and Akt**

Immunoprecipitated AMPK  $\alpha$ 1 (kinase-inactive) was incubated in the presence of calf intestine alkaline phosphatase (CIAP) for 30 min at 30 °C prior to extensive washing. Immunoprecipitated AMPK  $\alpha$ 1 was then incubated with purified rat brain PKC, or recombinant Akt1 (with the indicated units of activity) for 30 min at 30 °C in the presence of  $\text{Ca}^{2+}$  and phosphatidyl serine (PtdSer). **i.** Proteins were resolved by SDS-PAGE and analysed by immunoblotting with the antibodies indicated. Blot shown is representative of two independent experiments. The migration of molecular mass markers is indicated on the right and **ii.** densitometric quantification of immunoblots from **i.**

*This experiment was performed by Dr Ian Salt.*

Figure 5-15

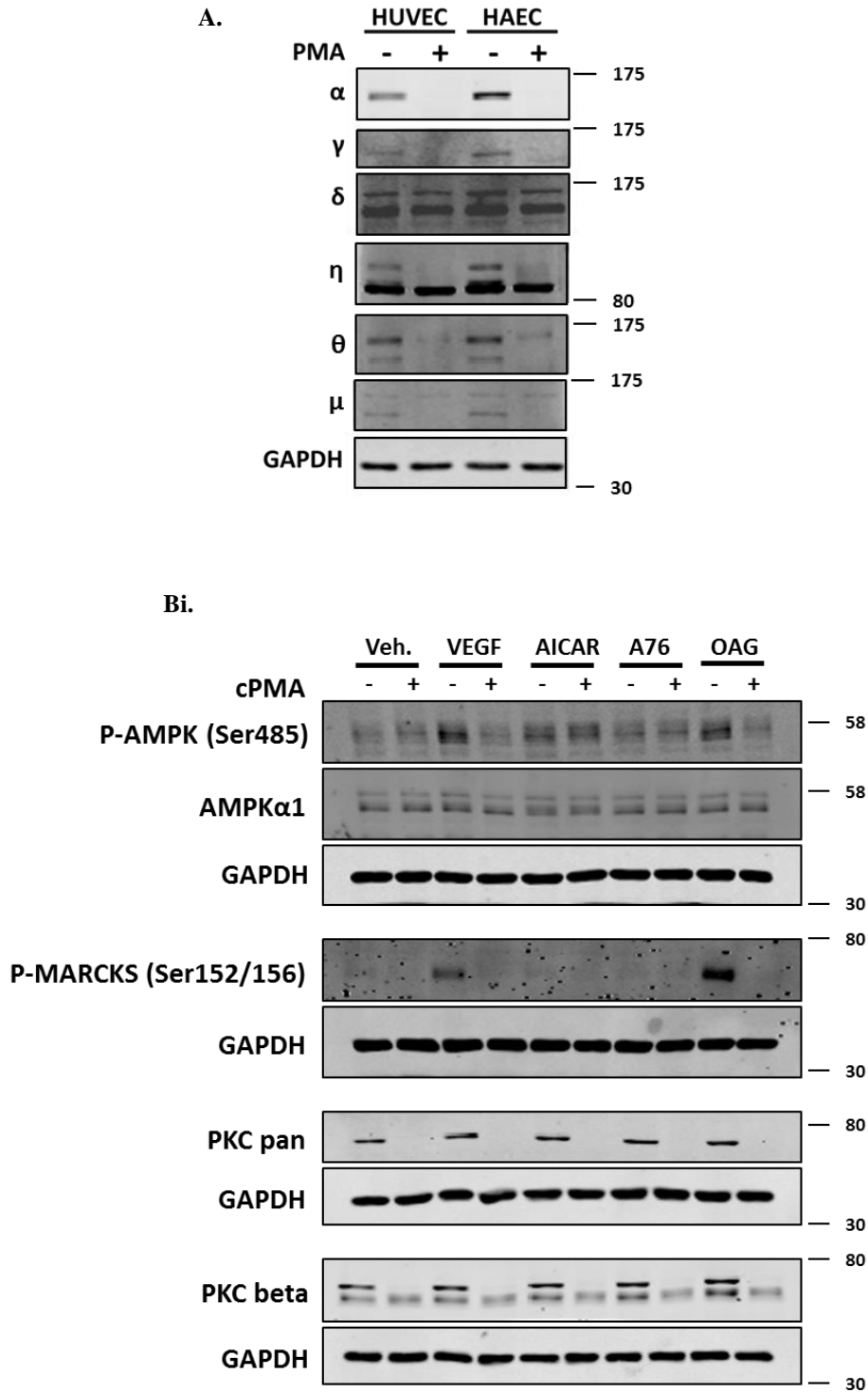
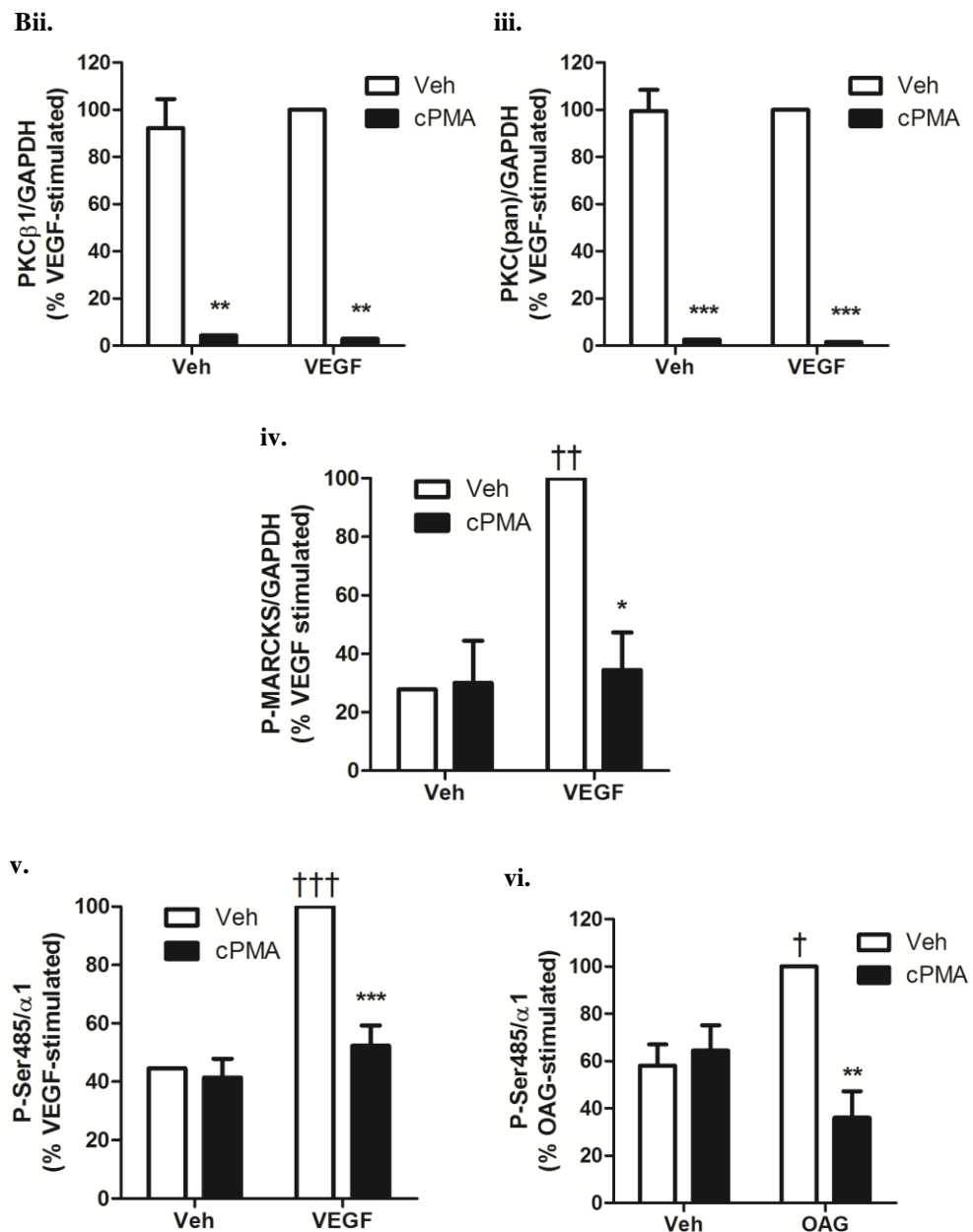


Figure continues on facing page...



**Figure 5-15: Chronic down regulation of PKC prevents VEGF-stimulated  $\alpha$ 1 Ser485 phosphorylation**

**A.** HUVEC or HAEC, or **B.** HUVEC were cultured for 20 h in the presence of 200 nM PMA (cPMA) **A.** prior to lysis, or **B.** stimulation with VEGF (10 ng/mL, 5 min), AICAR (2 mM 45 min), A769662 (100  $\mu$ M 60 min) or OAG (100  $\mu$ M, 20 min). Cell lysates were prepared and subjected to immunoblotting with the antibodies indicated. **A.** and **Bi.** Representative immunoblots are shown with the migration of molecular mass markers indicated on the right, and **Bii-vi** Densitometric quantification of immunoblots from three independent experiments (Veh = vehicle). \* $p$ <0.05, \*\* $p$ <0.01 and \*\*\* $p$ <0.001 relative to absence of cPMA pre-treatment and †  $p$ <0.05, ††  $p$ <0.01 and †††  $p$ <0.001 relative to absence of VEGF or OAG as indicated.

Figure 5-16

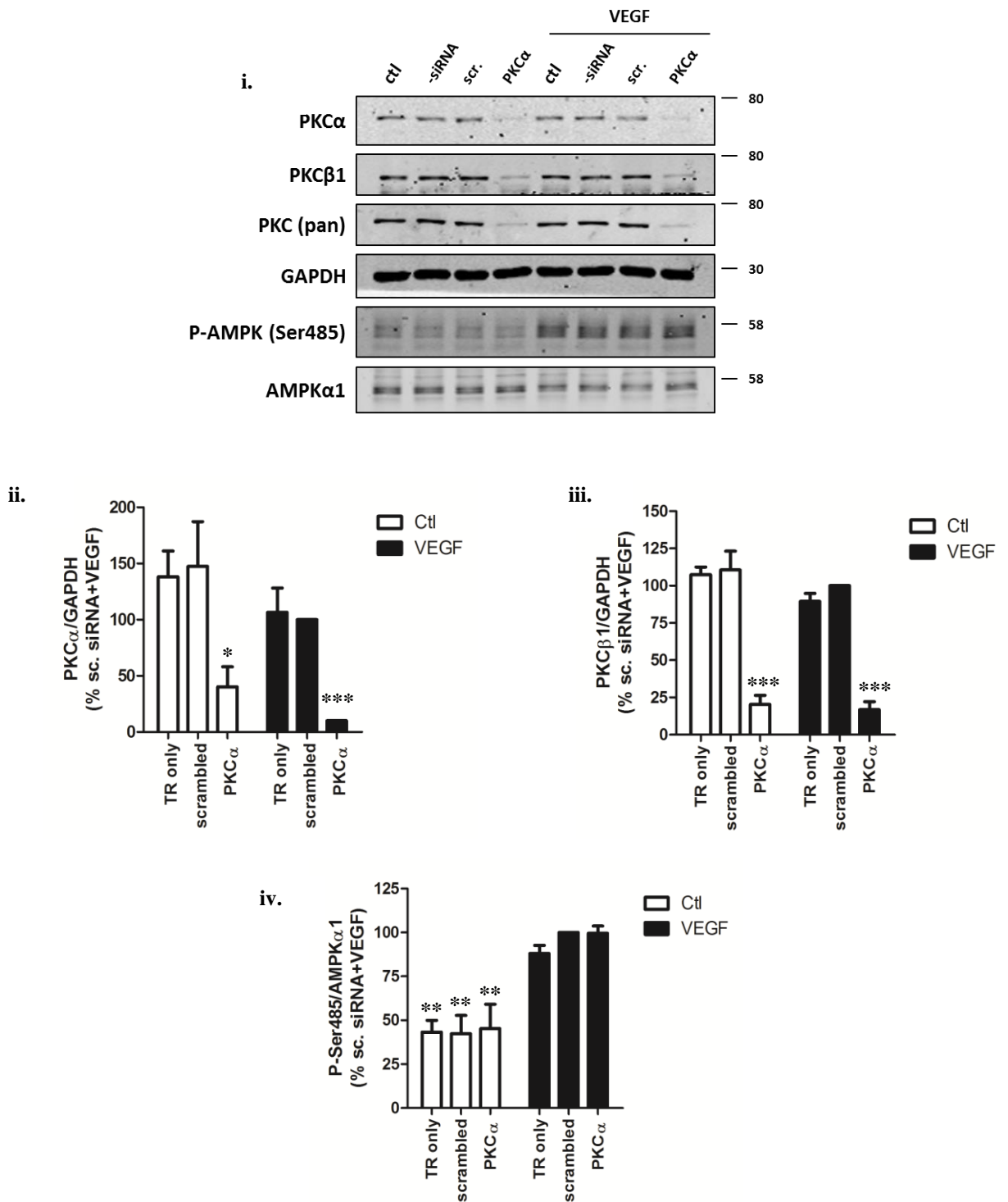


**Figure 5-16: siRNA-mediated downregulation of PKC  $\alpha$  has no effect on VEGF-stimulated AMPK  $\alpha$  Ser485 phosphorylation**

HUVEC were treated with 200 nM siRNA targeting PKC $\alpha$  for 48 hours prior to stimulation with VEGF (10 ng/mL) for 5 min. Cell lysates were prepared and subjected to SDS-PAGE/immunoblotting with the antibodies indicated. **i.** Blots shown are representative of three independent experiments with the migration of molecular mass markers indicated on the right, and **ii-iv.** Densitometric quantification of **i.** \* $p$ <0.05, \*\* $p$ <0.01 and \*\*\* $p$ <0.001 relative to scrambled siRNA treated cells in the presence of VEGF. (TR = transfection reagent with no siRNA).

Figure 5-17

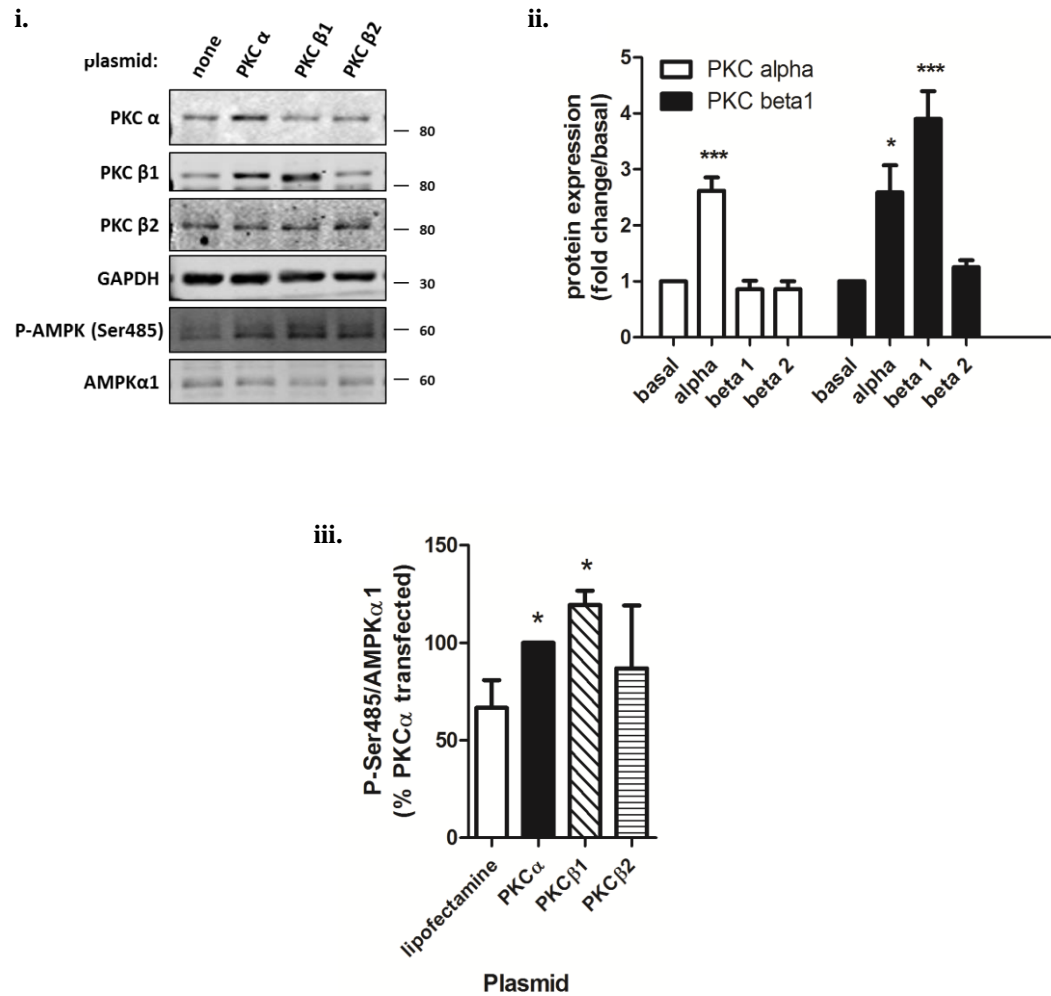


**Figure 5-17: Overexpression of PKC is sufficient to increase basal AMPK  $\alpha$ 1 Ser485 phosphorylation**

HeLa were transfected with 2  $\mu$ g plasmid DNA/well in a 6 well plate, 24 hours prior to cell lysis. Cell lysates were subjected to SDS-PAGE/immunoblotting with the antibodies indicated. **i.** a representative blot is shown with the migration of molecular mass markers indicated on the right. **ii. and iii.** Densitometric quantification of immunoblots in **i.** Data shown represents three independent experiments. \* $p$ <0.05 and \*\*\* $p$ <0.001 relative to basal expression.

To determine whether PKC activation stimulates AMPK  $\alpha$ 1 Ser485 phosphorylation in other cell types, HeLa (LKB1-null) were treated with PMA in the presence or absence of STO-609. PKC-stimulated AMPK  $\alpha$ 1 Ser485 phosphorylation is not unique to human endothelial cells nor is it dependent on the characterised AMPK-kinases LKB1 and CaMKK. In HeLa, inhibition of CaMKK with STO-609 significantly reduced AMPK activity (assessed by ACC Ser79 phosphorylation) in both the presence and absence of PMA, and in the absence of STO-609 PMA did not alter ACC Ser79 phosphorylation (Figure 5-18ii). PMA stimulated a 7.9-fold increase in AMPK  $\alpha$ 1 Ser485 phosphorylation (Figure 5-18iii) and 2.1-fold increase in MARCKS Ser152/156 phosphorylation (Figure 5-18iv), in both the absence and presence of STO-609 ( $p < 0.001$ ).

As HeLa cells are LKB1 null, in order to assess the inhibitory effect of AMPK  $\alpha$ 1 Ser485 phosphorylation on AICAR-stimulated AMPK activation HeLa expressing tetracyclin inducible LKB1 described previously (Boyle et al. 2008) were used. In HeLa cells expressing LKB1, stimulation with AICAR causes a 3-fold increase in ACC Ser79 phosphorylation (Figure 5-19ii). Acute pre-treatment of HeLa with PMA significantly reduces AICAR-stimulated ACC Ser79 phosphorylation (Figure 5-19ii). In the presence of PMA, basal AMPK Thr172 phosphorylation is also reduced in these cells whereas AICAR stimulation has no effect on PMA-stimulated AMPK  $\alpha$ 1 Ser485 phosphorylation.

Furthermore, PMA stimulates AMPK  $\alpha$ 1 Ser485 phosphorylation, and reduces AMPK Thr172 phosphorylation in cells from other species. Stimulation of mouse embryonic fibroblasts (MEFs) with 1  $\mu$ M PMA resulted in a 4.1-fold increase in Ser485 phosphorylation ( $p < 0.05$ ), and concurrently reduced basal Thr172 phosphorylation by approximately half ( $p < 0.001$ ) (Figure 5-20ii). ACC Ser79 phosphorylation was also markedly reduced (Figure 5-20i) in agreement with previous data (Figure 5-19ii).

Figure 5-18

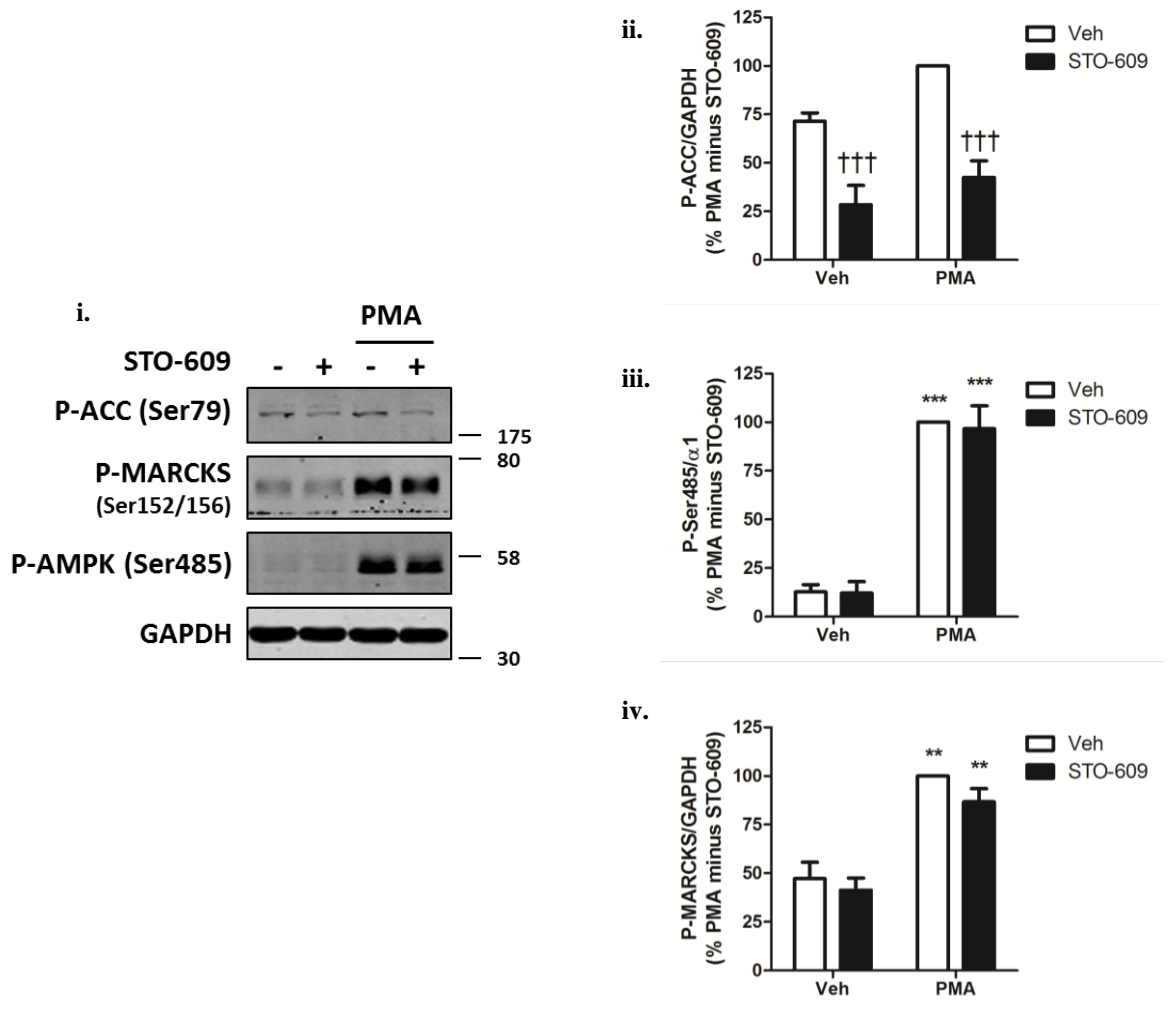
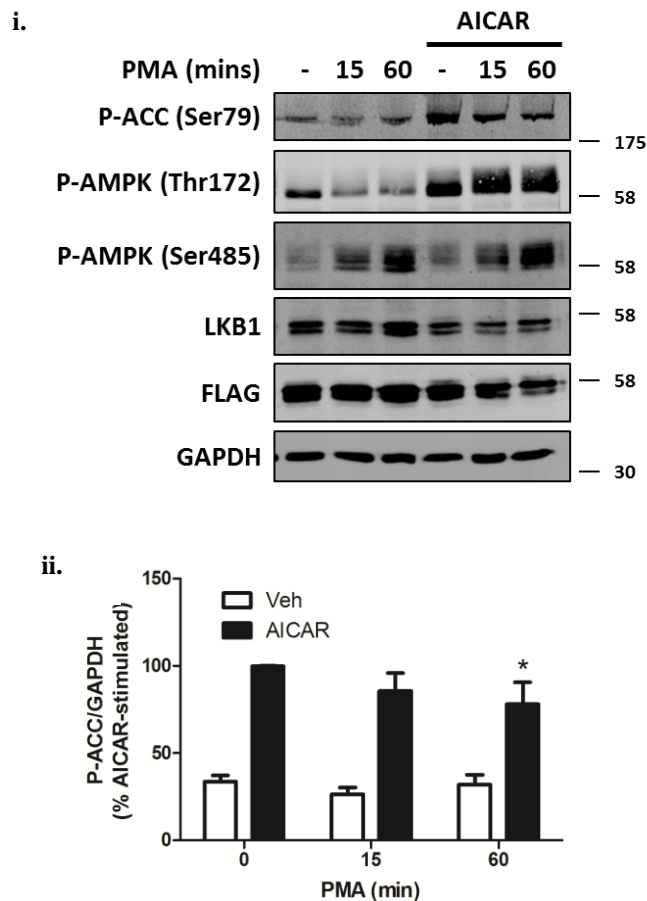


**Figure 5-18: PMA stimulates AMPK  $\alpha$ 1 Ser485 phosphorylation in HeLa independently of CaMKK**

Cell lysates were prepared from HeLa cells incubated with 10  $\mu$ M STO-609 for 1 hr prior to stimulation with 1  $\mu$ M PMA (20 min). Lysates were resolved by SDS-PAGE and immunoblotting with the antibodies indicated **i**. A representative immunoblot is shown, the migration of molecular mass markers is indicated on the right. This was repeated with similar results on four further occasions. **ii-iv**. Quantification of immunoblots in **i**. ††† $p$ <0.001 vs absence of STO-609. \*\* $p$ <0.01 and \*\*\* $p$ <0.001 vs absence of PMA.

*This experiment was performed with the help of Kunzah Jamal*

Figure 5-19

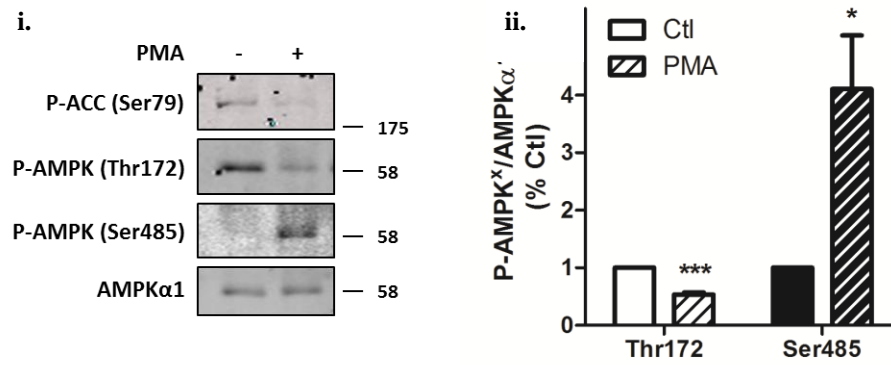


**Figure 5-19: PMA stimulates AMPK  $\alpha$ 1 Ser485 phosphorylation and inhibits AICAR-stimulated ACC Ser79 phosphorylation in HeLa cells expressing LKB1**

Cell lysates were prepared from HeLa cells stably expressing LKB1 incubated in the presence or absence of AICAR (1 mM, 45 min) and/or PMA (1  $\mu$ M) for 15 or 60 min as indicated. Lysates were resolved by SDS-PAGE and immunoblotting with the antibodies indicated. **i.** A representative immunoblot is shown, repeated with similar results two further occasions. The migration of molecular mass markers is indicated on the right. **ii.** Densitometric quantification of ACC Ser79 phosphorylation in **i.** \* $p$ <0.05 relative to absence of PMA.

*This experiment was performed by Kunzah Jamal*

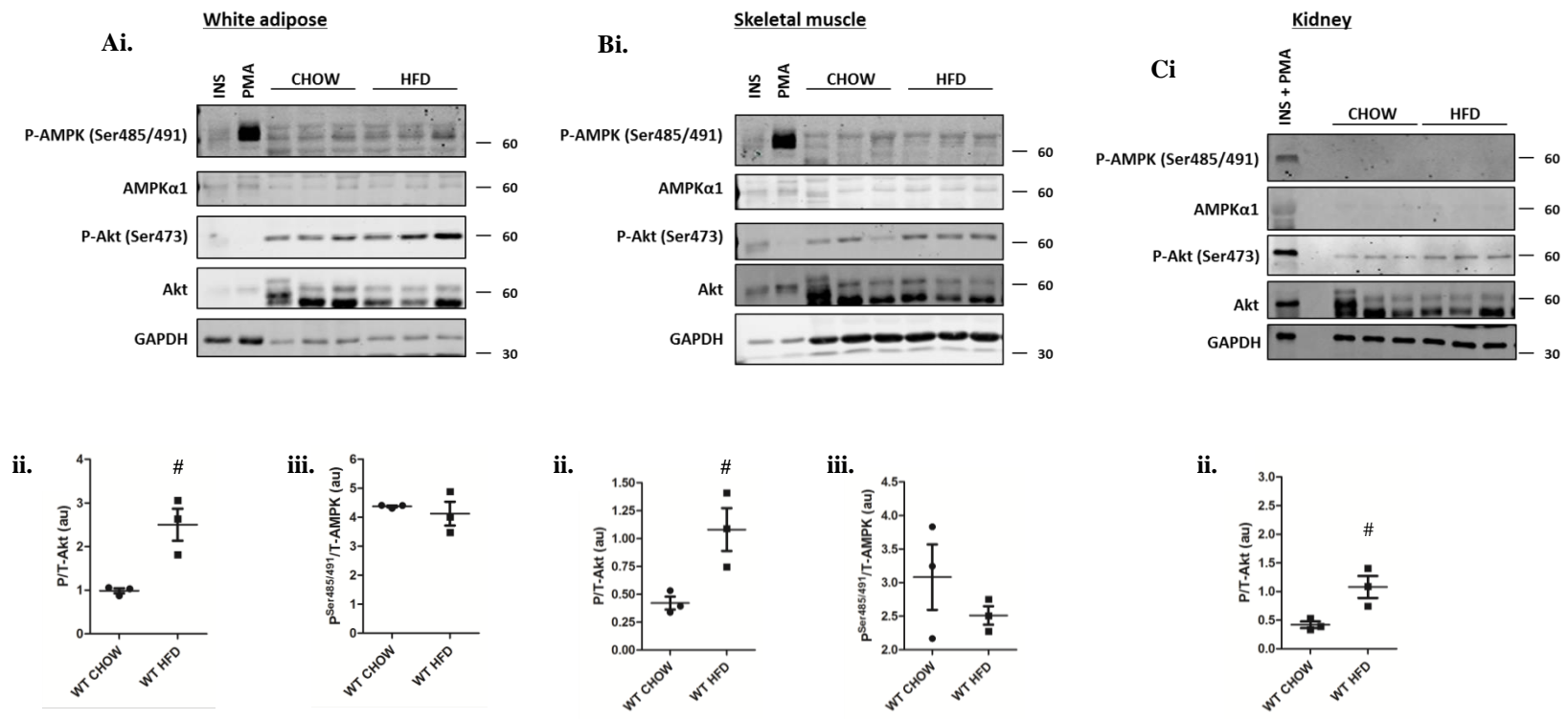
Figure 5-20

**Figure 5-20: PMA stimulates AMPK  $\alpha$ 1 Ser485 phosphorylation in MEFs**

Mouse embryonic fibroblasts were stimulated with 1  $\mu$ M PMA for 20 min. Cell lysates were prepared and subjected to SDS-PAGE and immunoblotting with the antibodies indicated. **i.** representative blots are shown with the migration of molecular mass markers indicated on the right. **ii.** Densitometric quantification of immunoblots shown in **i.** Data represents three independent experiments. \* $p$ <0.05 and \*\*\* $p$ <0.001 relative to absence of PMA.

Given that AMPK  $\alpha$ 1 Ser485 phosphorylation in response to PKC activation is seen in both human and murine tissue, and that caloric excess is associated with elevated PKC activity, we assessed the AMPK Ser485/491 phosphorylation status of mice fed either a normal chow or high fat diet (HFD). In white adipose tissue, skeletal muscle and kidney, Akt Ser473 phosphorylation was significantly increased in mice fed a HFD compared to chow ( $p < 0.05$ ; Figure 5-21), however no difference in AMPK Ser485/491 phosphorylation was detected between the two groups, in either white adipose or skeletal muscle; Ser485/491 was not detected in kidney tissue lysate. Given the discrepancies between mouse and human models of diabetes, and that PKC activation is reported to mediate lipid-induced insulin resistance in muscle, liver and vascular tissues, which has previously been reported to be associated with reduced AMPK activity in humans (Geraldes and King 2010, Schmitz-Peiffer 2013), the AMPK  $\alpha$ 1 Ser485 phosphorylation status of muscle biopsy membrane fractions obtained from a previous study of European men in which insulin sensitivity index (ISI) had been also been calculated (Hall et al. 2010), was therefore assessed (Figure 5-22). A significant ( $p < 0.05$ ) increase in AMPK  $\alpha$ 1 Ser485 phosphorylation was observed in individuals with an ISI score  $< 7$  (less insulin sensitive) compared to  $> 7$  (more insulin sensitive) (Figure 5-22ii). Furthermore, AMPK  $\alpha$ 1 Ser485 phosphorylation showed a significant inverse relationship with ISI ( $p < 0.05$ ,  $r^2 = 0.7337$ ; Figure 5-22iii). MARCKS phosphorylation was not detected in any muscle biopsy sample tested (not shown).

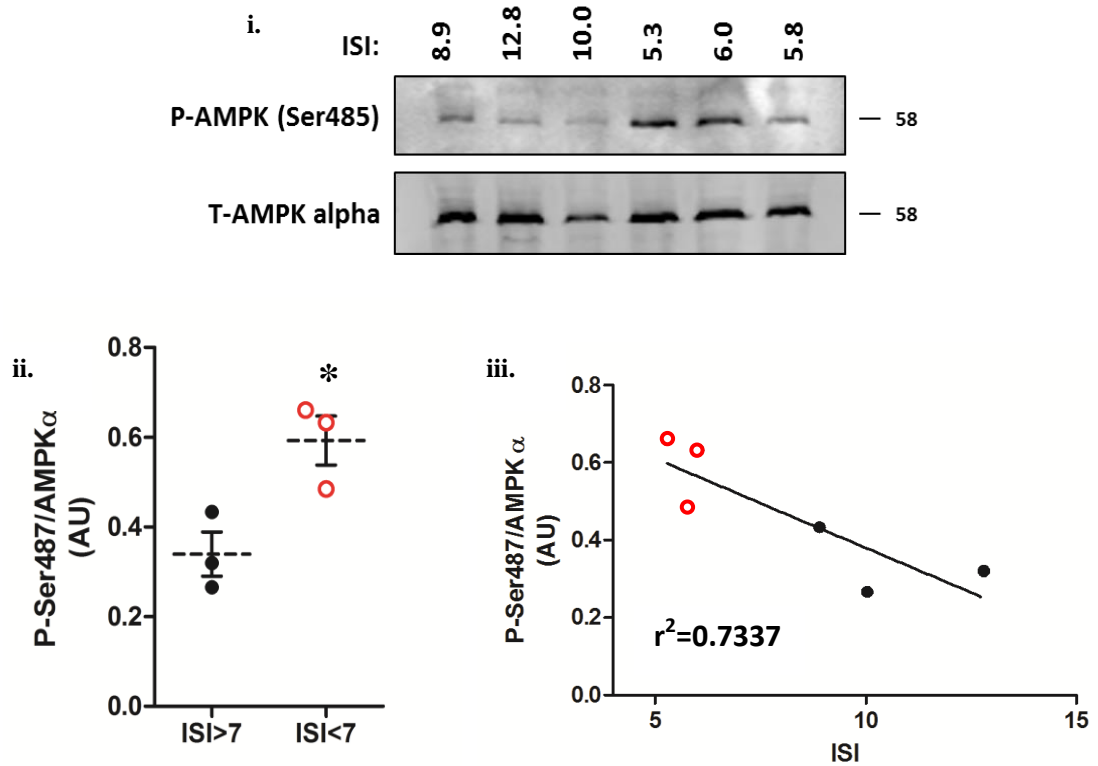
**Figure 5-21**



**Figure 5-21: Assessment of Akt and AMPK Ser485/491 phosphorylation in murine tissue**

Tissue (**A.** white adipose, **B.** skeletal muscle and **C.** kidney) harvested from wild type mice fed either chow or high fat diet (a kind gift from Dr Colin Selman, University of Glasgow) was homogenized. Prepared lysates were subjected to SDS-PAGE/immunoblotting using the antibodies indicated. Lysate prepared from HAEC treated with either 1  $\mu$ M insulin (INS) or PMA (1  $\mu$ M, 20 min), or pooled INS and PMA lysates (kidney immunoblots) was used as a positive control in each case (lane 1 and 2 respectively, or lane 1 for kidney). Tissue from three animals in each sample group was assessed. The migration of molecular mass markers is indicated on the right. <sup>#</sup> $p < 0.05$  vs chow diet.

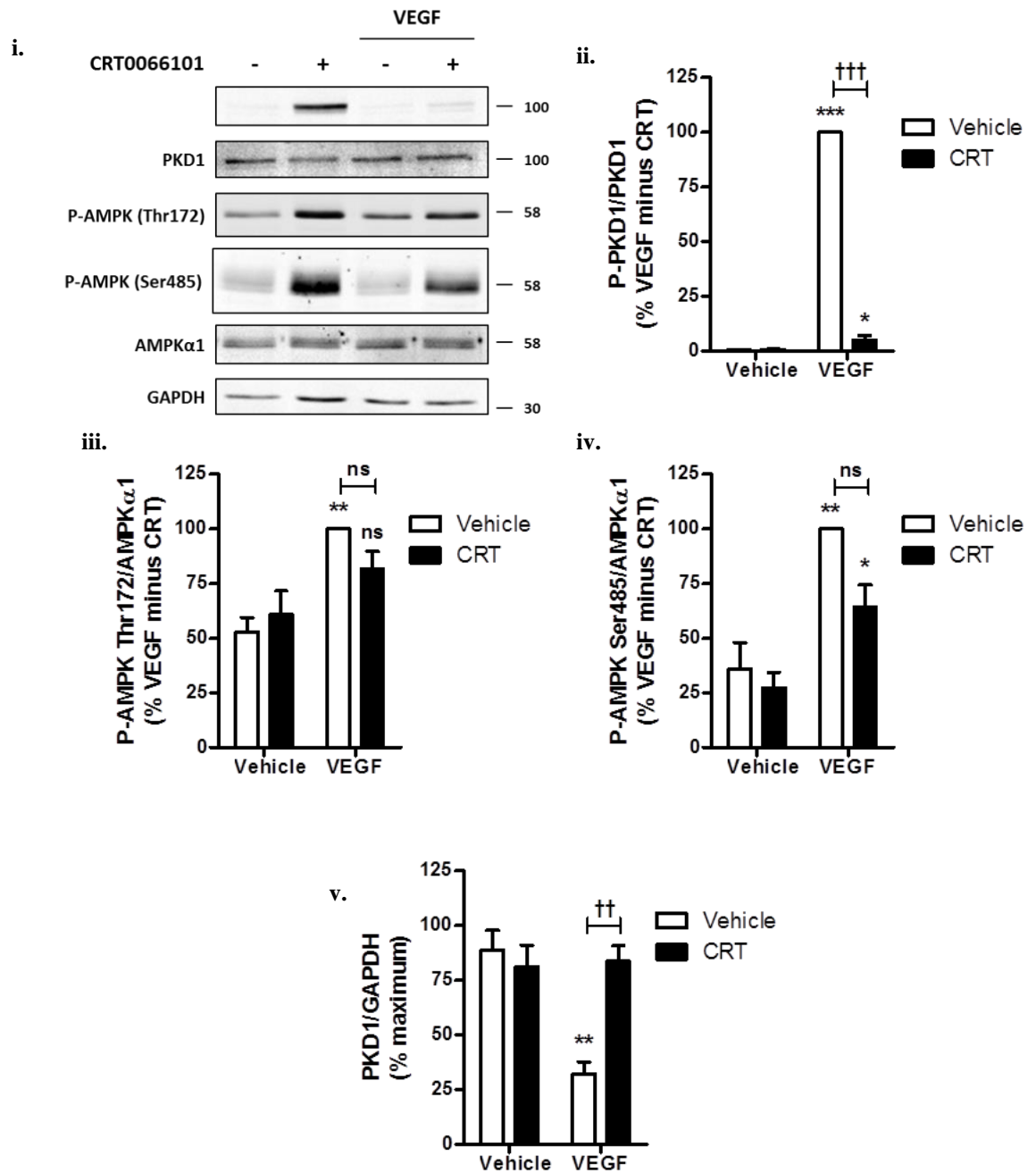
Figure 5-22



**Figure 5-22: AMPK  $\alpha$ 1 Ser485 phosphorylation is inversely related to insulin sensitivity in human muscle**

Human muscle biopsy membrane fractions were prepared in a previous study (Hall et al. 2010) and stored at  $-80^{\circ}\text{C}$ . **i.** Membrane fraction proteins of individuals with the indicated insulin sensitivity index (ISI) were resolved by SDS-PAGE and immunoblotting using the antibodies shown. **ii. and iii.** Quantification of AMPK  $\alpha$ 1 Ser485 phosphorylation relative to total AMPK  $\alpha$ . \* $p < 0.05$  comparing individuals with an ISI  $< 7$  to those with an ISI  $> 7$ .

Figure 5-23

**Figure 5-23: The effect of CRT0066101 on VEGF-stimulated AMPK phosphorylation**

HAEC were incubated in the presence or absence of 10  $\mu$ M CRT0066101 for 60 min prior to stimulation with VEGF (10 ng/mL, 5 min). HAEC lysates were prepared and proteins resolved by SDS-PAGE and immunoblotted with the antibodies indicated. **i.** a representative blot is shown with the migration of molecular mass markers indicated on the right. **ii.–v.** Densitometric quantification of immunoblots from four independent experiments showing mean  $\pm$  SEM. \* $p$ <0.05, \*\* $p$ <0.01 and \*\*\* $p$ <0.001 compared to absence of VEGF, †† $p$ <0.01 and ††† $p$ <0.001.

*This experiment was performed by Dr Sarah Mancini*

## 5.3 Discussion

Data presented here demonstrates for the first time that in addition to activating AMPK, VEGF also stimulates the inhibitory phosphorylation of AMPK  $\alpha$ 1 Ser485 in human vascular endothelial cells.

### 5.3.1 VEGF and AICAR stimulate both AMPK Thr172 and Ser485 phosphorylation, but by different mechanisms

Data presented here is in agreement with the previous findings of Reihill and co-workers, confirming that VEGF-stimulated AMPK  $\alpha$  Thr172 phosphorylation is dependent on CaMKK activity (Reihill et al., 2007) and  $\text{Ca}^{2+}$  influx (Reihill, 2009), although the identity of the  $\text{Ca}^{2+}$  channel mediating VEGF-stimulated  $\text{Ca}^{2+}$  influx has still to be determined (discussed in Chapter 4). AICAR-stimulated AMPK activation is neither CaMKK nor  $\text{Ca}^{2+}$ -dependent. The present study further demonstrates that VEGF-stimulated AMPK Ser485 phosphorylation is  $\text{Ca}^{2+}$  dependent but independent of CaMKK. AMPK  $\alpha$ 2 Ser491 is proposed to be a poor substrate for Akt *in vivo* (Hawley et al. 2014). Phosphorylation of this residue ( $\alpha$ 2 Ser491) is likely to result from auto-phosphorylation by active AMPK. Data demonstrating that inhibition of VEGF-stimulated AMPK activation (using STO-609) has no effect on AMPK  $\alpha$ 1 Ser485 phosphorylation argues against an AMPK auto-phosphorylation event in response to AMPK activation. Furthermore, AMPK activation using the direct AMPK activator A769662 does not stimulate AMPK  $\alpha$ 1 Ser485 phosphorylation. In agreement with previous reports (Javadov et al. 2009, Lu et al. 2010, Stone et al. 2012), AICAR was also demonstrated to stimulate AMPK  $\alpha$ 1 Ser485 phosphorylation however the mechanism of AICAR-stimulated AMPK Ser485 phosphorylation has not been described to date. However, AICAR-stimulated AMPK  $\alpha$ 1 Ser485 phosphorylation is not sensitive to  $\text{Ca}^{2+}$  depletion indicating that VEGF and AICAR stimulate AMPK  $\alpha$ 1 Ser485 phosphorylation via different mechanisms. AICAR has previously been reported to activate Akt in HAEC (Morrow et al. 2003) such that it remains possible that AICAR-stimulated AMPK  $\alpha$ 1 Ser485 phosphorylation is mediated via Akt, and it would be interesting to assess this hypothesis in future studies.

### 5.3.2 Investigating the Akt and ERK1/2 dependence of AMPK $\alpha$ 1 Ser485 phosphorylation

Previous reports have demonstrated that Akt and ERK1/2 (or an ERK1/2 regulated kinase) can act as AMPK Ser485 kinases (Horman et al. 2006, Lopez-Cotarelo et al. 2015). Insulin or IGF-1 (insulin-like growth factor) has been shown to stimulate Akt activity and concomitantly reduce AMPK Thr172 phosphorylation (or activity) in multiple model systems, including heart (Kovacic et al. 2003, Horman et al. 2006), adipocytes (Berggreen et al. 2009), tumour cells (Hawley et al. 2014), vascular smooth muscle (Ning et al. 2011) and hepatocytes and myotubes (Valentine et al. 2014). In all of these studies, with the exception of Kovacic and colleagues who were not able to define the mechanism explaining the observed insulin-stimulated reduction in AMPK activity, Akt-mediated inhibition of AMPK activity in response to insulin/IGF-1 was attributed to increased AMPK Ser485/491 phosphorylation.

Further mechanisms describing the regulation of AMPK  $\alpha$ 1 Ser485 phosphorylation independent of Akt have also been described. Cyclic AMP-dependent protein kinase (PKA) is reported to phosphorylate AMPK  $\alpha$ 1 at Ser485 in addition to Ser173, Ser497, and AMPK  $\beta$ 1-Ser24 (Djouder et al. 2010). More recently, IKK inhibition in neutrophils and macrophages was reported to effectively diminish LPS-induced AMPK  $\alpha$ 1 Ser485 phosphorylation and Thr172 de-phosphorylation, whereas Akt inhibition had negligible effects on LPS-induced Thr172 de-phosphorylation and cytokine production (Park et al. 2014). Furthermore, CCR7 is reported to promote the survival of mature dendritic cells via  $G_{\alpha}/G_{\beta/\gamma}$ -mediated activation of the MEK1/2-ERK1/2 cascade resulting in AMPK  $\alpha$ 1 Ser485 phosphorylation (Lopez-Cotarelo et al. 2015).

VEGF stimulates the phosphorylation of Akt and ERK1/2. Therefore, to assess the dependence of VEGF-stimulated AMPK Ser485 phosphorylation on Akt and ERK1/2, selective kinase inhibitors were used. Contrary to previously described mechanisms, the present study demonstrates that VEGF-stimulated AMPK  $\alpha$ 1 Ser485 phosphorylation is not dependent on ERK1/2 or Akt, as complete inhibition of VEGF-stimulated ERK1/2 Thr202/Try204 and Akt Ser473 phosphorylation using the MEK inhibitor PD184352 or the Akt inhibitor Akti-1/2 respectively had no effect on either VEGF-stimulated Thr172 or  $\alpha$ 1 Ser485 phosphorylation. At the inhibitor concentration used here (1  $\mu$ M), VEGF-stimulated ERK and Akt phosphorylation were not affected by Akt and ERK inhibition

respectively, suggesting specific inhibition by these compounds as reported previously (Logie et al. 2007, Allen et al. 2003).

Furthermore, pre-treatment of endothelial cells with the PI3K inhibitor wortmannin, had no effect on VEGF-stimulated AMPK Thr172 or  $\alpha 1$  Ser485 phosphorylation, while both basal and VEGF-stimulated Akt Ser473 phosphorylation were significantly reduced suggesting that AMPK phosphorylation at both Thr172 and  $\alpha 1$  Ser485 is independent of PI3K activity. In the absence of wortmannin, VEGF stimulated only a modest increase in Akt Ser473 phosphorylation. This was not however unexpected, given the modest increase in Akt Ser473 phosphorylation observed after 5 min of VEGF treatment).

Together this data strongly suggests that Akt activity is not *necessary* for VEGF-stimulated AMPK  $\alpha 1$  Ser485 phosphorylation. To determine whether Akt activation is *sufficient* to induce AMPK  $\alpha 1$  Ser485 phosphorylation, HAEC were stimulated with the Akt activator insulin, which has previously been reported to stimulate AMPK  $\alpha 1$  Ser485 phosphorylation in other cell types (Horman et al. 2006, Soltys et al. 2006, Berggreen et al. 2009, Ning et al. 2011). Robust Akt activation was indicated by increased phosphorylation of Akt at Ser473, however no increase in AMPK  $\alpha 1$  Ser485 phosphorylation was observed, whereas in these cells VEGF stimulated substantial AMPK  $\alpha 1$  Ser485 phosphorylation. Akt activation by insulin is therefore not *sufficient* to stimulate AMPK  $\alpha 1$  Ser485 phosphorylation in human vascular endothelial cells.

Previous studies in cultured immune cells (neutrophils and B cell chronic lymphocytic leukaemia cells) report that Akt is activated in response to PMA (Barragan et al. 2006, Douda et al. 2014). To assess the effect of PMA-stimulation on Akt phosphorylation in endothelial cells, HUVEC were pre-treated with Akti-1/2 or wortmannin prior to PMA or insulin stimulation. Both Akt Thr308 and Ser473 phosphorylation are robustly stimulated by insulin, an effect ablated by pre-treatment with wortmannin or Akti. As previously demonstrated, insulin-mediated Akt activation does not stimulate AMPK  $\alpha 1$  Ser485 phosphorylation.

PMA treatment however causes robust stimulation of AMPK  $\alpha 1$  Ser485 phosphorylation which is not affected by PI3K or Akt inhibition. PMA stimulation actually reduces Akt phosphorylation at both Thr308 and Ser473, and is ablated in the presence of wortmannin or Akt. This data strongly supports our previous findings in endothelial cells indicating that

VEGF-, and now PMA-stimulated AMPK  $\alpha$ 1 Ser485 phosphorylation is not mediated via a PI3K/Akt signalling axis.

Together these data indicate that VEGF-stimulated AMPK  $\alpha$ 1 Ser485 phosphorylation is independent of PI3K/Akt and ERK1/2 signalling in vascular endothelial cells, contrary to findings in other model systems and to our expectations. We therefore conclude that Akt activation is neither necessary, nor sufficient for AMPK  $\alpha$ 1 Ser485 phosphorylation in primary human vascular endothelial cells. Activation of PKC using the synthetic phorbol ester PMA decreases Akt activity and as such is unlikely to stimulate AMPK  $\alpha$ 1 Ser485 phosphorylation via increased Akt activity as suggested previously (Djouder et al. 2010). Previous reports suggesting that Akt is an AMPK  $\alpha$ 1 Ser485 kinase might be describing cell and/or stimuli specific effects/mechanisms.

### **5.3.3 Investigating the mechanism of VEGF-stimulated AMPK $\alpha$ 1 Ser485 phosphorylation**

In light of these findings, we hypothesised that an alternative, novel and as yet uncharacterised,  $\text{Ca}^{2+}$ -dependent mechanism mediates VEGF- and PMA-stimulated AMPK  $\alpha$ 1 Ser485 phosphorylation. Given the  $\text{Ca}^{2+}$  dependence of VEGF-stimulated AMPK  $\alpha$ 1 Ser485 phosphorylation and previous suggestions that DAG-regulated  $\text{Ca}^{2+}$  channels may be mediating VEGF-stimulated  $\text{Ca}^{2+}$  influx in endothelial cells (Chapter 4), we asked whether the PKC family of protein kinases were involved in regulating AMPK activity.

The protein kinase C (PKC) family contains of a number of structurally and functionally related serine-threonine kinases, derived from multiple genes and alternative mRNA splicing. At least 15 isoforms have been identified in humans and these can be further subcategorised according to their primary domain structures and second messenger requirements, summarised in Table 5.1. Conventional or classical PKCs ( $\alpha$ ,  $\beta$ I,  $\beta$ II,  $\gamma$ ) require calcium and diacylglycerol for activation, whereas the novel PKCs ( $\delta$ ,  $\epsilon$ ,  $\eta$ ,  $\theta$ ) require DAG but not calcium. Because they both require DAG for activation, both the conventional and novel PKCs can be activated via phospholipase C-mediated signalling cascades, including those downstream of VEGF-receptor activation. The final PKC subfamily, the atypical PKCs ( $\zeta$ ,  $\iota/\lambda$ ) require neither DAG nor calcium for activation.

**Table 5-1: Protein kinase C subfamily categorisation and co-factor requirements**

subcategory	isoforms	Co-factor requirements		
		Ca <sup>2+</sup>	DAG	Phospholipid
conventional	$\alpha$ , $\beta$ I, $\beta$ II, $\gamma$	✓	✓	✓
novel	$\delta$ , $\epsilon$ , $\eta$ , $\theta$ , $\mu$	-	✓	✓
atypical	$\zeta$ , $\nu$ , $\lambda$	-	-	✓

Inhibition of the classical PKCs or PKC  $\beta$  using GF109203X or LY333531 respectively abolished VEGF-stimulated AMPK  $\alpha$ 1 Ser485 phosphorylation without significantly altering VEGF-stimulated AMPK Thr172 phosphorylation. The mechanism by which VEGF stimulates AMPK activity (Thr172) was investigated and discussed in Chapter 4, however, since only AMPK  $\alpha$ 1 Ser485 phosphorylation is ablated by PKC inhibition we hypothesised that these phosphorylation events are regulated via different mechanisms: Thr172 independently of PKC, and  $\alpha$ 1 Ser485 in a PKC dependent manner.

Although not significant ( $p > 0.05$ ) treatment of HUVEC with LY333531 caused a modest increase in VEGF-stimulated Thr172 phosphorylation (23 % increase in mean phosphorylation) suggesting that inhibition of PKC may increase AMPK activity. Basal AMPK activity was later shown to be significantly increased by the PKC inhibitor GF109203X, which also tended to increase VEGF-stimulated AMPK activity indicating that PKC negatively regulates AMPK activity. There are contradictory reports in the literature as to whether PKC positively or negatively regulates AMPK activity. Saberi and colleagues report that H<sub>2</sub>O<sub>2</sub> induced necrosis in primary hepatocytes is associated with increased PKC activation and reduced AMPK activity, and inhibition of PKC using multiple different PKC inhibitors (Ro-31-8425 and Gö6850) increased AMPK activity and protected against H<sub>2</sub>O<sub>2</sub> induced necrosis (Saberi et al. 2008). Furthermore, in rat cardiac myocytes PMA treatment reduced AMPK activity in a GF109203X sensitive manner (Tsuchiya et al. 2012) such that PKC-mediated AMPK inhibition may underlie these previous reports. Contrary to this, Nishino and colleagues report that AMPK activation and GLUT4 upregulation stimulated by ischemic preconditioning was abrogated by prior infusion with GF109203X (Nishino et al. 2004), whereas Chang and co-workers report that AMPK activation is required for PMA-stimulated monocyte adhesion, suggesting that PKC is upstream of LKB1 and AMPK activation (Chang et al. 2012). LY333531 (10  $\mu$ M) has previously been reported to inhibit AMPK activity in a cell free assay of activity (Komander et al. 2004). LY333531 at the concentration used in the present study (1  $\mu$ M) did not influence AMPK activity in a cell free assay of AMPK activity (either increase or

decrease), and did not inhibit AMPK activation by VEGF. At the highest concentration we have used in the present study, LY333531 is neither a direct activator nor inhibitor of AMPK, and as such PKC inhibition tends to increase AMPK activity only in intact cells.

The present study also demonstrates that PKC activation using the synthetic phorbol ester PMA, or the diacylglycerol mimetic OAG stimulates the phosphorylation of AMPK  $\alpha$ 1 at Ser485, and not AMPK  $\alpha$ 2 Ser491. We have assessed the relative contribution of AMPK  $\alpha$ 1 and  $\alpha$ 2 containing complexes in vascular endothelial cell lysates. AMPK  $\alpha$ 1 containing complexes account for the vast majority of vascular AMPK activity (basal and VEGF-/AICAR-stimulated) such that abrogation of AMPK  $\alpha$ 1 activity has the potential to significantly influence AMPK activity in the vascular endothelium. Specific anti-phospho-AMPK  $\alpha$ 2 Ser491 antibodies were not widely available at the time of these studies although have become commercially available since. These conclusions were therefore reached using a phospho-specific AMPK  $\alpha$ 1/ $\alpha$ 2 Ser485/491 antibody after successful separation of AMPK  $\alpha$ 1 and  $\alpha$ 2 containing complexes by immunoprecipitation. It would be interesting to reassess these results with specific anti-phospho-AMPK  $\alpha$ 2 Ser491 antibodies. Data to this point also indicates that in addition to VEGF, other activators of PKC (PMA and OAG) also preferentially stimulate AMPK  $\alpha$ 1 Ser485 phosphorylation in primary human vascular endothelial cells. Therefore, PKC activation, rather than a VEGF-specific signalling event stimulates AMPK  $\alpha$ 1 Ser485 phosphorylation and inhibition of AMPK activity.

### **5.3.4 Characterising the PKC isoform(s) responsible for PKC-mediated AMPK $\alpha$ 1 Ser485 phosphorylation**

Phosphorylation of MARCKS is often used as a surrogate marker for PKC activity. In Sf9 insect cells, a heterologously expressed human MARCKS was found to be phosphorylated by PKCs  $\alpha$ ,  $\beta$ <sub>1</sub>,  $\beta$ <sub>2</sub>,  $\gamma$ ,  $\delta$ ,  $\epsilon$  and  $\eta$  but not PKC  $\zeta$  (Cabell et al. 1996). MARCKS phosphorylation is therefore a surrogate marker of PKC activity, representing the activity of multiple PKC isoforms.

The time course of PMA-stimulated AMPK  $\alpha$ 1 Ser485 and MARCKS Ser152/156 was assessed, in addition to the sensitivity of PMA- and VEGF-stimulated AMPK and MARCKS phosphorylation to PKC inhibition using LY333531. In response to PMA, MARCKS was rapidly phosphorylated with the time taken to reach half-maximal phosphorylation calculated as being 1 min. The time taken to reach half-maximal AMPK  $\alpha$ 1 Ser485 phosphorylation was calculated to be 2.6 min. LY333531 inhibited VEGF-

stimulated MARCKS and AMPK  $\alpha$ 1 Ser485 phosphorylation with remarkably similar kinetics and significant inhibition of phosphorylation of both MARCKS and AMPK  $\alpha$ 1 Ser485 at the lowest concentration tested (0.1  $\mu$ M). PMA-stimulated MARCKS phosphorylation was however less sensitive to inhibition by low concentrations of LY333531 such that significant inhibition of PMA-stimulated MARCKS was only measured at LY333531 concentrations  $\geq 0.5$   $\mu$ M, whereas the inhibition of PMA-stimulated AMPK  $\alpha$ 1 Ser485 phosphorylation demonstrated kinetics similar to VEGF-stimulated AMPK  $\alpha$ 1 Ser485 phosphorylation. Together, this data suggests that AMPK  $\alpha$ 1 Ser485 may be a substrate for only a subset of PKC isoforms, whereas MARCKS is a substrate for more PKC isoforms.

Chronic stimulation of PKC activity with nanomolar concentrations of PMA has been shown to downregulate PKC expression by increasing its degradation via the lysosome machinery (Young et al. 1987). Downregulation of the PKC isoforms  $\alpha$ ,  $\beta$ 1,  $\gamma$ ,  $\eta$ ,  $\theta$  and  $\mu$  by chronic PMA treatment (200 nM, overnight) inhibited both VEGF- and OAG-stimulated AMPK  $\alpha$ 1 Ser485 phosphorylation, however siRNA-mediated PKC  $\alpha$  downregulation (~90 % reduction) had no effect on VEGF-stimulated AMPK  $\alpha$ 1 Ser485 phosphorylation. Conversely, over expression of either PKC  $\alpha$  or  $\beta$ 1 was sufficient to increase AMPK  $\alpha$ 1 Ser485 phosphorylation, even in the absence of a stimulus. Together these data indicate that over expression of a single PKC isoform is sufficient to increase AMPK  $\alpha$ 1 Ser485 phosphorylation, but alternate PKC isoforms may be able to compensate for depletion of single PKC isoforms.

It was interesting to observe that down regulation of PKC  $\alpha$  stimulated a concurrent decrease in PKC  $\beta$ 1 levels. Conversely, overexpression of PKC  $\beta$ 1 caused a concurrent increase in PKC  $\alpha$  expression. Data presented therefore raises the interesting concept of PKC isoenzyme trans-regulation. Such coordinated regulation has been described previously in murine hemopoietic cells (Baf3) and a murine myeloid cell line (32D), in which PKC  $\alpha$  upregulated PKC  $\delta$  protein levels by increasing mRNA transcription and stability (Romanova et al. 1998). PKC  $\beta$  and  $\gamma$  expression was not detected in these cell lines so the effect of PKC  $\alpha$  overexpression on the level of these was not studied and cannot be compared with the present study.

Despite previous suggestions that PKC stimulates AMPK  $\alpha$ 1 Ser485 phosphorylation, no data demonstrating this has been made available to date (Kodiha and Stochaj 2011). We have established in this study that PKC is an AMPK  $\alpha$ 1 Ser485 kinase *in vitro*. Purified rat-

brain PKC consisting of mostly  $\alpha$ ,  $\beta$  and  $\gamma$  ( $\delta$  and  $\zeta$  to a lesser extent) phosphorylated isolated kinase-dead (therefore not capable of auto-phosphorylation) AMPK at least as well as a quantity of Akt with comparable kinase activity. This is the first demonstration to our knowledge of PKC acting as a direct AMPK  $\alpha$ 1 Ser485 kinase *in vitro*. The identity of the PKC isoform(s) mediating AMPK  $\alpha$ 1 Ser485 phosphorylation however is not clear. The calcium dependence of VEGF-stimulated AMPK  $\alpha$ 1 Ser485 phosphorylation, and the demonstration that purified PKC consisting of predominantly PKC  $\alpha$ ,  $\beta$  and  $\gamma$  ( $\delta$  and  $\zeta$  to a lesser extent) phosphorylate AMPK  $\alpha$ 1 Ser485 *in vitro*, indicates that the PKC isoform mediating this effect is likely to be one of the classical ( $\text{Ca}^{2+}$  regulated) isoforms.

### **5.3.5 PKC inhibition as a therapeutic approach for ameliorating reduced AMPK activity in metabolic disease**

LY333531 is a compound also known as ruboxistaurin and has previously been reported to reverse vascular abnormalities in animal models of diabetes (Ishii et al. 1996), and normalise diabetes induced elevations in PKC activity in the retina and kidney of diabetic animals (Kowluru et al. 1996). Furthermore, LY333531 ameliorated abnormal hemodynamics in patients with diabetes and enhanced endothelium dependent vasodilation impaired by hyperglycaemia (Aiello et al. 1999, Beckman et al. 2002). Ruboxistaurin (64 mg) administered as a daily oral dose was found to be well tolerated in human subjects. It was further shown to pass into the systemic circulation after oral administration where it is extensively metabolised by CYP3A4 (Yeo et al. 2006). The major metabolite of ruboxistaurin is *N*-desmethyl ruboxistaurin and was found to be an equally potent inhibitor of PKC  $\beta$ . The plasma concentration of ruboxistaurin and *N*-desmethyl ruboxistaurin in 17 men after an oral dose of 64 mg was found to be 200 and 128 nmol/L respectively (Yeo et al. 2006). Later reports characterising the metabolism and excretion of [ $^{14}\text{C}$ ]-ruboxistaurin in six human subjects achieved plasma concentrations of 204 nmol/L. and 87.4 nmol/L for ruboxistaurin and *N*-desmethyl ruboxistaurin respectively (Burkey et al. 2006) consistent with previous reports. We have demonstrated that therapeutically achievable concentrations of LY333531 significantly reduce AMPK  $\alpha$ 1 Ser485 phosphorylation >60%. Given that ruboxistaurin and *N*-desmethyl ruboxistaurin are equipotent, it would be interesting to assess *in vitro* the combined inhibitory effect of ruboxistaurin and *N*-desmethyl ruboxistaurin on AMPK  $\alpha$ 1 Ser485 phosphorylation, under more biologically relevant conditions.

### 5.3.6 AMPK $\alpha$ 1 Ser485 phosphorylation in mouse and human models of metabolic disease

The present study demonstrates that PKC-mediated AMPK  $\alpha$ 1 Ser485 phosphorylation is not limited to vascular endothelial cells and therefore has the potential to influence AMPK activity at the level of the whole organism. We have also demonstrated that AMPK  $\alpha$ 1 Ser485 phosphorylation is associated with reduced AMPK activity (Thr172 phosphorylation) in both human and murine derived cultured cells. In both HeLa and MEFs, basal Thr172 phosphorylation is reduced in the presence of PMA. Additionally, AICAR-stimulated ACC Ser79 phosphorylation is significantly reduced with prior PMA treatment, confirming previous reports of the inhibitory effect of AMPK  $\alpha$ 1 Ser485 phosphorylation on AMPK activity. Together, these studies suggest that Ser485/491 phosphorylation may underlie reduced AMPK activity observed under conditions where PKC activity is known to be elevated *e.g.* diabetes. After determining the greater efficiency of the AMPK  $\alpha$ 1/ $\alpha$ 2 Ser485/491 antibody for detecting Ser485/491 phosphorylation in murine tissue (not shown), the Ser485/491 phosphorylation status of wild type mice, fed either normal chow or HFD was investigated. Significantly elevated Akt phosphorylation was measured in skeletal muscle, white adipose and kidney tissue from HFD fed mice compared to chow, however no difference in Ser485/491 phosphorylation was measured between the groups. If, as suggested by previous reports (Horman et al. 2006, Soltys et al. 2006, Berggreen et al. 2009, Ning et al. 2011), Akt activation stimulates AMPK  $\alpha$ 1 Ser485 phosphorylation, we might have expected to observe concurrent increase in AMPK  $\alpha$ 1 Ser485 phosphorylation, in these tissues.

Given the striking differences observed previously between mouse models of diabetes and human subjects, we also assessed the AMPK  $\alpha$ 1 Ser485 phosphorylation status in muscle biopsies obtained from European men in a previous study in which Akt phosphorylation levels and insulin sensitivity index (ISI) had been determined:  $10000/\sqrt{[(\text{fasting glucose} \times \text{fasting insulin}) \times (\text{mean glucose during OGTT} \times \text{mean insulin during OGTT})]}$  (Matsuda and DeFronzo 1999). A strong inverse correlation ( $r^2=0.7337$ ) between ISI and AMPK  $\alpha$ 1 Ser485 phosphorylation was observed, and subjects who were determined to be less sensitive to insulin (ISI <7) demonstrated significantly elevated AMPK  $\alpha$ 1 Ser485 phosphorylation ( $p<0.05$ ). Inhibition of AMPK  $\alpha$ 1, which is reported to contribute 50 % of basal AMPK activity in human vastus lateralis muscle (Deshmukh et al. 2010), therefore has the potential to markedly influence AMPK activity. Crucially, no relationship was observed between previously reported Akt phosphorylation levels (Hall et al. 2010), and

AMPK  $\alpha$ 1 Ser485 such that it remains possible that PKC mediates AMPK  $\alpha$ 1 Ser485 phosphorylation in human muscle despite not being able to detect the phosphorylation of MARCKS in these samples. The samples used in this analysis were chosen to represent a range of insulin sensitivities although none of the volunteers had diabetes. Reduced AMPK activity due to Ser485 phosphorylation may therefore occur during metabolic dysfunction preceding the development of insulin resistance and diabetes thus providing a therapeutic window to ameliorate or slow the development of diabetes. We believe this to be the first report of an inverse correlation between insulin sensitivity and AMPK  $\alpha$ 1 Ser485 phosphorylation, and propose that AMPK  $\alpha$ 1 Ser485 phosphorylation may explain some of the reduced AMPK activity associated with insulin resistance. Whether AMPK  $\alpha$ 1 Ser485 phosphorylation contributes to vascular dysfunction or cardiovascular disease associated with insulin resistance remains to be established.

During the preparation of this thesis, Coughlan and co-workers reported that PKD1 inhibits AMPK  $\alpha$ 2 through phosphorylation of Ser491 and impairs insulin signalling in skeletal muscle cells (Coughlan et al. 2016). The authors of this study report that PMA stimulates PKD1 activation which catalyses the phosphorylation of AMPK  $\alpha$ 2 at Ser491, resulting in the inhibition of AMPK  $\alpha$ 2 activity resulting in impaired insulin signalling. Broad-spectrum PKC inhibition or PKD1 specific inhibition prevented PMA-stimulated AMPK  $\alpha$ 2 Ser491 phosphorylation. Our study reports that PKC activation, either by the addition of PMA, or the endogenous signalling molecule VEGF stimulates AMPK  $\alpha$ 1 Ser485 phosphorylation, and furthermore, we see no effect of PMA on AMPK  $\alpha$ 2 Ser491 phosphorylation. In light of this recent report, we sourced the PKD1 inhibitor (CRT0066101) used by Coughlan and co-workers and assessed the effect of inhibiting PKD1 (murine designation for human PKC $\mu$ ) on VEGF-stimulated AMPK  $\alpha$ 1 Ser485 phosphorylation in primary human vascular endothelial cells.

VEGF stimulates significant phosphorylation of PKD (Ser916) which is prevented by prior incubation with the PKD1 inhibitor, CRT0066101. PKD1 inhibition has no effect on AMPK Thr172 phosphorylation whereas we see a (not-significant) reduction in VEGF-stimulated AMPK  $\alpha$ 1 Ser485 phosphorylation in the presence of CRT0066101. Furthermore, the presence of CRT0066101 does not prevent VEGF stimulating a significant increase in AMPK  $\alpha$ 1 Ser485 phosphorylation. Together these suggest that PKD1 may contribute to VEGF-stimulated AMPK  $\alpha$ 1 Ser485 phosphorylation but PKD1 cannot account for all the AMPK  $\alpha$ 1 Ser485 kinase activity we observe in response to VEGF.

Coughlan and co-workers also report that PMA-stimulated AMPK  $\alpha 2$  Ser491 is independent of the previously reported AMPK  $\alpha 1$  Ser485 kinases Akt and ERK1/2, in agreement with our findings using VEGF. The authors of this study also report that PKD1 phosphorylates AMPK  $\alpha 2$  *in vitro*. Phosphorylation of AMPK  $\alpha 2$  Ser491 has previously been reported to likely be a result of AMPK auto-phosphorylation (Hawley et al. 2014). For our *in vivo* assessment of AMPK  $\alpha 1$  Ser485 phosphorylation by PKC, we have utilised kinase-dead AMPK  $\alpha 1$ , excluding the possibility that the PKC-mediated AMPK  $\alpha 1$  Ser485 phosphorylation we measured is a result of AMPK auto-phosphorylation unlike Coughlan and co-workers. Furthermore, contrary to their findings, we have no evidence that PMA stimulates the phosphorylation of AMPK  $\alpha 2$  in human vascular endothelial cells. While this article reports that PKD1 is an AMPK  $\alpha 2$  Ser491 kinase in murine muscle cells stimulated by the addition of exogenous PMA via a PKC-PKD-AMPK  $\alpha 2$  Ser491 signalling cascade, our study was conducted in primary human vascular endothelial cells, and furthermore we report that the physiologically relevant stimulus VEGF stimulates AMPK  $\alpha 1$  Ser485 phosphorylation, in addition to the application of synthetic PMA. Comparing our findings with those of this recent report generates a number of interesting questions. Given that we found altering the expression of specific PKC isoforms, whether downregulation using siRNA or transient overexpression using plasmids, caused concurrent alterations in the expression of other PKC isoforms, it would be interesting to know what concentration of siRNA was required by Coughlan and co-workers to induce the downregulation of phospho-PKD1 reported (total PKD1 was not reported) and whether any other PKC isoforms were affected. Furthermore, we report that AMPK  $\alpha 1$  Ser485 phosphorylation is dependent on  $\text{Ca}^{2+}$ , despite not being  $\text{Ca}^{2+}$  regulated itself it would be interesting to assess the  $\text{Ca}^{2+}$  dependence of PKD1 activation in response to PMA, such that it remains possible that a  $\text{Ca}^{2+}$ -regulated PKC isoform regulates PKD1 activity. We are also able to report that AMPK  $\alpha 1$  Ser485 phosphorylation is inversely correlated with insulin sensitivity in *human* muscle; the findings of the current study are therefore still of significant relevance.

## 5.4 Conclusion

Data presented here demonstrates for the first time that PKC activation stimulates the inhibitory phosphorylation of AMPK  $\alpha$ 1 at Ser485 in primary human vascular endothelial cells, independently of LKB1 and CaMKK, and has established that PKC is a novel AMPK  $\alpha$ 1 Ser485 kinase *in vitro*. Previous reports that Akt and ERK1/2 are AMPK  $\alpha$ 1 Ser485 kinases may describe cell and or stimuli specific effects. Furthermore, AMPK  $\alpha$ 1 Ser485 phosphorylation levels show a strong inverse correlation with insulin sensitivity in human muscle. Elevated PKC activity and reduced AMPK activity are observed in metabolic diseases such as diabetes, as such these findings report a novel mechanism of AMPK regulation by PKC, which may be of therapeutic interest in the treatment of metabolic disease.

Despite recent reports that PKD1 is an AMPK  $\alpha$ 2 Ser491 kinase, we can show that inhibition of PKD1 does not prevent VEGF significantly inducing AMPK  $\alpha$ 1 Ser485 phosphorylation, such that PKD1 may contribute to AMPK  $\alpha$ 1 Ser485 phosphorylation but PKD1 does not account for all the AMPK  $\alpha$ 1 Ser485-kinase activity seen in response to VEGF.

## **Chapter 6 – Discussion**

## 6.1 Final discussion

Our laboratory has previously reported that AMPK is activated in response to VEGF (Reihill et al. 2007), and that AMPK is required for VEGF-stimulated endothelial cell ‘proliferation’ (Reihill et al. 2011), in contrast to reports that AMPK activation by other agents *e.g.* AICAR, is anti-proliferative. We therefore sought to determine the specific effect of VEGF on AMPK activity in order to assess whether VEGF activated a specific  $\alpha$  isoform-containing complex or subcellular pool of AMPK in order to mediate this paradoxical effect. As reported in Chapter 3, VEGF activates AMPK complexes containing the same  $\alpha 1$  catalytic subunit as AICAR;  $\alpha 1$  account for the vast majority of both basal and VEGF-/AICAR-stimulated AMPK activity in agreements with previous reports that AMPK  $\alpha 1$  is the predominant isoform expressed in vascular endothelial cells. It is however, also the predominant isoform reported to be expressed in SMC derived from rat aortae and porcine carotid arteries (Horman et al. 2008, Rubin et al. 2005) suggesting that targeting AMPK  $\alpha 1$  in the endothelium *in vivo* has the potential to also influence the underlying VSM. It is worth noting that most of the experiments performed in the current study were performed using cultured cells. Extrapolating the findings in the current study to the situation *in vivo* must be done with caution. Intact vessels *in vivo* are comprised of numerous cell populations *e.g.* endothelial cells, smooth muscle, pericytes etc. and endothelial cells *in vivo* are exposed to sheer stress, blood components and the influence of immune cells. Furthermore, at any given time, the percentage of endothelial cells undergoing proliferation is reported to be in the region of 0.01 %, a minute proportion of the estimated  $2 \times 10^{12}$  endothelial cells that line the human vasculature (Bianconi et al. 2013). Culturing endothelial cells inadvertently selects for an enhanced proliferative phenotype during sequential passaging, such that cells in culture may not best represent native endothelial cells.

Contrary to previous reports from our laboratory (Reihill et al. 2011), infection of HUVEC with Ad.AMPK-DN had no effect on cell proliferation, when it measured with the RTCA xCELLigence system. This was in contrast to concurrent MTS proliferation assays showing that AMPK *is* required for cell proliferation. Together, these experiments suggest that experiments using the MTS assay as a measure of proliferation need to be supported by other methods *e.g.* xCELLigence or BrdU incorporation, to accurately differentiate between effects on cell proliferation and mitochondrial activity.

Previous work in our laboratory also reported that VEGF activates AMPK in a CaMKK (Reihill et al. 2007) and extracellular  $\text{Ca}^{2+}$  dependent manner, and that this could be mimicked by the DAG mimetic OAG (Reihill 2009). It was therefore hypothesised that VEGF-stimulated AMPK activation is facilitated by one or more members of the DAG sensitive  $\text{Ca}^{+2}$  channel family (TRPCs 3, 6 and 7). The present study was neither able to confirm, nor exclude the possibility of TRPC channel expression in human vascular endothelial cells, contrary to numerous previous reports. We show here that the pharmacological and molecular analysis tools available, at the time of this study into TRPC channel activity are, at least in our hands, insufficiently efficacious, nor specific enough to enable the contribution of their targets in the mechanism of VEGF-stimulated AMPK activation to be resolved fully.

Numerous reports however claim to have characterised the expression profile of TRPC channels in vascular tissues summarised well by Yao and Garland (2005), with widely varying results. As such no consensus expression profile of TRPC isoforms in endothelial cells has been reached. Furthermore, numerous reports claim that different individual TRPC isoforms are crucial in regulating vascular homeostasis and/or pathological states without necessarily reporting the effect of modulating the activity of other TRPC isoforms in the same models. TRPC channels form heteromeric in addition to homomeric complexes, with an ever-increasing number of combinations reported. The tetrameric composition of the TRPC channel complex therefore has the capacity to affect channel characteristics (Vazquez et al. 2004). Until such time that the subunit composition of TRPCs can be determined with high resolution, studies reporting that channel a or b, and not c are responsible for effect x, should be interpreted with caution. Furthermore, we have shown for the first time that hyperforin activates AMPK in vascular endothelial cells, consistent with recent reports (Wiechmann et al. 2015) that hyperforin disrupts mitochondrial processes, activating AMPK in leukemic cells.

We report that activation of PKC stimulates AMPK  $\alpha 1$  Ser485 phosphorylation and concomitantly reduces AMPK activity, whereas inhibition of PKC tends to increase AMPK activity; together this data suggests that PKC is a negative regulator of AMPK activity. We have further demonstrated that active PKC phosphorylates AMPK  $\alpha 1$  Ser485 in a cell free assay, indicating that at least *in vitro*, PKC is a direct AMPK  $\alpha 1$  Ser485-kinase. Furthermore, AMPK  $\alpha 1$  Ser485 phosphorylation is inversely correlated with insulin sensitivity in human muscle, such that it remains possible that the elevated PKC

activity observed in response to over-nutrition may contribute to the reduction in AMPK activity observed in animal and human models of metabolic disease.

This study demonstrates that PKC is a direct AMPK  $\alpha 1$  Ser485 kinase, and reports for the first time to our knowledge that AMPK  $\alpha 1$  Ser485 phosphorylation is inversely correlated with insulin sensitivity in biopsies of human muscle from volunteers who are not clinically classified as diabetic. Probably the most interesting finding from the current study is that the endogenous signalling molecule VEGF stimulates PKC activation to mediate this in intact primary human vascular endothelial cells. AMPK  $\alpha 1$  Ser485 has previously been reported to be an inhibitory phosphorylation event, with Akt, and a MEK1/2- or ERK1/2-dependent kinase reported to mediate this phosphorylation (Horman et al. 2006, Lopez-Cotarelo et al. 2015). The finding that PKC activation also stimulates AMPK  $\alpha 1$  Ser485 phosphorylation adds to our understanding of the mechanisms by which AMPK activity is downregulated.

After the completion of the experimental work for this project, and during the preparation of this thesis, Coughlan and co-workers reported that PKD1 inhibits AMPK  $\alpha 2$  by phosphorylation of Ser491 kinase and impaired insulin signalling in murine muscle cells (C2C12) (Coughlan et al. 2016), results similar to what we present in the current study. Their findings however support those in our current study and indicate that PMA stimulates AMPK Ser485 phosphorylation via PKC/PKD1. We have since demonstrated that PKD1 does not fully account for the VEGF-stimulated activation of the kinase mediating AMPK  $\alpha 1$  Ser485 phosphorylation in human vascular endothelial cells. As such PKC-mediated regulation of AMPK activity may still contribute to the downregulated AMPK activity observed in models of metabolic disease independent of PKD1-stimulated AMPK  $\alpha 1$  Ser485 phosphorylation.

## 6.2 Future work

The current study presents a number of avenues warranting further investigation:

- What is the significance of AMPK translocating to the Golgi apparatus when confluent and is this unique to endothelial cells?

At this time we can only speculate as to why AMPK is localised to the Golgi body of confluent endothelial cells but to the ER when sub-confluent. Furthermore, we do not

know whether the targeting of AMPK to these different subcellular compartments affects its activity or interaction with substrates. We assessed the feasibility of expressing GFP tagged AMPK in HUVEC during the current study, in order to obtain a real-time images of AMPK distribution. Unfortunately, we were not able to distinguish between GFP and GFP-tagged AMPK, which both shared a similar distribution, such that this requires further optimisation. Should this be better resolved, it would be of considerable interest to synthesise Golgi or ER-targeted AMPK in order to assess the effect of AMPK localisation on its activity and cell phenotype. This could be achieved using the Golgi and ER targeting sequences ‘GRIP-domain’ and ‘KDEL sequence’, described previously (Munro and Nichols 1999, Stornaiuolo et al. 2003).

- Can mitochondrial mass and biogenesis be quantified in endothelial cells and is it altered by VEGF?

Initial experiments assessing the effect of downregulating AMPK on mitochondrial oxygen consumption have proven inconclusive, such that we have not conclusively determined the mechanism by which Ad.AMPK-DN virus affects the outcome of the MTS assay, independently of inhibiting VEGF-stimulated cell proliferation. Given the greater resolution achievable, transmission electron microscopy would allow for a relative and absolute measurement of the area within cells occupied by mitochondria to be determined, rather than by confocal microscopy as we have tried. Highly sensitive qRT-PCR might also be used to assess the copy number of mtDNA encoded genes. Given the small volume of protein lysate recovered after the Seahorse XF Mito Stress Test we assessed only the expression of mitochondrial complexes I-V. If conditions permitted enough lysate to be recovered it would be interesting to assess the mRNA, or protein expression level of factors involved in mitochondrial biogenesis, such as PGC-1 $\alpha$ , the nuclear respiratory factors NRF-1 and 2, and the mitochondrial transcription factor mtTFA.

- What are the downstream targets of VEGF-stimulated AMPK?

The obvious omission from the current study is the effect of VEGF downstream of AMPK activation. Once we have established an efficient protocol to induce siRNA-mediated AMPK knockdown, it would be interesting to assess this on metabolic parameters, rather than relying on recombinant adenoviral vector infection, a process which itself is likely to have effects on the cells. During the current study, the feasibility of isolating primary aortic endothelial cells from *PRKAA1*<sup>-/-</sup> mice and their wild type littermates was explored.

Despite successfully developing a protocol for isolating murine aortic endothelial cells, the absolute number of isolated cells recovered was low, and expanding them in culture was not possible. Should this be overcome, it would be of particular interest to assess the effect of VEGF on potential targets in WT derived murine endothelial cells and compare this in cells derived from their *PRKAA1*<sup>-/-</sup> littermates to determine their AMPK dependence.

- Are TRPCs mediating VEGF-stimulated Ca<sup>2+</sup> influx and AMPK activation?

The development of better tools is required in order to determine if TRPCs are actually involved in VEGF-stimulated AMPK activation, however we report here for the first time that hyperforin activates AMPK in an extracellular Ca<sup>2+</sup>-independent manner. In addition to its effects on TRPC6 (Leuner et al. 2007), there are suggestions that hyperforin acts as a protonophore and upregulates the expression of the drug metabolising enzyme CYP3A4 (Friedland and Harteneck 2015). It would be interesting to further study the mechanism by which hyperforin stimulates AMPK activity and its downstream effects, in order to better understand the reported pleiotropic effects of hyperforin, given the over-the-counter availability and use of St John's Wort preparations for the treatment of mild to moderate depression (Linde et al. 2008).

- Does AMPK  $\alpha$ 1 Ser485 phosphorylation correlate with, or contribute to reduced insulin sensitivity in the larger population?

The most interesting finding in the current study was that increased PKC activity such as that seen during over-nutrition, stimulates the inhibitory phosphorylation of AMPK  $\alpha$ 1 at Ser485 in primary human vascular endothelial cells. We also report that AMPK  $\alpha$ 1 Ser485 phosphorylation is significantly, inversely correlated with insulin sensitivity in human muscle although we had access to only a limited number of biopsy samples. It is important that this be expanded in the future, including a large number of samples across a range of insulin sensitivities, and ideally from a range of diverse ethnic populations. Given that none of the biopsy volunteers in the current study were clinically classified as having diabetes, it remains possible that PKC-mediated inhibition of AMPK activity precedes, or underlies the development of insulin resistance and diabetes. Although initial clinical trials with the PKC inhibitor LY333531 (Ruboxistaurin) showed promising results in the treatment of diabetic retinopathy, the overall benefit was not deemed significant enough to warrant further investigation therapeutically; oral delivery of the drug was however very well tolerated. Furthermore, clinically achievable concentrations of ruboxistaurin

decreased AMPK  $\alpha$ 1 Ser485 phosphorylation by >60 %. It might therefore be interesting in the future to investigate whether PKC inhibitors like ruboxistaurin augment the activation of AMPK by drugs such as metformin and TZDs, under conditions where AMPK activity may have been previously impaired

## Summary

Our current understanding of the mechanism by which VEGF regulates AMPK activity is summarised (Figure 6-1). VEGF binds to its cognate receptor stimulating PLC $\gamma$ -mediated PIP<sub>2</sub> hydrolysis. The resultant DAG stimulates Ca<sup>2+</sup> influx but we cannot, at this time identify the channel mediating this Ca<sup>2+</sup> influx. CaMKK $\beta$  is activated by this influx of extracellular Ca<sup>2+</sup> resulting in transient activation of AMPK  $\alpha$ 1. This Ca<sup>2+</sup> influx, also appears to stimulate PKC, which either directly as we have demonstrated here, or indirectly as suggested by others, stimulates the phosphorylation of AMPK  $\alpha$ 1 Ser485, thereby negatively regulating its activity. PKC can also be activated by endogenous DAG, or the application of DAG mimetics such as PMA, but the contribution of DAG-mediated PKC activation to VEGF-stimulated Ser485 phosphorylation is not clear.

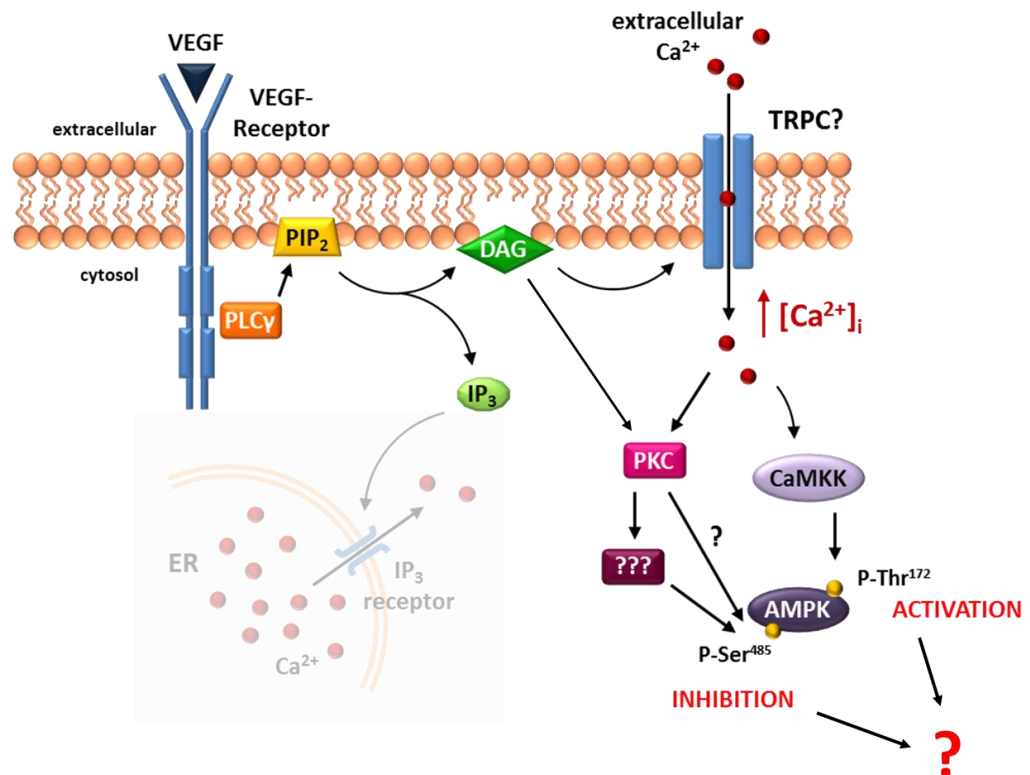


**Figure 6-1: Mechanism of VEGF-stimulated phosphorylation of AMPK at Thr172 and Ser485**

VEGF binds to its receptor on the extracellular surface of endothelial cells stimulating PIP<sub>2</sub> hydrolysis by PLC $\gamma$  to generate IP<sub>3</sub> and DAG. IP<sub>3</sub> stimulates Ca<sup>2+</sup> release from intracellular stores (ER; endoplasmic reticulum) however previous reports indicate that Ca<sup>2+</sup> mobilisation from the ER is not sufficient to activate AMPK. DAG however stimulates the influx of extracellular Ca<sup>2+</sup>, potentially via DAG-sensitive TRPC channels. Influx of extracellular Ca<sup>2+</sup> stimulates CaMKK $\beta$  which further activates AMPK. Ca<sup>2+</sup> influx also stimulates PKC activity resulting in the phosphorylation of AMPK  $\alpha$ 1 Ser485 by PKC, therefore directly or indirectly causing AMPK activity to be inhibited.

## References

Aarhus, R., Graeff, R. M., Dickey, D. M., Walseth, T. F., Lee, H. C. (1995) 'ADP-ribosyl cyclase and CD38 catalyze the synthesis of a calcium-mobilizing metabolite from NADP', *Journal of Biological Chemistry*, 270(51), 30327-33

Adis (2007) 'Ruboxistaurin: LY 333531', *Drugs in R&D*, 8(3), 193-199

Ahluwalia, A., Tarnawski, A. S. (2011) 'Activation of the metabolic sensor-AMP activated protein kinase reverses impairment of angiogenesis in aging myocardial microvascular endothelial cells. Implications for the aging heart', *Journal of Physiology and Pharmacology*, 62(5), 583-7

Aiello, L., Bursell, S., Devries, T., Alatorre, C., King, G., Ways, K. (1999) 'Protein kinase C beta-selective inhibitor LY333531 ameliorates abnormal retinal hemodynamics in patients with diabetes', *Diabetes*, 48, A19

Allen, L. F., Sebolt-Leopold, J., Fau-Meyer, M. B., Meyer, M. B. (2003) 'CI-1040 (PD184352), a targeted signal transduction inhibitor of MEK (MAPKK)', *Seminars in Oncology*, 30(5-16), 105-116

Altieri, D. C., Duperray, A., Plescia, J., Thornton, G. B., Languino, L. R. (1995) 'Structural recognition of a novel fibrinogen chain sequence (117133) by intercellular adhesion molecule-1 mediates leukocyte-endothelium interaction', *Journal of Biological Chemistry*, 270(2), 696-699

Anderson, K. A., Lin, F., Ribar, T. J., Stevens, R. D., Muehlbauer, M. J., Newgard, C. B. and Means, A. R. (2012) 'Deletion of CaMKK2 from the liver lowers blood glucose and improves whole-body glucose tolerance in the mouse', *Molecular Endocrinology*, 26(2), 281-291.

Anderson, K. A., Means, R. L., Huang, Q. H., Kemp, B. E., Goldstein, E. G., Selbert, M. A., Edelman, A. M., Fremeau, R. T. and Means, A. R. (1998) 'Components of a Calmodulin-dependent Protein Kinase Cascade: molecular cloning, functional characterization and cellular localization of Ca<sup>2+</sup>/calmodulin-dependent protein kinase kinase  $\beta$ ', *Journal of Biological Chemistry*, 273(48), 31880-31889

Antoniotti, S., Fiorio Pla, A., Barral, S., Scalabrino, O., Munaron, L., Lovisolo, D. (2006) 'Interaction between TRPC channel subunits in endothelial cells', *Journal of Receptor and Signal Transduction Research*, 26(4), 225-240

Antoniotti, S., Lovisolo, D., Fiorio Pla, A., Munaron, L. (2002) 'Expression and functional role of bTRPC1 channels in native endothelial cells', *FEBS Letters*, 510(3), 189-195

Bair, A. M., Thippogowda, P. B., Freichel, M., Cheng, N., Ye, R. D., Vogel, S. M., Yu, Y., Flockerzi, V., Malik, A. B., Tiruppathi, C. (2009) 'Ca<sup>2+</sup> entry via TRPC channels is necessary for thrombin-induced NF- $\kappa$ B activation in endothelial cells through AMP-activated protein kinase and protein kinase Cdelta', *Journal of Biological Chemistry*, 284(1), 563-574

Baldwin, M. E., Halford, M. M., Roufail, S., Williams, R. A., Hibbs, M. L., Grail, D., Kubo, H., Stacker, S. A., Achen, M. G. (2005) 'Vascular endothelial growth factor d is dispensable for development of the lymphatic system', *Molecular and Cellular Biology*, 25(6), 2441-2449

Barleon, B., Sozzani, S., Zhou, D., Weich, H. A., Mantovani, A., Marmé, D. (1996) 'Migration of human monocytes in response to vascular endothelial growth factor (VEGF) is mediated via the VEGF receptor Flt-1', *Blood*, 87(8), 3336-3343

Barragan, M., de Frias, M., Iglesias-Serret, D., Campas, C., Castano, E., Santidrian, A. F., Coll-Mulet, L., Cosialls, A. M., Domingo, A., Pons, G., Gil, J. (2006) 'Regulation of Akt/PKB by phosphatidylinositol 3-kinase-dependent and -independent pathways in B-cell chronic lymphocytic leukemia cells: role of protein kinase C $\beta$ ', *Journal of Leukocyte Biology*, 80, 1473-9.

- Bateman, A. (1997) 'The structure of a domain common to archaebacteria and the homocystinuria disease protein', *Trends in Biochemical Sciences*, 22(1), 12-13
- Bates, D. O., Harper, S. J. (2002) 'Regulation of vascular permeability by vascular endothelial growth factors', *Vascular Pharmacology*, 39(4-5), 225-237
- Bates, D. O., Heald, R. I., Curry, F. E., Williams, B. (2001) 'Vascular endothelial growth factor increases Rana vascular permeability and compliance by different signalling pathways', *The Journal of Physiology*, 533(1), 263-272
- Becker, P. M., Verin, A. D., Booth, M. A., Liu, F., Birukova, A., Garcia, J. G. (2001) 'Differential regulation of diverse physiological responses to VEGF in pulmonary endothelial cells', *American Journal of Physiology. Lung, Cellular and Molecular Physiology*, 281(6), 1500-1511
- Beckman, J. A., Goldfine, A. B., Gordon, M. B., Garrett, L. A., Creager, M. A. (2002) 'Inhibition of protein kinase C $\beta$  prevents impaired endothelium-dependent vasodilation caused by hyperglycemia in humans', *Circulation Research*, 90(1), 107-111
- Beg, Z. H., Allmann, D. W., Gibson, D. M. (1973) 'Modulation of 3-hydroxy-3-methylglutaryl coenzyme A reductase activity with cAMP and with protein fractions of rat liver cytosol', *Biochemical and Biophysical Research Communications*, 54(4), 1362-1369
- Bellomo, D., Headrick, J. P., Silins, G. U., Paterson, C. A., Thomas, P. S., Gartside, M., Mould, A., Cahill, M. M., Tonks, I. D., Grimmond, S. M., Townson, S., Wells, C., Little, M., Cummings, M. C., Hayward, N. K., Kay, G. F. (2000) 'Mice lacking the vascular endothelial growth factor-B gene (Vegfb) have smaller hearts, dysfunctional coronary vasculature, and impaired recovery from cardiac ischemia', *Circulation Research*, 86(2), 29-35
- Berggreen, C., Gormand, A., Omar, B., Degerman, E., Goransson, O. (2009) 'Protein kinase B activity is required for the effects of insulin on lipid metabolism in adipocytes', *American Journal of Physiology. Endocrinology and Metabolism*, 296, 635-646
- Berridge, M. V., Tan, A. S. (1993) 'Characterization of the cellular reduction of 3-(4, 5-dimethylthiazol-2-yl)-2, 5-diphenyltetrazolium bromide (MTT): subcellular localization, substrate dependence, and involvement of mitochondrial electron transport in MTT reduction'. *Archives of Biochemistry and Biophysics*, 303(2), 474-482
- Berse, B., Hunt, J. A., Diegel, R. J., Morganelli, P., Yeo, K., Brown, F., Fava, R. A. (1999) 'Hypoxia augments cytokine (transforming growth factor-beta (TGF- $\beta$ ) and IL-1)-induced vascular endothelial growth factor secretion by human synovial fibroblasts', *Clinical & Experimental Immunology*, 115(1), 176-182
- Bianconi, E., Piovesan, A., Facchin, F., Beraudi, A., Casadei, R., Frabetti, F., Vitale, L., Pelleri, M. C., Tassani, S., Piva, F., Perez-Amodio, S., Strippoli, P. and Canaider, S. (2013) 'An estimation of the number of cells in the human body', *Annals of Human Biology*, 40(6), 463-471
- Boyle, J. G., Logan, P. J., Ewart, M. A., Reihill, J. A., Ritchie, S. A., Connell, J. M., Cleland, S. J., Salt, I. P. (2008) 'Rosiglitazone stimulates nitric oxide synthesis in human aortic endothelial cells via AMP-activated protein kinase', *Journal of Biological Chemistry*, 283, 11210-11217
- Bradford, M. M. (1976) 'A rapid and sensitive method for the quantitation of microgram quantities of protein utilizing the principle of protein-dye binding', *Analytical Biochemistry*, 72, 248-254
- Broggi, E., Wu, T., Namiki, A., Isner, J. M. (1994) 'Indirect angiogenic cytokines upregulate VEGF and bFGF gene expression in vascular smooth muscle cells, whereas hypoxia upregulates VEGF expression only', *Circulation*, 90(2) 649-650

- Buhl, E. S., Jessen, N., Schmitz, O., Pedersen, S. B., Pedersen, O., Holman, G. D., Lund, S. (2001) 'Chronic treatment with 5-Aminoimidazole-4-Carboxamide-1- $\beta$ -D-Ribofuranoside increases insulin-stimulated glucose uptake and GLUT4 translocation in rat skeletal muscles in a fiber type-specific manner', *Diabetes*, 50(1), 12-17
- Burkey, J. L., Campanale, K. M., Barbuch, R., O'Bannon, D., Rash, J., Benson, C., Small, D. (2006) 'Disposition of [ $^{14}$ C]ruboxistaurin in humans', *Drug Metabolism and Disposition. The Biological Fate of Chemicals*, 34, 1909-17
- Cabell, C. H., Verghese G. M., Rankl, N. B., Blackshear, P. J. (1996) 'MARCKS phosphorylation by individual protein kinase C isozymes in insect Sf9 cells', *Proceedings of the Association of American Physicians*, 108(1) 37-46
- Calcraft, P. J., Ruas, M., Pan, Z., Cheng, X., Arredouani, A., Hao, X., Tang, J., Rietdorf, K., Teboul, L., Chuang, K. T., Lin, P., Xiao, R., Wang, C., Zhu, Y., Lin, Y., Wyatt, C. N., Parrington, J., Ma, J., Evans, A. M., Galione, A. and Zhu, M. X. (2009) 'NAADP mobilizes calcium from acidic organelles through two-pore channels', *Nature*, 459(7246), 596-600
- Calvert, J. W., Gundewar S., Jha, S., Greer, J. J., Bestermann, W. H., Tian, R., Lefer, D. J. (2008) 'Acute metformin therapy confers cardioprotection against myocardial infarction via AMPK-eNOS-mediated signalling', *Diabetes*, 57(3) 696-705
- Carling, D., Sanders, M. J., Woods, A. (2008) 'The regulation of AMP-activated protein kinase by upstream kinases', *International Journal of Obesity (London)*, 32 Suppl 4, 55-59
- Carling, D., Zammit, V. A. and Hardie, D. G. (1987) 'A common bicyclic protein kinase cascade inactivates the regulatory enzymes of fatty acid and cholesterol biosynthesis', *FEBS Letters*, 223(2), 217-22
- Carlson, C. A., Kim, K. H. (1973) 'Regulation of hepatic acetyl coenzyme A carboxylase by phosphorylation and dephosphorylation', *Journal of Biological Chemistry*, 248(1), 378-80
- Carmeliet, P., Ferreira, V., Breier, G., Pollefeyt, S., Kieckens, L., Gertsenstein, M., Fahrig, M., Vandenhoeck, A., Harpal, K., Eberhardt, C., Declercq, C., Pawling, J., Moons, L., Collen, D., Risau, W. and Nagy, A. (1996) 'Abnormal blood vessel development and lethality in embryos lacking a single VEGF allele', *Nature*, 380(6573), 435-439
- Ceolotto, G., Gallo, A., Papparella, I., Franco, L., Murphy, E., Iori, E., Pagnin, E., Fadini, G. P., Albiero, M., Semplicini, A., Avogaro, A. (2007) 'Rosiglitazone reduces glucose-induced oxidative stress mediated by NAD(P)H oxidase via AMPK-dependent mechanism', *Atherosclerosis, Thrombosis and Vascular Biology*, 27(12), 2627-2633
- Chabowski, A., Coort, S. L., Calles-Escandon, J., Tandon, N. N., Glatz, J. F., Luiken, J. J., Bonen, A. (2005) 'The subcellular compartmentation of fatty acid transporters is regulated differently by insulin and by AICAR', *FEBS Letters*, 579(11), 2428-2432
- Chabowski, A., Momken, I., Coort, S. L., Calles-Escandon, J., Tandon, N. N., Glatz, J. F., Luiken, J. J. and Bonen, A. (2006) 'Prolonged AMPK activation increases the expression of fatty acid transporters in cardiac myocytes and perfused hearts', *Molecular and Cellular Biochemistry*, 288(1-2), 201-212
- Chang, M. Y., Huang, D. Y., Ho, F. M., Huang, K. C., Lin, W. W. (2012) 'PKC-dependent human monocyte adhesion requires AMPK and Syk activation', *PLoS One*, 7(7)
- Chappell, L. C., Duckworth, S., Seed, P. T., Griffin, M., Myers, J., Mackillop, L., Simpson, N., Waugh, J., Anumba, D., Kenny, L. C., Redman, C. W. G. and Shennan, A. H. (2013) 'Diagnostic accuracy of placental growth factor in women with suspected preeclampsia: a prospective multicenter study', *Circulation*, 128(19), 2121-2131

- Chen, H., Montagnani, M., Funahashi, T., Shimomura, I., Quon, M. J. (2003) 'Adiponectin stimulates production of nitric oxide in vascular endothelial cells', *Journal of Biological Chemistry*, 278(45), 45021-45026
- Chen, J., Crossland, R. F., Noorani, M. M. and Marrelli, S. P. (2009) 'Inhibition of TRPC1/TRPC3 by PKG contributes to NO-mediated vasorelaxation', *American Journal of Physiology. Heart and Circulation Physiology*, 297(1), H417-24
- Chen, L., Jiao, Z. H., Zheng, L. S., Zhang, Y. Y., Xie, S. T., Wang, Z. X., Wu, J. W. (2009) 'Structural insight into the auto-inhibition mechanism of AMP-activated protein kinase', *Nature*, 459(7250), 1146-9114
- Chen, Z., Gibson T. B., Robinson, F., Silvestro, L., Pearson, G., Xu, B., Wright, A., Vanderbilt, C., Cobb, M. H. (2001) 'MAP kinases', *Chemical Reviews*, 101(8) 2449-2476
- Chen, Z., Peng I. C., Sun, W., Su, M. I., Hsu, P. H., Fu, Y., Zhu, Y., DeFea, K., Pan, S., Tsai, M. D., Shyy, J. Y. (2009) 'AMP-activated protein kinase functionally phosphorylates endothelial nitric oxide synthase Ser633', *Circulation Research*, 104(4), 496-505
- Cheng, H. W., James, A. F., Foster, R. R., Hancox, J. C., Bates, D. O. (2006) 'VEGF activates receptor-operated cation channels in human microvascular endothelial cells', *Arteriosclerosis, Thrombosis and Vascular Biology*, 26(8), 1768-1776
- Cheung, P. C., Salt I. P., Davies, S. P., Hardie, D. G., Carling, D. (2000) 'Characterization of AMP-activated protein kinase gamma-subunit isoforms and their role in AMP binding', *The Biochemical Journal*, 346(3) 659-669
- Clapham, D. E., Runnels, L. W., Strubing, C. (2001) 'The TRP ion channel family', *Nature Reviews. Neuroscience*, 2(6), 387-396
- Clark, D. E., Smith, S. K., Licence, D., Evans, A. L., Charnock-Jones, D.S. (1998) 'Comparison of expression patterns for placenta growth factor, vascular endothelial growth factor (VEGF), VEGF-B and VEGF-C in the human placenta throughout gestation', *Journal of Endocrinology*, 159(3), 459-467
- Cohen, R. A. (1995) 'The role of nitric oxide and other endothelium-derived vasoactive substances in vascular disease', *Progress in Cardiovascular Diseases*, 38(2), 105-128
- Cool, B., Zinker, B., Chiou, W., Kifle, L., Cao, N., Perham, M., Dickinson, R., Adler, A., Gagne, G., Iyengar, R., Zhao, G., Marsh, K., Kym, P., Jung, P., Camp, H. S., Frevert, E. (2006) 'Identification and characterization of a small molecule AMPK activator that treats key components of type 2 diabetes and the metabolic syndrome', *Cell Metabolism*, 3(6), 403-416
- Coughlan, K. A., Valentine, R. J., Sudit, B. S., Allen, K., Dagon, Y., Kahn, B. B., Ruderman, N. B. and Saha, A. K. (2016) 'PKD1 inhibits AMPK $\alpha$ 2 through phosphorylation of Serine 491 and impairs insulin signalling in skeletal muscle cells', *Journal of Biological Chemistry*, 291(11), 5664-5675
- Craven, P. A. and DeRubertis, F. R. (1989) 'Protein kinase C is activated in glomeruli from streptozotocin diabetic rats. Possible mediation by glucose', *Journal of Clinical Investigation*, 83(5), 1667-16675
- Cross, M. J., Dixelius, J., Matsumoto, T., Claesson-Welsh, L. (2003) 'VEGF-receptor signal transduction', *Trends in Biochemical Sciences*, 28(9), 488-494
- Crute, B. E., Seefeld, K., Gamble, J., Kemp, B. E., Witters, L. A. (1998) 'Functional domains of the alpha1 catalytic subunit of the AMP-activated protein kinase', *Journal of Biological Chemistry*, 273(52), 35347-54

- Cudmore, M. J., Hewett, P. W., Ahmad, S., Wang, K. Q., Cai, M., Al-Ani, B., Fujisawa, T., Ma, B., Sissaoui, S., Ramma, W., Miller, M. R., Newby, D. E., Gu, Y., Barleon, B., Weich, H., Ahmed, A. (2012) 'The role of heterodimerization between VEGFR-1 and VEGFR-2 in the regulation of endothelial cell homeostasis', *Nature Communications*, 3, 972
- Cullen, V. C., Mackarel, A. J., Hislip, S. J., O'Connor, C. M., Keenan, A. K. (2000) 'Investigation of vascular endothelial growth factor effects on pulmonary endothelial monolayer permeability and neutrophil transmigration', *General Pharmacology*, 35(3), 149-57
- Cébe Suarez, S., Pieren, M., Cariolato, L., Arn, S., Hoffmann, U., Bogucki, A., Manlius, C., Wood, J., Ballmer-Hofer, K. (2006) 'A VEGF-A splice variant defective for heparan sulfate and neuropilin-1 binding shows attenuated signalling through VEGFR-2', *Cellular and Molecular Life Sciences*, 63(17), 2067-77
- Dagher, Z., Ruderman, N., Tornheim, K., Ido, Y. (2001) 'Acute regulation of fatty acid oxidation and amp-activated protein kinase in human umbilical vein endothelial cells', *Circulation Research*, 88(12), 1276-82
- Davidson, S. M., Duchon, M. R. (2007) 'Endothelial mitochondria: contributing to vascular function and disease', *Circulation Research*, 100(8), 1128-41
- Davidson, S. M., Foote, K., Kunuthur, S., Gosain, R., Tan, N., Tyser, R., Zhao, Y. J., Graeff, R., Ganesan, A., Duchon, M. R., Patel, S., Yellon, D. M. (2015) 'Inhibition of NAADP signalling on reperfusion protects the heart by preventing lethal calcium oscillations via two-pore channel 1 and opening of the mitochondrial permeability transition pore', *Cardiovascular Research*, 108(3), 357-366
- Davies, M. J., Gordon, J. L., Gearing, A. J. H., Pigott, R., Woolf, N., Katz, D., Kyriakopoulos, A. (1993) 'The expression of the adhesion molecules ICAM-1, VCAM-1, PECAM, and E-selectin in human atherosclerosis', *The Journal of Pathology*, 171(3), 223-229
- Davis, B. J., Xie, Z., Viollet, B., Zou, M. H. (2006) 'Activation of the AMP-activated kinase by anti-diabetes drug metformin stimulates nitric oxide synthesis *in vivo* by promoting the association of heat shock protein 90 and endothelial nitric oxide synthase', *Diabetes*, 55(2), 496-505
- Deshmukh, A. S., Long, Y. C., de Castro Barbosa, T., Karlsson, H. K., Glund, S., Zavadoski, W. J., Gibbs, E. M., Koistinen, H. A., Wallberg-Henriksson, H., Zierath, J. R. (2010) 'Nitric oxide increases cyclic GMP levels, AMP-activated protein kinase (AMPK)alpha1-specific activity and glucose transport in human skeletal muscle', *Diabetologia*, 53(6), 1142-1150
- Dickinson, R. J., Keyse, S. M. (2006) 'Diverse physiological functions for dual-specificity MAP kinase phosphatases', *Journal of Cell Science*, 119(22), 4607-4615
- Dietrich, A., Mederos, Y. S. M., Gollasch, M., Gross, V., Storch, U., Dubrovskaja, G., Obst, M., Yildirim, E., Salanova, B., Kalwa, H., Essin, K., Pinkenburg, O., Luft, F. C., Gudermann, T., Birnbaumer, L. (2005) 'Increased vascular smooth muscle contractility in TRPC6<sup>-/-</sup> mice', *Molecular and Cellular Biology*, 25(16), 6980-6989
- Djouder, N., Tuerk, R. D., Suter, M., Salvioni, P., Thali, R. F., Scholz, R., Vahtomeri, K., Auchli, Y., Rechsteiner, H., Brunisholz, R. A., Viollet, B., Makela, T. P., Wallimann, T., Neumann, D., Krek, W. (2010) 'PKA phosphorylates and inactivates AMPKalpha to promote efficient lipolysis', *EMBO Journal*, 29(2), 469-481
- Domigan, C. K., Warren, C. M., Antanesian, V., Happel, K., Ziyad, S., Lee, S., Krall, A., Duan, L., Torres-Collado, A. X., Castellani, L. W., Elashoff, D., Christofk, H. R., van der Bliek, A. M., Potente, M., Iruela-Arispe, M. L. (2015) 'Autocrine VEGF maintains endothelial survival through regulation of metabolism and autophagy', *Journal of Cell Science*, 128(12), 2236-2248

- Douda, D. N., Yip, L., Khan, M. A., Grasmann, H., Palaniyar, N. (2014) 'Akt is essential to induce NADPH-dependent NETosis and to switch the neutrophil death to apoptosis', *Blood*, 123, 597-600
- Dougher, M., Terman, B. I. (1999) 'Autophosphorylation of KDR in the kinase domain is required for maximal VEGF-stimulated kinase activity and receptor internalization', *Oncogene*, 18(8), 1619-1627
- Dumont, D. J., Jussila, L., Taipale, J., Lymboussaki, A., Mustonen, T., Pajusola, K., Breitman, M., Alitalo, K. (1998) 'Cardiovascular failure in mouse embryos deficient in VEGF receptor-3', *Science*, 282(5390), 946-949
- El-Mir, M. Y., Nogueira, V., Fontaine, E., N., Averet, N., Rigoulet, M., Leverve, X., (2000) 'Dimethylbiguanide inhibits cell respiration via an indirect effect targeted on the respiratory chain complex I', *Journal of Biological Chemistry*. 275(1) 223-228
- Emerling, B. M., Weinberg, F., Snyder, C., Burgess, Z., Mutlu, G. M., Viollet, B., Budinger, G. R. S., Chandel, N. S. (2009) 'Hypoxic activation of AMPK is dependent on mitochondrial ROS but independent of an increase in AMP/ATP ratio', *Free Radical Biology and Medicine*, 46(10), 1386-1391
- Endemann, D. H., Schiffrin, E. L. (2004) 'Endothelial dysfunction', *Journal of the American Society of Nephrology*, 15(8), 1983-1992
- Ewart, M. A., Kohlhaas, C. F. and Salt, I. P. (2008) 'Inhibition of tumor necrosis factor alpha-stimulated monocyte adhesion to human aortic endothelial cells by AMP-activated protein kinase', *Arteriosclerosis, Thrombosis and Vascular Biology*, 28(12), 2255-2257
- Fan, F., Wey, J. S., McCarty, M. F., Belcheva, A., Liu, W., Bauer, T. W., Somcio, R. J., Wu, Y., Hooper, A., Hicklin, D. J., Ellis, L. M. (2005) 'Expression and function of vascular endothelial growth factor receptor-1 on human colorectal cancer cells', *Oncogene*, 24(16), 2647-2653
- Favia, A., Desideri, M., Gambarà, G., D'Alessio, A., Ruas, M., Esposito, B., Del Bufalo, D., Parrington, J., Ziparo, E., Palombi, F., Galione, A., Filippini, A. (2014) 'VEGF-induced neoangiogenesis is mediated by NAADP and two-pore channel-2-dependent Ca<sup>2+</sup> signaling', *Proceedings of the National Academy of Sciences of the United States of America*, 111(44), 4706-4715
- Ferrara, N., Carver-Moore, K., Chen, H., Dowd, M., Lu, L., O'Shea, K. S., Powell-Braxton, L., Hillan, K. J., Moore, M. W. (1996) 'Heterozygous embryonic lethality induced by targeted inactivation of the VEGF gene', *Nature*, 380(6573), 439-442
- Ferri, N. (2012) 'AMP-activated protein kinase and the control of smooth muscle cell hyperproliferation in vascular disease', *Vascular Pharmacology*, 56(1-2), 9-13
- Flockerzi, V., Jung, C., Aberle, T., Meissner, M., Freichel, M., Philipp, S., Nastainczyk, W., Maurer, P., Zimmermann, R. (2005) 'Specific detection and semi-quantitative analysis of TRPC4 protein expression by antibodies', *Pflügers Archiv: European Journal of Physiology*, 451(1), 81-86
- Fong, G. H., Rossant, J., Gertsenstein, M., Breitman, M. L. (1995) 'Role of the Flt-1 receptor tyrosine kinase in regulating the assembly of vascular endothelium', *Nature*, 376(6535), 66-70
- Foretz, M., Ancellin, N., Andreelli, F., Saintillan, Y., Grondin, P., Kahn, A., Thorens, B., Vaulont, S., Viollet, B. (2005) 'Short-term overexpression of a constitutively active form of AMP-activated protein kinase in the liver leads to mild hypoglycemia and fatty liver', *Diabetes*, 54(5), 1331-1339
- Freichel, M., Vennekens, R., Olausson, J., Stolz, S., Philipp, S. E., Weissgerber, P. and Flockerzi, V. (2005) 'Functional role of TRPC proteins in native systems: implications from knockout and knock-down studies', *Journal of Physiology*, 567(Pt 1), 59-66

- Friday, B. B., Adjei, A. A. (2008) 'Advances in targeting the Ras/Raf/MEK/Erk mitogen-activated protein kinase cascade with MEK inhibitors for cancer therapy', *Clinical Cancer Research*, 14(2), 342-346
- Friedland, K., Harteneck, C. (2015) 'Hyperforin: to be or not to be an activator of TRPC(6)', *Reviews of Physiology, Biochemistry and Pharmacology*, 169, 1-24
- Fulton, D., Gratton, J.-P., McCabe, T. J., Fontana, J., Fujio, Y., Walsh, K., Franke, T. F., Papapetropoulos, A., Sessa, W. C. (1999) 'Regulation of endothelium-derived nitric oxide production by the protein kinase Akt', *Nature*, 399(6736), 597-601
- Galione, A., Morgan, A. J., Arredouani, A., Davis, L. C., Rietdorf, K., Ruas, M., Parrington, J. (2010) 'NAADP as an intracellular messenger regulating lysosomal calcium-release channels', *Biochemical Society Transactions*, 38(6), 1424-1431
- García-Prieto, C. F., Gil-Ortega, M., Aránguez, I., Ortiz-Besoain, M., Somoza, B. and Fernández-Alfonso, M. S. (2015) 'Vascular AMPK as an attractive target in the treatment of vascular complications of obesity', *Vascular Pharmacology*, 67-69, 10-20
- Ge, R., Tai, Y., Sun, Y., Zhou, K., Yang, S., Cheng, T., Zou, Q., Shen, F., Wang, Y. (2009) 'Critical role of TRPC6 channels in VEGF-mediated angiogenesis', *Cancer Letters*, 283(1), 43-51
- Geraldes, P., King, G. L. (2010) 'Activation of protein kinase C isoforms and its impact on diabetic complications', *Circulation Research*, 106, 1319-1331
- Goad, D. L., Rubin, J., Wang, H., Tashjian, A. H., Patterson, C. (1996) 'Enhanced expression of vascular endothelial growth factor in human SaOS-2 osteoblast-like cells and murine osteoblasts induced by insulin-like growth factor I', *Endocrinology*, 137(6), 2262-8
- Gohil, V. M., Gvozdenovic-Jeremic, J., Schlame, M., Greenberg, M. L. (2005) 'Binding of 10-N-nonyl acridine orange to cardiolipin-deficient yeast cells: implications for assay of cardiolipin', *Analytical Biochemistry*, 343(2), 350-352
- Goirand, F., Solar, M., Athea, Y., Viollet, B., Mateo, P., Fortin, D., Leclerc, J., Hoerter, J., Ventura-Clapier, R., Garnier, A. (2007) 'Activation of AMP kinase  $\alpha$ 1 subunit induces aortic vasorelaxation in mice', *Journal of Physiology*, 581(3), 1163-1171
- Goldman, C. K., Kim, J., Wong, W., King, V., Brock, T., Gillespie, G. (1993) 'Epidermal growth factor stimulates vascular endothelial growth factor production by human malignant glioma cells: a model of glioblastoma multiforme pathophysiology', *Molecular Biology of the Cell*, 4(1), 121-133
- Goransson, O., McBride, A., Hawley, S. A., Ross, F. A., Shpiro, N., Foretz, M., Viollet, B., Hardie, D. G., Sakamoto, K. (2007) 'Mechanism of action of A-769662, a valuable tool for activation of AMP-activated protein kinase', *Journal of Biological Chemistry*, 282(45) 32549-32960
- Gowans, G. J., Hawley, S. A., Ross, F. A., Hardie, D. G. (2013) 'AMP is a true physiological regulator of AMP-activated protein kinase by both allosteric activation and enhancing net phosphorylation', *Cell Metabolism*, 18(4), 556-566
- Graziani, A., Poteser, M., Heupel, W.-M., Schleifer, H., Krenn, M., Drenckhahn, D., Romanin, C., Baumgartner, W. and Groschner, K. (2010) 'cell-cell contact formation governs  $\text{Ca}^{2+}$  signaling by TRPC4 in the vascular endothelium: evidence for a regulatory TRPC4- $\beta$ -catenin interaction', *Journal of Biological Chemistry*, 285, 4213-4223
- Green, M. F., Anderson, K. A., Means, A. R. (2011) 'Characterization of the CaMKK $\beta$ -AMPK signaling complex', *Cellular Signalling*, 23(12), 2005-2012

- Gupta, K., Gupta, P., Wild, R., Ramakrishnan, S., Hebbel, R. P. (1999) 'Binding and displacement of vascular endothelial growth factor (VEGF) by thrombospondin: effect on human microvascular endothelial cell proliferation and angiogenesis', *Angiogenesis*, 3(2), 147-158
- Hall, L. M., Moran, C. N., Milne, G. R., Wilson, J., MacFarlane, N. G., Forouhi, N. G., Hariharan, N., Salt, I. P., Sattar, N. and Gill, J. M. (2010) 'Fat oxidation, fitness and skeletal muscle expression of oxidative/lipid metabolism genes in South Asians: implications for insulin resistance?', *PLoS One*, 5(12), e14197
- Hamdollah Zadeh, M. A., Glass, C. A., Magnussen, A., Hancox, J. C., Bates, D. O. (2008) 'VEGF-mediated elevated intracellular calcium and angiogenesis in human microvascular endothelial cells *in vitro* are inhibited by dominant negative TRPC6', *Microcirculation*, 15(7), 605-614
- Hanks, S. K. (2003) 'Genomic analysis of the eukaryotic protein kinase superfamily: a perspective', *Genome Biology*, 4(5), 111
- Hardie, D. G. (2011) 'AMP-activated protein kinase—an energy sensor that regulates all aspects of cell function', *Genes & Development*, 25(18), 1895-1908
- Hardie, D. G., Carling, D., Carlson, M. (1998) 'The AMP-activated/SNF1 protein kinase subfamily: metabolic sensors of the eukaryotic cell?', *Annual Review of Biochemistry*, 67, 821-855
- Harteneck, C., Gollasch, M. (2011) 'Pharmacological modulation of diacylglycerol-sensitive TRPC3/6/7 channels', *Current Pharmaceutical Biotechnology*, 12(1), 35-41
- Hawley, S. A., Boudeau, J., Reid, J. L., Mustard, K. J., Udd, L., Mäkelä, T. P., Alessi, D. R., Hardie, D. G. (2003) 'Complexes between the LKB1 tumor suppressor, STRAD alpha/beta and MO25 alpha/beta are upstream kinases in the AMP-activated protein kinase cascade', *Journal of Biology*, 2(4), 28
- Hawley, S. A., Fullerton, M. D., Ross, F. A., Schertzer, J. D., Chevtzoff, C., Walker, K. J., Peggie, M. W., Zibrova, D., Green, K. A., Mustard, K. J., Kemp, B. E., Sakamoto, K., Steinberg, G. R., Hardie, D. G. (2012) 'The ancient drug salicylate directly activates AMP-activated protein kinase', *Science*, 336(6083), 918-922
- Hawley, S. A., Gadalla, A. E., Olsen, G. S., Hardie, D. G. (2002) 'The antidiabetic drug metformin activates the AMP-activated protein kinase cascade via an adenine nucleotide-independent mechanism', *Diabetes*, 51(8) 2420-2425
- Hawley, S. A., Pan, D. A., Mustard, K. J., Ross, L., Bain, J., Edelman, A. M., Frenguelli, B. G., Hardie, D. G. (2005) 'Calmodulin-dependent protein kinase kinase- $\beta$  is an alternative upstream kinase for AMP-activated protein kinase', *Cell Metabolism*, 2(1), 9-19
- Hawley, S. A., Ross, F. A., Gowans, G. J., Tibarewal, P., Leslie, N. R., Hardie, D. G. (2014) 'Phosphorylation by Akt within the ST loop of AMPK-alpha1 down-regulates its activation in tumour cells', *Biochemical Journal*, 459, 275-287
- Herbert, S. P., Ponambolam, S., Walker, J. H. (2005) 'Cytosolic phospholipase A<sub>2</sub>- $\alpha$  mediates endothelial cell proliferation and is inactivated by association with the Golgi apparatus', *Molecular Biology of the Cell*, 16, 3800-3809
- Hiratsuka, S., Minowa, O., Kuno, J., Noda, T., Shibuya, M. (1998) 'Flt-1 lacking the tyrosine kinase domain is sufficient for normal development and angiogenesis in mice', *Proceedings of the National Academy of Sciences of the United States of America*, 95(16), 9349-9354
- Hofmann, T., Obukhov, A. G., Schaefer, M., Harteneck, C., Gudermann, T., Schultz, G. (1999) 'Direct activation of human TRPC6 and TRPC3 channels by diacylglycerol', *Nature*, 397(6716), 259-263

- Holmes, B. F., Kurth-Kraczek, E. J., Winder, W. W. (1999) 'Chronic activation of 5'-AMP-activated protein kinase increases GLUT-4, hexokinase, and glycogen in muscle', *Journal of Applied Physiology*, 87(5), 1990-1995
- Hong, S. P., Leiper, F. C., Woods, A., Carling, D., Carlson, M. (2003) 'Activation of yeast Snf1 and mammalian AMP-activated protein kinase by upstream kinases', *Proceedings of the National Academy of Sciences of the United States of America*, 100(15), 8839-8843
- Horman, S., Morel, N., Vertommen, D., Hussain, N., Neumann, D., Beauloye, C., El Najjar, N., Forcet, C., Viollet, B., Walsh, M. P., Hue, L., Rider, M. H. (2008) 'AMP-activated protein kinase phosphorylates and desensitizes smooth muscle myosin light chain kinase', *Journal of Biological Chemistry*, 283(27), 18505-18512
- Horman, S., Vertommen, D., Heath, R., Neumann, D., Mouton, V., Woods, A., Schlattner, U., Wallimann, T., Carling, D., Hue, L., Rider, M. H. (2006) 'Insulin antagonizes ischemia-induced Thr172 phosphorylation of AMP-activated protein kinase alpha-subunits in heart via hierarchical phosphorylation of Ser485/491', *Journal of Biological Chemistry*, 281, 5335-5340
- Houck, K. A., Ferrara, N., Winer, J., Cachianes, G., Li, B., Leung, D. W. (1991) 'The vascular endothelial growth factor family: identification of a fourth molecular species and characterization of alternative splicing of RNA', *Molecular Endocrinology*, 5(12), 1806-1814
- Hudson, E. R., Pan, D. A., James, J., Lucocq, J. M., Hawley, S. A., Green, K. A., Baba, O., Terashima, T., Hardie, D. G. (2003) 'A novel domain in AMP-activated protein kinase causes glycogen storage bodies similar to those seen in hereditary cardiac arrhythmias', *Current Biology*, 13(10), 861-866
- Hurley, R. L., Anderson, K. A., Franzone, J. M., Kemp, B. E., Means, A. R., Witters, L. A. (2005) 'The Ca<sup>2+</sup>/calmodulin-dependent protein kinase kinases are AMP-activated protein kinase kinases', *Journal of Biological Chemistry*, 280(32), 29060-29066
- Hurley, R. L., Barre, L. K., Wood, S. D., Anderson, K. A., Kemp, B. E., Means, A. R., Witters, L. A. (2006) 'Regulation of AMP-activated protein kinase by multisite phosphorylation in response to agents that elevate cellular cAMP', *Journal of Biological Chemistry*, 281, 36662-36672
- Igata, M., Motoshima, H., Tsuruzoe, K., Kojima, K., Matsumura, T., Kondo, T., Taguchi, T., Nakamaru, K., Yano, M., Kukidome, D., Matsumoto, K., Toyonaga, T., Asano, T., Nishikawa, T., Araki, E. (2005) 'Adenosine monophosphate-activated protein kinase suppresses vascular smooth muscle cell proliferation through the inhibition of cell cycle progression', *Circulation Research*, 97(8), 837-844
- Iglesias, T., Waldron, R. T., Rozengurt, E. (1998) 'Identification of *in vivo* phosphorylation sites required for protein kinase D activation', *Journal of Biological Chemistry*, 273(42), 27662-27667
- Inoguchi, T., Battan, R., Handler, E., Sportsman, J. R., Heath, W., King, G. L. (1992) 'Preferential elevation of protein kinase C isoform beta II and diacylglycerol levels in the aorta and heart of diabetic rats: differential reversibility to glycemic control by islet cell transplantation', *Proceedings of the National Academy of Sciences of the United States of America*, 89, 11059-11063
- Inoki, K., Ouyang, H., Zhu, T., Lindvall, C., Wang, Y., Zhang, X., Yang, Q., Bennett, C., Harada, Y., Stankunas, K., Wang, C. Y., He, X., MacDougald, O. A., You, M., Williams, B. O., Guan, K. L. (2006) 'TSC2 integrates Wnt and energy signals via a coordinated phosphorylation by AMPK and GSK3 to regulate cell growth', *Cell*, 126(5), 955-968
- Inoue, E., Yamauchi, J. (2006) 'AMP-activated protein kinase regulates PEPCCK gene expression by direct phosphorylation of a novel zinc finger transcription factor', *Biochemical and Biophysical Research Communications*, 351(4), 793-799

- Irrthum, A., Karkkainen, M. J., Devriendt, K., Alitalo, K., Vikkula, M. (2000) 'Congenital hereditary lymphedema caused by a mutation that inactivates VEGFR3 tyrosine kinase', *American Journal of Human Genetics*, 67(2), 295-301
- Ishida, A., Murray, J., Saito, Y., Kanthou, C., Benzakour, O., Shibuya, M., Wijelath, E. S. (2001) 'Expression of vascular endothelial growth factor receptors in smooth muscle cells', *Journal of Cellular Physiology*, 188(3), 359-368
- Ishii, H., Jirousek, M. R., Koya, D., Takagi, C., Xia, P., Clermont, A., Bursell, S. E., Kern, T. S., Ballas, L. M., Heath, W. F., Stramm, L. E., Feener, E. P., King, G. L. (1996) 'Amelioration of vascular dysfunctions in diabetic rats by an oral PKC beta inhibitor', *Science*, 272(5262), 728-731
- Itani, S. I., Zhou, Q., Pories, W. J., MacDonald, K. G., Dohm, G. L. (2000) 'Involvement of protein kinase C in human skeletal muscle insulin resistance and obesity', *Diabetes*, 49, 1353-1358
- Javadov, S., Rajapurohitam, V., Kilić, A., Zeidan, A., Choi, A., Karmazyn, M. (2009) 'Anti-hypertrophic effect of NHE-1 inhibition involves GSK-3beta-dependent attenuation of mitochondrial dysfunction', *Journal of Molecular and Cellular Cardiology*, 46(6), 998-1007
- Jeltsch, M., Jha S. K., Tvorogov, D., Anisimov, A., Leppanen, V.-M., Holopainen, T., Kivela, R., Ortega, S., Karpanen, T., Alitalo, K. (2014) 'CCBE1 enhances lymphangiogenesis via A disintegrin and metalloprotease with thrombospondin motifs-3-mediated vascular endothelial growth factor-C activation', *Circulation*, 129(19) 1962-1971
- Jho, D., Mehta, D., Ahmmed, G., Gao, X. P., Tirupathi, C., Broman, M., Malik, A. B. (2005) 'Angiopoietin-1 opposes VEGF-induced increase in endothelial permeability by inhibiting TRPC1-dependent  $Ca^{2+}$  influx', *Circulation Research*, 96(12), 1282-1290
- Johannes, F. J., Prestle, J., Eis, S., Oberhagemann, P., Pfizenmaier, K. (1994) 'PKC $\epsilon$  is a novel, atypical member of the protein kinase C family', *Journal of Biological Chemistry*, 269(8), 6140-6148
- Jones, N. M. (2011) Single-cell RT-PCR analysis and CRF effects on TRPC channels expressed in rat brain, Unpublished Thesis, University of Illinois
- Joukov, V., Sorsa, T., Kumar, V., Jeltsch, M., Claesson-Welsh, L., Cao, Y., Saksela, O., Kalkkinen, N., Alitalo, K. (1997) 'Proteolytic processing regulates receptor specificity and activity of VEGF-C', *EMBO Journal*, 16(13) 3898-3911
- Ju, T.-C., Chen, H.-M., Lin, J.-T., Chang, C.-P., Chang, W.-C., Kang, J.-J., Sun, C.-P., Tao, M.-H., Tu, P.-H., Chang, C., Dickson, D. W., Chern, Y. (2011) 'Nuclear translocation of AMPK- $\alpha$ 1 potentiates striatal neurodegeneration in Huntington's disease', *Journal of Cell Biology*, 194(2), 209-227
- Jäger, S., Handschin, C., St.-Pierre, J., Spiegelman, B. M. (2007) 'AMP-activated protein kinase (AMPK) action in skeletal muscle via direct phosphorylation of PGC-1 $\alpha$ ', *Proceedings of the National Academy of Sciences of the United States of America*, 104(29), 12017-12022
- Kahn, B. B., Alquier, T., Carling, D., Hardie, D. G. (2005) 'AMP-activated protein kinase: Ancient energy gauge provides clues to modern understanding of metabolism', *Cell Metabolism*, 1(1), 15-25
- Kato, K., Tokuda, H., Adachi, S., Matsushima-Nishiwaki, R., Natsume, H., Yamakawa, K., Gu, Y., Otsuka, T., Kozawa, O. (2010) 'AMP-activated protein kinase positively regulates FGF-2-stimulated VEGF synthesis in osteoblasts', *Biochemical and Biophysical Research Communications*, 400(1), 123-127

- Katoh, O., Tauchi, H., Kawaishi, K., Kimura, A., Satow, Y. (1995) 'Expression of the vascular endothelial growth factor (VEGF) receptor gene, KDR, in hematopoietic cells and inhibitory effect of VEGF on apoptotic cell death caused by ionizing radiation', *Cancer Research*, 55(23), 5687-5692
- Kawakami, Y., Nishimoto, H., Kitaura, J., Maeda-Yamamoto, M., Kato, R. M., Littman, D. R., Leitges, M., Rawlings, D. J., Kawakami, T. (2004) 'Protein kinase C betaII regulates Akt phosphorylation on Ser-473 in a cell type- and stimulus-specific fashion', *Journal of Biological Chemistry*, 279(46), 47720-47725
- Kim, J., Kundu, M., Viollet, B., Guan, K. L. (2011) 'AMPK and mTOR regulate autophagy through direct phosphorylation of Ulk1', *Nature Cell Biology*, 13(2), 132-141
- Kiselyov, K., Kim, J. Y., Zeng, W., Muallem, S. (2005) 'Protein-protein interaction and function of TRPC channels', *Pflugers Archiv: European Journal of Physiology*, 451(1), 116-124
- Kiyonaka, S., Kato, K., Nishida, M., Mio, K., Numaga, T., Sawaguchi, Y., Yoshida, T., Wakamori, M., Mori, E., Numata, T., Ishii, M., Takemoto, H., Ojida, A., Watanabe, K., Uemura, A., Kurose, H., Morii, T., Kobayashi, T., Sato, Y., Sato, C., Hamachi, I., Mori, Y. (2009) 'Selective and direct inhibition of TRPC3 channels underlies biological activities of a pyrazole compound', *Proceedings of the National Academy of Sciences of the United States of America*, 106(13), 5400-5405
- Kleinbongard, P., Heusch, G., Schulz, R. (2010) 'TNF $\alpha$  in atherosclerosis, myocardial ischemia/reperfusion and heart failure', *Pharmacology & Therapeutics*, 127(3), 295-314
- Kobori, T., Smith, G. D., Sandford, R., Edwardson, J. M. (2009) 'The transient receptor potential channels trpp2 and trpc1 form a heterotetramer with a 2:2 stoichiometry and an alternating subunit arrangement', *Journal of Biological Chemistry*, 284(51), 35507-35513
- Koch, M., Dettori, D., van Nuffelen, A., Souffreau, J., Marconcini, L., Wallays, G., Moons, L., Bruyere, F., Oliviero, S., Noel, A., Foidart, J.-M., Carmeliet, P., Dewerchin, M. (2009) 'VEGF-D deficiency in mice does not affect embryonic or postnatal lymphangiogenesis but reduces lymphatic metastasis', *Journal of Pathology*, 219(3) 356-364
- Koch, S., Tugues, S., Li, X., Gualandi, L., Claesson-Welsh, L. (2011) 'Signal transduction by vascular endothelial growth factor receptors', *Biochemical Journal*, 437(2), 169-183
- Kochukov, M. Y., Balasubramanian, A., Noel, R. C., Marrelli, S. P. (2012) 'Role of TRPC1 and TRPC3 channels in contraction and relaxation of mouse thoracic aorta', *Journal of Vascular Research*, 50(1) 11-20
- Kodiha, M., Rassi J. G., Brown, C. M., Stochaj, U. (2007) 'Localization of AMP kinase is regulated by stress, cell density, and signaling through the MEK->ERK1/2 pathway', *American Journal of Physiology. Cell Physiology*, 293(5) 1427-1436
- Kodiha, M., Stochaj, U. (2011) 'Targeting AMPK for therapeutic intervention in type 2 diabetes' in Croniger, C., (ed.) *Frontiers in Biosciences (Landmark Edition)*14, 3380-3400
- Koenig, S., Scherthaner, M., Maechler, H., Kappe, C. O., Glasnov, T. N., Hoefler, G., Braune, M., Wittchow, E., Groschner, K. (2013) 'A TRPC3 blocker, ethyl-1-(4-(2,3,3-trichloroacrylamide)phenyl)-5-(trifluoromethyl)-1H-pyrazole-4-carboxylate (Pyr3), prevents stent-induced arterial remodeling', *Journal of Pharmacology and Experimental Therapeutics*, 344(1), 33-40
- Koga, J., Matoba, T., Egashira, K., Kubo, M., Miyagawa, M., Iwata, E., Sueishi, K., Shibuya, M., Sunagawa, K. (2009) 'Soluble Flt-1 gene transfer ameliorates neointima formation after wire injury in flt-1 tyrosine kinase-deficient mice', *Arteriosclerosis, Thrombosis and Vascular Biology*, 29(4), 458-464

- Kohler, R., Brakemeier, S., Kuhn, M., Degenhardt, C., Buhr, H., Pries, A., Hoyer, J. (2001) 'Expression of ryanodine receptor type 3 and TRP channels in endothelial cells: comparison of *in situ* and cultured human endothelial cells', *Cardiovascular Research*, 51(1), 160-168
- Komander, D., Kular, G. S., Schuttelkopf, A. W., Deak, M., Prakash, K. R., Bain, J., Elliott, M., Garrido-Franco, M., Kozikowski, A. P., Alessi, D. R., van Aalten, D. M. (2004) 'Interactions of LY333531 and other bisindolyl maleimide inhibitors with PDK1', *Structure*, 12, 215-226
- Kovacic, S., Soltys, C. L., Barr, A. J., Shiojima, I., Walsh, K., Dyck, J. R. (2003) 'Akt activity negatively regulates phosphorylation of AMP-activated protein kinase in the heart', *Journal of Biological Chemistry*, 278, 39422-39427
- Kowluru, R., Jirousek, M., Stramm, L., Engerman, R., Kern, T. (1996) Diabetes-induced disorders of retinal protein kinase C and Na, K-ATPase are inhibited by LY333531, *Diabetes*, 45, 50-50
- Kubota, N., Terauchi, Y., Kubota, T., Kumagai, H., Itoh, S., Satoh, H., Yano, W., Ogata, H., Tokuyama, K., Takamoto, I., Mineyama, T., Ishikawa, M., Moroi, M., Sugi, K., Yamauchi, T., Ueki, K., Tobe, K., Noda, T., Nagai, R., Kadowaki, T. (2006) 'Pioglitazone ameliorates insulin resistance and diabetes by both adiponectin-dependent and -independent pathways', *Journal of Biological Chemistry*, 281(1) 8748-8755
- Kukidome, D., Nishikawa, T., Sonoda, K., Imoto, K., Fujisawa, K., Yano, M., Motoshima, H., Taguchi, T., Matsumura, T., Araki, E. (2006) 'Activation of AMP-activated protein kinase reduces hyperglycemia-induced mitochondrial reactive oxygen species production and promotes mitochondrial biogenesis in human umbilical vein endothelial cells', *Diabetes*, 55(1), 120-127
- Lamallice, L., Houle, F., Jourdan, G., Huot, J. (2004) 'Phosphorylation of tyrosine 1214 on VEGFR2 is required for VEGF-induced activation of Cdc42 upstream of SAPK2/p38', *Oncogene*, 23(2), 434-445
- LeBrasseur, N. K., Kelly, M., Tsao, T.-S., Farmer, S. R., Saha, A. K., Ruderman, N. B., Tomas, E. (2006) 'Thiazolidinediones can rapidly activate AMP-activated protein kinase in mammalian tissues', *American Journal of Physiology - Endocrinology and Metabolism*, 291(1), E175-E181
- Lee, M., Hwang, J. T., Lee, H. J., Jung, S. N., Kang, I., Chi, S. G., Kim, S. S., Ha, J. (2003) 'AMP-activated protein kinase activity is critical for hypoxia-inducible factor-1 transcriptional activity and its target gene expression under hypoxic conditions in DU145 cells', *Journal of Biological Chemistry*, 278(41), 39653-39661
- Lee, M., Hwang, J. T., Yun, H., Kim, E. J., Kim, M. J., Kim, S. S., Ha, J. (2006) 'Critical roles of AMP-activated protein kinase in the carcinogenic metal-induced expression of VEGF and HIF-1 proteins in DU145 prostate carcinoma', *Biochemical Pharmacology*, 72(1), 91-103
- Lehmann, J. M., Moore, L. B., Smith-Oliver, T. A., Wilkison, W. O., Willson, T. M., Kliewer, S. A. (1995) 'An antidiabetic thiazolidinedione is a high affinity ligand for peroxisome proliferator-activated receptor gamma (PPAR gamma)', *Journal of Biological Chemistry*, 270(22), 12953-12956
- Leppänen, V. M., Prota, A. E., Jeltsch, M., Anisimov, A., Kalkkinen, N., Strandin, T., Lankinen, H., Goldman, A., Ballmer-Hofer, K., Alitalo, K. (2010) 'Structural determinants of growth factor binding and specificity by VEGF receptor 2', *Proceedings of the National Academy of Sciences of the United States of America*, 107(6), 2425-2430
- Leuner, K., Kazanski, V., Muller, M., Essin, K., Henke, B., Gollasch, M., Harteneck, C., Muller, W. E. (2007) 'Hyperforin--a key constituent of St. John's wort specifically activates TRPC6 channels', *FASEB Journal*, 21(14), 4101-4111
- Leung, D. W., Cachianes, G., Kuang, W. J., Goeddel, D. V., Ferrara, N. (1989) 'Vascular endothelial growth factor is a secreted angiogenic mitogen', *Science*, 246(4935), 1306-1309

- Levy, A. P., Levy, N. S., Wegner, S. and Goldberg, M. A. (1995) 'Transcriptional regulation of the rat vascular endothelial growth factor gene by hypoxia', *Journal of Biological Chemistry*, 270(22), 13333-13340
- Li, D., Wang, D., Wang, Y., Ling, W., Feng, X., Xia, M. (2010) 'Adenosine monophosphate-activated protein kinase induces cholesterol efflux from macrophage-derived foam cells and alleviates atherosclerosis in apolipoprotein E-deficient mice', *Journal of Biological Chemistry*, 285(43), 33499-33509
- Lihn, A. S., Jessen, N., Pedersen, S. B., Lund, S., Richelsen, B. (2004) 'AICAR stimulates adiponectin and inhibits cytokines in adipose tissue', *Biochemical and Biophysical Research Communications*, 316(3) 853-858
- Lin, F., Ribar, T. J., Means, A. R. (2011) 'The Ca<sup>2+</sup>/calmodulin-dependent protein kinase kinase, CaMKK2, inhibits pre-adipocyte differentiation', *Endocrinology*, 152(10), 3668-3679
- Lin, J., Handschin, C., Spiegelman, B. M. (2005) 'Metabolic control through the PGC-1 family of transcription coactivators', *Cell Metabolism*, 1(6), 361-370
- Linde, K., Berner, M., Kriston, L. (2008) 'St John's wort for major depression', *Cochrane Database of Systematic Reviews*, 4.
- Liu, Y., Cox, S. R., Morita, T., Kourembanas, S. (1995) 'Hypoxia regulates vascular endothelial growth factor gene expression in endothelial cells. Identification of a 5' enhancer', *Circulation Research*, 77(3), 638-643
- Logie, L., Ruiz-Alcaraz, A. J., Keane, M., Woods, Y. L., Bain, J., Marquez, R., Alessi, D. R., Sutherland, C. (2007) 'Characterization of a protein kinase B inhibitor *in vitro* and in insulin-treated liver cells', *Diabetes*, 56(9), 2218-2227
- Lopez-Cotarelo, P., Escribano-Diaz, C., Gonzalez-Bethencourt, I. L., Gomez-Moreira, C., Deguiz, M. L., Torres-Bacete, J., Gomez-Cabanas, L., Fernandez-Barrera, J., Delgado-Martin, C., Mellado, M., Regueiro, J. R., Miranda-Carus, M. E. and Rodriguez-Fernandez, J. L. (2015) 'A novel MEK-ERK-AMPK signaling axis controls chemokine receptor CCR7-dependent survival in human mature dendritic cells', *Journal of Biological Chemistry*, 290, 827-840
- Lu, D. Y., Tang, C. H., Chen, Y. H., Wei, I. H. (2010) 'Berberine suppresses neuroinflammatory responses through AMP-activated protein kinase activation in BV-2 microglia', *Journal of Cellular Biochemistry*, 110(3), 697-705
- Manning, B. D., Cantley, L. C. (2007) 'AKT/PKB signaling: navigating downstream', *Cell*, 129(7), 1261-1274
- Marsin, A. S., Bertrand, L., Rider, M. H., Deprez, J., Beauloye, C., Vincent, M. F., van den Berghe, G., Carling, D., Hue, L. (2001) 'Phosphorylation and activation of heart PFK-2 by AMPK has a role in the stimulation of glycolysis during ischaemia', *Current Biology*, 10(20) 1247-1255
- Martini, M., De Santis, M. C., Braccini, L., Gulluni, F., Hirsch, E. (2014) 'PI3K/AKT signaling pathway and cancer: an updated review', *Annals of Medicine*, 46(6), 372-383
- Matsuda, M., DeFronzo, R. A. (1999) 'Insulin sensitivity indices obtained from oral glucose tolerance testing: comparison with the euglycemic insulin clamp', *Diabetes Care*, 22(9), 1462-1470
- Matsumoto, K., Ohi, H., Kanmatsuse, K. (1997) 'Interleukin 10 and interleukin 13 synergize to inhibit vascular permeability factor release by peripheral blood mononuclear cells from patients with lipoid nephrosis', *Nephron*, 77(2), 212-218

- Matsumoto, T., Bohman, S., Dixelius, J., Berge, T., Dimberg, A., Magnusson, P., Wang, L., Wikner, C., Qi, J. H., Wernstedt, C., Wu, J., Bruheim, S., Mugishima, H., Mukhopadhyay, D., Spurrkland, A., Claesson-Welsh, L. (2005) 'VEGF receptor-2 Y951 signaling and a role for the adapter molecule TSAd in tumor angiogenesis', *EMBO Journal*, 24(13), 2342-2353
- Matsumoto, T., Claesson-Welsh, L. (2001) 'VEGF receptor signal transduction', *Science's STKE*, 112,(21)
- Matsumoto, T., Mugishima, H. (2006) 'Signal transduction via vascular endothelial growth factor (VEGF) receptors and their roles in atherosclerosis', *Journal of Atherosclerosis and Thrombosis*, 13(3), 130-135
- Matthews, S. A., Rozengurt, E., Cantrell, D., (1999) 'Characterization of serine 916 as an *in vivo* autophosphorylation site for protein kinase D/Protein kinase Cmu', *Journal of Biological Chemistry*, 274(37) 26543-26549
- Maxwell, P. H., Wiesener, M. S., Chang, G.-W., Clifford, S. C., Vaux, E. C., Cockman, M. E., Wykoff, C. C., Pugh, C. W., Maher, E. R., Ratcliffe, P. J. (1999) 'The tumour suppressor protein VHL targets hypoxia-inducible factors for oxygen-dependent proteolysis', *Nature*, 399(6733), 271-275
- Maynard, S. E., Min, J. Y., Merchan, J., Lim, K. H., Li, J., Mondal, S., Libermann, T. A., Morgan, J. P., Sellke, F. W., Stillman, I. E., Epstein, F. H., Sukhatme, V. P., Karumanchi, S. A. (2003) 'Excess placental soluble fms-like tyrosine kinase 1 (sFlt1) may contribute to endothelial dysfunction, hypertension, and proteinuria in preeclampsia', *Journal of Clinical Investigation*, 111(5), 649-658
- McBride, A., Ghilagaber, S., Nikolaev, A., Hardie, D. G. (2009) 'The glycogen-binding domain on the AMPK  $\beta$  subunit allows the kinase to act as a glycogen sensor', *Cell Metabolism*, 9(1), 23-34
- McColl, B. K., Baldwin, M., E. Roufail, S., Freeman, C., Moritz, R. L., Simpson, R. J., Alitalo, K., Stacker, S. A., Achen, M. G., (2003) 'Plasmin activates the lymphangiogenic growth factors VEGF-C and VEGF-D', *Journal of Experimental Medicine*, 198(7) 863-868
- McGarry, J. D. (1995) 'The mitochondrial carnitine palmitoyltransferase system: its broadening role in fuel homeostasis and new insights into its molecular features', *Biochemical Society Transactions*, 23(2) 321-324
- McMahon, G. (2000) 'VEGF receptor signaling in tumor angiogenesis', *The Oncologist*, 5(Supplement 1), 3-10
- Mebratu, Y., Tesfagzi, Y. (2009) 'How ERK1/2 activation controls cell proliferation and cell death is subcellular localization the answer?', *Cell Cycle*, 8(8), 1168-1175
- Medeiros, D. M. (2008) 'Assessing mitochondria biogenesis', *Methods*, 46(4), 288-294
- Mitchell, K. I., Michell, B. J., House, C. M., Stapleton, D., Dyck, J., Gamble, J., Ullrich, C., Witters, L. A., Kemp, B. E. (1997) 'Posttranslational modifications of the 5'-AMP-activated protein kinase beta1 subunit', *Journal of Biological Chemistry*, 272(39), 24475-24479
- Mizrachy-Schwartz, S., Kravchenko-Balasha, N., Ben-Bassat, H., Klein, S., Levitzki, A. (2007) 'Optimization of energy-consuming pathways towards rapid growth in HPV-transformed cells', *PLoS One*, 2(7), e628
- Mizutani, J., Tokuda, H., Matsushima-Nishiwaki, R., Kato, K., Kondo, A., Natsume, H., Kozawa, O., Otsuka, T. (2012) 'Involvement of AMP-activated protein kinase in TGF- $\beta$ -stimulated VEGF synthesis in osteoblasts', *International Journal of Molecular Medicine*, 29(4), 550-556

- Morrow, V. A., Foufelle, F., Connell, J. M., Petrie, J. R., Gould, G. W., Salt, I. P. (2003) 'Direct activation of AMP-activated protein kinase stimulates nitric-oxide synthesis in human aortic endothelial cells', *Journal of Biological Chemistry*, 278(34), 31629-31639
- Motoshima, H., Goldstein, B. J., Igata, M., Araki, E. (2006) 'AMPK and cell proliferation-AMPK as a therapeutic target for atherosclerosis and cancer', *Journal of Physiology*, 574(1), 63-71
- Munday, M. R., Campbell, D. G., Carling, D., Hardie, D. G. (1988) 'Identification by amino acid sequencing of three major regulatory phosphorylation sites on rat acetyl-CoA carboxylase', *European Journal of Biochemistry*, 175(2), 331-338
- Munro, S., Nichols, B. J. (1999) 'The GRIP domain – a novel Golgi-targeting domain found in several coiled-coil proteins', *Current Biology*, 9(7), 377-380
- Nagata, D., Mogi, M., Walsh, K. (2003) 'AMP-activated protein kinase (AMPK) signaling in endothelial cells is essential for angiogenesis in response to hypoxic stress', *Journal of Biological Chemistry*, 278(33), 31000-31006
- Neumann, P., Gertzberg, N., Johnson, A. (2004) 'TNF- $\alpha$  induces a decrease in eNOS promoter activity', *American Journal of Physiology - Lung Cellular and Molecular Physiology*, 286(2), L452-L459
- Ning, J., Xi, G., Clemmons, D. R. (2011) 'Suppression of AMPK activation via S485 phosphorylation by IGF-I during hyperglycemia is mediated by AKT activation in vascular smooth muscle cells', *Endocrinology*, 152, 3143-3154
- Nishino, Y., Miura, T., Miki, T., Sakamoto, J., Nakamura, Y., Ikeda, Y., Kobayashi, H., Shimamoto, K. (2004) 'Ischemic preconditioning activates AMPK in a PKC-dependent manner and induces GLUT4 up-regulation in the late phase of cardioprotection', *Cardiovascular Research*, 61, 610-619
- Nissen, S. E., Nicholls, S. J., Sipahi, I., Libby, P., Raichlen, J. S., Ballantyne, C. M., Davignon, J., Erbel, R., Fruchart, J. C., Tardif, J. C., Schoenhagen, P., Crowe, T., Cain, V., Wolski, K., Goormastic, M., Tuzcu, E. M. (2006) 'Effect of very high-intensity statin therapy on regression of coronary atherosclerosis: The asteroid trial', *JAMA*, 295(13), 1556-1565
- O'Brien, A. J., Villani, L. A., Broadfield, L. A., Houde, V. P., Galic, S., Blandino, G., Kemp, B. E., Tsakiridis, T., Muti, P., Steinberg, G. R. (2015) 'Salicylate activates AMPK and synergizes with metformin to reduce the survival of prostate and lung cancer cells *ex vivo* through inhibition of *de novo* lipogenesis', *Biochemical Journal*, 469(2) 177-187
- Odell, A. F., Hollstein, M., Ponnambalam, S., Walker, J. H. (2011) 'A VE-cadherin-PAR3- $\alpha$ -catenin complex regulates the Golgi localization and activity of cytosolic phospholipase A<sub>2</sub> $\alpha$  in endothelial cells', *Molecular Biology of the Cell*, 23, 1783-1796
- Ogawa, S., Asuke, O., Sawano, A., Yamaguchi, S., Yazaki, Y., Shibuya, M. (1998) 'A novel type of vascular endothelial growth factor, VEGF-E (NZ-7 VEGF), Preferentially Utilizes KDR/Flk-1 receptor and carries a potent mitotic activity without heparin-binding domain' *Journal of Biological Chemistry*, 273(47) 31273-31282
- Ohmstede, C., Jensen, K., Sahyoun, N. (1989) 'Ca<sup>2+</sup>/calmodulin-dependent protein kinase enriched in cerebellar granule cells. Identification of a novel neuronal calmodulin-dependent protein kinase', *Journal of Biological Chemistry*, 264(10), 5866-5875
- Olofsson, B., Pajusola, K., Kaipainen, A., von Euler, G., Joukov, V., Saksela, O., Orpana, A., Pettersson, R. F., Alitalo, K., Eriksson, U. (1996a) 'Vascular endothelial growth factor B, a novel growth factor for endothelial cells', *Proceedings of the National Academy of Sciences of the United States of America*, 93(6), 2576-2581

- Olofsson, B., Pajusola, K., von Euler, G., Chilov, D., Alitalo, K., Eriksson, U. (1996b) 'Genomic organization of the mouse and human genes for vascular endothelial growth factor B (VEGF-B) and characterization of a second splice isoform', *Journal of Biological Chemistry*, 271(32), 19310-19317
- Olsson, A. K., Dimberg, A., Kreuger, J., Claesson-Welsh, L. (2006) 'VEGF receptor signalling - in control of vascular function', *Nature Reviews Molecular, Cell Biology*, 7(5), 359-371
- Ong, H. L., Chen, J., Chataway, T., Brereton, H., Zhang, L., Downs, T., Tsiokas, L., Barritt, G. (2002) 'Specific detection of the endogenous transient receptor potential (TRP)-1 protein in liver and airway smooth muscle cells using immunoprecipitation and Western-blot analysis', *Biochemical Journal*, 364(3), 641-648
- Osol, G., Celia, G., Gokina, N., Barron, C., Chien, E., Mandala, M., Luksha, L., Kublickiene, K. (2008) 'Placental growth factor is a potent vasodilator of rat and human resistance arteries', *American Journal of Physiology. Heart and Circulatory Physiology*, 294(3), H1381-1387
- Ouchi, N., Shibata, R., Walsh, K. (2005) 'AMP-activated protein kinase signaling stimulates VEGF expression and angiogenesis in skeletal muscle', *Circulation Research*, 96(8), 838-846
- Owen, M. R., Doran, E., Halestrap, A. P., (2000) 'Evidence that metformin exerts its anti-diabetic effects through inhibition of complex 1 of the mitochondrial respiratory chain', *Biochemical Journal*, 348(3), 607-614
- Pajusola, K., Aprelikova, O., Armstrong, E., Morris, S., Alitalo, K., (1993) 'Two human FLT4 receptor tyrosine kinase isoforms with distinct carboxy terminal tails are produced by alternative processing of primary transcripts', *Oncogene*, 8(11)
- Palmer, T. M., Stiles, G. L. (1999) 'Stimulation of A(2A) adenosine receptor phosphorylation by protein kinase C activation: evidence for regulation by multiple protein kinase C isoforms', *Biochemistry*, 38(45), 14833-14842
- Paria, B. C., Malik, A. B., Kwiatek, A. M., Rahman, A., May, M. J., Ghosh, S., Tiruppathi, C. (2003) 'Tumor necrosis factor- $\alpha$  induces nuclear factor- $\kappa$ B-dependent TRPC1 expression in endothelial cells', *Journal of Biological Chemistry*, 278(39), 37195-37203
- Park, D. W., Jiang, S., Liu, Y., Siegal, G. P., Inoki, K., Abraham, E., Zmijewski, J. W. (2014) 'GSK3 $\beta$ -dependent inhibition of AMPK potentiates activation of neutrophils and macrophages and enhances severity of acute lung injury', *American Journal of Physiology. Lung Cellular and Molecular Physiology*, 307, L735-745
- Parker, P. J., Murray-Rust, J. (2004) 'PKC at a glance', *Journal of Cell Science*, 117, 131-132
- Pedram, A., Razandi, M., Levin, E. R. (1998) 'Extracellular signal-regulated protein kinase/jun kinase cross-talk underlies vascular endothelial cell growth factor-induced endothelial cell proliferation', *Journal of Biological Chemistry*, 273(41), 26722-26728
- Pertovaara, L., Kaipainen, A., Mustonen, T., Orpana, A., Ferrara, N., Saksela, O., Alitalo, K. (1994) 'Vascular endothelial growth factor is induced in response to transforming growth factor- $\beta$  in fibroblastic and epithelial cells', *Journal of Biological Chemistry*, 269(9), 6271-6274
- Pinter, K., Jefferson, A., Czibik, G., Watkins, H., Redwood, C. (2012) 'Subunit composition of AMPK trimers present in the cytokinetic apparatus: Implications for drug target identification', *Cell Cycle*, 11(5), 917-921

- Pitt, S. J., Funnell, T. M., Sitsapesan, M., Venturi, E., Rietdorf, K., Ruas, M., Ganesan, A., Gosain, R., Churchill, G. C., Zhu, M. X., Parrington, J., Galione, A., Sitsapesan, R. (2010) 'TPC2 is a novel NAADP-sensitive  $\text{Ca}^{2+}$  release channel, operating as a dual sensor of luminal pH and  $\text{Ca}^{2+}$ ', *Journal of Biological Chemistry*, 285(45), 35039-35046
- Pocock, T. M., Foster, R. R., Bates, D. O. (2004) 'Evidence of a role for TRPC channels in VEGF-mediated increased vascular permeability *in vivo*', *American Journal of Physiology. Heart and Circulatory Physiology*, 286(3), H1015-1026
- Popovic, M., Smiljanic, K., Dobutovic, B., Syrovets, T., Simmet, T., Isenovic, E. R., (2011) 'Thrombin and vascular inflammation', *Molecular and Cellular Biochemistry*, 359(1-2), 301-313
- Poteser, M., Graziani, A., Eder, P., Yates, A., Machler, H., Romanin, C., Groschner, K. (2008) 'Identification of a rare subset of adipose tissue-resident progenitor cells, which express CD133 and TRPC3 as a VEGF-regulated  $\text{Ca}^{2+}$  entry channel', *FEBS Letters*, 582(18), 2696-2702
- Poteser, M., Graziani, A., Rosker, C., Eder, P., Derler, I., Kahr, H., Zhu, M. X., Romanin, C., Groschner, K., (2006) 'TRPC3 and TRPC4 associate to form a redox-sensitive cation channel. Evidence for expression of native TRPC3-TRPC4 heteromeric channels in endothelial cells', *Journal of Biological Chemistry*, 281(19), 13588-13599
- Procopio, C., Andreozzi, F., Laratta, E., Cassese, A., Beguinot, F., Arturi, F., Hribal, M. L., Perticone, F., Sesti, G. (2009) 'Leptin-stimulated endothelial nitric-oxide synthase via an adenosine 5'-monophosphate-activated protein kinase/Akt signaling pathway is attenuated by interaction with C-reactive protein', *Endocrinology*, 150(8), 3584-3593
- Quentin, T., Kitz, J., Steinmetz, M., Poppe, A., Bär, K., Krätzner, R. (2011) 'Different expression of the catalytic alpha subunits of the AMP activated protein kinase--an immunohistochemical study in human tissue', *Histol Histopathol*, 26(5), 589-596
- Raman, M., Chen, W., Cobb, M. H., (2007) 'Differential regulation and properties of MAPKs', *Oncogene*, 26, 3100-3112
- Reihill, J. A. (2009) The role of AMP-activated protein kinase in endothelial VEGF signalling, Unpublished Thesis, University of Glasgow
- Reihill, J. A., Ewart, M. A., Hardie, D. G., Salt, I. P. (2007) 'AMP-activated protein kinase mediates VEGF-stimulated endothelial NO production', *Biochemical and Biophysical Research Communications*, 354(4), 1084-1088
- Reihill, J. A., Ewart, M. A., Salt, I. P. (2011) 'The role of AMP-activated protein kinase in the functional effects of vascular endothelial growth factor-A and -B in human aortic endothelial cells', *Vascular Cell*, 3, 9
- Riccio, A., Medhurst, A. D., Mattei, C., Kellsell, R. E., Calver, A. R., Randall, A. D., Benham, C. D., Pangalos, M. N. (2002) 'mRNA distribution analysis of human TRPC family in CNS and peripheral tissues', *Brain Research. Molecular Brain Research*, 109(1-2), 95-104
- Romanova, L. Y., Alexandrov, I. A., Nordan, R. P., Blagosklonny, M. V., Mushinski, J. F. (1998) 'Cross-talk between protein kinase C-alpha (PKC-alpha) and -delta (PKC-delta): PKC-alpha elevates the PKC-delta protein level, altering its mRNA transcription and degradation', *Biochemistry*, 37, 5558-5565
- Rozengurt, E. (2011) 'Protein kinase D signaling: multiple biological functions in health and disease', *Physiology*, 26(1), 23-33
- Rubin, L. J., Magliola, L., Feng, X., Jones, A. W., Hale, C. C. (2005) 'Metabolic activation of AMP kinase in vascular smooth muscle', *Journal of Applied Physiology (1985)*, 98(1), 296-306

- Saberi, B., Shinohara, M., Ybanez, M. D., Hanawa, N., Gaarde, W. A., Kaplowitz, N., Han, D. (2008) 'Regulation of H<sub>2</sub>O<sub>2</sub>-induced necrosis by PKC and AMP-activated kinase signaling in primary cultured hepatocytes', *American Journal of Physiology. Cell Physiology*, 295(1), C50-63
- Saeedi, R., Parsons H. I., Wambolt, R. B., Paulson, K., Sharma, V., Dyck, J. R. B., Brownsey, R. W., Allard, M. F., (2008) 'Metabolic actions of metformin in the heart can occur by AMPK-independent mechanisms', *American Journal of Physiology. Heart and Circulatory Physiology*. 294(6), 2497-2506
- Saha, A. K., Persons, K., Safer, J. D., Luo, Z., Holick, M. F., Ruderman, N. B. (2006) 'AMPK regulation of the growth of cultured human keratinocytes', *Biochemical and Biophysical Research Communications*, 349(2), 519-24
- Sakurai, Y., Ohgimoto, K., Kataoka, Y., Yoshida, N., Shibuya, M., (2005) 'Essential role of Flk-1 (VEGF receptor 2) tyrosine residue 1173 in vasculogenesis in mice', *Proceedings of the National Academy of Sciences of the United States of America*, 102(4), 1076-1081
- Salt, I., Celler, J. W., Hawley, S. A., Prescott, A., Woods, A., Carling, D., Hardie, D. G. (1998) 'AMP-activated protein kinase: greater AMP dependence, and preferential nuclear localization, of complexes containing the alpha2 isoform', *Biochemical Journal*, 334 (1), 177-187
- Sambrook, J., Fritsch, E.F., Maniatis, T. (1989) *Molecular Cloning: A laboratory manual*, New York: Cold Spring Harbour Laboratory Press
- Sanders, M. J., Ali, Z. S., Hegarty, B. D., Heath, R., Snowden, M. A., Carling, D., (2007a) 'Defining the mechanism of activation of AMP-activated protein kinase by the small molecule A-769662, a member of the thienopyridone family', *Journal of Biological Chemistry*, 282(45) 32539-32548
- Sanders, M. J., Grondin, P. O., Hegarty, B. D., Snowden, M. A., Carling, D. (2007b) 'Investigating the mechanism for AMP activation of the AMP-activated protein kinase cascade', *Biochemical Journal*, 403(1), 139-148
- Sapkota, G. P., Deak, M., Kieloch, A., Morrice, N., Goodarzi, A. A., Smythe, C., Shiloh, Y., Lees-Miller, S. P., Alessi, D. R. (2002) 'Ionizing radiation induces ataxia telangiectasia mutated kinase (ATM)-mediated phosphorylation of LKB1/STK11 at Thr-366', *Biochemical Journal*, 368(2), 507-516
- Schindl, R., Fritsch, R., Jardin, I., Frischauf, I., Kahr, H., Muik, M., Riedl, M. C., Groschner, K., Romanin, C., Romanin, C. (2012) 'Canonical transient receptor potential (TRPC) 1 acts as a negative regulator for vanilloid TRPV6-mediated Ca<sup>2+</sup> influx', *Journal of Biological Chemistry*, 287(42), 35612-35620
- Schmitz-Peiffer, C. (2013) 'The tail wagging the dog--regulation of lipid metabolism by protein kinase C', *FEBS Journal*, 280(21), 5371-5383
- Schuhmacher, S., Foretz, M., Knorr, M., Jansen, T., Hortmann, M., Wenzel, P., Oelze, M., Kleschyov, A. L., Daiber, A., Keaney, J. F., Wegener, G., Lackner, K., Münzel, T., Viollet, B., Schulz, E. (2011) 'α1AMP-activated protein kinase preserves endothelial function during chronic angiotensin II treatment by limiting Nox2 upregulation', *Arteriosclerosis, Thrombosis, and Vascular Biology*, 31(3), 560-566
- Schulz, E., Anter, E., Zou, M.-H., Keaney, J. F. (2005) 'Estradiol-mediated endothelial nitric oxide synthase association with heat shock protein 90 requires adenosine monophosphate-dependent protein kinase', *Circulation*, 111(25), 3473-3480

- Scott, J. W., van Denderen, B. J., Jorgensen, S. B., Honeyman, J. E., Steinberg, G. R., Oakhill, J. S., Iseli, T. J., Koay, A., Gooley, P. R., Stapleton, D., Kemp, B. E. (2008) 'Thienopyridone drugs are selective activators of AMP-activated protein kinase beta1-containing complexes', *Chemistry & Biology*, 15(11), 1220-1230
- Seghezzi, G., Patel, S., Ren, C. J., Gualandris, A., Pintucci, G., Robbins, E. S., Shapiro, R. L., Galloway, A. C., Rifkin, D. B., Mignatti, P. (1998) 'Fibroblast Growth Factor-2 (FGF-2) Induces Vascular Endothelial Growth Factor (VEGF) Expression in the Endothelial Cells of Forming Capillaries: An Autocrine Mechanism Contributing to Angiogenesis', *Journal of Cell Biology*, 141(7), 1659-1673
- Seo, K., Rainer, P. P., Shalkey Hahn, V., Lee, D. I., Jo, S. H., Andersen, A., Liu, T., Xu, X., Willette, R. N., Lepore, J. J., Marino, J. P., Jr., Birnbaumer, L., Schnackenberg, C. G., Kass, D. A. (2014) 'Combined TRPC3 and TRPC6 blockade by selective small-molecule or genetic deletion inhibits pathological cardiac hypertrophy', *Proceedings of the National Academy of Sciences of the United States of America*, 111(4), 1551-1556
- Shalaby, F., Rossant, J., Yamaguchi, T. P., Gertsenstein, M., Wu, X. F., Breitman, M. L., Schuh, A. C. (1995) 'Failure of blood-island formation and vasculogenesis in Flk-1-deficient mice', *Nature*, 376(6535), 62-66
- Shen, Q., Rigor, R. R., Pivetti, C. D., Wu, M. H., Yuan, S. Y. (2010) 'Myosin light chain kinase in microvascular endothelial barrier function', *Cardiovascular Research*, 87(2), 272-280
- Shi, J., Takahashi, S., Jin, X. H., Li, Y. Q., Ito, Y., Mori, Y., Inoue, R. (2007) 'Myosin light chain kinase-independent inhibition by ML-9 of murine TRPC6 channels expressed in HEK293 cells', *British Journal of Pharmacology*, 152(1), 122-131
- Shiba, T., Inoguchi, T., Sportsman, J. R., Heath, W. F., Bursell, S., King, G. L. (1993) 'Correlation of diacylglycerol level and protein kinase C activity in rat retina to retinal circulation', *American Journal of Physiology. Endocrinology and Metabolism*, 265(5), E783-E793
- Siegfried, G., Basak, A., Cromlish, J. A., Benjannet, S., Marcinkiewicz, J., Chretien, M., Seidah, N. G., Khatib, A.-M., (2003) 'The secretory proprotein convertases furin, PC5, and PC7 activate VEGF-C to induce tumorigenesis', *Journal of clinical Investigation*, 111(11), 1723-1732
- Soares, S., Thompson, M., White, T., Isbell, A., Yamasaki, M., Prakash, Y., Lund, F. E., Galione, A., Chini, E. N. (2007) 'NAADP as a second messenger: neither CD38 nor base-exchange reaction are necessary for *in vivo* generation of NAADP in myometrial cells', *American Journal of Physiology. Cell Physiology*, 292(1), C227-239
- Soetikno, V., Watanabe, K., Lakshamanan, A. P., Arumugam, S., Sari, F. R., Sukumaran, V., Thandavarayan, R. A., Harima, M., Suzuki, K., Kawachi, H. (2012) 'Role of Protein Kinase C-MAPK, oxidative stress and inflammation pathways in diabetic nephropathy', *Journal of Nephrology & Therapeutics*, S2:001
- Soltys, C. L., Kovacic, S., Dyck, J. R. (2006) 'Activation of cardiac AMP-activated protein kinase by LKB1 expression or chemical hypoxia is blunted by increased Akt activity', *American Journal of Physiology. Heart and Circulatory Physiology*, 290(6), H2472-2479
- Song, H. B., Jun, H. O., Kim, J. H., Fruttiger, M. (2015) 'Suppression of transient receptor potential canonical channel 4 inhibits vascular endothelial growth factor-induced retinal neovascularization', *Cell Calcium*, 57, 101-108
- Song, M. S., Salmena, L., Pandolfi, P. P. (2012) 'The functions and regulation of the PTEN tumour suppressor', *Nature Reviews. Molecular Cell Biology*, 13(5), 283-296

- Stahmann, N., Woods, A., Carling, D., Heller, R. (2006) 'Thrombin activates AMP-activated protein kinase in endothelial cells via a pathway involving Ca<sup>2+</sup>/calmodulin-dependent protein kinase kinase beta', *Molecular and Cellular Biology*, 26(16), 5933-5945
- Stahmann, N., Woods, A., Spengler, K., Heslegrave, A., Bauer, R., Krause, S., Viollet, B., Carling, D., Heller, R. (2010) 'Activation of AMP-activated protein kinase by vascular endothelial growth factor mediates endothelial angiogenesis independently of nitric-oxide synthase', *Journal of Biological Chemistry*, 285(14), 10638-10652
- Stapleton, D., Mitchelhill, K. I., Gao, G., Widmer, J., Michell, B. J., Teh, T., House, C. M., Fernandez, C. S., Cox, T., Witters, L. A., Kemp, B. E. (1996) 'Mammalian AMP-activated protein kinase subfamily', *Journal of Biological Chemistry*, 271(2), 611-614
- Stone, J. D., Narine, A., Shaver, P. R., Fox, J. C., Vuncannon, J. R., Tulis, D. A. (2013) 'AMP-activated protein kinase inhibits vascular smooth muscle cell proliferation and migration and vascular remodeling following injury', *American Journal of Physiology. Heart and Circulatory Physiology*, 304(3), H369-381
- Stone, J. D., Narine, A., Tulis, D. A. (2012) 'Inhibition of vascular smooth muscle growth via signaling crosstalk between AMP-activated protein kinase and cAMP-dependent protein kinase', *Frontiers in Physiology*, 3, 409
- Stornaiuolo, M., Lotti, L.V., Borgese, N., Torrisi, M.-R., Mottola, G., Martire, G., Bonatti, S., (2003) 'KDEL and KKXX retrieval signals appended to the same reporter protein determine different trafficking between endoplasmic reticulum, intermediate compartment, and Golgi complex', *Molecular Biology of the Cell*, 14(3) 889-902
- Stuttfield, E., Ballmer-Hofer, K. (2009) 'Structure and function of VEGF receptors', *IUBMB Life*, 61(9), 915-922
- Sukhodub, A., Jovanović, S., Du, Q., Budas, G., Clelland, A. K., Shen, M., Sakamoto, K., Tian, R., Jovanović, A. (2007) 'AMP-activated protein kinase mediates preconditioning in cardiomyocytes by regulating activity and trafficking of sarcolemmal ATP-sensitive K(+) channels', *Journal of Cellular Physiology*, 210(1), 224-236
- Sun, W., Lee, T. S., Zhu, M., Gu, C., Wang, Y., Zhu, Y., Shyy, J. Y. (2006) 'Statins activate AMP-activated protein kinase *in vitro* and *in vivo*', *Circulation*, 114(24), 2655-2662
- Suter, M., Riek, U., Tuerk, R., Schlattner, U., Wallimann, T., Neumann, D. (2006) 'Dissecting the role of 5'-AMP for allosteric stimulation, activation, and deactivation of AMP-activated protein kinase', *Journal of Biological Chemistry*, 281(43), 32207-32216
- Sutherland, C. M., Hawley, S. A., McCartney, R. R., Leech, A., Stark, M. J., Schmidt, M. C., Hardie, D. G. (2003) 'Elm1p is one of three upstream kinases for the *Saccharomyces cerevisiae* SNF1 complex', *Current Biology*, 13(15), 1299-1305
- Takagi, H., King, G. L., Robinson, G. S., Ferrara, N., Aiello, L. P. (1996) 'Adenosine mediates hypoxic induction of vascular endothelial growth factor in retinal pericytes and endothelial cells', *Investigative Ophthalmology and Visual Science*, 37(11), 2165-2176
- Takahashi, T., Yamaguchi, S., Chida, K., Shibuya, M. (2001) 'A single autophosphorylation site on KDR/Flk-1 is essential for VEGF-A-dependent activation of PLC-gamma and DNA synthesis in vascular endothelial cells', *EMBO Journal*, 20(11), 2768-2778

- Tammela, T., Zarkada, G., Wallgard, E., Murtomaki, A., Suchting, S., Wirzenius, M., Waltari, M., Hellstrom, M., Schomber, T., Peltonen, R., Freitas, C., Duarte, A., Isoniemi, H., Laakkonen, P., Christofori, G., Yla-Herttuala, S., Shibuya, M., Pytowski, B., Eichmann, A., Betsholtz, C., Alitalo, K., (2008) 'Blocking VEGFR-3 suppresses angiogenic sprouting and vascular network formation', *Nature*, 454(7204)
- Tiruppathi, C., Freichel, M., Vogel, S. M., Paria, B. C., Mehta, D., Flockerzi, V., Malik, A. B. (2002) 'Impairment of store-operated  $Ca^{2+}$  entry in TRPC4(-/-) mice interferes with increase in lung microvascular permeability', *Circulation Research*, 91(1), 70-76
- Tokumitsu, H., Hatano, N., Fujimoto, T., Yurimoto, S., Kobayashi, R. (2011) 'Generation of autonomous activity of  $Ca^{2+}$ /calmodulin-dependent protein kinase kinase  $\beta$  by autophosphorylation', *Biochemistry*, 50(38), 8193-8201
- Tokumitsu, H., Iwabu M Fau - Ishikawa, Y., Ishikawa Y Fau - Kobayashi, R., Kobayashi, R. (2001) 'Differential regulatory mechanism of  $Ca^{2+}$ /calmodulin-dependent protein kinase kinase isoforms', *Biochemistry*, 40(46)13925-13932
- Tsuchiya, Y., Denison, F. C., Heath, R. B., Carling, D., Saggerson, D. (2012) '5'-AMP-activated protein kinase is inactivated by adrenergic signalling in adult cardiac myocytes', *Bioscience Reports*, 32(2), 197-209
- Um, J.-H., Park, S.-J., Kang, H., Yang, S., Foretz, M., McBurney, M. W., Kim, M. K., Violette, B., Chung, J. H. (2010) 'AMP-activated protein kinase-deficient mice are resistant to the metabolic effects of resveratrol', *Diabetes*, 59(3), 554-563
- Unterluggauer, H., Mazurek, S., Lener, B., Hütter, E., Eigenbrodt, E., Zwerschke, W., Jansen-Dürr, P. (2008) 'Premature senescence of human endothelial cells induced by inhibition of glutaminase', *Biogerontology*, 9(4), 247-259
- Urban, N., Hill, K., Wang, L., Kuebler, W. M., Schaefer, M. (2012) 'Novel pharmacological TRPC inhibitors block hypoxia-induced vasoconstriction', *Cell Calcium*, 51(2), 194-206
- Valbuena, N., Moreno, S. (2012) 'AMPK phosphorylation by Ssp1 is required for proper sexual differentiation in fission yeast', *Journal of Cell Science*, 125(11), 2655-2664
- Valentine, R. J., Coughlan, K. A., Ruderman, N. B., Saha, A. K. (2014) 'Insulin inhibits AMPK activity and phosphorylates AMPK Ser485/491 through Akt in hepatocytes, myotubes and incubated rat skeletal muscle', *Archives of Biochemistry and Biophysics*, 562, 62-69
- Valverde, A. M., Sinnott-Smith, J., van Lint, J., Rozengurt, E., (1994) 'Molecular cloning and characterization of protein kinase D: a target for diacylglycerol and phorbol esters with a distinctive catalytic domain',
- Vannier, B., Peyton, M., Boulay, G., Brown, D., Qin, N., Jiang, M., Zhu, X., Birnbaumer, L. (1999) 'Mouse trp2, the homologue of the human trpc2 pseudogene, encodes mTrp2, a store depletion-activated capacitative  $Ca^{2+}$  entry channel', *Proceedings of the National Academy of Sciences of the United States of America*, 96(5), 2060-2064
- Vazquez, G., Wedel, B. J., Aziz, O., Trebak, M., Putney, J. W., Jr. (2004) 'The mammalian TRPC cation channels', *Biochimica et Biophysica Acta*, 1742(1-3), 21-36
- Vincenti, V., Cassano, C., Rocchi, M., Persico, G. (1996) 'Assignment of the vascular endothelial growth factor gene to human chromosome 6p21.3', *Circulation*, 93(8), 1493-1495
- Violette, B., Lantier, L., Devin-Leclerc, J., Hebrard, S., Amouyal, C., Mounier, R., Foretz, M., Andreelli, F., (2009) 'Targeting the AMPK pathway for the treatment of Type 2 diabetes', *Frontiers in Bioscience (Landmark Edition)* 14, 3380-3400

Waltenberger, J., Claesson-Welsh, L., Siegbahn, A., Shibuya, M., Heldin, C. H. (1994) 'Different signal transduction properties of KDR and Flt1, two receptors for vascular endothelial growth factor', *Journal of Biological Chemistry*, 269(43), 26988-26995

Wang, S., Zhang, M., Liang, B., Xu, J., Xie, Z., Liu, C., Viollet, B., Yan, D., Zou, M.-H. (2010) 'AMPK $\alpha$ 2 deletion causes aberrant expression and activation of NAD (P) H oxidase and consequent endothelial dysfunction *in vivo* role of 26S proteasomes', *Circulation Research*, 106(6), 1117-1128

Wang, Y., Huang, Y., Lam, K. S., Li, Y., Wong, W. T., Ye, H., Lau, C.-W., Vanhoutte, P. M., Xu, A. (2009) 'Berberine prevents hyperglycemia-induced endothelial injury and enhances vasodilatation via adenosine monophosphate-activated protein kinase and endothelial nitric oxide synthase', *Cardiovascular Research*, 82(3), 484-492

Ward, Y., Gupta, S., Jensen, P., Wartmann, M., Davis, R. J., Kelly, K., (1994) 'Control of MAP kinase activation by the mitogen-induced threonine/tyrosine phosphatase PAC1', *Nature*, 367(6464), 651-654

Wiechmann, K., Muller, H., Fischer, D., Jauch, J., Werz, O. (2015) 'The acylphloroglucinols hyperforin and myrtilone A cause mitochondrial dysfunctions in leukemic cells by direct interference with mitochondria', *Apoptosis*, 20, 1508-1517

Wong, A. K., Howie, J., Petrie, J. R., Lang, C. C. (2009) 'AMP-activated protein kinase pathway: a potential therapeutic target in cardiometabolic disease', *Clinical Science (London)*, 116(8), 607-620

Woods, A., Azzout-Marniche, D., Foretz, M., Stein, S. C., Lemarchand, P., Ferré, P., Foufelle, F., Carling, D. (2000) 'Characterization of the role of AMP-activated protein kinase in the regulation of glucose-activated gene expression using constitutively active and dominant negative forms of the kinase', *Mol Cell Biol*, 20(18), 6704-11

Woods, A., Dickerson, K., Heath, R., Hong, S. P., Momcilovic, M., Johnstone, S. R., Carlson, M., Carling, D. (2005) 'Ca<sup>2+</sup>/calmodulin-dependent protein kinase kinase-beta acts upstream of AMP-activated protein kinase in mammalian cells', *Cell Metabolism*, 2(1), 21-33

Woods, A., Johnstone, S. R., Dickerson, K., Leiper, F. C., Fryer, L. G., Neumann, D., Schlattner, U., Wallimann, T., Carlson, M., Carling, D. (2003a) 'LKB1 is the upstream kinase in the AMP-activated protein kinase cascade', *Current Biology*, 13(22), 2004-2008

Woods, A., Munday, M. R., Scott, J., Yang, X., Carlson, M., Carling, D., (1994) 'Yeast SNF1 is functionally related to mammalian AMP-activated protein kinase and regulates acetyl-CoA carboxylase *in vivo*', *Journal of Biological Chemistry*, 269(30), 19505-19515

Woods, A., Vertommen, D., Neumann, D., Turk, R., Bayliss, J., Schlattner, U., Wallimann, T., Carling, D., Rider, M. H. (2003b) 'Identification of phosphorylation sites in AMP-activated protein kinase (AMPK) for upstream AMPK kinases and study of their roles by site-directed mutagenesis', *Journal of Biological Chemistry*, 278, 28434-28442

Wright, G. L., Maroulakou, I. G., Eldridge, J., Liby, T. L., Sridharan, V., Tsihchlis, P. N., Muise-Helmericks, R. C. (2008) 'VEGF stimulation of mitochondrial biogenesis: requirement of AKT3 kinase', *FASEB Journal*, 22(9), 3264-3275

Wu, H. M., Yuan, Y., Zawieja, D. C., Zawieja, D. C., Tinsley, J., Tinsley, J., Granger, H. J., (1999) 'Role of phospholipase C, protein kinase C, and calcium in VEGF-induced venular hyperpermeability', *American Journal of Physiology*, 276(2), H535-542

Xiao, B., Heath, R., Saiu, P., Leiper, F. C., Leone, P., Jing, C., Walker, P. A., Haire, L., Eccleston, J. F., Davis, C. T., Martin, S. R., Carling, D., Gamblin, S. J., (2007) 'Structural basis for AMP binding to mammalian AMP-activated protein kinase', *Nature*, 449(7161), 469-500

- Xiao, B., Sanders, M. J., Underwood, E., Heath, R., Mayer, F. V., Carmena, D., Jing, C., Walker, P. A., Eccleston, J. F., Haire, L. F., Saiu, P., Howell, S. A., Aasland, R., Martin, S. R., Carling, D., Gamblin, S. J. (2011) 'Structure of mammalian AMPK and its regulation by ADP', *Nature*, 472(7342), 230-233
- Yasuo Yamazaki, Y., Takani, K., Atoda, H., Morita, T. (2003) Snake venom vascular endothelial growth factors (VEGFs) exhibit potent activity through their specific recognition of KDR (VEGF Receptor 2), *Journal of Biological Chemistry*, 278(52) 5198-51988
- Yang, Q., Huang, J.-H., Underwood, M. J., Yao, X.-Q., He, G.-W. (2011) 'Endothelial TRPC3 channel and Associated NO release under hypoxia-reoxygenation', *FASEB Journal*, 25(1), 820.6
- Yao, X., Garland, C. J. (2005) 'Recent developments in vascular endothelial cell transient receptor potential channels', *Circulation Research*, 97(9), 853-863
- Yeo, K. P., Lowe, S. L., Lim, M. T., Voelker, J. R., Burkey, J. L., Wise, S. D. (2006) 'Pharmacokinetics of ruboxistaurin are significantly altered by rifampicin-mediated CYP3A4 induction', *British Journal of Clinical Pharmacology*, 61(2), 200-210
- Yip, H., Chan, W. Y., Leung, P. C., Kwan, H. Y., Liu, C., Huang, Y., Michel, V., Yew, D. T., Yao, X. (2004) 'Expression of TRPC homologs in endothelial cells and smooth muscle layers of human arteries', *Histochemistry and Cell Biology*, 122(6), 553-561
- Young, S., Parker, P. J., Ullrich, A., Stabel, S. (1987) 'Down-regulation of protein kinase C is due to an increased rate of degradation', *Biochemical Journal*, 244, 775-779
- Yun, H., Lee, M., Kim, S. S., Ha, J. (2005) 'Glucose deprivation increases mRNA stability of vascular endothelial growth factor through activation of AMP-activated protein kinase in DU145 prostate carcinoma', *Journal of Biological Chemistry*, 280(11), 9963-9972
- Zagranichnaya, T. K., Wu, X., Villereal, M. L. (2005) 'Endogenous TRPC1, TRPC3, and TRPC7 proteins combine to form native store-operated channels in HEK-293 cells', *Journal of Biological Chemistry*, 280(33), 29559-29569
- Zhang, J., Xie, Z., Dong, Y., Wang, S., Liu, C., Zou, M. H. (2008) 'Identification of nitric oxide as an endogenous activator of the AMP-activated protein kinase in vascular endothelial cells', *Journal of Biological Chemistry*, 283(41), 27452-27461
- Zhang, L., Dai, F., Cui, L., Jing, H., Fan, P., Tan, X., Guo, Y., Zhou, G. (2015) 'Novel role for TRPC4 in regulation of macroautophagy by a small molecule in vascular endothelial cells', *Biochimica et Biophysica Acta*, 1853(2), 377-387
- Zhang, W., Wang, Q., Wu, Y., Moriasi, C., Liu, Z., Dai, X., Liu, W., Yuan, Z. Y., Zou, M. H. (2014) 'Endothelial cell-specific liver kinase B1 deletion causes endothelial dysfunction and hypertension in mice *in vivo*', *Circulation*, 129(13), 1428-1439
- Zhou, G., Myers, R., Li, Y., Chen, Y., Shen, X., Fenyk-Melody, J., Wu, M., Ventre, J., Doebber, T., Fujii, N., Musi, N., Hirshman, M. F., Goodyear, L. J., Moller, D. E. (2001) 'Role of AMP-activated protein kinase in mechanism of metformin action', *Journal of Clinical Investigation*, 108(8), 1167-1174
- Zou, M. H., Kirkpatrick, S. S., Davis, B. J., Nelson, J. S., Wiles, W. G., Schlattner, U., Neumann, D., Brownlee, M., Freeman, M. B., Goldman, M. H. (2004) 'Activation of the AMP-activated protein kinase by the anti-diabetic drug metformin *in vivo*. Role of mitochondrial reactive nitrogen species', *Journal of Biological Chemistry*, 279(42), 43940-43951

Zugaza, J. L., Sinnett-Smith, J., Van Lint, J., Rozengurt, E. (1996) 'Protein kinase D (PKD) activation in intact cells through a protein kinase C-dependent signal transduction pathway', *EMBO Journal*, 15(22), 6220-6230